Ecological considerations of thermal and nutritional interactions in *Metarhizium* host range evolution

A multidimensional analysis of niche width in insect-pathogenic fungi

Anna R. Slowik

Submitted in accordance with
the requirements for the degree
of Doctor of Philosophy

The University of Leeds
School of Biology
October 2023

I confirm that the work submitted is my own, except where work which has formed part of jointly authored publications has been included. My contribution and the other authors to this work has been explicitly indicated below. I confirm that appropriate credit has been given within the thesis where reference has been made to the work of others.

The work in Chapter 2 of the thesis has appeared in a publication as follows:

> **Slowik, A.R.**, Hesketh, H., Sait, S.M., & De Fine Licht, H.H. (2023). A Rapid Method for Measuring In Vitro Growth in Entomopathogenic Fungi. *Insects, 14*(8), 703. https://doi.org/10.3390/insects14080703
>
> Conceptualization, A.R.S., H.H., S.M.S. and H.H.D.F.L.; methodology, A.R.S. and H.H.D.F.L.; formal analysis, A.R.S..; investigation, A.R.S.; writing—original draft preparation, A.R.S.; writing—review and editing, A.R.S., H.H., S.M.S. and H.H.D.F.L.; supervision, H.H., S.M.S. and H.H.D.F.L.

The work in Chapter 3 of the thesis will be submitted for publication as follows:

> **Slowik, A.R.**, Hesketh, H., Sait, S.M., & De Fine Licht, H.H. Quantification of nutritional niche width in *Metarhizium* with different host ranges.
>
> Conceptualization, A.R.S., H.H., S.M.S. and H.H.D.F.L.; methodology, A.R.S. and H.H.D.F.L.; formal analysis, A.R.S..; investigation, A.R.S.; writing—original draft preparation, A.R.S.; writing—review and editing, A.R.S., H.H., S.M.S. and H.H.D.F.L.; supervision, H.H., S.M.S. and H.H.D.F.L.

The work in Chapter 4 of the thesis is under review for publication as follows:

Slowik, A.R., Hesketh, H., Sait, S.M., & De Fine Licht, H.H. Thermal ecology shapes disease outcomes of entomopathogenic fungi infecting warm-adapted insects. Submitted to *Journal of Invertebrate Pathology*.

A.R.S., S.M.S., H.H. and H.H.D.F.L. conceived the ideas and designed methodology; A.R.S. collected the data; A.R.S. analysed the data; A.R.S., S.M.S., H.H. and H.H.D.F.L led the writing of the manuscript.

This research has received funding from the European Union's Horizon 2020 research and innovation program INSECT DOCTORS under the Marie Skłodowska-Curie grant agreement No. 859850.

Preface

Ecological considerations of thermal and nutritional interactions in *Metarhizium* host range evolution

A multidimensional analysis of niche width in insect-pathogenic fungi

By Anna R. Slowik

This PhD thesis has been submitted as a double doctoral degree to the PhD School of the Faculty of Science, University of Copenhagen, and to the University of Leeds School of Biology. The project work was supervised by Associate Professor Henrik Hjarvard De Fine Licht, Associate Professor Steven Sait, and Dr. Helen Hesketh.

This research has received funding from the European Union's Horizon 2020 research and innovation program INSECT DOCTORS under the Marie Skłodowska-Curie grant agreement No. 859850 and was supported by grants to H. H. De Fine Licht from a Sapere Aude: Independent Research Fund Denmark Starting Grant (No. 8049-00086A), and a Young Researcher Fellowship from the Carlsberg Foundation, Denmark (No. CF20-0609). All experimental work was conducted at the University of Copenhagen, Department of Plant and Environmental Sciences, Section for Organismal Biology, at the University of Leeds, Faculty of Biological Sciences, School of Biology, and the UK Centre for Ecology and Hydrology in Wallingford.

Acknowledgements

First and foremost, I extend my deepest gratitude to my supervisors, Henrik, Steve and Helen, for everything I have learned from them, and whose unwavering support and exceptional guidance have been my north star throughout this journey.

I am deeply grateful to those who have welcomed me into their homes and hearts across Europe, providing me with shelter and incredible company: Sophie & Smila in Nørrebro, Tanya and Themos and all of Rose Dale in Iffley Village, my dear friends Henry and Ieva (and Lyra & Baguira) in Littlemore, and Frank and Charlotte in Østerbro.

I want to thank my dear friends and family for making me a home away from home, especially Nicki and Charlie, Pascal, and Carlotta. Thank you Nicki for letting me keep mealworms in your freezer. Thanks to Pascal for all the Erdingers and for teaching me about *Tenebrio* rearing and pouring plates left-handed. Thanks to Carlotta for the many precious moments together, as well as all the voice notes of support from across many borders.

Tak til Sophie, min punk rock fairy godmother, for den afgørende kulturelle uddannelse.

Thanks to Autumn for always believing in me.

I express my sincere appreciation to the Applied Evolutionary Ecology research group at KU, the Environmental Change Group at Leeds, the student group at UKCEH, and all members of SOBI for the friendships, enriching intellectual engagement, and collaborative atmospheres you've provided. Special acknowledgment is extended to the INSECT DOCTORS PhD cohort, whose friendship, support, and camaraderie have been invaluable. My gratitude is also due to everyone involved in putting (and keeping) this program together, and for providing me with this invaluable opportunity.

Big big ups to my partner in life and love, Ed Spencer, for supporting me and accompanying me through this crazy journey. Thank you for always being there for me.

Thanks to my family for coping without me for three years; to my parents for instilling in me a love of nature and letting me play in the compost pile; to my Mom, who has not only inspired my pursuit of a doctoral degree but has also been my anchor and greatest support in life, you are truly my role model; and to my Dad for first teaching me about bugs and mushrooms and awakening my curiosity to the mysteries of the Universe.

Abstract

Host-pathogen interactions are fundamental to the ecological and evolutionary processes in ecosystems, influencing community dynamics, species distribution, and the evolutionary trajectories of both hosts and pathogens. Such interactions are often dictated by coevolutionary forces that drive pathogens to exhibit specialized host-specific adaptations or generalist strategies encompassing multiple hosts. Entomopathogenic fungi (EPF) serve as key models for studying these interactions, exemplifying different degrees of niche specialization - the extent to which an organism is adapted to specific ecological parameters such as host or environmental conditions - in their ecological functionality. This thesis integrates thermal and nutritional ecology to provide a multidimensional analysis of the environmental niche breadth and host range in *Metarhizium* species, employing experimental and quantitative methods to deepen insights into the ecological dynamics of EPF. The **introductory chapter** reviews current knowledge on the interactions between EPF and their thermal and nutritional environments, focusing on how these interactions influence host range specifically in the genus *Metarhizium*.

In **Chapter 2**, the objective was to develop a rapid, high-throughput method for measuring fungal growth in liquid media cultures using microplates and microspectrophotometry. This method, compared and validated against traditional approaches, enhances the precision and speed in assessing growth patterns among various *Metarhizium* isolates, and offers a high throughput technique for multidimensional niche quantification.

Chapter 3 aimed to quantify the nutritional niches of a specialist and a generalist EPF and determine whether host range correlates with nutritional niche width. It was hypothesized that the nutritional niche width of specialist EPF would be narrower, reflecting their ecological lifestyles. Employing the growth assay from Chapter 2 in conjunction with the Geometric Framework for Nutrition, which generates nutritional landscapes by mapping the effects of various nutrient combinations as response topologies, nutrient profiles were produced for the specialist *Metarhizium acridum* and the more-generalized *Metarhizium*

guizhouense. This approach revealed distinct growth patterns in response to different nutrient availabilities for each fungus. *Metarhizium acridum* demonstrated greater efficiency in nutrient utilization, growing more overall across various conditions, and protein was more of a limiting factor for *M. acridum* at lower concentrations compared to *M. guizhouense*. These findings align with *M. acridum's* ecological role as a specialist pathogen that rapidly infects and proliferates in large protein-rich insect populations. *Metarhizium guizhouense* had a broader nutritional niche and was less sensitive to protein limitation, which reflects its association with carbohydrate-rich plant roots. These findings suggest a relationship between the nutritional niche breadth of these EPF and their ecological host niches.

The **final data chapter** explores thermal ecology, assessing the influence of thermal adaptation on host-pathogen interactions using EPF with different host ranges and the yellow meal worm, *Tenebrio molitor*. Central to this study was the Thermal Mismatch Hypothesis (TMH), which proposes that in host-pathogen interactions there is often a mismatch between the optimal temperatures for the growth and virulence of the pathogen and the optimal temperature for the host's immune response or survival. Experiments conducted across ecologically relevant temperatures aimed to construct thermal performance curves for growth and virulence and identify critical thresholds for these traits. It was found that both EPF species and the host shared a growth optima at 28°C, with the host's growth response to infection mediated by the species of fungus and temperature during sublethal infections. However, *M. brunneum*, the generalist EPF, displayed a broader optimal temperature range for virulence (23–28°C) compared to *M. flavoviride*, the specialist EPF, which had a multiphasic virulence pattern peaking at 18 and 28°C. Contrary to TMH predictions, peak virulence of both fungi occurred at the host's optimal temperature. Furthermore, the thermal growth profile of *M. flavoviride* closely matched its temperature-dependent virulence profile, whereas *M. brunneum's* virulence did not align with its growth across temperatures, indicating that the generalist pathogen may achieve higher virulence even under constrained growth conditions. This investigation uncovers distinct relationships between virulence thermal profiles and individual thermal

profiles for *Metarhizium brunneum* and *M. flavoviride*, corresponding to their respective evolutionary histories and ecological adaptations.

In **Chapter 5**, I discuss how the cumulative insights into the interactions between abiotic factors and host-pathogen dynamics in these experimental chapters, particularly in *Metarhizium* species with varied host ranges, contribute to the fundamental understanding of ecological and evolutionary mechanisms driving host-specialization and environmental adaptation in entomopathogenic fungi. In combination with a general review of the current knowledge of the relationship between thermal and nutritional ecology and host specificity in the fungal genus *Metarhizium*, this thesis presents an integrated approach to understanding the multifaceted adaptations and specializations of *Metarhizium* species, informing both ecological theory and advancing our knowledge of EPF ecological interactions and roles.

Contents

List of figures

List of tables

List of acronyms and abbreviations

ANOVA	Analysis of variance
ARSEF	Agricultural Research Service collection of Entomopathogenic Fungal cultures
°C	Degrees Celsius
C	Carbohydrate
CI	Confidence interval
CTmax	Critical thermal minimum
CTmin	Critical thermal minimum
df	Degrees of freedom
DI	Deionized
EPF	Entomopathogenic fungi
ES	Ecological Stoichiometry
EU	European Union
g	Grams
GFN	Geometric Framework for Nutrition
hrs	Hours
HSD	Honestly Significant Difference
HGT	Horizontal gene transfer
L	Liters
LD	Lethal dose
mg	Milligrams
mL	Milliliters
mm	Millimeters

MYA	Million years ago
N	Nitrogen
NG	Nutritional Geometry
nm	Nanometers
OD	Optical density
P	Protein
RH	Relative humidity
rpm	Revolutions per minute
SDAY/4	1⁄4 Sabouraud Dextrose Yeast Agar
SE	Standard error
spp.	Species
TER	Threshold elemental ratio
TMH	Thermal Mismatch Hypothesis
UK	United Kingdom
µL	Microliters
US	United States
USDA	United States Department of Agriculture
v/v	Volume per volume
w/v	Weight per volume
$\chi 2$	Chi-square

Chapter 1

General introduction

1.1 Chapter outline

Entomopathogenic fungi (EPF), especially within the diverse genus *Metarhizium* Sorokīn (Hypocreales: Clavicipitaceae), are key regulators of natural insect populations and important agents in the biological control of insect pests, offering environmentally friendly alternatives to chemical pesticides (Chandler, 2017; Mantzoukas & Eliopoulos, 2020). Their adaptability and varying host range emphasize the multifaceted interactions between these fungi, their insect hosts, and the surrounding environment (St. Leger & Wang, 2020). This ecological interplay is central to the thesis, as it explores the ecological aspects and evolutionary trajectories that influence the adaptability and host specificity of different *Metarhizium* species.

This thesis explores the multi-faceted ecological interactions that characterize the adaptability and host specificity of *Metarhizium* species. It seeks to unravel the influence of abiotic factors, specifically temperature and nutrition, in mediating these interactions. In this opening chapter, the foundational concepts and overarching themes central to this work are introduced and explored. Initially, I provide an overview of ecological specialization and habitat adaptation in pathogens (section 1.2) and the basis for using EPF as a model for investigating specificity in host-pathogen relationships (1.3). Subsequently I introduce the complexities of interactions between EPF, their insect hosts, and environmental variables (1.4) with particular emphasis on the effects of nutrition (section 1.4.1) and temperature (1.4.2) in these interactions. A detailed description of the study organisms utilized in the experimental chapters is provided in section 1.5, and the chapter concludes with an outline of the thesis plan (section 1.6).

1.2 Ecological specialization and habitat adaptation

Understanding ecological specialization and habitat adaptation is essential for analyzing pathogens' evolution, diversity, and distribution. The ecology of these pathogens drives their specialization in various niches and their ability to parasitize specific ranges and types of hosts (Harvell, 2004; St. Leger & Wang, 2020). Host range, or the number of species a pathogen is capable of infecting, is a simple but fundamental ecological and epidemiological metric in understanding the virluenceof a pathogen and its potential as a biocontrol agent (Brodeur, 2012). The capability of a pathogen to infect a specific host or a range of hosts is determined by a suite of factors central to host-pathogen interaction theory. Primarily, the genetic compatibility between the host's immune responses and the pathogen's virulence genes dictates the outcome of the interaction (Bohannan & Lenski, 2000). Additionally, environmental conditions, host immune responses, pathogen adaptation strategies, and the evolution of resistance mechanisms collectively influence the dynamics of infection (Casadevall & Pirofski, 2001). The pathogen's ability to adhere, invade, and evade host defenses, as well as its transmission strategy, also modulate its host range (Finlay & Falkow, 1997; Ewald, 1983). Level of host specificity is thought to be the consequence of interactive effects between host population dynamics (e.g. host abundance), molecular mechanisms shaping evolutionary processes in the genome (e.g. genome size, sexuality, and molecular correction mechanisms), and ecological and environmental factors (e.g. spatiotemporal overlap of host and pathogen populations), and is the main determinant in important processes of disease ecology like transmission and survival (Sexton *et al.,* 2017; Hajek & Shapiro-Ilan, 2018; Webster *et al.,* 2017; Kelly *et al.,* 2011; Fargues & Remaudiere, 1977; St. Leger & Wang, 2020).

Traditionally, pathogens have been classified as either generalists, capable of infecting a wide range of taxonomically diverse species, or specialists, which are limited in their infective ability to one or a few closely related taxa (Fargues & Remaudiere, 1977). However, there is a distinction between ecological host range, the range of species a pathogen infects under field conditions, and physiological host range, the range a pathogen infects under

optimized conditions using laboratory tests (Hajek & Goettel, 2007). Ecological host range is generally considered to be narrower than the physiological range, because conditions in natural environments are not always conducive to infection. Humidity, temperature, pathogen dose, and host behavior (i.e. for example behavioral fever and diet modification) are all important variables that are optimized under laboratory manipulated infections. As such, these two metrics can be very different, indicating the importance of ecological factors influencing specificity, like environment and species interactions. There are often multiple levels of trophic interaction involved in host-parasite relationships, like in entomopathogenic fungi (EPF), which parasitize insects as well as forming mutualistic symbioses with plants in the rhizosphere (Stone & Bidochka, 2020). Classifying pathogens solely as generalists or specialists is challenged by the existence of those with "transitional" host ranges, exhibiting infective capabilities that are neither strictly specialized nor generalized (Wang *et al.,* 2016).

The delineation between generalists and specialists is often nebulous, despite the ubiquity of these terms in describing species' ecologies. The multifaceted nature of organisms' niches, spread across various axes, complicates these classifications. Niche breadth, representing the extent of a species' niche along various dimensions, e.g. moisture niche breadth and thermal niche breadth, serves as a tangible measure of ecological specialization (Sexton *et al*., 2017). A fundamental question in evolutionary ecology is whether a specialist's adaptation is confined to a specific niche dimension or extends across multiple, and conversely, the extent of a generalist's adaptability. In other words, "Is a specialist a specialist in all niche dimensions?" (Bebber & Chaloner, 2022). Yet, while ample studies and models have explored niche breadth evolution on a singular axis, the interconnection between multiple niche dimensions remains relatively understudied (Bebber & Chaloner, 2022).

Carscadden *et al.* (2020) investigated these cross-niche axis relationships in plant-pathogenic fungi, where they found correlations among niche axes are tied to the interplay between climatic and edaphic variables. These findings challenge the notion of universal generalists or specialists, unveiling species capable of being 'masters of some, jacks of others' (Bebber & Chaloner; 2022).

They propose that co-varying environmental fluctuations in combination with functional limitations (e.g. genetic ability to adapt inherent to the genome) underpin niche breadth correlations (Carscadden *et al.,* 2020). They suggested correlations in the variability of environmental conditions, rather than their absolute levels, are shaping these correlations (Carscadden *et al.,* 2020). For example, a study of North American basidiomycetes found a strong positive correlation across niche axes between temperature and moisture, which was attributed to similar variation in temperature and moisture in the soil environment (Maynard *et al.,* 2019).

The fundamental question of how ecological and evolutionary interactions between organisms drive specialization and generalization has inspired many biological studies (Futuyma & Moreno, 1988). Host range is determined by both extrinsic factors related to the pathogen, as in its ecology and epidemiology, and intrinsic factors, like genetic traits that influence pathogen fitness in various hosts (Hu *et al.,* 2014). Extrinsic factors encompass the ecological and epidemiological attributes of the pathogen, including the environment it inhabits, its transmission dynamics, and the interactions with various host species (Hu *et al.,* 2014). These factors are significantly influenced by environmental conditions, host availability, and the spatial-temporal distribution of hosts, which collectively delineate the boundaries of a pathogen's host range (Hajek & Shapiro-Ilan, 2018; Fargues & Remaudiere, 1977). On the other hand, intrinsic factors stem from the genetic and physiological attributes of the pathogen. Genetic traits, including those that confer resistance to host immune responses, adaptation to different environmental conditions, or the ability to exploit host resources, play a pivotal role in determining a pathogen's fitness across different host species (Harvell, 2004). These genetic traits, in turn, are shaped by evolutionary processes like natural selection, mutation, and genetic drift, conferring the pathogen's ability to infect, proliferate, and transmit among specific hosts (Harvell, 2004).

Previous explanations of host range evolution have focused primarily on the intrinsic, genetic components at play (Wang *et al.,* 2016; Hu *et al.,* 2014), but it is the interplay between genetic mechanisms interacting with ecological factors that determine evolutionary outcomes (Futuyma & Moreno, 1988; Araújo &

Hughes, 2016). The importance of ecological factors in determining host range becomes apparent when we consider that while most pathogens are classified as generalists, it is widely regarded that evolution often favor specialization (Woolhouse *et al.,* 2001; McDonald & Linde, 2002). This theory is based on differential fitness tradeoffs and competition between generalists and specialists for host resources – as the pathogen's main environment is the host, selection for a variety of hosts would limit pathogen fitness in any one specific host, and generalists would be outcompeted by specialists in any one specific host (Futuyma & Moreno, 1988). Such a scenario is exemplified by a pathogen that can infect multiple species but is less effective in causing disease or reproducing within any given specific host compared to a pathogen that has adapted to primarily infect a single species, highlighting the trade-off between host range and virulence or replication efficiency.

Furthermore, tradeoffs in virulence play a critical role in shaping these dynamics. Virulence can be defined as the degree of damage a pathogen causes to its host, and it is closely tied to the pathogen's evolutionary strategy. Specialists, adapted to a narrow host range, may evolve higher virulence towards their specific hosts due to co-evolutionary dynamics, optimizing their reproductive success within these hosts (Råberg & Stjernman, 2012). In contrast, generalists may exhibit lower virulence across a broader host range to maintain a wider infectious profile, thus balancing transmission opportunities with the mortality risk to their host pool (Day, 2001). The tradeoff between host range and virulence is exemplified by pathogens that can infect multiple species but may be less effective in causing disease or reproducing within any given specific host compared to a pathogen that has adapted to primarily infect a single species (Råberg & Stjernman, 2012).

Analysis of across-host fitness trade-offs mediating host range expansion has received much attention due to the applied relevance to disease emergence (host shifts) and biocontrol applications (St. Leger & Wang, 2020; Asplen *et al.,* 2012; Joshi & Thompson, 1995; Boomsma *et al.,* 2014). Most theoretical and experimental evidence is derived from research examining host-pathogen interactions in homogenous environments, however, and fails to account for the

multifunctional lifestyles and heterogenous conditions EPF in particular will encounter throughout their varied life histories. The limited understanding of how environment modulates host range in EPF indicates a need for more comprehensive research that incorporates ecological perspectives.

From here, I review the existing knowledge on the interactions between EPF and their varied thermal and nutritional environments, and examine their influence on host range. I focus on species in the fungal genus *Metarhizium*, which provides a model that offers a detailed look into the interplay of these factors, helping us to understand the broader implications for pathogenic adaptation and diversity.

1.3 Entomopathogenic fungi as a model for investigating host specificity

Many examples of host-pathogen coevolution arise from the interactions between insects and fungi, which collectively account for 80% of all known extant species, and 25% of Earth's biomass respectively (Larsen *et al.,* 2017). An incredible variety of ecological relationships formed as these organisms passed through evolutionary deep time together: mutualisms and symbioses, like fungi as obligate food sources for fungus farming ants, and more antagonistic relationships: fungal parasitism of insects (Humber, 2008). In insects, fungi are the most common agents of disease, and entomopathogenicity has evolved independently and repeatedly in every major phylum of the Fungal Kingdom (Araújo & Hughes, 2016; Humber, 2008). Plants also played a role in evolutionary dynamics: insect-derived nitrogen transfer to plants by endophytic insect-pathogen fungi is now understood to be ubiquitous in soil ecosystems and an important part of the Soil Nitrogen Cycle (Behie & Bidochka, 2014). Humber captures the sentiment of the diverse and unpredictable ecological nature of EPF in his comment regarding their evolution: "the great 'Perpetual Fungal Banquet and Heterotrophic Ball' continues: the rich assortment of dishes available may change or substitutions made with little notice; in the ball-room the styles of music being played will keep changing, and dancers may change partners at any time" (Humber, 2008).

Research on the evolution of host range in EPF has been particularly focused on the biochemical and molecular basis for toxic secondary metabolites produced by EPF that allow them to overcome insect immunity and kill their hosts, as this ability is the basis for their application as microbial control agents (Wang *et al.,* 2019). Understanding the genetic basis for pathogenicity in EPF has also helped to address fundamental questions in evolution and ecology involving host-pathogen co-evolution, host preference and host shifts, as well as provide insights into the mechanisms of speciation (Wang *et al.,* 2016; Hu *et al.,* 2014). A significant amount of this understanding is attributable to research using the experimentally tractable hypocrealean genus *Metarhizium* (family Clavicipitaceae), which has arisen as an exemplar model for answering such questions. The *Metarhizium* genus exhibits very different host ranges between closely taxonomically related species (Wang *et al.,* 2016). Genetic research on *Metarhizium* has provided a number of insights into the intrinsic determinants of host range, as well as raised extrinsic questions. Hu *et al.* (2014) found that in each *Metarhizium* species analyzed, over half of the species-specific genes lack conserved domains (St. Leger & Wang, 2020). This suggests there are unknown ecological interactions involving these fungi.

Metarhizium, a cosmopolitan insect-pathogenic fungus with diverse lifestyles, ranks together with *Beauveria* as the most extensively characterized genera of insect-pathogenic fungi (Roberts & St. Leger, 2004). It is thought to have evolved between 88-114 MYA from grass endophytes after the acquisition of insect pathogenesis genes, and subsequently diverged based on insect host range into generalists and specialists 30-50 MYA (Gao *et al.,* 2011). At least seventy species of *Metarhizium* have been resolved using multilocus analyses and it is unknown and unestimated how many species exist (Mongkolsamrit *et al.,* 2020). An endophytic root symbiont, *Metarhizium* has come to inhabit soil communities from the artic to the tropics in forests, swamps, savannahs, coastal zones and deserts, as one of the most abundant fungi isolated from soils at 10^6 conidia per gram in grasslands (Roberts & St. Leger, 2004; Moonjely *et al.,* 2019; Vänninen, 1996).

Understanding the life cycle of *Metarhizium* spp. is crucial to grasping its ecological versatility and host-pathogen dynamics. Most *Metarhizium* species reproduce clonally (Kepler *et al.,* 2014). The lifecycle begins with the sporulation phase, where *Metarhizium* produces conidia, which are asexual spores. The conidia are highly resistant to environmental stress and can persist in the soil for extended periods (Lovett & St. Leger, 2015). They can be dispersed by wind, water, or contact with other organisms, such as insects, which facilitates their spread to new hosts and environments. When conidia come into contact with a suitable insect host, they adhere to the insect cuticle (Figure 1.1). Adhesion is facilitated by hydrophobic interactions and possibly by specific adhesive compounds produced by the spores upon sensing an appropriate host surface, which is conferred by the waxy surface and chitinous cues (St. Leger, 1995). Upon adhering to the host, the conidia germinate and form a germ tube. The germ tube grows and differentiates into a specialized infection structure called an appressorium, which exerts mechanical pressure and releases enzymes that degrade the insect's cuticle, primarily chitinase and protease, allowing the fungus to penetrate the host's body (St. Leger, 1995; Gao *et al.,* 2011). Once inside the insect, the fungus transitions into a yeast-like phase, producing blastospores that proliferate within the insect hemocoel. The fungus utilizes the nutrients from the insect's body, avoiding and suppressing the host's immune response (Li & Xia*,* 2022). This internal growth phase is characterized by extensive mycelial growth and the production of secondary metabolites, like destruxins, including toxins that contribute to death of the insect (Wang *et al.,* 2012). After the insect host succumbs to the infection, the fungal cells return to filamentous form and emerges from the cadaver. It then sporulates, producing a new generation of conidia which can infect a new insect host, enter a symbiotic relationship with plants, or enter the saprotrophic lifecycle wherein hyphae consume organic material (St. Leger & Wang, 2020; Sheng *et al.,* 2022). This saprophytic phase allows the fungus to persist in the environment between infections of living insect hosts, completing its lifecycle from pathogen to saprophyte and back as it encounters suitable hosts.

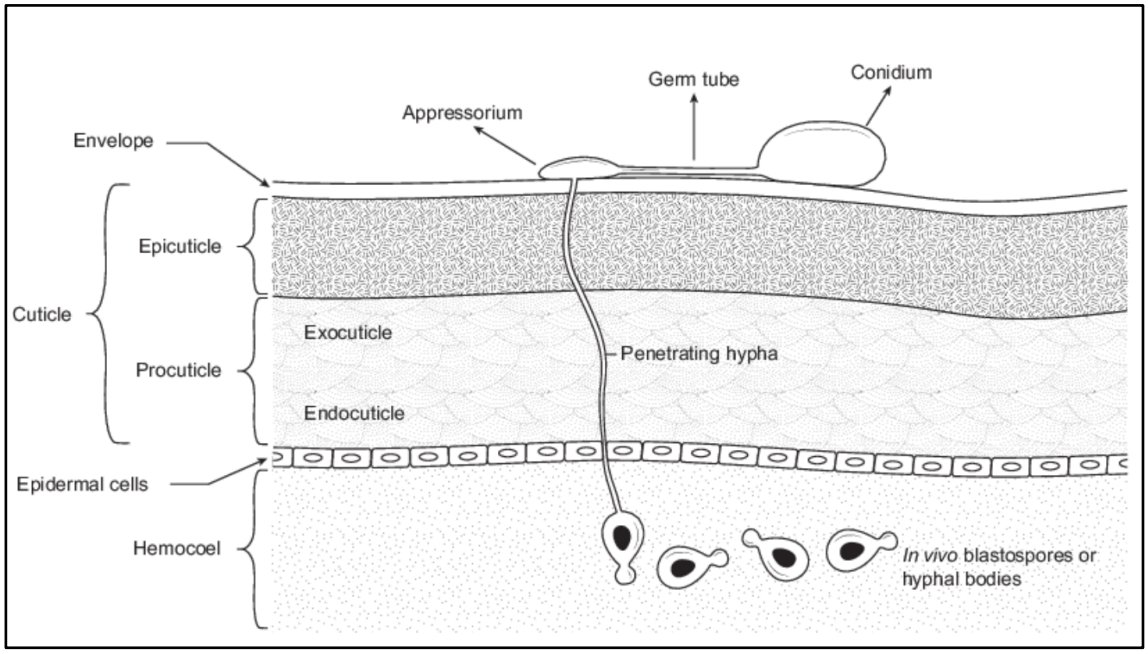

Figure 1.1 How entomopathogenic fungi grow: Colonization process of an insect host by EPF adapted from Vega *et al.,* (2009). Upon encountering the host cuticle, the fungus adheres, germinates, and determines host appropriateness through sensing physical and chemical cues. The fungal spore then begins to penetrate the cuticle and form a germ tube. The cuticle is degraded with cuticle-degrading enzymes and an appressorium is formed, which delivers mechanical pressure. After penetration, hyphae colonize the haemocoel, forming *in vivo* blastospores and hyphal bodies. The fungus then competes for nutrients in the insect body while avoiding the insect immune response, which includes anti-microbial proteins and circulating cells (haemocytes) capable of phagocytosis and encapsulation. Following complete colonization of the insect body, the fungus emerges from the mycosed cadaver and sporulates.

While less common, some specialist *Metarhizium* species are known to undergo sexual reproduction. The sexual phase involves the formation of fruiting bodies that produce sexual spores (ascospores), contributing to genetic recombination and diversity. These species are known to have narrow host ranges and are geographically restricted (Mongkolsamrit *et al.,* 2020; Kepler *et al.,* 2016).

Apart from being pathogens to insects, some *Metarhizium* species can also enter into a mutualistic endophytic relationship with plants (Stone & Bidochka, 2020; Sheng *et al.,* 2022). As endophytes, they colonize plant roots as well as other tissues and provide benefits such as increased nutrient uptake and resistance to plant pathogens or pests (Alves *et al.,* 2021; Ahmad *et al.,* 2020). These commensal or mutualistic symbiotic relationships broaden the ecological niche of *Metarhizium* species and contributes to their persistence in various ecosystems (Shang & Song, 2023).

Capable of infecting hundreds of insect species as a genus, as well as arachnids, nematodes and lizards, *Metarhizium* spp. play a major role in ecosystems and are used to great success as a biological control agent (St. Leger & Wang, 2020). Perhaps one of the first biocontrol agents, *Metarhizium anisopliae* was used to combat the wheat cockchafer *Anisoplia austriaca* by Elie Metchnickoff in 1879, and now boasts one of the most successful biocontrol programs in the world, used to treat two million hectares of sugar cane each year for spittlebugs in Brazil (St. Leger & Wang, 2020). Use of insect-pathogenic fungi as biocontrol agents is only expected to increase due to interest in chemical pesticide alternatives.

1.4 Insect-entomopathogenic fungi-environment interactions

In host-pathogen relationships, the phenotype of either organism is determined by the interaction between its genotype (G), the environment which it exists (E), and the host or pathogen's genotype (G): G X G X E interaction (Thomas & Blanford, 2003). For the purpose of this review, I will focus on the environmental and ecological factors of temperature and nutrition. While temperature is an abiotic, environmental variable, it is important to note that in the case of parasitism, nutrition is both an abiotic and an interactive, biotic, ecological factor (Bernot & Poulin, 2018). Nutrition can be considered an environmental factor in that diet is at its most basic a combination of various inert elements at different ratios. In a host-pathogen relationship, though, nutrition for the pathogen is an interaction between the pathogen's own nutritional and physiological processes

and the host's, as the host is the essential nutritive source (Bernot & Poulin, 2018).

Entomopathogenic fungi in particular are exposed to a broad and diverse range of environmental conditions throughout their complex lifecycles and due to complex ecological systems. The multifunctional lifestyles of *Metarhizium* compose a tripartite association of saprotrophism, endophytism, and insect pathogenesis (Stone & Bidochka, 2020). They are exposed to the stress of the rhizosphere as root endophytes, growing within or between cortical cells in their plant symbionts, are exposed to oxidative stress under the sun, and navigate their way through the various tissues once inside their insect host, evading potentially lethal immune defenses, and behavioral defenses such as induced fever (Behie & Bidochka, 2014; Ouedraogo *et al.,* 2003). As such, EPF are adapted to withstand a range of environmental stresses and have an extremely flexible metabolism (Lovett & St. Leger, 2015).

Insect-pathogenic fungi are known to have a high degree of phenotypic plasticity, which can be adaptive or non-adaptive, depending on whether the phenotypic response results in advantageous fitness outcomes (Rangel *et al.,* 2015; Ghalambor *et al.,* 2007; Acasuso-Rivero *et al.,* 2019). Pathogenic potential and thermal tolerance of conidia of insect pathogenic fungi has been shown to be highly dependent on environmental conditions during mycelial growth in studies producing conidia at different temperatures and on different substrates (Rangel *et al.,* 2015). Conidia produced by *M. robertsii* mycelia from stressed conditions, such as poor nutrients and heat shock, have very different phenotypes than those produced under ambient environmental conditions (Rangel *et al.,* 2015).

There are a variety of different lifestyle options and ecologies represented in the *Metarhizium* genus. While some *Metarhzium* species are important root symbionts, a significant proportion are not known to be symbiotic (St. Leger & Wang, 2020). Those that are symbiotic are typically generalist pathogens, the plant interaction life-style being their primary source of nutrition (St. Leger & Wang, 2020). Specialist species, on the other hand, rely on abundant populations of above ground insects like locusts and cockroaches (St. Leger & Wang, 2020).

This pattern is also reflected in the reproductive strategy of different *Metarhizium* species. *Metarhizium* species reproduce both clonally and sexually. Generalists have primarily clonal reproduction while some specialist species, such as *Metarhizium acridum*, show evidence for more frequent sexual reproduction (Nielsen *et al.,* 2021). The sex life of *Metarhizium* is enigmatic, as the requirements for sexual reproduction are unknown. Molecular phylogenetic analyses reveal sexually reproducing species are interspersed among clades of isolates assumed to be asexual (Kepler *et al.,* 2014). It is thought sexual reproduction is limited to a narrow range of host insects in geographically isolated areas, while asexual forms cover a broad spectrum of niches across extensive geographical distributions (Kepler *et al.,* 2016).

In general, host-specificity is linked to genome size: specialist species have smaller and more compacted genomes than generalists, and have a larger number of genes under selection that are rapidly evolving (Hu *et al.,* 2014; St. Leger & Wang, 2020). This is attributed to existing protein sequences being involved in rapid evolution in specialists, compared to generalists' large genomes undergoing extensive gene duplication (Hu *et al.,* 2014). Also unsurprisingly, generalists produce more enzymes associated with pathogenesis, as generalist pathogens employ a larger enzymatic "arsenal" suitable for attacking a greater number of species (Hu *et al.,* 2014).

1.4.1 Effects of nutrition on host-pathogen interactions

From an ecological perspective, specialist and generalist *Metarhizium* species have essentially different nutritional lifestyles and mechanisms for accessing nutrients. Specifically, generalist *Metarhizium* species are thought to form relationships with plants in the rhizosphere, while specialist species are limited to foliar insects (St. Leger & Wang, 2020). In forming multiple associations with host species, generalist pathogens will encounter a greater degree of variation of nutritional compositions and ratios, while host-specific pathogens may only have a limited diet with a more uniform nutritional composition. It follows that this fundamental difference in nutritional lifestyles may convey different nutritional requirements and optimal profiles, a question aptly addressed by the theoretical

framework Geometric Stoichiometry (GS) which integrates Ecological Stoichiometry (ES) and the Geometric Framework for Nutrition (GFN) (Simpson & Raubenheimer, 2012). Ecological Stoichiometry is based on the basic hypothesis that for every organism there is an optimal diet which will maximize performance in different areas of life history, and different organisms are better or worse at accessing limiting nutrients as well as storing them for use during periods of scarcity (Sterner & Elser, 2017; Sanders & Taylor, 2018). The Geometric Framework for Nutrition is a model that provides an approach to understanding how organisms make trade-offs in nutrient allocation, emphasizing the interaction between multiple nutrients or dietary components. This framework considers the balance and interaction of multiple nutrients or dietary components using a graphical approach, plotting two or more nutrients against each other to visualize how dietary composition affects performance of different traits or biological functions (Figure 1.2) (Simpson & Raubenheimer, 2012). This visualization helps identify the optimal nutritional balance and demonstrates how nutrients interact.

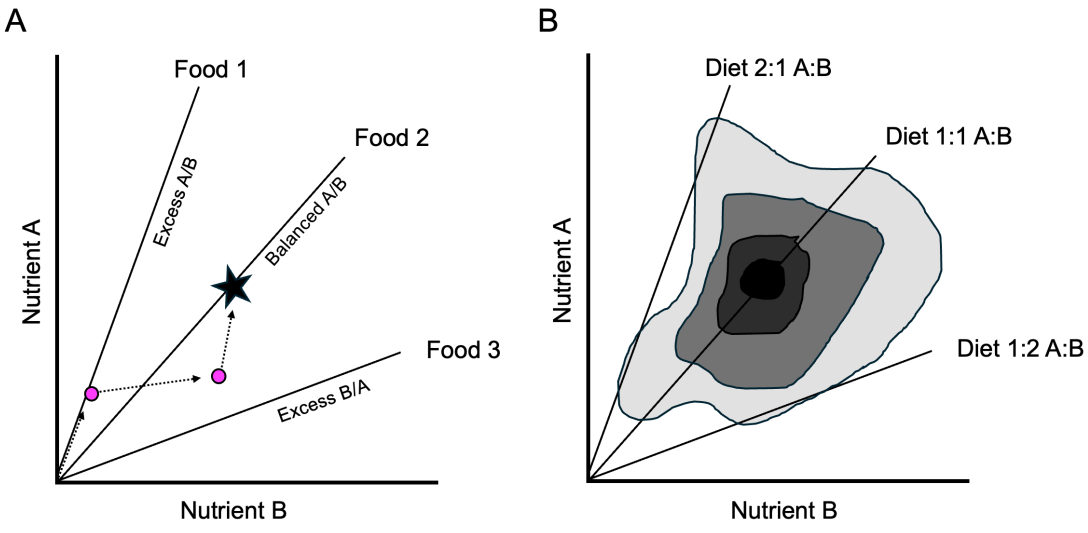

Figure 1.2 The Geometric Framework for Nutrition. Panel **(A)** illustrates the core concept of the Geometric Framework for Nutrition. Nutrient A and Nutrient B are plotted on the axes, representing two essential dietary components. The star symbol denotes the “Intake Target,” which is the optimal ratio of Nutrients A and

B for the organism's health and growth. Radial lines from the origin to the points labeled "Food 1", "Food 2", and "Food 3" depict the nutrient ratios of these food sources. Food 1 has a balanced ratio of Nutrient A to Nutrient B, allowing direct alignment with the Intake Target. Foods 2 and 3 are imbalanced, having excesses of Nutrient A/B and B/A, respectively, and do not align directly with the Intake Target. The dotted arrows show the theoretical dietary path an organism could take by combining these foods to achieve the optimal nutrient balance, indicated by the transition from Food 3 to the Intake Target via a mixed intake path. (Modified from Simpson *et al.,* 2017). Panel **(B)** provides a graphical representation of a hypothetical organism's performance when fed artificial experimental diets at specific ratios of Nutrient A to Nutrient B. The shaded contours map out the organism's performance outcomes, with darker areas indicating higher performance levels and allowing visualization of nutritional optima.

Building on these principles, the integration of Nutritional Geometry (NG) with ES through the concept of Geometric Stoichiometry offers a more comprehensive understanding of nutritional ecology. The concept of a nutritional optimum that optimizes the performance of traits of interest in an organism culminated from advances in nutritional ecology theory which integrated Raubenheimer and Simpson's theoretical framework of Nutritional Geometry (NG) with that of Sterner and Elser's Ecological Stoichiometry (Anderson *et al.,* 2020). In the new framework of Geometric Stoichiometry, the equations used to balance elemental ratios in ES are extended to include core concepts in NG, mainly that of macromolecules (i.e. proteins and lipids) as nutritional currencies and the influence of organismal behavior, like diet modification, which works to balance nutrient deficits and surplus (Anderson *et al.,* 2020).

Most research in nutritional ecology has focused on the aspect of limiting nutrients determining fitness outcomes, but recently the idea of excess nutrients imposing fitness costs and impacting performance and growth has been proposed (Boersma & Elser, 2006). The Threshold Elemental Ratio's (TERs)

hypothesis extends this concept, suggesting a hump-shaped relationship between diet and performance due to the energy costs associated with excreting excess nutrients (Boersma & Elser, 2006). In this sense there really can be “too much of a good thing”, because there is energy required to remove the nutrients that are in excess. The GFN can be used to test the TERs hypothesis, and is also useful for visualizing niche breadth (Figure 1.2 B).

Looking at the TERs hypothesis from a host-parasite perspective adds another level of complexity, because the host is the essential diet for the parasite. This interaction between individual nutritional requirements and nutritional optima of host and pathogen, which may or may not overlap, has ecological and evolutionary consequences for disease outcomes and pathogen performance. Povey *et al.* (2013) found insects engage in diet-modifying behavior in response to fungal infections in an effort to recoup specific resources involved in mounting effective resistance, and also by balancing their intake of essential nutrients, which can impact defensive ability. I suggest this could also be a reaction to deprive the pathogen of essential nutrients required for growth.

1.4.1.1 The relationship between entomopathogenic fungi nutritional requirements and host specificity

While the nutritional ecology of EPF is relatively understudied, there has been ample research investigating virulence, germination, conidial yield, and growth in commercially important EPF species on different media as a proxy for host tissues (Li & Holdom, 1995). Safavi *et. al.* found *M. anisopliae* grew best in high-C:N ratio agar media (75:1) compared to two other ratios (35:1 and 10:1), but with low conidial yield (Safavi *et al.,* 2007). Conidial yield was found to be greatest at lower C:N ratio medias, with 35:1 producing the most conidia (Safavi *et al.,* 2007). A study by Kamp & Bidochka showed similar results, but found the greatest C:N ratio for conidial production to be 10:1 (Kamp & Bidochka, 2002). This indicates resource investment into spore production has the greatest fitness payoffs when EPF are nutritionally challenged (2002). Vega *et. al.* (2003) showed the same results at a 10:1 C:N ratio, but in liquid media (Vega *et al.,* 2003)

The source of nutrients also affects fungal performance (measured as spore germination, hyphal growth, and sporulation) as different types of carbon are more or less bioavailable and nutritionally appropriate for EPF (Sun & Liu, 2006). Sun and Liu evaluated *M. anisopliae* growth with 33 different carbon sources and 11 EPF isolates and found some isolates of the same species differed in their ability to utilize different carbon sources, suggesting fungal nutritional requirements might be strain dependent (2006). Differences among isolates varied with the geographical location and host from which the strain was isolated (Sun & Liu, 2006).

1.4.2 Effects of temperature on host-pathogen interactions

Temperature as an environmental factor affecting performance in organisms is well-studied and considered to have a crucial role in mediating outcomes in host-pathogen interactions (Thomas & Blanford, 2003). In ectotherms, such as fungi and insects, thermal sensitivity, or performance over a range of different temperatures, has been shown to have a nonlinear asymmetric curve defining the relationship between performance and temperature (Figure 1.3) (Thomas & Blanford, 2003). This can be summarized as performance increasing up to an optimal temperature, after which performance decreases dramatically. Performance outcomes in host-pathogen interactions is a composite of the outcome of the interaction of the individual thermal performance curves of both organisms in the relationship. This adds complexity to possible outcomes: the two thermal profiles may overlap such that no effect is seen relative to temperature, or alternatively they differ in thermal optima, in which case temperature could have a substantial effect on disease outcomes (Thomas & Blanford, 2003).

The Thermal Mismatch Hypothesis (TMH) expands this narrative, positing that scenarios where hosts, especially those adapted to specific temperature ranges, find themselves vulnerable when environmental temperatures move away from their optimal range (Rohr & Cohen, 2020). In such instances, pathogens, often characterized by broader thermal optima, may have an advantage, as their virulence is accentuated by the host's thermal vulnerability (Rohr & Cohen, 2020). Support for the TMH isn't universal but is notably

pronounced in certain wildlife populations and specific host-pathogen pairs (Sun *et al.*, 2023; Cohen *et al.,* 2020). For instance, pathogens parasitizing warm-adapted hosts have displayed enhanced virulence in colder climates (Rohr & Cohen, 2020). There are three foundational assumptions underpinning the TMH. Firstly, the thermal breadth of parasites is generally broader than that of their host, particularly when environmental conditions vary (Rohr *et al.,* 2018). Secondly, there is a localized thermal adaptation of both hosts and parasites (Sternberg & Thomas, 2014). Each organism is adapted to its native thermal environment, a specialization that can either be an asset or a vulnerability depending on changing climatic conditions. The third assumption originates in the principles of population ecology: a critical threshold density of hosts is necessary to sustain parasite populations (Lloyd-Smith *et al.,* 2005).

The TMH illustrates scenarios where environmental conditions deviate from the typical thermal experiences of hosts and parasites. In these altered thermal environments, parasites are predicted to outcompete their hosts and infection rates and virulence are increased (Rohr & Cohen, 2020). Empirical support for the TMH is robust across wildlife populations (Cohen *et al.,* 2020). In the world of amphibians, particularly, the TMH has offered compelling insights, explaining the dynamics of declines and infections (Cohen *et al*., 2020).

Despite its empirical support, the TMH is not without challenges. Certain host-pathogen interactions reveal anomalies, where the expected outcomes based on thermal optima deviations are not observed. For example, in a zooplankton–fungus (*Daphnia dentifera–Metschnikowia bicuspidata*) disease system, Sun *et al.* observed that warmer temperatures can lead to strengthened physical barriers against infections in hosts but also weaken their cellular immune responses (2023). These exceptions pose questions on the universal applicability of TMH and beckon a deeper exploration to understand the underlying factors that might mediate such outcomes.

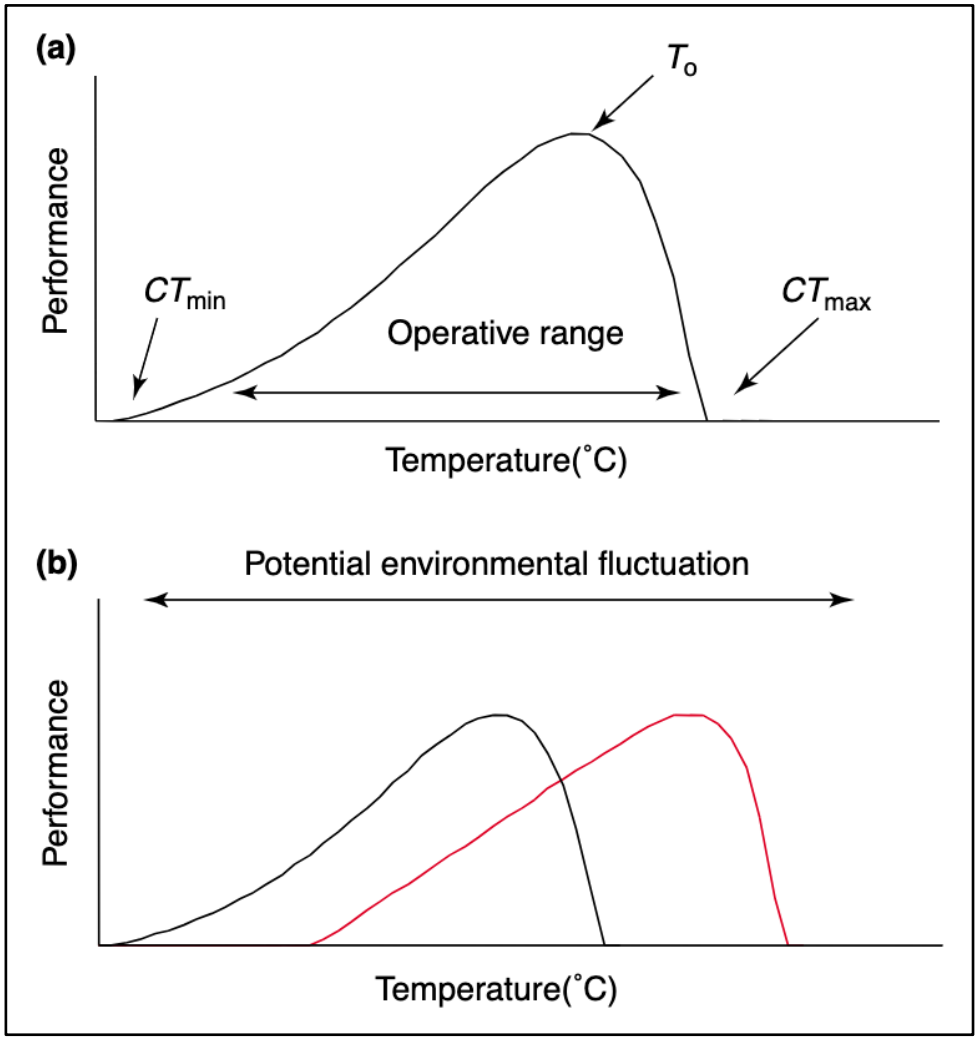

Figure 1.3 Graphical representation of ectotherm performance across temperatures **(a)**, and hypothetical interactions between thermal profiles of a host and parasite **(b)**. Adapted from "Thermal biology in insect-parasite interactions" (Thomas & Blanford, 2003). In (a), the optimal temperature for performance of a given trait (e.g. pathogen growth) for an organism is at point *To*, with critical thermal minimum and maximum at points *CTmin* and *CTmax*, respectively. A host-parasite relationship might have superimposing thermal profiles, in which case there would be no effect from temperature on performance outcomes for either symbiont. Figure 1.3(b) illustrates a hypothetical interaction between the thermal profiles of a host (red curve) and parasite (black curve) in which thermal profiles are different, showing separation. Temperature would have a strong effect on this relationship, as the thermal optima are separated. In this scenario,

at higher temperatures, growth of the pathogen would be limited and the performance of the host would be favored.

1.4.2.1 The relationship between entomopathogenic fungi thermal requirements and host specificity

Temperature can affect germination, growth, and virulence in insect-pathogenic fungi, and is a central factor determining the efficacy of their use in biocontrol (Keyser *et al.,* 2014). *Metarhizium* species have been shown to be very sensitive to changes in environmental and host body temperature in ticks (Polar *et al.,* 2005). While no study specifically addresses EPF thermotolerance in relation to host range, numerous studies have investigated the performance of *Metarhizium* species across thermal gradients and under thermal stress (Keyser *et al.,* 2014; (Polar *et al.,* 2005; Fernandes *et al.,* 2008; Ouedraogo *et al.,* 1997; Hallsworth & Megan, 1999; Rangel *et al.,* 2010).

Due to its potential as biocontrol agent, thermal death point has been determined for numerous *Metarhizium anisopliae* strains isolated from around the world from hemipterans, arthropods, coleopterans and hymenopterans. Results from these studies show thermal sensitivity in *M. anisopliae* varies from 35–60°C (Fernandes *et al.,* 2010; Zimmerman, 1982; Herlinda *et al.,* 2018). Interestingly, thermal tolerance of *M. anisopliae* is not necessarily correlated with geographic location (Bidochka & Small, 2005) but rather is associated with interspecific variation within the fungal species (Li & Feng, 2009; Constanski *et al.*, 2011), as well as the host it was isolated from, as the selective pressures on the host insects and fungal adaptability are related to the intraspecific strain characteristics of the fungi (Scully & Bidochka, 2005).

Among different species, phylogeography plays a more determining role in thermal tolerance of EPF, but only for cold activity (Fernandes *et al.,* 2008). No correlation between heat tolerance and latitude, or distance from the equator, was found in a study of thermotolerance for 60 EPF isolates by Fernandes *et. al.* (2008). Understanding the effect of transitory thermal stress on host and pathogen performance is also important in host- pathogen interactions. Transitory

stress differs from simple thermal stress in that they are temporary. Temporary thermal stressors, e.g. exposure to hot and cold “shocks”, are an intrinsic element of natural systems, and can produce unexpected and complex outcomes in pathogen performance. When exposed to heat stress for short periods, *Metarhizium* species have been found to experience a phase of growth inhibition thought to be a “re-tooling” period for recovery from heat damage (Keyser *et al.,* 2014). This is in contrast to mycelial reaction to cold shocks, where reactivation of mycelial growth after cold exposure is immediate upon returning to a growth-appropriate temperature (Keyser *et al.,* 2014).

1.5 Model organisms used in this study

1.5.1 *Metarhizium* spp.

In this thesis, I explore various *Metarhizium* species, selected for their distinct ecological and evolutionary characteristics that offer a diverse perspective on adaptability and host interactions. These species are ideal for examining my chosen parameters: growth and survival of the insect after infection. Growth, measured as the rate of fungal expansion and mycelial formation, and survival, observed as host mortality rates post-infection, are critical indicators of fungal virulence. *Virulence*, in the context of entomopathogenic fungi, refers to the degree to which the fungus can cause disease in its host, often measured by its lethality or the speed at which it incapacitates the host (Poulin & Combs, 1999). Virulence is a multifaceted characteristic that includes the fungus’s ability to infect, grow within, and ultimately kill its insect host. Key components of virulence include: aggressiveness or infection efficiency – how effectively the fungus can invade and establish itself in a host; growth and colonization (replication) – once inside, virulence encompasses the fungus’s ability to grow and spread within the host, utilizing the host’s resources; mortality induction and toxin production – the speed and efficiency with which the fungus can kill the host as well as the potency and quantity of toxins produced (Casadevall & Pirofski, 2001; Casadevall, 2007), *Pathogenicity,* on the other hand, refers to the ability of the fungus to infect and

cause disease in a host (Poulin & Combs, 1999). These concepts are directly linked to the ecological and evolutionary traits of *Metarhizium* species.

The phylogenetic relationships within the genus *Metarhizium* are essential to understand the evolutionary paths and ecological roles of different species (Figure 1.4). The distinct evolutionary trajectories of these species are particularly marked by their association with, or exclusion from, the PARB clade, a subset of the *Metarhizium anisopliae* complex, which includes broadly infective generalist species (Rehner & Kepler, 2017). Species within the PARB clade, comprised of *M. pinghaense*, *M. anisopliae*, *M. robertsii*, and *M. brunneum*, exhibit remarkable adaptability attributed to horizontal gene transfer (HGT) event that is thought to have conferred them with broadly infective virulence genes, expanding their host range and pathogenic potential (Zhang *et al.,* 2019). HGT can serve as a rapid adaptation mechanism, especially in microbial species (Woods *et al.,* 2020). Within the PARB clade, several instances of HGT might have played pivotal roles in determining host range and ecological niche adaptation. Older HGT events have introduced genes that assist in breaching insect cuticles, a crucial step in the infection process (Zhang *et al.,* 2019). The origin of these genes from soil bacteria suggests a soil-based ancestral ecological niche for these fungi (St. Leger & Wang, 2020). However, more recent HGTs have incorporated genes from both soil-dwelling and insect-dwelling bacteria, indicating an ongoing ecological overlap and continuous adaptation (Zhang *et al.,* 2019).

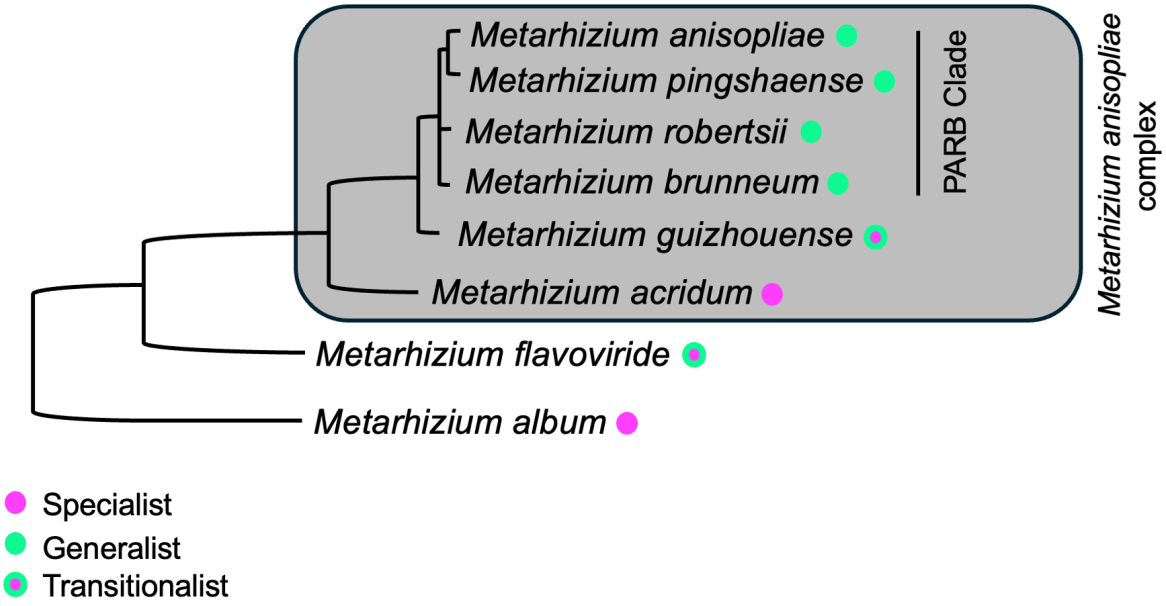

Figure 1.4 *Metarhizium* phylogeny (modified from Kumar *et al.,* 2021).

Conversely, species outside the PARB clade display a different evolutionary and ecological narrative. Their adaptational scope is relatively narrowed, confined to specific ecological niches and host ranges (St. Leger & Wang, 2020). Their exclusion from the clade's genetic diversity and HGT dynamics underscores a contrast in ecological distribution and adaptational capabilities. Together, the comparative analysis of these *Metarhizium* species unfolds a rich tapestry of evolutionary and ecological insights, essential for understanding their roles in ecosystems.

Here I offer an overview of the four species used in experimental chapters of this thesis. ***Metarhizium acridum*** ((Driver & Milner) J.F. Bisch., Rehner & Humber) (Hypocreales: Clavicipitaceae) stands out as a specialist, known to parasitize Orthopterans, or grasshoppers, locusts, and crickets (Hu *et al.,* 2014). Its evolutionary trajectory has likely been driven by the pressures of targeting specific foliar hosts (St. Leger & Wang, 2020).

I also include ***Metarhizium guizhouense*** (Chen & Guo) (Hypocreales: Clavicipitaceae) and ***Metarhizium flavoviride*** (Gams & Rozsypal) (Hypocreales:

Clavicipitaceae), both of which can be categorized as transitional species. Their evolutionary histories hint at an adaptation towards a broader host range, primarily encompassing lepidopterans and coleopterans, although they lack the broad infective capability of generalist species in the PARB clade. It is important to consider that the classification of a host range as either narrow or broad is context-dependent, varying according to the species under comparison; consequently, both *Metarhizium guizhouense* and *Metarhizium flavoviride* have been characterized as either specialists or generalists in different investigative contexts (see i.e. Mongkolsamrit *et al.,* 2020 and Moonjely & Bidochka, 2019).

Lastly, ***Metarhizium brunneum*** (Petch) (Hypocreales: Clavicipitaceae) serves as a powerful example of the remarkable adaptability characteristic of this genus. Its evolutionary history is distinguished by its generalism and versatility, with the capability to parasitize more than ten different insect orders and arachnids, and its associations with plants (Hu *et al.,* 2014). This generalist lifestyle exemplifies the adaptation inherent in the *Metarhizium* genus, emphasizing its ecological relevance and widespread presence in diverse ecosystems (St. Leger & Wang, 2020).

1.5.2 *Tenebrio molitor*

In my research, *Tenebrio molitor* Linnaeus, 1758 (Coleoptera: Tenebrionidae) serves as model host organism, a choice stemming from its rich history and biological studies and well-documented susceptibility to various *Metarhizium* species (Slowik *et al.*, 2023). This susceptibility is crucial for studying the parameters of growth and survival after infection. The growth of *Metarhizium* on *T. molitor* can be quantitatively measured, providing direct insights into the virulence of the fungus. Survival rates of *T. molitor* post-infection offer a clear measure of virulence, reflecting the ability of *Metarhizium* to infect and cause mortality in this host.

This beetle species originates from Europe but is now cosmopolitan in its distribution thanks to its association with being a pest of stored grains (Hagstrum *et al.,* 2016). Although there is little published research on its natural ecology, it

is a detritovore known to inhabit diverse environments such as leaf litter, birds' nests, and rotting wood. In the Anthropocene Epoch, its association with human-altered enviornments mean it is primarily known as being the largest stored grain beetle (USDA, 2016). Its frequent use in baiting to isolate EPF from the environment attests to its significant role in understanding host-pathogen dynamics (Kim *et al.,* 2018). Furthermore, the simplicity in rearing *T. molitor*, owing to its non-complex dietary and environmental requirements, as well as physiological robustness, has made it a favorite among researchers exploring population ecology, insect physiology, and genetics (de Souza *et al.,* 2015; Adamski *et al.,* 2019).

Tenebrio molitor plays a significant role not only in scientific research but also in human economies. These larvae are cultivated on a large scale for their protein and fats, potential for human consumption, use as animal feeds, and even their frass, a valuable option for fertilizers (Finke, 2015; Van Huis, 2013; Sogari *et al.,* 2019; Blakstad *et al.,* 2023). The dietary versatility of *T. molitor*, able to consume a diverse range of substances, positions them as efficient processors of waste and byproducts (Kuan *et al.,* 2022; Moruzzo *et al.,* 2021). Their demonstrated ability to digest plastics amplifies their importance, marking them as potential key players in circular economy systems in a resource-conscious world (Kuan *et al.,* 2022).

T. molitor's robustness is underscored by its ecological and physiological traits. Its lifecycle is notably plastic, with development typically spanning anywhere from 280 to 630 days, which is heavily influenced by temperature variations (Dinev, 2013). The lifecycle of *T. molitor* typically comprises 10-12 days in the egg stage, followed by a variable larval stage that can range from 3-4 months to 18 months depending on environmental conditions, and an adult stage lasting 2 to 3 months during which a female can lay up to 2,000 eggs (Truman, 2002; Dinev, 2013). Larvae exhibit a varied developmental trajectory, transitioning through anywhere from 9 to over 20 instars, the number of which increase under stress, depending on environmental factors including temperature, humidity, diet, and photoperiod (Rebeiro *et al.,* 2018; Morales-Ramos *et al.,* 2010*;* Esperk *et al*., 2007; Zim *et al.,* 2022). Biotic variables like

population density and parental age also affect development (Berggreen *et al.,* 2018).

The versatility of *T. molitor* is further highlighted by its resistance to low temperatures, with larvae capable of surviving up to 80 days at -5°C (Errico *et al.,* 2021; Loreto, 2019). This poikilothermic species, though warm-adapted, is distinguished by a robust overwintering capability due to its ability to produce antifreeze proteins and other biochemical adaptations that prevent ice formation within their cells, thus preventing freezing and allowing cellular functions to continue at low temperatures (Graham *et al.,* 2000). The developmental stages of *T. molitor*, from larva to adult, are highly dependent on temperature. At optimal temperatures (around 27-30°C), the larvae develop faster, while colder temperatures slow down their growth and metabolic rates (Rebeiro *et al.,* 2018; Dinev, 2013; Bjørge *et al.,* 2018). This adaptability allows them to exist in varied climates, adjusting their developmental speed according to the prevailing environmental conditions. Moreover, the thermal ecology of *T. molitor* is integral to understanding its interactions with entomopathogenic fungi like *Metarhizium*. Being ectotherms, the beetles' physiological processes, including immune responses, are highly influenced by ambient temperature (Bjørge *et al.,* 2018; Catalán *et al.,* 2012). The insects exhibit notable thermal plasticity, even affecting inheritance of traits like developmental speed and body size between generations, enabling survival in diverse climates (Morales-Ramos *et al.,* 2022). This adaptability doesn't only underscore their global distribution but also influences the dynamics of host-pathogen interactions.

In the context of ecological and evolutionary studies, understanding the thermal ecology of *T. molitor* can provide insights into their survival strategies, adaptability, and the dynamics of their interactions with pathogens in varying environmental contexts. This species offers a model to explore questions related to thermal adaptation, effects of temperature variations on host-pathogen interactions, and potential impacts of climate change on these dynamics. For these reasons I chose to use this species as a model host organism for the host-pathogen interaction experiment in Chapter 4.

1.6 Thesis plan

The dynamic interplay between *Metarhizium* species, their insect hosts, and the environment is characterized by a complex web of interactions that determine outcomes ranging from effective pest control to the emergence of potential problems for mass-reared insects. In this thesis, a systematic approach is employed to dissect and understand these interactions, with particular focus on the influence of thermal and nutritional factors.

Through a series of empirical studies detailed in subsequent chapters, this work aims to quantify and characterize the nutritional niches of *Metarhizium* species with different host ranges and explore the role of temperature in shaping host-pathogen interactions.

This thesis presents a multidimensional approach through three data chapters to understand the thermal and nutritional ecologies of *Metarhizium* with different host ranges and how these environmental factors mediate host-pathogen interactions. First, I develop a rapid high throughput method for measuring fungal growth. I then quantify the nutritional niches of a broad-host range (generalist) and a specialist species of EPF with this method using the Geometric Framework for Nutrition. Finally, I apply the rapid growth assay to determine thermal optima in EPF with different ecologies, alongside a host (*Tenebrio molitor),* and investigate the effect of temperature on host-pathogen interactions (virulence) and disease outcomes. Understanding the ecological interactions between EPF and their insect hosts will help in informing biological control strategies, evolutionary ecology research, and the broader understanding of insect-pathogen-environment interactions.

This thesis is composed of three empirical studies each forming an individual manuscript (Chapters 2-4). Experimental studies conducted in Chapters 2-4 involve *Metarhizium* spp., with an interaction experiment featuring *T. molitor* detailed in Chapter 4.

In Chapter 2, I introduce a novel, high-throughput method for measuring the growth of EPF using spectrophotometry in small-volume, liquid media cultures. This innovative approach allows for rapid, precise, and reproducible

assessments of fungal growth, laying a foundational methodology for the subsequent chapters. This chapter has been published in the journal *Insects* (Slowik *et al.,* 2023).

Chapter 3 explores the nutritional ecology of *Metarhizium*, investigating how the nutritional niche width is influenced by the fungi's host range. Utilizing the methodology established in Chapter 2, I examine the correlations between nutritional requirements and ecological lifestyle, providing insights into the fungi's performance in different environmental conditions. It is understood that each organism has a particular nutritional niche depending on its lifestyle and ecology (Simpson & Raubenheimer, 2012), and it is currently unclear how nutritional niche width relates to host range in EPF. In Chapter 3, I quantify the nutritional niches of a host generalist and a specialist species of *Metarhizium* fungi with the rapid growth assay using the Geometric Framework for Nutrition. I construct a nutritional landscape using 24 experimentally defined diets with 6 different ratios of C:P and varying media concentrations.

In Chapter 4, the focus shifts to thermal ecology, examining how temperature influences the interactions between EPF and warm-adapted insects. I evaluate the Thermal Mismatch Hypothesis and explore the thermal performance curves for growth and virulence, revealing how evolutionary histories and ecological adaptations of EPF species have resulted in distinct thermal niches during host interactions. This manuscript has been submitted to the *Journal of Invertebrate Pathology*.

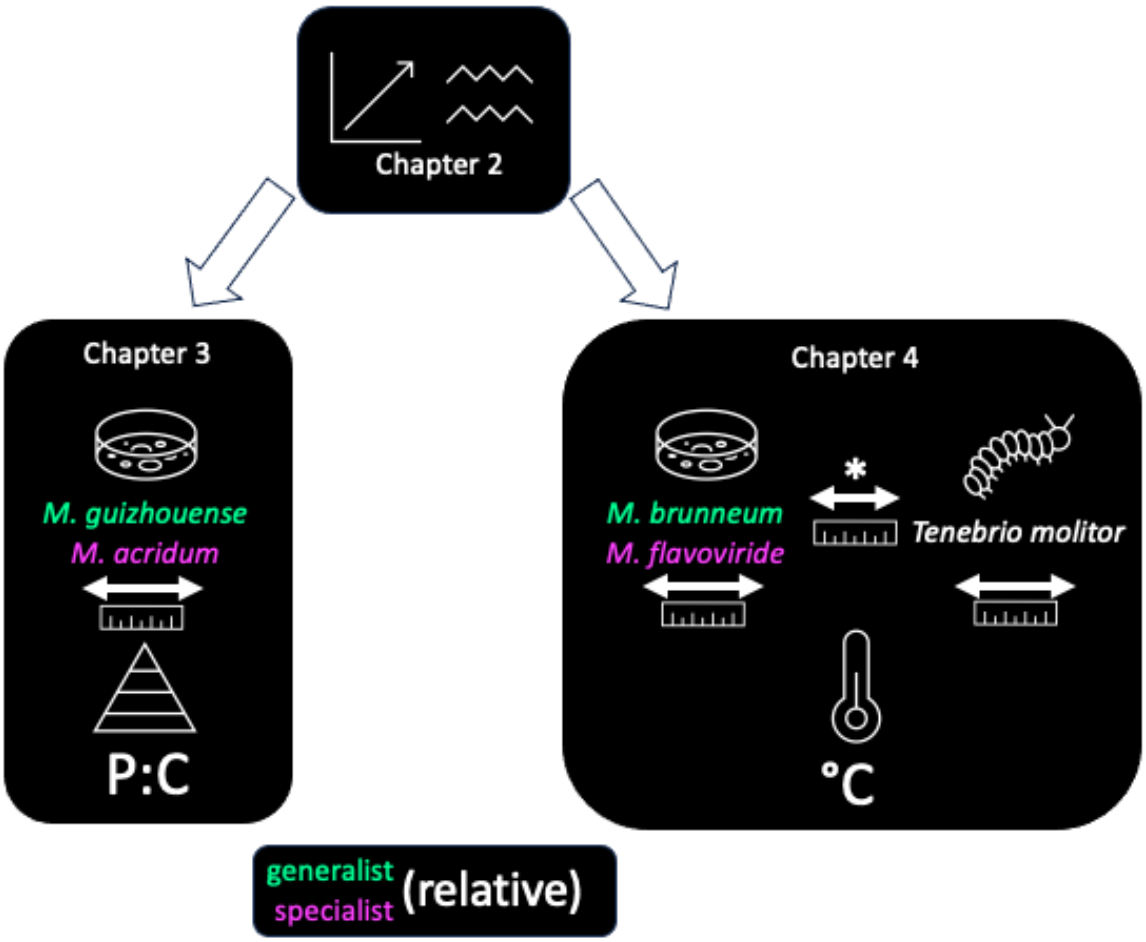

Figure 1.5 Thesis experimental framework.

1.6.1 Key objectives of the thesis with predictive hypotheses

Chapter 2

Objective 2.1: Develop a rapid and high throughput method for measuring fungal growth using small volume liquid media cultures in microplates and microspectrophotometry.

Hypothesis: The microspectrophotometric method will provide reliable and accurate measurements of fungal growth, showing a direct correlation with traditional measures of growth, such as biomass and colony expansion.

Chapter 3

Objective 3.1: Quantify the nutritional niche width of a specialist and a generalist EPF using the rapid growth assay developed in Chapter 2.

Hypothesis: Niche width can be quantified for EPF using the rapid growth assay and Geometric Framework for Nutrition.

Objective 3.2: Determine if host range of EPF correlates to nutritional niche width.

Hypothesis: Host-specialist EPF will exhibit a narrower nutritional niche, characterized by specialized nutrient requirements and less adaptability to varied nutrient ratios, compared to generalist EPF, reflecting their ecological lifestyles.

Chapter 4

Objective 4.1: Examine if individual pathogens and hosts exhibit overlapping or distinct thermal performance curves and optima in EPF-insect relationships.

Hypothesis: Host and pathogen curves might show overlaps indicating potential hotspots for effective infection.

Hypothesis: There will be a variation in thermal performance curves between different EPF species, reflecting their adaptation to specific environments and ecological lifestyles.

Objective 4.2: Examine how virulence outcomes reflect the interaction between the host and pathogen's individual thermal performance curve.

Hypothesis: EPF with broader thermal performance curves will exhibit consistent virulence across a range of temperatures, while those with narrower curves will show peak virulence at specific temperatures aligned with their thermal optima.

Hypothesis: *M. flavoviride* will demonstrate heightened virulence at lower temperatures compared to *M. brunneum*, reflecting its adaptation to cold environments and aligning with the predictions of the Thermal Mismatch Hypothesis.

1.7 References

Acasuso-Rivero, C., Murren, C. J., Schlichting, C. D., & Steiner, U. K. (2019). Adaptive phenotypic plasticity for life-history and less fitness-related traits. *Proceedings of the Royal Society B*, *286*(1904), 20190653.

Adamski, Z., Bufo, S.A., Chowanski, S., Falabella, P., Lubawy, J., Marciniak, P., Pacholska-Bogalska, J., Salvia, R., Scrano, L., Slocinska, M., Spochacz, M., Szymczak, M., Urbanski, A., Walkowiak-Nowicka, K., and Rosinski, G. (2019). Beetles as model organisms in physiological, biomedical and environmental studies–a review. *Frontiers in physiology*, *10*, 319.

Ahmad, I., del Mar Jiménez-Gasco, M., Luthe, D. S., Shakeel, S. N., & Barbercheck, M. E. (2020). Endophytic *Metarhizium robertsii* promotes maize growth, suppresses insect growth, and alters plant defense gene expression. *Biological Control, 144,* 104167.

Alves, G. S., Bertini, S. C. B., Barbosa, B. B., Pimentel, J. P., Junior, V. A. R., de Oliveira Mendes, G., & Azevedo, L. C. B. (2021). Fungal endophytes inoculation improves soil nutrient availability, arbuscular mycorrhizal colonization and common bean growth. *Rhizosphere, 18,* 100330.

Anderson, T. R., Raubenheimer, D., Hessen, D. O., Jensen, K., Gentleman, W. C., & Mayor, D. J. (2020). Geometric stoichiometry: unifying concepts of animal nutrition to understand how protein-rich diets can be “too much of a good thing”. *Frontiers in Ecology and Evolution*, *8*, 196.

Araújo, J. P., & Hughes, D. P. (2016). Diversity of entomopathogenic fungi: which groups conquered the insect body?. *Advances in genetics*, *94*, 1-39.

Asplen, M.K., Bruns, E., David, A.S., Denison, R.F., Epstein, B., Kaiser, M.C., Kaser, J.M., Lacroix, C., Mohl, E.K., Quiram, G. and Prescott, K. (2012). Do trade-offs have explanatory power for the evolution of organismal interactions?. *Evolution*, *66*(5), 1297-1307.

Bebber, D. P., & Chaloner, T. M. (2022). Specialists, generalists and the shape of the ecological niche in fungi. *The New Phytologist*, *234*(2), 345.

Behie, S. W., & Bidochka, M. J. (2014). Ubiquity of insect-derived nitrogen transfer to plants by endophytic insect-pathogenic fungi: an additional

branch of the soil nitrogen cycle. *Applied and environmental microbiology*, *80*(5), 1553-1560.

Berggreen, I. E., Offenberg, J., Calis, M., & Heckmann, L. H. (2018). Impact of density, reproduction period and age on fecundity of the yellow mealworm *Tenebrio molitor* (Coleoptera: Tenebrionidae). *Journal of Insects as Food and Feed*, *4*(1), 43-50.

Bernot, R. J., & Poulin, R. (2018). Ecological stoichiometry for parasitologists. *Trends in parasitology*, *34*(11), 928-933.

Bidochka, M. J., & Small, C. L. (2005). Phylogeography of *Metarhizium*, an insect pathogenic fungus. *Insect-fungal associations*, 28-49.

Bjørge, J. D., Overgaard, J., Malte, H., Gianotten, N., & Heckmann, L. H. (2018). Role of temperature on growth and metabolic rate in the tenebrionid beetles *Alphitobius diaperinus* and *Tenebrio molitor*. *Journal of Insect Physiology*, (*107)*, 89-96.

Blakstad, J. I., Strimbeck, R., Poveda, J., Bones, A. M., & Kissen, R. (2023). Frass from yellow mealworm (*Tenebrio molitor*) as plant fertilizer and defense priming agent. *Biocatalysis and Agricultural Biotechnology*, 102862.

Boersma, M., & Elser, J. J. (2006). Too much of a good thing: on stoichiometrically balanced diets and maximal growth. *Ecology*, *87*(5), 1325-1330.

Bohannan, B. J., & Lenski, R. E. (2000). Linking genetic change to community evolution: insights from studies of bacteria and bacteriophage. *Ecology Letters, 3*(4), 362-377.

Boomsma, J. J., Jensen, A. B., Meyling, N. V., & Eilenberg, J. (2014). Evolutionary interaction networks of insect pathogenic fungi. *Annual Review of Entomology*, *59*, 467-485.

Brodeur, J. (2012). Host specificity in biological control: insights from opportunistic pathogens. *Evolutionary applications*, *5*(5), 470-480.

Carscadden, K. A., Emery, N. C., Arnillas, C. A., Cadotte, M. W., Afkhami, M. E., Gravel, D., & Wiens, J. J. (2020). Niche breadth: causes and

consequences for ecology, evolution, and conservation. *The Quarterly Review of Biology*, *95*(3), 179-214.

Casadevall, A. (2007). Determinants of virulence in the pathogenic fungi. *Fungal biology reviews, 21*(4), 130-132.

Casadevall, A., & Pirofski, L. A. (2001). Host-pathogen interactions: the attributes of virulence. *The Journal of infectious diseases*, *184*(3), 337-344.

Catalán, T. P., Wozniak, A., Niemeyer, H. M., Kalergis, A. M., & Bozinovic, F. (2012). Interplay between thermal and immune ecology: effect of environmental temperature on insect immune response and energetic costs after an immune challenge. *Journal of Insect Physiology*, *58*(3), 310-317.

Chandler, D. (2017). Basic and applied research on entomopathogenic fungi. In *Microbial control of insect and mite pests* (pp. 69-89). Academic Press.

Cohen, J. M., Sauer, E. L., Santiago, O., Spencer, S. & Rohr, J. R. (2020). Divergent impacts of warming weather on wildlife disease risk across climates. *Science,* 370.

Constanski, K. C., Neves, P. M. O. J., Nogueira, L. M., Santoro, P. H., Amaro, J. T., & Zorzetti, J. (2011). Selection and evaluation of virulence of *Beauveria bassiana* (Bals.) Vuill. submitted to different temperature. *Semina: Ciencias Agrarias (Londrina)*, *32*(3), 875-882.

Day, T. (2001). Parasite transmission modes and the evolution of virulence. *Evolution, 55*(12), 2389-2400.

de Souza, P. C., Morey, A. T., Castanheira, G. M., Bocate, K. P., Panagio, L. A., Ito, F. A., & Almeida, R. S. (2015). *Tenebrio molitor* (Coleoptera: Tenebrionidae) as an alternative host to study fungal infections. *Journal of microbiological methods*, *118*, 182-186.

Dinev, I. (2013). The Darkling Beetle health hazard for broiler chicken production*. Trakia Journal o f Sciences, 1*, 1-4.

Errico, S., Dimatteo, S., Moliterni, S., & Baldacchino, F. (2021). Effects of long-lasting cold storage on *Tenebrio molitor* larvae (Coleoptera: Tenebrionidae). *Journal of Insects as Food and Feed*, *7*(7), 1111-1116.

Esperk, T., Tammaru, T., & Nylin, S. (2007). Intraspecific variability in number of larval instars in insects. *Journal of Economic Entomology, 100*(3), 627-645.

Ewald, P. W. (1983). Host-parasite relations, vectors, and the evolution of disease severity. *Annual Review of Ecology and Systematics, 14*(1), 465-485.

Fargues, J., & Remaudiere, G. (1977). Considerations on the specificity of entomopathogenic fungi. *Mycopathologia*, *62*(1), 31-37.

Fernandes, É. K., Keyser, C. A., Chong, J. P., Rangel, D. E., Miller, M. P., & Roberts, D. W. (2010). Characterization of *Metarhizium* species and varieties based on molecular analysis, heat tolerance and cold activity. *Journal of Applied Microbiology*, *108*(1), 115-128.

Fernandes, E. K., Rangel, D. E., Moraes, A. M., Bittencourt, V. R., & Roberts, D. W. (2008). Cold activity of *Beauveria* and *Metarhizium*, and thermotolerance of *Beauveria*. *Journal of invertebrate pathology*, *98*(1), 69-78.

Finke, M. D. (2015). Complete nutrient content of four species of commercially available feeder insects fed enhanced diets during growth. *Zoo biology*, *34*(6), 554-564.

Finlay, B. B., & Falkow, S. (1997). Common themes in microbial pathogenicity revisited. *Microbiology and Molecular Biology Reviews, 61*(2), 136-169.

Futuyma, D. J., & Moreno, G. (1988). The evolution of ecological specialization. *Annual review of Ecology and Systematics*, *19*(1), 207-233.

Gao, Q., Jin, K., Ying, S. H., Zhang, Y., Xiao, G., Shang, Y., & Wang, C. (2011). Genome sequencing and comparative transcriptomics of the model entomopathogenic fungi *Metarhizium anisopliae* and *M. acridum*. *PLoS genetics*, *7*(1), e1001264.

Ghalambor, C. K., McKay, J. K., Carroll, S. P., & Reznick, D. N. (2007). Adaptive versus non-adaptive phenotypic plasticity and the potential for contemporary adaptation in new environments. *Functional ecology, 21*(3), 394-407.

Graham, L. A., Walker, V. K., & Davies, P. L. (2000). Developmental and environmental regulation of antifreeze proteins in the mealworm beetle *Tenebrio molitor*. *European Journal of Biochemistry*, *267*(21), 6452-6458.

Hagstrum, D. (2016). *Atlas of stored-product insects and mites*. Elsevier.

Hajek, A. E., & Goettel, M. S. (2007). Guidelines for evaluating effects of entomopathogens on non-target organisms. *Field manual of techniques in invertebrate pathology*, 815-833.

Hajek, A. E., & Shapiro-Ilan, D. I. (Eds.). (2018). *Ecology of invertebrate diseases*. John Wiley & Sons.

Hallsworth, J. E., & Magan, N. (1999). Water and temperature relations of growth of the entomogenous fungi *Beauveria bassiana, Metarhizium anisopliae*, and *Paecilomyces farinosus*. *Journal of invertebrate pathology*, *74*(3), 261-266.

Harvell, D. (2004). Ecology and evolution of host-pathogen interactions in nature. *The American Naturalist*, *164*(S5), S1-S5.

Herlinda, S., Rizkie, L., Suwandi, Susilawati, Lakitan, B., Verawaty, M., & Hasbi. (2018). Effects of high temperature and ultraviolet-C irradiance on conidial viability and density of *Beauveria bassiana* and *Metarhizium anisopliae* isolated from soils of lowland ecosystems in Indonesia. *Eurasian Journal of Analytical Chemistry 13*(6), 209-216.

Hu, X., Xiao, G., Zheng, P., Shang, Y., Su, Y., Zhang, X., Liu, X., Zhan, S., St. Leger, R.J. & Wang, C. (2014). Trajectory and genomic determinants of fungal-pathogen speciation and host adaptation. *Proceedings of the National Academy of Sciences*, *111*(47), 16796-16801.

Humber, R. A. (2008). Evolution of entomopathogenicity in fungi. *Journal of invertebrate pathology*, *98*(3), 262-266.

Joshi, A., & Thompson, J. N. (1995). Trade-offs and the evolution of host specialization. *Evolutionary Ecology*, *9*, 82-92.

Kamp, A. M., & Bidochka, M. J. (2002). Conidium production by insect pathogenic fungi on commercially available agars. *Letters in Applied Microbiology*, *35*(1), 74-77.

Kelly, S. A., Panhuis, T. M., & Stoehr, A. M. (2011). Phenotypic plasticity: molecular mechanisms and adaptive significance. *Comprehensive Physiology*, *2*(2), 1417-1439.

Kepler, R. M., Humber, R. A., Bischoff, J. F., & Rehner, S. A. (2014). Clarification of generic and species boundaries for *Metarhizium* and related fungi through multigene phylogenetics. *Mycologia*, *106*(4), 811-829.

Kepler, R. M., Chen, Y., Kilcrease, J., Shao, J., & Rehner, S. A. (2016). Independent origins of diploidy in *Metarhizium*. *Mycologia*, *108*(6), 1091-1103.

Keyser, C. A., Fernandes, É. K., Rangel, D. E., & Roberts, D. W. (2014). Heat-induced post-stress growth delay: a biological trait of many *Metarhizium* isolates reducing biocontrol efficacy?. *Journal of invertebrate pathology*, *120*, 67-73.

Kim, J. C., Lee, M. R., Kim, S., Lee, S. J., Park, S. E., Nai, Y. S., & Kim, J. S. (2018). *Tenebrio molitor*-mediated entomopathogenic fungal library construction for pest management. *Journal of Asia-Pacific Entomology*, *21*(1), 196-204.

Koo, H. Y., Kim, S. G., Oh, H. K., Kim, J. E., Choi, D. S., Kim, D. I., & Kim, I. (2013). Temperature-dependent development model of larvae of mealworm beetle, *Tenebrio molitor* L.(Coleoptera: Tenebrionidae). *Korean journal of applied entomology*, *52*(4), 387-394.

Kuan, Z. J., Chan, B. K. N., & Gan, S. K. E. (2022). Worming the circular economy for biowaste and plastics: *Hermetia illucens, Tenebrio molitor*, and *Zophobas morio*. *Sustainability*, *14*(3), 1594.

Kumar, C. S., Jacob, T. K., Devasahayam, S., Geethu, C., & Hariharan, V. (2021). Characterization and biocontrol potential of a naturally occurring isolate of *Metarhizium pingshaense* infecting *Conogethes punctiferalis*. *Microbiological Research*, *243*, 126645.

Larsen, B. B., Miller, E. C., Rhodes, M. K., & Wiens, J. J. (2017). Inordinate fondness multiplied and redistributed: the number of species on earth and the new pie of life. *The Quarterly Review of Biology*, *92*(3), 229-265.

Li, D. P., & Holdom, D. G. (1995). Effects of nutrients on colony formation, growth, and sporulation of *Metarhizium anisopliae* (Deuteromycotina: Hyphomycetes). *Journal of Invertebrate Pathology*, *65*(3), 253-260.

Li, J., & Feng, M. G. (2009). Intraspecific tolerance of *Metarhizium anisopliae* conidia to the upper thermal limits of summer with a description of a quantitative assay system. *Mycological research*, *113*(1), 93-99.

Li, J., & Xia, Y. (2022). Host–Pathogen Interactions between *Metarhizium* spp. and Locusts. *Journal of Fungi, 8*(6), 602.

Lloyd-Smith, J. O., Cross, P. C., Briggs, C. J., Daugherty, M., Getz, W. M., Latto, J., & Swei, A. (2005). Should we expect population thresholds for wildlife disease?. *Trends in ecology & evolution*, *20*(9), 511-519.

Loreto, D.N. (2019). Larval performance, morphological, behavioural and elecrophisiological studies on *Tenebrio molitor* L. (Coleoptera: Tenebrionidae). Thesis.

Lovett, B., & St. Leger, R. J. (2015). Stress is the rule rather than the exception for *Metarhizium. Current genetics*, *61*, 253-261.

Mantzoukas, S., & Eliopoulos, P. A. (2020). Endophytic entomopathogenic fungi: A valuable biological control tool against plant pests. *Applied Sciences*, *10*(1), 360.

Maynard, D.S., Bradford, M.A., Covey, K.R., Lindner, D., Glaeser, J., Talbert, D.A., Tinker, P.J., Walker, D.M., and Crowther, T.W. (2019). Consistent trade-offs in fungal trait expression across broad spatial scales. *Nature Microbiology, 4*, 846–853.

McDonald, B. A., & Linde, C. (2002). Pathogen population genetics, evolutionary potential, and durable resistance. *Annual review of phytopathology*, *40*(1), 349-379.

Moonjely, S., Barelli, L., & Bidochka, M. J. (2016). Insect pathogenic fungi as endophytes. *Advances in genetics*, *94*, 107-135.

Mongkolsamrit, S., Khonsanit, A., Thanakitpipattana, D., Tasanathai, K., Noisripoom, W., Lamlertthon, S., Himaman, W., Houbraken, J., Samson, R.A. and Luangsa-Ard, J., 2020. Revisiting *Metarhizium* and the

description of new species from Thailand. *Studies in Mycology, 95*(1), pp.171-251.

Morales-Ramos, J. A., Rojas, M. G., Tweedy, D., Emery, V., & Kelstrup, H. C. (2022). Inheritance of Two Traits With High Plasticity, Developmental Speed, and Body Size, in *Tenebrio molitor* (Coleoptera: Tenebrionidae). *Journal of Insect Science*, *22*(6), 13.

Morales-Ramos, J. A., Rojas, M. G., Shapiro-Ilan, D. I., & Tedders, W. L. (2010). Developmental plasticity in *Tenebrio molitor* (Coleoptera: Tenebrionidae): Analysis of instar variation in number and development time under different diets. *Journal of Entomological Science*, *45*(2), 75-90.

Moruzzo, R., Riccioli, F., Espinosa Diaz, S., Secci, C., Poli, G., & Mancini, S. (2021). Mealworm (*Tenebrio molitor*): potential and challenges to promote circular economy. *Animals*, *11*(9), 2568.

Nielsen, K. N., Salgado, J. F. M., Natsopoulou, M. E., Kristensen, T., Stajich, J. E., & De Fine Licht, H. H. (2021). Diploidy within a haploid genus of entomopathogenic fungi. *Genome biology and evolution*, *13*(7), evab158.

Ouedraogo, R. M., Cusson, M., Goettel, M. S., & Brodeur, J. (2003). Inhibition of fungal growth in thermoregulating locusts, *Locusta migratoria*, infected by the fungus *Metarhizium anisopliae var acridum. Journal of invertebrate pathology*, *82*(2), 103-109.

Ouedraogo, A., Fargues, J., Goettel, M. S., & Lomer, C. J. (1997). Effect of temperature on vegetative growth among isolates of *Metarhizium anisopliae* and *M. flavoviride*. *Mycopathologia*, *137*, 37-43.

Polar, P., de Muro, M. A., Kairo, M. T., Moore, D., Pegram, R., John, S. A., & Roach-Benn, C. (2005). Thermal characteristics of *Metarhizium anisopliae* isolates important for the development of biological pesticides for the control of cattle ticks. *Veterinary parasitology*, *134*(1-2), 159-167.

Råberg, L., & Stjernman, M. (2012). The evolutionary ecology of infectious disease virulence. *Ecoimmunology*, *548*, 78.

Poulin, R., & Combes, C. (1999). The concept of virulence: interpretations and implications. *Parasitology Today, 15*(12), 474-475.

Povey, S., Cotter, S. C., Simpson, S. J., & Wilson, K. (2014). Dynamics of macronutrient self-medication and illness-induced anorexia in virally infected insects. *Journal of Animal Ecology*, *83*(1), 245-255.

Rangel, D. E., Braga, G. U., Fernandes, É. K., Keyser, C. A., Hallsworth, J. E., & Roberts, D. W. (2015). Stress tolerance and virulence of insect-pathogenic fungi are determined by environmental conditions during conidial formation. *Current genetics*, *61*, 383-404.

Rangel, D. E., Fernandes, É. K., Dettenmaier, S. J., & Roberts, D. W. (2010). Thermotolerance of germlings and mycelium of the insect-pathogenic fungus *Metarhizium* spp. and mycelial recovery after heat stress. *Journal of Basic Microbiology*, *50*(4), 344-350.

Rehner, S. A., & Kepler, R. M. (2017). Species limits, phylogeography and reproductive mode in the *Metarhizium anisopliae* complex. *Journal of invertebrate pathology*, *148*, 60-66.

Ribeiro, N., Abelho, M., & Costa, R. (2018). A review of the scientific literature for optimal conditions for mass rearing *Tenebrio molitor* (Coleoptera: Tenebrionidae). *Journal of Entomological Science*, *53*(4), 434-454.

Roberts, D. W., & St. Leger, R. J. (2004). *Metarhizium* spp., cosmopolitan insect-pathogenic fungi: mycological aspects. *Advances in applied microbiology*, *54*(1), 1-70.

Rohr, J. R., Civitello, D. J., Cohen, J. M., Roznik, E. A., Sinervo, B., & Dell, A. I. (2018). The complex drivers of thermal acclimation and breadth in ectotherms. *Ecology letters*, *21*(9), 1425-1439.

Safavi, S. A., Shah, F. A., Pakdel, A. K., Reza Rasoulian, G., Bandani, A. R., & Butt, T. M. (2007). Effect of nutrition on growth and virulence of the entomopathogenic fungus *Beauveria bassiana*. *FEMS Microbiology Letters*, *270*(1), 116-123.

Sanders, A. J., & Taylor, B. W. (2018). Using ecological stoichiometry to understand and predict infectious diseases. *Oikos*, *127*(10), 1399-1409.

Scully, L. R., & Bidochka, M. J. (2005). Serial passage of the opportunistic pathogen *Aspergillus flavus* through an insect host yields decreased saprobic capacity. *Canadian journal of microbiology*, *51*(2), 185-189.

Sexton, J. P., Montiel, J., Shay, J. E., Stephens, M. R., & Slatyer, R. A. (2017). Evolution of ecological niche breadth. *Annual Review of Ecology, Evolution, and Systematics*, *48*, 183-206.

Sheng, H., McNamara, P. J., & St. Leger, R. J. (2022). *Metarhizium*: an opportunistic middleman for multitrophic lifestyles. *Current Opinion in Microbiology, 69*, 102176.

Shang, J., Song, S., & Wang, C. (2023). *Metarhizium robertsii. Trends in Parasitology.* https://doi.org/10.1016/j.pt.2023.10.004

Simpson, S. J., Le Couteur, D. G., James, D. E., George, J., Gunton, J. E., Solon-Biet, S. M., & Raubenheimer, D. (2017). The geometric framework for nutrition as a tool in precision medicine. *Nutrition and healthy aging*, *4*(3), 217-226.

Simpson, S. J., & Raubenheimer, D. (2012). *The nature of nutrition: a unifying framework from animal adaptation to human obesity*. Princeton university press.

Slowik, A. R., Herren, P., Bessette, E., Lim, F. S., Hernández-Pelegrín, L., & Savio, C. (2023). Harmful and beneficial symbionts of *Tenebrio molitor* and their implications for disease management. *Journal of Insects as Food and Feed*, 1-16.

Smith, V. H., Jones, T. P., & Smith, M. S. (2005). Host nutrition and infectious disease: an ecological view. *Frontiers in Ecology and the Environment*, *3*(5), 268-274.

Sogari, G., Amato, M., Biasato, I., Chiesa, S., & Gasco, L. (2019). The potential role of insects as feed: A multi-perspective review. *Animals*, *9*(4), 119.

St. Leger, R. J. (1995). The role of cuticle-degrading proteases in fungal pathogenesis of insects. *Canadian Journal of Botany*, *73*(S1), 1119-1125.

St. Leger, R. J., & Wang, J. B. (2020). *Metarhizium:* Jack of all trades, master of many. *Open biology*, *10*(12), 200307.

Sternberg, E. D., & Thomas, M. B. (2014). Local adaptation to temperature and the implications for vector-borne diseases. *Trends in Parasitology*, *30*(3), 115-122.

Sterner, R. W., & Elser, J. J. (2017). Ecological stoichiometry: the biology of elements from molecules to the biosphere. In *Ecological stoichiometry*. Princeton university press.

Stone, L. B., & Bidochka, M. J. (2020). The multifunctional lifestyles of *Metarhizium*: Evolution and applications. *Applied microbiology and biotechnology*, *104*, 9935-9945.

Sun, S. J., Dziuba, M. K., Jaye, R. N., & Duffy, M. A. (2023). Temperature modifies trait-mediated infection outcomes in a *Daphnia*–fungal parasite system. *Philosophical Transactions of the Royal Society B*, *378*(1873), 20220009.

Sun, M., & Liu, X. (2006). Carbon requirements of some nematophagous, entomopathogenic and mycoparasitic hyphomycetes as fungal biocontrol agents. *Mycopathologia*, *161*, 295-305.

Thomas, M. B., & Blanford, S. (2003). Thermal biology in insect-parasite interactions. *Trends in Ecology & Evolution*, *18*(7), 344-350.

Truman, J. W., & Riddiford, L. M. (2002). Endocrine insights into the evolution of metamorphosis in insects. *Annual review of entomology*, *47*(1), 467-500.

United States Department of Agriculture (USDA). (2016). Stored Grain Insect Reference. Agricultural Marketing Service, Federal Grain Inspection Service, Washington, D.C.

Van Huis, A. (2013). Potential of insects as food and feed in assuring food security. *Annual review of entomology*, *58*, 563-583.

Vänninen, I. (1996). Distribution and occurrence of four entomopathogenic fungi in Finland: effect of geographical location, habitat type and soil type. *Mycological Research*, *100*(1), 93-101.

Vega, F. E., Jackson, M. A., Mercadier, G., & Poprawski, T. J. (2003). The impact of nutrition on spore yields for various fungal entomopathogens in liquid culture. *World journal of Microbiology and Biotechnology*, *19*, 363-368.

Vega, F. E., Goettel, M. S., Blackwell, M., Chandler, D., Jackson, M. A., Keller, S., & Roy, H. E. (2009). Fungal entomopathogens: new insights on their ecology. *Fungal ecology*, *2*(4), 149-159.

Wang, B., Kang, Q., Lu, Y., Bai, L., & Wang, C. (2012). Unveiling the biosynthetic puzzle of destruxins in *Metarhizium* species. *Proceedings of the National Academy of Sciences*, *109*(4), 1287-1292.

Wang, J., Lovett, B., & St. Leger, R. J. (2019). The secretome and chemistry of *Metarhizium*; a genus of entomopathogenic fungi. *Fungal Ecology, 38*, 7–11.

Wang, J. B., St. Leger, R., & Wang, C. (2016). Advances in genomics of entomopathogenic fungi. *Advances in genetics*, *94*, 67-105.

Webster, J. P., Borlase, A., & Rudge, J. W. (2017). Who acquires infection from whom and how? Disentangling multi-host and multi-mode transmission dynamics in the 'elimination' era. *Philosophical Transactions of the Royal Society B: Biological Sciences*, *372*(1719), 20160091.

Woods, L. C., Gorrell, R. J., Taylor, F., Connallon, T., Kwok, T., & McDonald, M. J. (2020). Horizontal gene transfer potentiates adaptation by reducing selective constraints on the spread of genetic variation. *Proceedings of the National Academy of Sciences*, *117*(43), 26868-26875.

Woolhouse, M. E., Taylor, L. H., & Haydon, D. T. (2001). Population biology of multihost pathogens. *Science*, *292*(5519), 1109-1112.

Zhang, Q., Chen, X., Xu, C., Zhao, H., Zhang, X., Zeng, G., Qian, Y., Liu, R., Guo, N., Mi, W., Meng, G., St. Leger, R. J., & Fang, W. (2019). Horizontal gene transfer allowed the emergence of broad host range entomopathogens. *Proceedings of the National Academy of Sciences*, *116*(16), 7982-7989.

Zim, J., Sarehane, M., Mazih, A., Lhomme, P., Elaini, R., & Bouharroud, R. (2022). Effect of population density and photoperiod on larval growth and reproduction of *Tenebrio molitor* (Coleoptera: Tenebrionidae). *International Journal of Tropical Insect Science*, *42*(2), 1795-1801.

Zimmermann, G. (1982). Effect of high temperatures and artificial sunlight on the viability of conidia of *Metarhizium anisopliae*. *Journal of Invertebrate Pathology*, *40*(1), 36-40.

Chapter 2

A rapid method for measuring in vitro growth in entomopathogenic fungi

Anna R. Slowik[1, 2, 3], Helen H. Hesketh[2], Steven M. Sait[3], and Henrik H. De Fine Licht[1]

[1]University of Copenhagen, Department of Plant and Environmental Sciences, Thorvaldsensvej 40, 1871 Frederiksberg C., Denmark.
[2]UK Centre for Ecology & Hydrology, Maclean Building, Benson Lane, Crowmarsh Gifford, Wallingford, OX10 8BB, United Kingdom.
[3]School of Biology, Faculty of Biological Sciences, University of Leeds, Leeds, LS2 9JT, United Kingdom.

Published in the journal Insects*.*
(2023). *14*(8), 703.

This chapter aimed to develop a rapid and efficient method for measuring the growth of entomopathogenic fungi, which are used as environmentally friendly alternatives to chemical insecticides. The traditional methods used to measure fungal growth are time-consuming and limited in their ability to capture important aspects of growth. In this research, I introduced a novel technique using a microplate reader, which uses the optical density of small volume cultures to estimate fungal biomass. I compared the results of this method with traditional measurements on solid agar plates and found that the microspectrophotometric approach provided accurate and reliable measurements. The findings revealed differences in growth rates and biomass production among different species and isolates of the fungi. This technique offers a valuable tool for studying the growth dynamics of entomopathogenic fungi and has practical applications in assessing their virulence and pathogenic potential. It can contribute to our understanding of how these fungi grow during infection and aid in the development of effective biological control strategies against insect pests.

A rapid method for measuring in vitro growth in entomopathogenic fungi

2.1 Abstract

Quantifying the growth of entomopathogenic fungi is crucial for understanding their virulence and pathogenic potential. Traditional methods for determining growth, such as biomass determination or colony growth area, are time-consuming and quantitatively and spatially limited in scope. In this study, we introduce a high-throughput method for rapidly measuring fungal growth using spectrophotometry in small-volume, liquid media cultures in 96-well microplates. Optical density (OD) changes were directly correlated with dry weight of samples for six isolates from three species of the genus *Metarhizium* to validate spectrophotometric growth measurements, and investigate species- and isolate-specific effects. We quantified fungal biomass from the microcultures by extracting, drying, and weighing mycelial mats. From the relationship established between OD and biomass, we generated standard curves for predicting biomass based on the OD values. The OD measurements clearly distinguished growth patterns among six isolates from three *Metarhizium* species. The logistic growth phase, as captured by the OD measurements, could be accurately assessed within a span of 80 h. Using isolates of *M. acridum*, *M. brunneum*, and *M. guizhouense*, this technique was demonstrated to be an effective, reproducible, and simple method for rapidly measuring filamentous fungal growth with high precision. This technique offers a valuable tool for studying the growth dynamics of entomopathogenic fungi and investigating the factors that influence their growth.

2.2 Introduction

Entomopathogenic fungi are important natural regulators of insect populations, and are widely used as environmentally friendly biological control alternatives to synthetic chemical insecticides (Augustyniuk-Kram & Kram, 2012; Goettel & Glare, 2010; Shah & Pell, 2003; Roberts & Hajek, 1992). In biological studies, measurements of fungal growth over time on different defined media serve as a

standard measure to assess performance and evaluate efficacy during isolation and testing (Jaronski, 2014; Yeo *et al.,* 2003). Being heterotrophic organisms with indeterminate growth, fungal growth often responds directly to the quality and availability of nutrients in the immediate environment (Gow & Gadd, 1995; Shah *et al.,* 2005). Fungal growth over time can be evaluated using various methods, generally classified as direct or indirect measures (Lee *et al.,* 2021). The most widely applied direct methods include measurement of hyphal extension (Meletiadis *et al.,* 2001), dry weight from liquid cultures, and radial expansion on solid agar (Trinci, 1971; Taniwaki *et. al,* 2006). Accepted indirect methods make use of spectrophotometry in liquid macro- or micro-cultures (Granade *et al.,* 1985; Langvad 1999; Meletiadis *et al.,* 2001), fluorescence of labeled fungi and light sheet fluorescence (Hickey *et al.,* 2004; Gutiérrez–Medina & Vázquez-Villa, 2021), multispectral imaging (Ebrahimi *et al.,* 2015), quantification of chitin production (Plassard *et al.*, 1971; Aidoo *et al.,* 1981), and advances in spectrophotometric analysis of microcultures on agar media (Canovas *et al.,* 2017).

Measurement of the radial expansion of fungal colonies on solid media is a widely-used direct method to quantify growth. The method is straightforward, and allows for measurement of other phenotypic traits such as spore production and colony morphology (e.g., color, branching pattern) (Poprawski & Majchrowicz, 1995; Shah *et al.,* 2005; Yeo *et al.* 2003). However, this approach fails to account for some important aspects of growth, such as the density of the mycelium (Canovas *et al.,* 2017). An expanding colony can exhibit varying degrees of mycelial density while covering the same area, which is not captured when using radial expansion measurements. Using a dry weight method to measure growth in liquid macrocultures accounts for this discrepancy in mycelial density, but requires interference with cultures through direct sampling for quantification, making real-time monitoring of in situ growth impractical (Granade *et al.,* 1985, Banerjee *et al.,* 1993).

In addition to this, the solid media environment may not be biologically appropriate for some fungi based on their specific ecologies. In entomopathogenic fungi, in vivo growth progresses primarily through the insect

hemocoel, which is a submerged liquid environment (Lovett *et al.,* 2017). The physiological and developmental biology of fungi can vary considerably, depending on whether they grow on a solid or liquid medium. For instance, solid media may support a higher production of secondary metabolites or enzymes compared to liquid media in some fungal isolates (VanderMolen *et al.,* 2013; Viniegra-González *et al.,* 2003). In terms of practicality, fungal growth on agar plates is also time-consuming to conduct. The timescale for growth of many entomopathogenic fungi when analyzing radial expansion spans multiple days, and in the case of measuring dry weight, the processing of samples involves a lengthy process of collection, drying, and weighing (Poprawski & Majchrowicz, 1995; Shah *et al.,* 2005; Lee *et al.,* 2021).

In situ spectrophotometry provides a viable alternative to these methods by directly correlating optical density (OD) values with an increase in fungal biomass. It is generally understood that growing fungus changes the OD of liquid cultures, because turbidity directly correlates with unit population size, which serves as the basis for the traditional spectrophotometric analysis of fungal growth (Stanier *et al.,* 1963). In this study, we apply spectrophotometric analysis to measure the growth of entomopathogenic fungi, which are typically performed on solid agar media, as previously described. Previous studies have demonstrated the use of spectrophotometric measurements for assessing filamentous fungal growth in microcultures. However, in these studies, the relationship between dry mycelial mass and OD is extrapolated using correlation coefficients (Granade *et al.,* 1985), or hyphal extension is employed as a growth metric (Meletiadis *et al.,* 2001). The aim of this study was to establish a direct correlation between the dry weight of mycelial cultures and their corresponding OD values for six isolates of *Metarhizium* spp. This correlation allows for the construction of isolate-specific standard curves, enabling the quantification of biomass based on OD measurements.

2.3 Materials and Methods

2.3.1 Fungal isolates and preparation of inoculum

The growth of two isolates within each of three different species of *Metarhizium* were compared to investigate variations among species and isolates. This was assessed in addition to the effect on the relationship between dry weight and OD. Six fungal isolates of the genus *Metarhizium* were used to produce standard curves of OD by dry weight: *M. brunneum* KVL 16_36 (Isolated from the commercial product Met52, Novozymes A/S, Krogshøjvej 36, Bagsværd, Denmark), *M. brunneum* KVL 12_30 (Steinwender *et al.,* 2014), *M. acridum* KVL 18_06 (ARSEF 6421), *M. acridum* KVL 04_55 (ARSEF 7486), *M. guizhouense* KVL 19_24 (ARSEF 977), and *M guizhouense* KVL 19_28 (ARSEF 3611). The acronym ARSEF refers to the United States Department of Agriculture (USDA) Agricultural Research Service (ARS) collection of Entomopathogenic Fungal cultures (https://data.nal.usda.gov/dataset/ars-collection-entomopathogenic-fungal-cultures-arsef. URL accessed on 11 March 2022). The acronym KVL refers to the entomopathogenic fungus culture collection maintained at the Section for Organismal Biology, Department of Plant and Environmental Sciences, University of Copenhagen. *Metarhizium* (Metschnikoff) Sorokin (Order Hypocreales: Family Clavicipitaceae) was selected as the focus of our study, due to its multifaceted importance in both evolutionary ecology and practical applications in pest management (Goettel & Glare, 2010; Shah & Pell, 2003; Roberts & Hajek, 1992).

The fungal cultures were grown on quarter-strength Sabouraud dextrose agar + yeast media (SDAY/4: 2.5 g/L 1:1 animal:bacterial peptone (bacteriological peptone and Acuferm Neoeptone, Neogen Corp., 620 Lesher Place, Lansing, MI, USA), 10 g/L dextrose (Bacteriological, Oxoid Ltd., Wade Road, Hampshire, UK), 2.5 g/L yeast extract (Neogen Corp.), 15 g/L agar (Bacteriological (European Type) No. 1, Neogen Corp.))) in Petri dishes (90 mm × 15 mm triple-vented, Sterilin Ltd., 1 Ashley Road, Altrincham, Cheshire, UK) at 23°C, and conidia were harvested after 14 days. The conidia were collected in 0.1% (*v*/*v*) Tween® 80 (Merk KgaA, Frankfurter Straße 250, Darmstadt,

Germany) via agitation with a Drigalski spatula from sporulating colonies, and the resulting suspension was centrifuged; the supernatant was removed, and the colonies were rinsed twice with 0.1% (*v*/*v*) Tween® 80 to remove all fragments of mycelia. Conidial suspensions were prepared at a concentration of 2×10^6 conidia per mL by dilution using 0.1% (*v*/*v*) Tween® 80. The concentration of the stock suspension was determined by counting conidia from 1000× serially diluted stock suspension in a Fuchs Rosenthall hemocytometer (×400 magnification). To verify germination, 100 µL of 100× diluted stock suspension was spread with a Drigalski spatula on an agar plate of SDAY/4 and incubated for 24 h at 23°C. Four microscope coverslips (22 mm × 22 mm) were then placed over the culture surface, and 100 conidia were counted under each coverslip. Conidia were considered to have germinated with the germ tube that was at least as long as the width of the conidium, and conidial germination after 24 h was verified as >98% in all cases before being used in further assays.

2.3.2 Continuous growth curve

To determine whether measurement by spectrophotometry in liquid microcultures can accurately capture the growth curve of an entomopathogenic fungus, a growth curve of *M. brunneum* KVL 12_30 was produced. The microcultures were prepared in 96 wells of a clear flat-bottom vented microplate (Starlab International GmbH, Neuer Höltigbaum 38, Hamburg, Germany) by inoculating 100 µL of 2×10^6 conidial suspension into 100 µL Sabouraud dextrose + yeast media (SDY/4: 2.5 g/L 1:1 animal:bacterial peptone, 10 g/L dextrose, 2.5 g/L yeast extract). The OD of each well was measured at 405nm in a Synergy™ HT MultiDetection Microplate Reader (BioTek Instruments Ltd., Cheadle, UK) with Gen5 software Version 2.00.18 every 10 minutes for 96 hours at 24°C, without removal of the microplate from the plate reader. The wavelength of 405nm was previously described as being fit for this purpose (Meletiadis *et al.,* 2001). Pilot assays were performed comparing a range of wavelengths for measuring growth in microcultures that confirmed this. The microcultures were checked visually for bacteria using a compound microscope upon completion to ensure they were uncontaminated.

2.3.3 Standard curve for fungal dry weight and OD

To establish a correlation between OD and fungal biomass, OD values were measured, and the mycelial mats were subsequently extracted and weighed for the six isolates at four time points (20, 40, 60, and 80 h post-inoculation) during the linear growth phase. The period of logistic growth was determined from the continuous growth curve generated, as detailed in Section 2.2, utilizing the described parameters for media and conidial suspension. The fungal microcultures were prepared as described in Section 2.2. For each measurement at the four time points, a single microplate containing 60 wells was utilized to assess the determination of dry weight, resulting in a total of 240 wells analyzed across the four measurements. To mitigate edge effects arising from temperature and evaporation, the 36 wells around the edge of the plate were excluded from analysis and loaded with 200 µL of blank media (Mansoury *et al.,* 2021). The microplates were incubated at 23 ± 0.5°C, and the OD measured at 405 nm at 20, 40, 60, and 80 h post-inoculation using a SynergyTM HT MultiDetection microplate reader with Gen5 software. At each time point, one microplate per isolate was collected after OD measurement and stored at -20°C. The OD values of all of the microplates were also measured after conidia settled (15 min post-inoculation) to establish the baseline reading OD of each culture. This baseline reading was subtracted from subsequent measurements to determine changes in OD for the construction of standard curves.

To quantify the changes in biomass of the microcultures, mycelial mats were extracted for the determination of dry weight. Thawed microplates were centrifuged in an Eppendorf Centrifuge 5810R (1968× *g*) at 4000 rpm for three minutes to force fungal material to the bottom of the wells, and the remaining media supernatant was removed using a pipette. The wells were then filled with 200 µL of 99% ethanol, and mycelia were scraped from the bottom of the well with a pipette tip to re-suspend the fungal material. The entire content of the well was then transferred to a pre-weighed aluminum weigh boat using a cut pipette tip. The process was repeated three times, refilling each well with 200 µL of ethanol and scraping to ensure complete removal of residual mycelial matter and rinsing of the pipette tip. Thus, a total of 600 µL of ethanol was utilized to

thoroughly wash each well. Complete extraction of mycelial material from the wells was confirmed through microscopic examination of the microplates. If any residual mycelial material was observed, the extraction process was repeated until the wells were free of any remaining matter. For each isolate, ten replicate wells containing resultant mycelial suspensions were pooled into pre-weighed aluminum boats, resulting in a total of six pooled dry weight measurements per microplate with an approximate volume of 6 mL. The pooled samples were subsequently dried in an oven for 72 h at 60 @C within a heat-resistant, lidded box. Finally, the dried samples were weighed on a precision scale (Sartorius ME36S Ultra Micro Balance, 31 g × 0.001 mg, Sartorius UK Ltd., Epsom, UK).

Standard curves were produced to establish the correlation between OD and change in biomass correlated using the OD measurements and their corresponding pooled biomass samples. At each measurement time point, the base OD values were subtracted from the measured OD values, and the resulting OD values for the 10 pooled wells in the sample were averaged. Regression analysis was performed to construct standard curves of OD by dry weight using the R package stats (R Core Team, 2023). To test for differences in relationship between OD and dry weight between isolates, a pairwise comparison of slope estimates was conducted using lsmeans (Lenth, 2016). This analysis applies a P value multiplicity adjustment to the least squares means of each isolate using Tukey's HSD. Linear regression was also performed to determine slope estimates for biomass added over time for each isolate. All statistical calculations were conducted in R Version 1.4.1717 (R Core Team, 2023).

2.3.4 Comparison of OD growth measure to radial growth measure on agar plates

To evaluate how the microspectrophotometric method compared to traditional growth assays performed on solid media, the growth of two isolates (*M. guizhouense* KVL 19_28 and *M. acridum* KVL 04_55) was measured using both microspectrophotometry and radial expansion methods. These experiments were conducted under the same conditions at 23°C in SDY/4 and SDAY/4 media, respectively. For the microspectrophotmetric analysis, media and conidial

suspensions were prepared as described in Section 2.3.2 in a microplate (n = 96). OD measurements were taken during the linear phase of the logistic growth curve (24 h post-inoculation) at 405 nm in 8-hour intervals. This provided a total of five measurements. To estimate the biomass, the linear equations deduced from the standard curves were applied to the spectrophotometric measurements. This allowed for the determination of the biomass estimation based on the spectrophotometric data.

To conduct the radial expansion analysis, for each isolate, four Petri dishes (90 mm × 15 mm, vented) of SDAY/4 were each inoculated with five cultures (n = 20), such that each Petri dish provided 5 cultures. The inoculation was performed using 5 µL of a conidial suspension with a concentration of 2.4×10^4 spores per mL, prepared according to the methods described in Section 2.3.1. Germination of the conidial suspension was confirmed as >99% after 24 h on a plate of SDAY/4, following the methods detailed in Section 2.3.1. The growth was recorded every 4 days, starting from the first day of detectable mycelium formation (day 4) until day 11. To calculate the radial expansion, the plates were digitally photographed at each measurement time point, and the colony area was calculated in ImageJ Version 1.53s (Schneider *et al.,* 2012).

2.4 Results

2.4.1 Growth curves and correlation of biomass with OD

First, it was determined that the entire growth curve of a *Metarhizium* fungus (isolate KVL 12_37, *M. brunneum*) could be captured within a short time period (96 h) using microspectrophotometry (Figure 2.1D). The distinct phases of fungal growth, namely the lag, log (exponential), and stationary phases, were clearly discernible in the preliminary growth curves obtained during the pilot study (Supplemental Figure S2.1). Second, standard curves were produced to quantify the change in culture OD with a corresponding increase in dry weight of fungal biomass over the linear growth phase of the logistic growth curve for two isolates each of *M. guizhouense* (Figure 2.1A), *M. acridum* (Figure 2.1B) and *M. brunneum* (Figure 2.1C). The linear growth phase was determined between 20

and 80 h after inoculation, based on the specified parameters for media and concentration of conidial suspension (Figure 2.1A). The resulting standard curves for dry weight and OD showed high correlation coefficients across all isolates (R2 = 0.93–0.95) (Figure 2.1), but with varying biomass incorporation (i.e., slopes) between isolates (Figure 2.2). In the pairwise comparison of the slope estimates for different isolates, some slope estimates for the relationship between OD and dry weight significantly differed from others (Figure 2.2 and Table 2.1). Notably, the *M. guizhouense* isolates (KVL 19_28 and KVL 19_24) exhibited distinct slope estimates compared to most other isolates, as well as each other (Table 2.1). The slope for isolate KVL 19_28 differed from all other isolates, with significantly larger dry weight estimation compared to all other isolates, with the exception of KVL 16_36 (*M. brunneum*; Table 2.1). Isolate KVL 19_24 was significantly different from KVL 18_06 (*M. acridum*) and KVL 16_36 ($p < 0.05$), with a smaller dry weight estimation compared to these two isolates (Supplemental Figure S2.2).

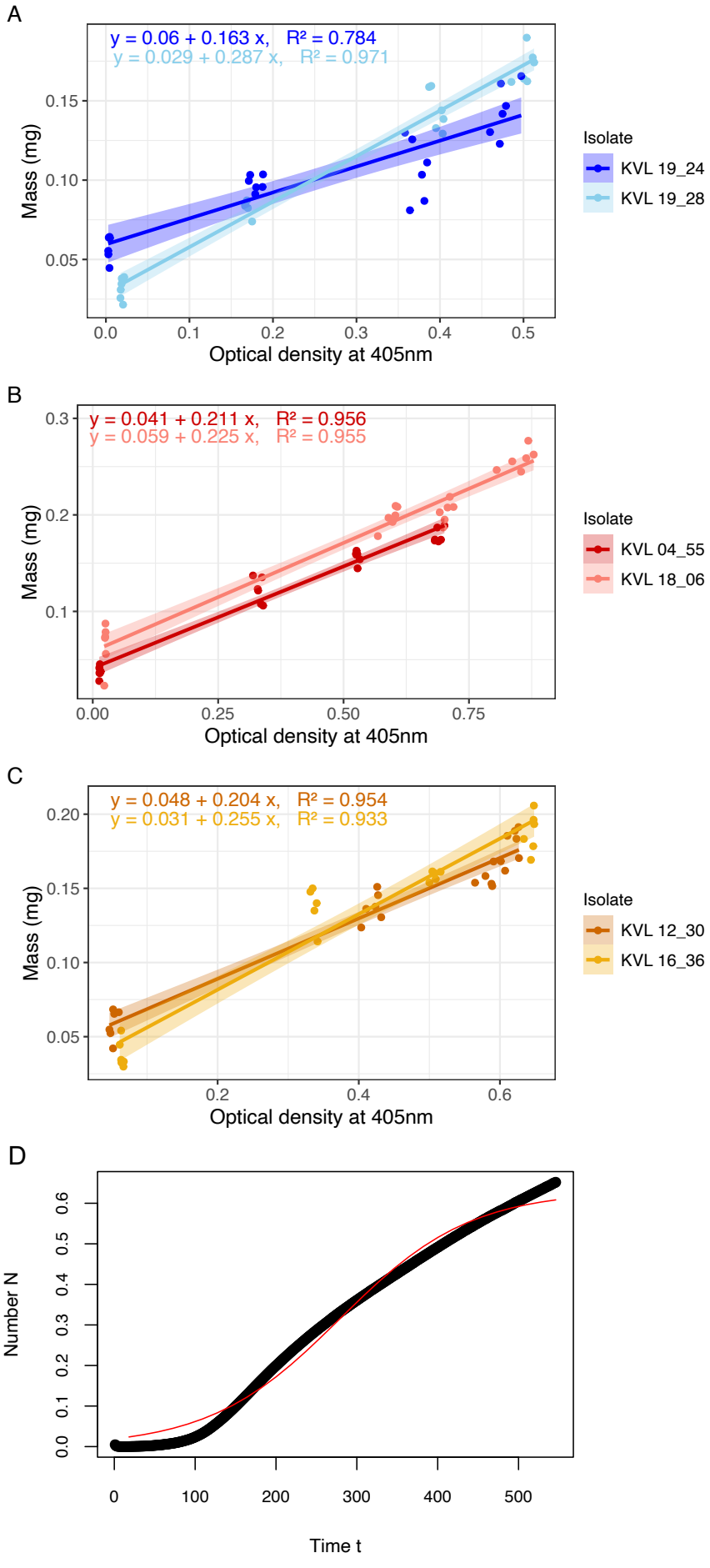
A
y = 0.06 + 0.163 x, R² = 0.784
y = 0.029 + 0.287 x, R² = 0.971
Mass (mg)
Optical density at 405nm
Isolate
KVL 19_24
KVL 19_28
B
y = 0.041 + 0.211 x, R² = 0.956
y = 0.059 + 0.225 x, R² = 0.955
Mass (mg)
Optical density at 405nm
Isolate
KVL 04_55
KVL 18_06
C
y = 0.048 + 0.204 x, R² = 0.954
y = 0.031 + 0.255 x, R² = 0.933
Mass (mg)
Optical density at 405nm
Isolate
KVL 12_30
KVL 16_36
D
Number N
Time t

Figure 2.1 Standard curves and growth curve for *Metarhizium* spp. Standard curves for change in dry weight as a function of optical density (OD) for three species of *Metarhizium*: **(A)** *M. guizhouense* KVL 19_24 and KVL 19_28 (blue and light blue), **(B)** *M. acridum* KVL 04_55 and KVL 18_06 (red and light red) and **(C)** *M. brunnuem* KVL 12_30 and KVL 16_36 (dark yellow and yellow) cultured in a 96-well microplate. Shaded bands around regression lines indicate 95% Confidence Intervals. **(D)** Fitted growth curve over 96 hours using continuous measurement for *M. brunneum* KVL 12_30 for 96 averaged microcultures. Red line indicates fitted logistic growth model and black line is average absorbance readings for 96 wells at each timepoint.

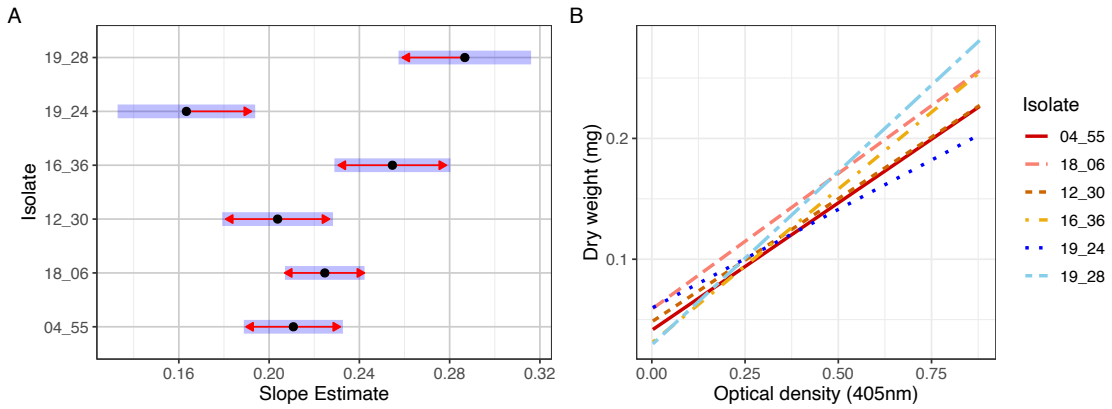

Figure 2.2 Comparison of slope estimates for dry weight as a function of change in optical density over time (OD) among six *Metarhizium* isolates. **(A)** Graphical comparisons of least squares means for each isolate's slope estimate. Black dots indicate slope estimates for biomass as a function of change in OD. The shaded bands are corresponding confidence intervals at an alpha level of 0.1. Arrow lengths indicate the amount by which confidence intervals for differences cover the value 0. **(B)** Corresponding regression lines for dry weight as a function of change in OD for six *Metarhizium* isolates.

Table 2.1 Pairwise comparison of slope estimates for dry weight as a function of change in OD for six *Metarhizium* isolates.

Contrast	Estimate	SE	*p* value[1]
04_55 – 12_30	0.0069	0.0167	0.998
04_55 – 16_36	-0.0439	0.0171	0.113
04_55 – 18_06	-0.0139	0.0142	0.924
04_55 – 19_24	0.0474	0.019	0.133
04_55 – 19_28	-0.076	0.0185	0.001
12_30 – 16_36	-0.0509	0.018	0.059
12_30 – 18_06	-0.0209	0.0153	0.746
12_30 – 19_24	0.0404	0.0198	0.324
12_30 – 19_28	-0.0829	0.0194	0.0005
16_36 – 18_06	0.03	0.0158	0.406
16_36 – 19_24	0.0913	0.0202	0.0002
16_36 – 19_28	-0.0321	0.0197	0.583
18_06 – 19_24	0.0613	0.0178	0.009
18_06 – 19_28	-0.062	0.0173	0.006
19_24 – 19_28	-0.123	0.0214	<.0001

[1] *p* values were adjusted for multiplicity using Tukey's HSD.

The biomass accumulated over time was determined for each isolate using slope coefficients extracted from the linear models (Figure 2.3A) and differences in growth rate among isolates were clearly distinguishable between some isolates (Figure 2.3B). Isolates KVL 19_24 (*M. guizhouense*) grew more slowly and had lower overall biomass than all other isolates (Figure 2.2B, Supplemental Figure S2.2). In contrast, isolate KVL 18_06 of *M. acridum* displayed more rapid growth and achieved a higher overall biomass compared to the other isolates (Figure 2.2B, Supplemental Figure S2.2).

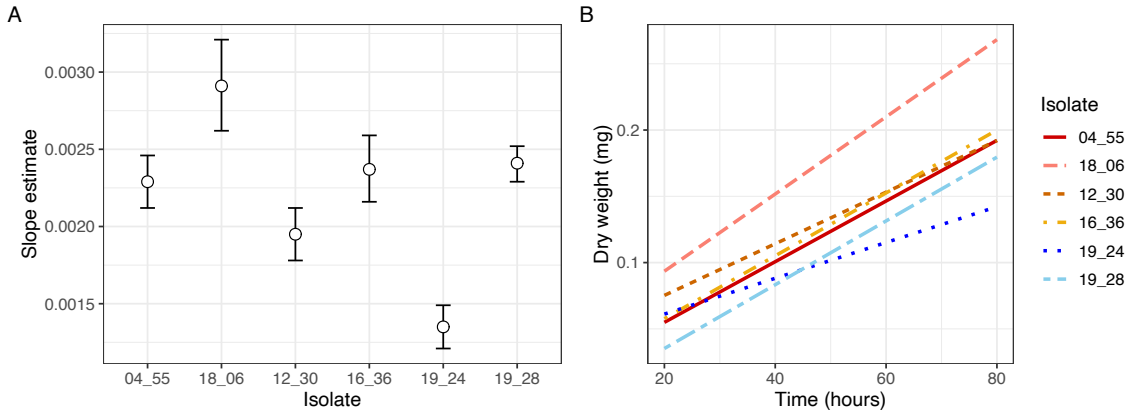

Figure 2.3 Biomass added over time for six *Metarhizium* isolates. **(A)** Slope estimates for linear phase growth rate of six isolates and three species of *Metarhizium* calculated using dry weight measured at 20-hour intervals from 20 to 80 hours (milligrams of dry weight ~ time*isolate). Estimates are for ten pooled microcultures collected from 60 wells in a 96-well microplate, n = 6. White dots indicate the slope estimates with SE bars calculated at an alpha level of 0.1. **(B)** Corresponding regression lines for dry weight (mg) as a function of time in hours in six *Metarhizium* isolates.

2.4.2. Comparison to traditional method and proof of concept

We applied this method to measure the growth rates of two species of *Metarhizium* (*M. guizhouense* KVL 19_28 and *M. acridum* KVL 04_55) over 56 hours from 20 to 80 hours after inoculation (Figure 2.4A), in conjunction with performing the same growth analysis using a radial expansion assay over 11 days (Figure 2.4B). In the microspectrophotometric analysis, the respective linear equations for the two isolates derived from the standard curves were applied to the measured OD values to predict dry weight per well. End point values between both methods showed similar results: both methods indicated the KVL 04_55 (*M. acridum*) isolate had a faster growth rate, growing more overall compared to KVL 19_28 (*M. guizhouense*) whether that was on solid agar media (Figure 2.4A) or using the new technique in liquid media (Figure 2.4B).

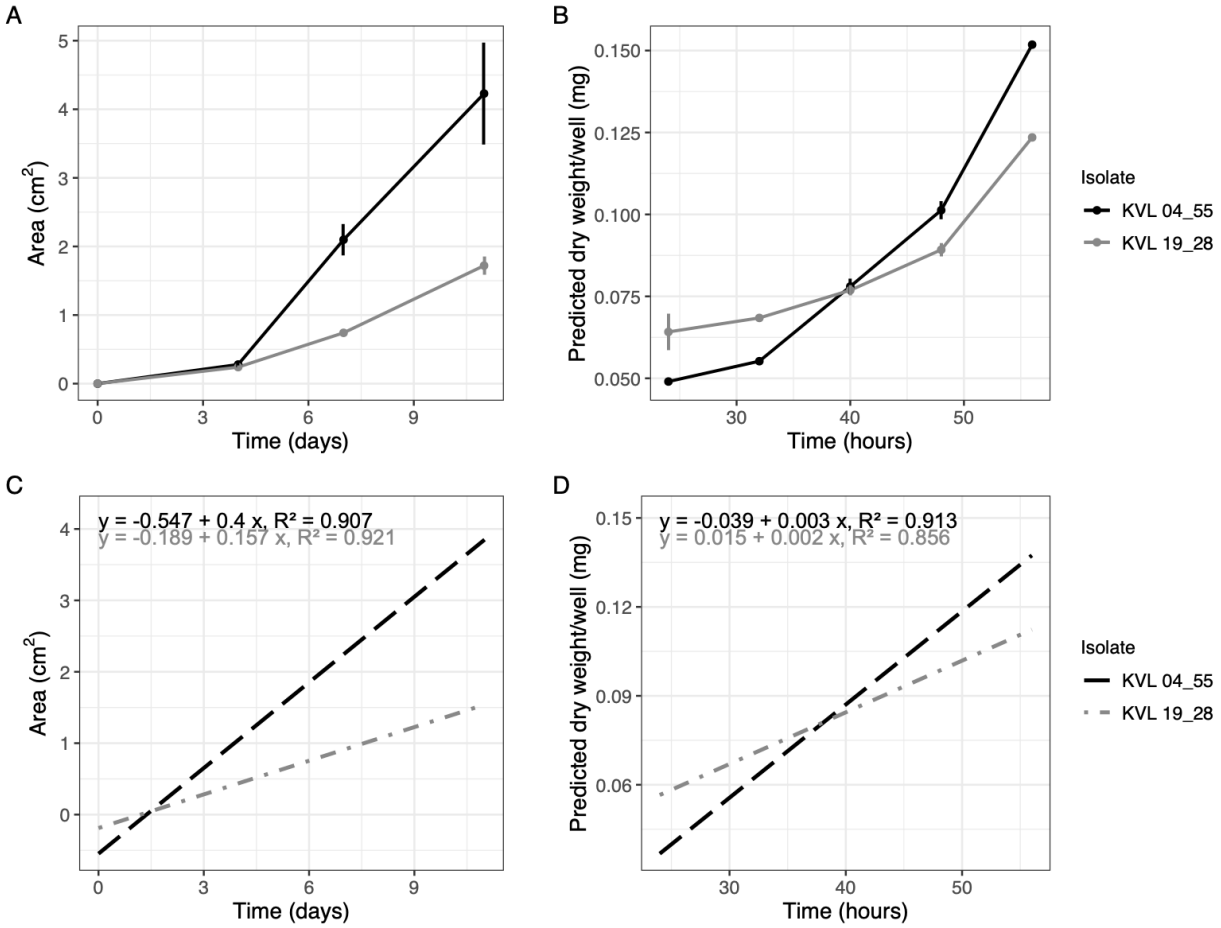

Figure 2.4 Growth curves for *Metarhizium acridum* KVL 04_55 and *M. guizhouense* KVL 19_28 produced on solid agar SDAY/4 media (n = 20) **(A)**, using the new technique in SDY/4 liquid media (n = 96) **(B)**, and regression lines for each **(C, D)**. The equations derived from the standard curves for the relationship between absorbance and dry weight were applied to OD values measured from plates of *Metarhizium* grown over 56 hours to deduce the biomass added over time for each isolate (A). Dots are mean area/colony or predicted biomass/well at each timepoint, and bars indicate standard error. Regression lines (C, D) were obtained using the lm function with the method of least squares.

It is important to note that Figure 2.4A represents a shorter time period of 9 days, whereas Figure 2.4B covers the first 56 h only (approximately 2.33 days). This distinction underscores the significance of our method, as it reveals detailed differences in growth rates that would not be apparent otherwise. While the end points in both figures show similar results, the microspectrophotometric method

provides a more detailed analysis, exposing variations in the initial growth rate. For instance, the KVL 04_55 isolate exhibits slower initial growth, only overtaking the KVL 19_28 isolate after the 40-hour sampling time point (Figure 2.4B). This level of detail allows us to discern growth rate differences that would not be evident from the 1–3 day growth analysis on solid media. Furthermore, an important aspect of the new assay (Figure 2.4A) is the low measurement error observed over this short time period. This reduced error enhances the reliability and accuracy of the growth rate measurements obtained. Finally, we developed linear models to assess the relationship between time and growth for the two measurement methods. Despite the inability to directly compare the regression lines due to the utilization of different measurement methods, the relationship between time and growth appears similar for the different isolates. The remarkable similarity observed in the regression lines (Figure 2.4C,D) indicates that the slopes of the growth rates for the two species of *Metarhizium* are quite similar between assays, although they are at different time scales. This similarity suggests that, regardless of potential variations in initial growth rates or growth patterns observed between the two assays (Figure 2.4A,B), the overall growth rates for both species exhibit a comparable trajectory over time in the context of both measurement methods.

Continuous measurement of OD over time allowed in situ fungal growth to be monitored at a fine scale and with low measurement error, which demonstrated this as a feasible technique for the two isolates of *M. brunneum* (Figures 2.1C and S2.1). This method can also be used to measure ODs at greater intervals, or for end point determination of growth (Figure 2.4). The growth curve generated for *M. brunneum* KVL 12_37 and KVL 12_30 clearly differentiates the lag, exponential, and stationary phases of the growth curve from continuous readings (Figures 2.1A and S2.1).

2.5 Discussion

In this study, we demonstrate that microspectrophotometry can be used to capture the growth curve of entomopathogenic fungi in situ, and that the change

in absorbance can be directly correlated with an increase in fungal biomass. Optical density (OD) values correlated strongly with biomass, and it was demonstrated that it is possible to produce a standard curve for the quantification of dry weight from OD by extracting, drying, and weighing the microcultures of mycelia on a precision scale (Figure 2.1).

In addition, we showed that change in the OD accurately represents biomass accumulation. This is not always the case in measurements of radial expansion, as the expansion of fungal colonies on solid media can often be equal in area, while having significantly different densities of mycelial growth (Cavonas *et al.*, 2017). Fungal cultures grow in multiple planar dimensions on agar (i.e., upwards and downwards, as well as across the substrate surface), and the hyphal mass can thus be more or less dense depending on nutrient availability (Olsson, 2001).

The microspectrophotometric technique provides a quantitative measurement of hyphal density that is more uniformly distributed throughout the microculture, which produces a better representation of three-dimensional hyphal density than measuring two dimensions. This technique also makes it possible to capture specific effects from environmental changes on different fungal growth phase features that are only detectable at small time scales (Figure 2.4B), which produce atypical growth curves, e.g., rapid depletion of a primary nutrient source followed by a secondary phase of logarithmic growth (Vrabl *et al.,* 2019). Furthermore, the solid medium does not accurately represent the environment which entomopathogenic fungi encounter during infection (i.e., insect hemolymph). Given that most entomopathogenic fungi are filamentous with similar ecologies (i.e., penetration of host cuticle and subsequently spreading as individual cells through the insect hemocoel), this technique could be applied to investigate growth in other entomopathogenic species (Mantzoukas *et al.,* 2022). However, differences in biomass accumulation during growth as represented in the relationship between fungal dry weight and OD necessitates the production of standard curves specific to the isolate under investigation, although this would only need to be undertaken once per isolate to be applied to subsequent high throughput measurements.

In this study, we compared the use of microspectrophotometry with radial expansion analysis to assess the growth dynamics of two species of *Metarhizium, M. acridum* and *M. guizhouense*. Our findings demonstrated that the microspectrophotometric analysis yielded similar end point results and linear growth rates compared to the radial growth assay (Figure 2.4A–C). However, the microspectrophotometric technique provided the additional advantage of capturing differences in early growth rates that were not evident in the radial growth assay (Figure 2.4). The finer scale of measurement provided by the microspectrophotometric technique illustrates its value in accurately capturing different aspects of fungal growth curves that might be otherwise undetectable when measuring macroculture growth over many days. Compared to methods with fewer measurement points, this technique is better suited for detecting subtle differences in growth (Figure 2.4).

Importantly, our study revealed a different relationship between *M. acridum* and *M. guizhouense* through finer measurement intervals during critical growth phases, particularly the early linear phase, which could not be discerned through radial expansion measurements performed over several days (Figure 2.4). This development is significant for understanding the growth dynamics of fungi, as it has been previously shown that the classical growth curve does not always adequately describe the growth patterns of filamentous fungi (Vrabl *et al.*, 2019). Different aspects of the growth curve can change due to variables such as nutrition and the host insect environment. Capturing the growth pattern can offer important insights into various aspects of how fungi grow during infection. Notably, atypically shaped growth curves have been suggested to be the rule rather than the exception (Vrabl *et al.,* 2019). This arises from the depletion of distinct nutrients occurring at different rates, resulting in atypical-shaped growth curves, like bimodal growth peaks (Vrabl *et al.,* 2019). These curves reveal nutritive preferences that might be otherwise overlooked without the necessary sensitivity in measurements. Our study revealed that the *M. acridum* KVL 04_55 isolate generally exhibited more growth over time compared to other isolates (Figure 2.4). However, a notable finding was that in the early stages, this isolate displayed a significantly slower growth rate compared to the other isolate

examined, *M. guizhouense* KVL 19_28. This observation provides important insights into the growth dynamics and pathogenic potential during early infection processes for this particular isolate (Frank, 1996).

Additionally, our findings have practical implications regarding the pathogenic potential of the different isolates and species measured. By comparing the growth rates and total biomass produced between isolates, our findings shed light on the potential speed of host invasion (e.g. rate of spread through the haemocoel) across different species of *Metarhizium*. Significantly differing slope estimates and total biomass production were observed not only between species, but also among isolates, indicating variations in pathogenicity potential within this in vitro setting (Figures 2.3 and S2.2). This highlights the practical application of the method in assessing the virulence and pathogenic potential of the examined isolates and species.

Previous studies demonstrated the use of microspectrophotometry in monitoring the growth of filamentous fungi, but were unable to determine the dry weight of individual microcultures, and therefore relied on comparisons of indirect metrics to extrapolate the relationship between OD and fungal dry weight (Granade *et al.,* 1985; Meletiadis *et al.,* 2001), or used microscopic measurements of hyphal extension to infer growth (Meletiadis *et al.,* 2001). In this research, we inferred growth in microculture using mycelial dry weight, and generated standard curves for direct correlation. While the microspectrophotometric technique may provide limited phenotypic information compared to solid media bioassays, such as the measurement of spore production and colony color, it offers complementary advantages in capturing biomass build-up during the early phases of the growth curve, and obtains data rapidly. The speed at which growth data can be obtained using microspectrophotometry is a clear advantage, as linear growth of the tested *Metarhizium* isolates could be measured within a few days, whereas radial growth on agar plates typically takes 10–14 days.

The need to produce entomopathogenic fungi for biocontrol at massive scales makes it important to be able to investigate the effects of different media

and nutrients on entomopathogenic fungal growth, and identify optimal growth parameters (Barra-Bucare *et al.,* 2016). In addition, for experimental biologists, this method allows for large-scale experiments using growth as a primary measure of performance in areas of research such as fitness costs, adaptation (Schoustra *et al.,* 2009), and niche quantification (Shik *et al.,* 2016). A more detailed picture of the different growth phases could provide an understanding of nutritional adaptation, for example, in revealing nutritive preferences (Vrabl *et al.,* 2019).

In conclusion, this technique allows for the rapid generation of growth curves of entomopathogenic fungi at a fine timescale with many replicates, and in a medium that is more ecologically relevant to entomopathogenic fungi than what typical solid media bioassays provide. Furthermore, this approach has the potential for application to other species of filamentous entomopathogenic fungi under investigation, such as *Beauveria* spp., *Hirsutella* spp., *Cordyceps* spp., and *Lecanicillium* spp. (Shah & Pell, 2003). The methodological developments described advance the applications of spectrophotometry to the monitoring of filamentous fungal growth in entomopathogenic fungi, and resolve the infeasibility of producing standard curves directly correlating change in OD with mycelial mass. This automated and high-throughput method for monitoring in situ fungal growth presented here will aid further studies on aspects affecting growth of these ecologically and commercially important organisms.

2.6 Supplemental Figures

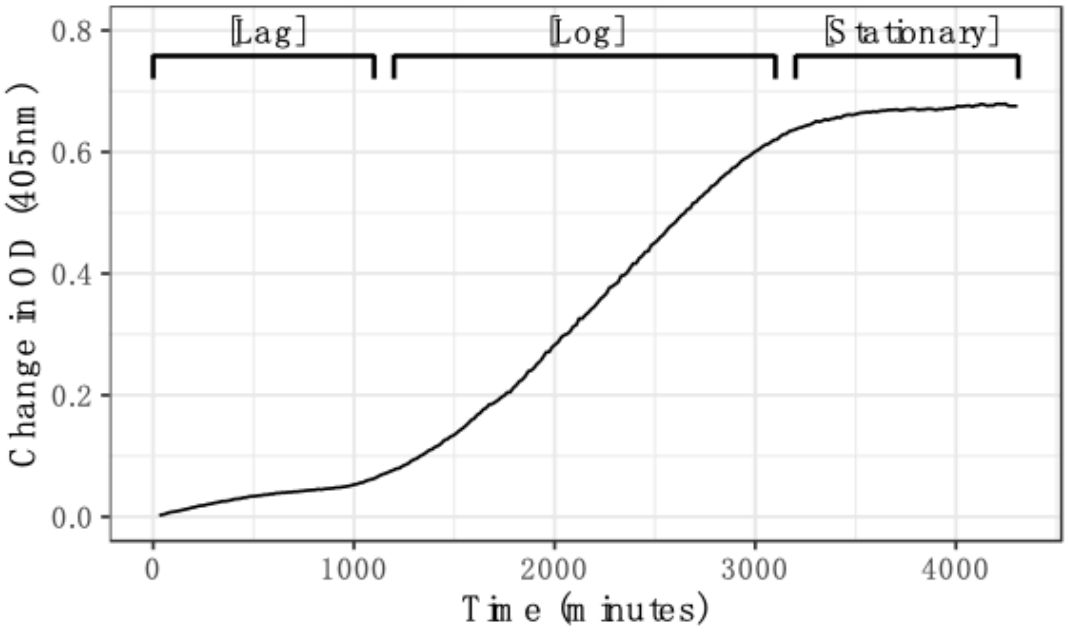

Supplemental Figure S2.1. Growth of *M. brunneum* KVL 12_37. Line indicates OD of 12 cultures grown at 24°C in 100 µL of SDY/4 liquid media in a 96-well plate over 96 h. Absorbance readings were taken every 10 minutes at 405 nm. Demonstrates full growth curve can be captured rapidly using high concentration conidial suspensions. For our purposes we used a lower concentration and longer period of measurement.

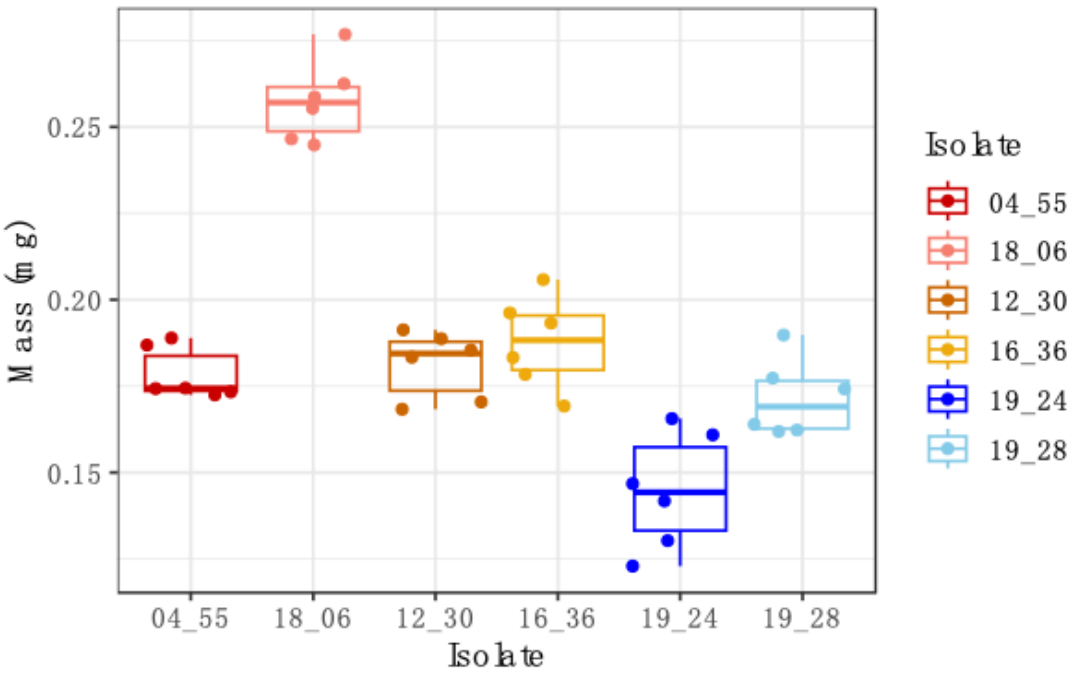

Supplemental Figure S2.2. Dry weight after 80 h in six *Metarhizium* isolates. Dry weight was calculated for mycelial material extracted from ten pooled microcultures grown for 80 h in 60 wells of a microplate (n = 60).

2.7 References

Aidoo, K. E., Hendry, R., & Wood, B. J. B. (1981). Estimation of fungal growth in a solid state fermentation system. *European journal of applied microbiology and biotechnology*, *12*, 6-9.

Augustyniuk-Kram, A., & Kram, K. J. (2012). Entomopathogenic fungi as an important natural regulator of insect outbreaks in forests. *Forest Ecosystems-More Than Just Trees. InTech, Rijeka, Poland*, 265-294.

Banerjee, U. C., Chisti, Y., & Moo-Young, M. (1993). Spectrophotometric determination of mycelial biomass. *Biotechnology techniques*, *7*, 313-316.

Barra-Bucarei, L., Vergara, P., & Cortes, A. (2016). Conditions to optimize mass production of *Metarhizium anisopliae* (Metschn.) Sorokin 1883 in different substrates. *Chilean journal of agricultural research, 76(4), 448-454.*

Cánovas, D., Studt, L., Marcos, A. T., & Strauss, J. (2017). High-throughput format for the phenotyping of fungi on solid substrates. *Scientific Reports*, *7*(1), 1-9.

Ebrahimi, P., van den Berg, F., Aunsbjerg, S. D., Honoré, A., Benfeldt, C., Jensen, H. M., & Engelsen, S. B. (2015). Quantitative determination of mold growth and inhibition by multispectral imaging. *Food Control*, *55*, 82-89.

Frank, S. A. (1996). Models of parasite virulence. *The Quarterly review of biology*, *71*(1), 37-78.

Goettel, M. S., & Glare, T. (2010). 11 Entomopathogenic Fungi and their Role in Regulation of Insect Populations. In *Insect Control*: *Biological and Synthetic Agents.* Elsevier: Amsterdam, The Netherlands.

Gow, N. A., & Gadd, G. M. (Eds.). (1995). *Growing fungus*. Springer Science & Business Media.

Granade, T. C., Hehmann, M. F., & Artis, W. M. (1985). Monitoring of filamentous fungal growth by in situ microspectrophotometry, fragmented mycelium absorbance density, and 14C incorporation: alternatives to mycelial dry weight. *Applied and environmental microbiology*, *49*(1), 101-108.

Gutiérrez–Medina, B., & Vázquez-Villa, A. (2021). Visualizing three-dimensional fungal growth using light sheet fluorescence microscopy. *Fungal Genetics and Biology*, *150*, 103549.

Hickey, P. C., Swift, S. R., Roca, M. G., & Read, N. D. (2004). Live-cell imaging of filamentous fungi using vital fluorescent dyes and confocal microscopy. *Methods in microbiology*, *34*, 63-87.

Jaronski, S. T. (2023). Mass production of entomopathogenic fungi—state of the art. *Mass production of beneficial organisms*, 317-357.

Langvad, F. (1999). A rapid and efficient method for growth measurement of filamentous fungi. *Journal of microbiological methods*, *37*(1), 97-100.

Lee, S. K., Lee, J. H., Kim, H. R., Chun, Y., Lee, J. H., Park, C., & Kim, S. W. (2021). Rapid and concise quantification of mycelial growth by

microscopic image intensity model and application to mass cultivation of fungi. *Scientific reports*, *11*(1), 1-9.

Lovett, B., & St. Leger, R. J. (2017). The insect pathogens. *Microbiology Spectrum*, 5(2), 5-2.

Mansoury, M., Hamed, M., Karmustaji, R., Al Hannan, F., & Safrany, S. T. (2021). The edge effect: A global problem. The trouble with culturing cells in 96-well plates. *Biochemistry and Biophysics Reports 26,* 100987.

Mantzoukas, S., Kitsiou, F., Natsiopoulos, D., & Eliopoulos, P. A. (2022). Entomopathogenic fungi: interactions and applications. *Encyclopedia, 2*(2), 646-656.

Meletiadis, J., Meis, J. F., Mouton, J. W., & Verweij, P. E. (2001). Analysis of growth characteristics of filamentous fungi in different nutrient media. *Journal of Clinical microbiology*, *39*(2), 478-484.

Olsson, S. (2001). Colonial growth of fungi. *Biology of the fungal cell*, 125-141.

Plassard, C. S., Mousain, D. G., & Salsac, L. E. (1982). Estimation of mycelial growth of basidiomycetes by means of chitin determination. *Phytochemistry, 21*(2), 345-348.

Poprawski, T. J., & Majchrowicz, I. (1995). Effects of herbicides on in vitro vegetative growth and sporulation of entomopathogenic fungi. *Crop Protection*, *14*(1), 81-87.

Rangel, D. E., Fernandes, É. K., Dettenmaier, S. J., & Roberts, D. W. (2010). Thermotolerance of germlings and mycelium of the insect-pathogenic fungus *Metarhizium* spp. and mycelial recovery after heat stress. *Journal of Basic Microbiology*, *50*(4), 344-350.

Roberts, D. W., & Hajek, A. E. (1992). Entomopathogenic fungi as bioinsecticides. In *Frontiers in Industrial Mycology*; Springer: Boston, MA, USA, 144-159.

R Core Team (2023). R: A language and environment for statistical computing. R Foundation for Statistical Computing, Vienna, Austria. URL https://www.R-project.org/.

Lenth, R.V. (2016). Least-Squares Means: The R Package lsmeans. *Journal of Statistical Software*, 69(1), 1-33. doi:10.18637/jss.v069.i01

Schneider, C. A., Rasband, W. S., & Eliceiri, K. W. (2012). NIH Image to ImageJ: 25 years of image analysis. *Nature methods*, *9*(7), 671-675.

Schoustra, S. E., Bataillon, T., Gifford, D. R., & Kassen, R. (2009). The properties of adaptive walks in evolving populations of fungus. *PLoS biology*, 7(11), e1000250.

Shah, P. A., & Pell, J. K. (2003). Entomopathogenic fungi as biological control agents. *Applied microbiology and biotechnology*, *61*(5), 413-423.

Shah, F. A., Wang, C. S., & Butt, T. M. (2005). Nutrition influences growth and virulence of the insect-pathogenic fungus *Metarhizium anisopliae*. *FEMS Microbiology Letters*, *251*(2), 259-266.

Shik, J. Z., Kooij, P. W., Donoso, D. A., Santos, J. C., Gomez, E. B., Franco, M., & Boomsma, J. J. (2021). Nutritional niches reveal fundamental domestication trade-offs in fungus-farming ants. *Nature ecology & evolution*, *5*(1), 122-134.

Stanier, R. Y., Doudoroff, M., & Adelberg, E. A. (1976). The microbial world.

Steinwender, B. M., Enkerli, J., Widmer, F., Eilenberg, J., Thorup-Kristensen, K., & Meyling, N. V. (2014). Molecular diversity of the entomopathogenic fungal *Metarhizium* community within an agroecosystem. *Journal of invertebrate pathology*, *123*, 6-12.

Taniwaki, M. H., Pitt, J. I., Hocking, A. D., & Fleet, G. H. (2006). Comparison of hyphal length, ergosterol, mycelium dry weight, and colony diameter for quantifying growth of fungi from foods. In *Advances in food mycology* (pp. 49-67). Boston, MA: Springer US.

Trinci, A. P. J. (1971). Influence of the width of the peripheral growth zone on the radial growth rate of fungal colonies on solid media. *Microbiology*, *67*(3), 325-344.

VanderMolen, K. M., Raja, H. A., El-Elimat, T., & Oberlies, N. H. (2013). Evaluation of culture media for the production of secondary metabolites in a natural products screening program. *Amb Express, 3*, 1-7.

Viniegra-González, G., Favela-Torres, E., Aguilar, C. N., de Jesus Rómero-Gomez, S., Dıaz-Godınez, G., & Augur, C. (2003). Advantages of fungal

enzyme production in solid state over liquid fermentation systems. *Biochemical Engineering Journal*, *13*(2-3), 157-167.

Vrabl, P., Schinagl, C. W., Artmann, D. J., Heiss, B., & Burgstaller, W. (2019). Fungal growth in batch culture–what we could benefit if we start looking closer. *Frontiers in microbiology*, *10*, 2391.

Yeo, H., Pell, J. K., Alderson, P. G., Clark, S. J., & Pye, B. J. (2003). Laboratory evaluation of temperature effects on the germination and growth of entomopathogenic fungi and on their pathogenicity to two aphid species. *Pest Management Science: formerly Pesticide Science*, *59*(2), 156-165.

Chapter 3

Phenotypic variation in nutritional niche breadth among *Metarhizium* species with different host ranges

Anna R. Slowik[1, 2, 3], Helen H. Hesketh[2], Steven M. Sait[3], and Henrik H. De Fine Licht[1]

[1]University of Copenhagen, Department of Plant and Environmental Sciences, Thorvaldsensvej 40, 1871 Frederiksberg C., Denmark.
[2]UK Centre for Ecology & Hydrology, Maclean Building, Benson Lane, Crowmarsh Gifford, Wallingford, OX10 8BB, United Kingdom.
[3]School of Biology, Faculty of Biological Sciences, University of Leeds, Leeds, LS2 9JT, United Kingdom.

Manuscript in preparation for submission.

This chapter explores the nutritional needs and preferences of the *Metarhizium* fungal genus, which includes species with different host ranges, e.g. the number of species that they are capable of parasitizing. Using a method called nutritional geometry, models were created to illustrate the optimal nutrition in terms of protein and carbohydrates for different *Metarhizium* species. It was discovered that *M. acridum*, which is a locust specialist, has specific nutritional preference. In contrast, *M. guizhouense*, which is considered to have broader host range, can utilize a wider range of nutrient sources. The link between nutrition and how generalized or specialized these species are can offer insights into their ecological roles.

Phenotypic variation in nutritional niche breadth among *Metarhizium* species with different host ranges

3.1 Abstract

This study explores the phenotypic variation in nutritional niches among *Metarhizium* species, a globally distributed entomopathogenic fungal genus with diverse ecological roles and host ranges, ranging from highly specialized insect pathogens to endophytic opportunistic pathogens. Through an experimentally constructed nutritional landscape, with varying carbohydrate (C) to protein (P) ratios (C:P) and concentrations, we utilized nutritional geometry to quantify and compare the fundamental nutritional niches of generalist and specialist species. We constructed generalized linear mixed-effects models to compare growth at different ratios and between species. *M. acridum* grew more overall at higher diet concentrations, while *M. guizhouense* performed better in lower, nutrient-poor diets. The findings reveal a wider nutritional niche breadth in the broad host-range species, *M. guizhouense,* compared to the locust-specific pathogen, *M. acridum,* corroborating our hypothesis that organisms with narrower ecological niches also exhibit nutritional specialization. This research demonstrates the relationship between ecological niche breadth and nutritional ecology in the *Metarhizium* genus.

3.2 Introduction

The genus *Metarhizium* is a diverse group of entomopathogenic fungi (EPF) globally distributed and recognized for its adaptability across varied ecological niches (St. Leger, 2024). *Metarhizium's* multifunctional lifestyles range from parasites of highly specific above ground insect populations to plant-root symbionts generally adapted to opportunistically parasitize a broad range of soil-dwelling insects (St. Leger & Wang, 2020). These fungi exemplify the breadth of adaptational strategies of specialization and generalization, with some species demonstrating a high degree of host specificity while others maintain a generalized ability to infect a broad range of insects. Specialist species are

restricted in pathogenic potential, like *M. acridum* which is found only on locusts and grasshoppers, while more generalist species like *M. guizhouense* have been shown to be pathogenic to at least two orders of insects (Hu *et al.,* 2014). The breadth of the ecological adaptability of *Metarhizium* is further illustrated by its resilience and ability to thrive in diverse environmental conditions, from temperate to tropical ecosystems (St. Leger & Wang, 2020; Lovett & St. Leger, 2015). This versatility raises questions about the genus's niche breadth—the range of conditions and resources it can utilize—and how this breadth may relate to its success in various ecological roles.

It is currently not entirely clear how niche width on different niche axes correlates in fungal symbionts (Bebber & Chaloner, 2022). In a metanalysis of plant pathogens investigating correlation between host range (determined by phylogenetic distances of hosts) and temperature, Carscadden *et al.* (2020) found no indication that specialization on those axes were correlated. They suggested that the extent of correlation in niche width might be influenced by factors like environmental stimuli or functional limitations, and that it is the fluctuations in environmental conditions, not their absolute values, that could potentially shape these correlations (Carscadden *et al.,* 2020). Bebber and Chaloner (2022) summarize this relationship as “rather than a generalist being ‘Jack of all trades, master of none’, a species can be ‘Jack of some trades, master of others’.” When we specifically consider the *Metarhizium* genus, this genus has been described as “jack of all trades, master of many”, exhibiting the versatility to thrive in a variety of environments and different species functioning either as specialist or generalist fungal pathogens of insects (St. Leger & Wang, 2020). Such adaptability arises from the fungus's significant flexibility across genetic, physiological, and ecological dimensions (St. Leger & Wang 2020).

The genus *Metarhizium* presents a unique and tractable model for investigating nutritional ecology and host-specialization within the context of host-pathogen interactions. Characterized by its diverse host range and complex ecological adaptations, *Metarhizium* spp. provide an opportunity to examine the nuanced relationships between nutrient acquisition, utilization efficiency, and ecological niche specialization. The interaction dynamics between these fungi

and their respective hosts represent a broad spectrum of adaptive strategies, offering a comprehensive model to study the morphological, physiological, and biochemical adaptations resulting from nutritional constraints and opportunities within their specific ecological contexts, which can be explored using Nutritional Geometry.

The framework of nutritional geometry (Raubenheimer *et al.,* 2009), allows for the quantification of nutritional niches in the context of both quantity and ratio of essential nutrients, thus allowing for an understanding of the nutritional interactions driving organisms' feeding behavior, growth, and survival. Nutritional geometry has been recognized as a useful tool in exploring the nutritional adaptability of organisms, grounding the understanding of their ecological roles and evolutionary trajectories within a quantifiable matrix of nutritional parameters. It provides a lens through which the correlation between the ecological niches and nutritional needs of *Metarhizium* species can be methodically examined and understood. Though many studies have explored the host-pathogen dynamics of *Metarhizium*, a comprehensive understanding of how these interactions are influenced by, and in turn influence, their nutritional ecology is still emerging (Cotter & Al Shareefi, 2022).

Nutritional ecology in entomopathogenic fungi (EPF) is complex, yet essential for understanding the adaptational strategies of species in the genus *Metarhizium*. Previous research has primarily focused on virulence, germination, and conidial yield in response to varied media compositions. (Li & Holdom, 1995). Safavi *et al.* (2007) reported optimal growth of *M. anisopliae* in high-Carbon to Nitrogen (C:N) ratio (75:1) agar media, but alongside a decrease in conidial yield. This finding aligns with studies by Kamp & Bidochka (2002) and Vega *et al*. (2003), where a 10:1 C:N ratio was identified as optimal for conidial production, indicating a shift in resource allocation from spore production to growth under nutrient limitations. The performance (e.g. spore germination, hyphal growth, and sporulation) of EPF is also influenced by the type and availability of carbon sources, as different types of carbon are more or less available and nutritionally appropriate for EPF (Sun & Liu, 2006). Sun and Liu evaluated the growth of 11 *M. anisopliae* isolates with 33 different carbon sources and reported variability in

nutrient utilization, also among isolates of the same species (2006). This strain-dependent variability in nutritional preference was correlated with the geographical location and host from which the isolates were derived, indicating a potential influence of ecological factors on nutritional adaptation (Sun & Liu, 2006). These findings highlight the importance of considering strain-specific, geographical, and host-dependent variables in studies of *Metarhizium* nutritional ecology.

Here we investigate phenotypic variation in nutritional niches between EPF with different host ranges. It is often inferred that organisms have different nutritional needs based on their specific ecologies (Simpson & Raubenheimer, 2012). The diverse ecological roles and adaptational strategies of *Metarhizium* fungi could suggest that different nutritional requirements are associated with their distinct ecological niches, e.g. generalist or specialist, rhizosphere colonizer or insect-pathogen. Furthermore, in our current understanding of evolutionary ecology, it is not clear to what extent specialist symbionts are specialized across different aspects of their existences, and whether their specialization is limited to certain areas or even a single aspect of their lifestyle (Bebber & Chaloner, 2022). Here, our aim is to determine if, and how, the ecological lifestyles between two species of *Metarhizium* translate to varied nutritional adaptations by quantifying the fundamental nutritional niches of a generalist and specialist species, which we define as the niche without any biotic interactions (Carscadden *et al.,* 2020).

3.3 Materials and Methods

We used the method described in Slowik *et al.* (2023) to measure fungal growth in liquid media microcultures using spectrophotometry. We constructed nutritional landscapes using 24 experimentally defined artificial media varying in total amounts and relative (C:P ratio) amounts of carbohydrates and protein for a specialist EPF, the locust-specific pathogen *M. acridum,* and an EPF with a broader host range, *M. guizhouense.* Pilot studies informed our choice of C:P ratios, which indicated protein was a highly limiting nutrient, and we therefore used four concentrations (1, 4, 8, and 12 g/L) of six C:P ratios (90:1, 60:1, 30:1, 10:1, 1:1 and 1:10) for the different medias. Stock solutions of each C:P ratio

were prepared and diluted to the desired concentrations. Growth was then measured in 96-well microplates for two fungal isolates, *M. guizhouense* (KVL 19-28) and *M. acridum* (ARSEF_5735; KVL 18-06) over 80 hours. The abbreviation KVL designates the EPF fungal collection maintained at the section for Organismal Biology, Dept. of Plant and Environmental Sciences, University of Copenhagen.

Each concentration treatment with every ratio treatment was used to grow both isolates in microplates, with two replicated plates and two replicates of spore suspensions. For every ratio present on each plate, 10 cultures were grown. The two replicates of each concentration and spore suspension resulted in a total of 40 microcultures for each ratio and concentration for both species. Initial optical density (OD) values, which were measured using a SPECTRAmax 340PC microplate spectrophotometer for each individual well taken at 0 hrs, were subtracted from the subsequent measurements, and endpoint measurements after 80 hours were used as a measure of total growth to construct the landscapes. We used R version 4.1.1 to construct nutritional landscapes with the package “fields” (R Core Team, 2016; Nychka *et al.,* 2021). This package creates continuous surfaces or “heatmaps” from spatially referenced data points. It does so by interpolating the data across a grid, using methods like kriging, a form of Bayesian optimization, to visualize spatial patterns and relationships in the data (Williams, 1998).

We then created general linearized mixed effects models (GLMMs) using the “lme4” package at each diet concentration for each species to compare the growth responses to diet concentration using the formula “overall growth ~ ratio + (1 | spore suspension/replicate)” (Bates *et al.,* 2015). We used the R package “multcomp” to perform post-hoc pairwise comparisons between diet ratios, with Bonferroni p value adjustment for multiple comparisons (Hothorn *et al.,* 2008). To determine differences in growth between species at each ratio, we created GLMMs defined by the formula “overall growth ~ species * ratio + (1 | spore suspension/replicate)” at each concentration, and performed post-hoc pairwise comparisons using “multcomp” with Bonferroni p value adjustment (Bates *et al.,* 2015; Hothorn *et al.,* 2008). The overall difference in growth between species at

each concentration was determined using Tukey's HSD test on anovas of each model R (Hothorn *et al*., 2008; R Core Team, 2023).

3.4 Results

We obtained data for the fundamental nutritional niche for the two species of *Metarhzium* fungi with different host ranges. The data collected in the growth assay was used to create nutritional landscape models for each fungus (Figure 3.1). These models reveal the areas of optimal nutrition and the niche breadth across different ratios and concentrations of proteins and carbohydrates. For *M. guizhouense*, a species with intermediate host range, a wider area of nutrient utilization was observed (Figure 3.1B). This species was capable of growing well across a broad range of protein-limited diet compositions. Conversely, *M. acridum*, an orthopteran specialist, exhibited a more constrained nutritional profile (Figure 3.1A). Its growth was optimal in specific 2:1 carbohydrate:protein ratios, reflecting a more specialized nutritional niche.

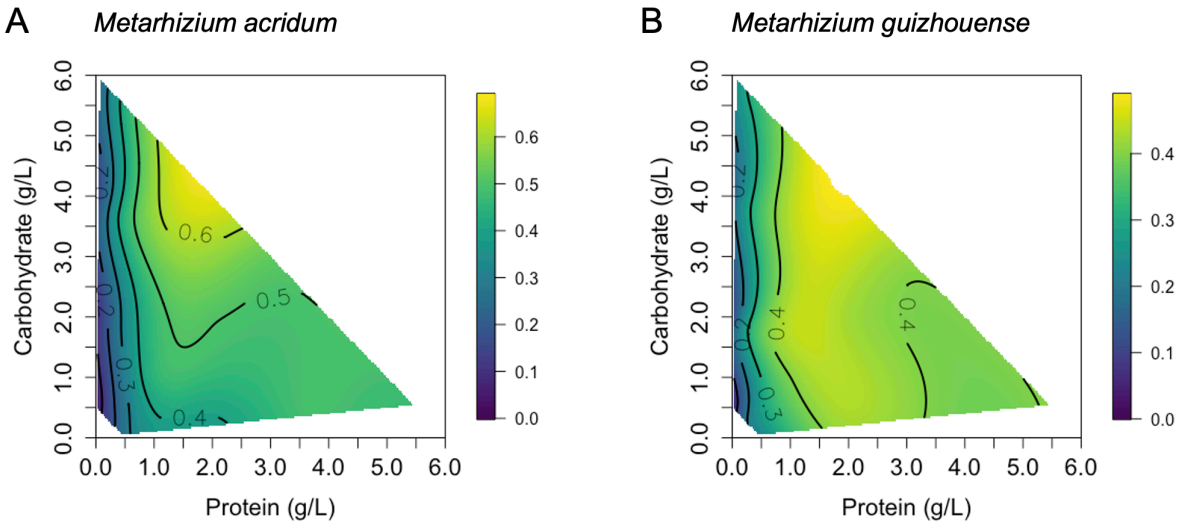

Figure 3.1 Nutritional landscapes of *M. acridum* and *M. guizhouense.* Fungal isolate performance mapped across a landscape of 24 experimentally defined artificial media varying in total amounts and relative (C:P ratio) amounts of carbohydrates and protein for a specialist EPF, *M. acridum* **(A)**, and a transitionalist, *M. guizhouense* **(B)**. Growth is measured as the increase in OD

from the initial (blanked) to the final measurement. Dark blue indicates lowest value for growth area and yellow highest.

We modeled growth as a response variable to diet ratios at each diet concentration to determine effect from C:P ratios (Figure 3.2, Supplemental Tables S3.1 – S3.8) and also compared growth at each concentration and ratio combination between the two species (Figure 3.3, Supplemental Tables S3.9 – S3.12). There was a pronounced optima observed in *M. acridum,* where growth increased between the 1:10 C:P diet and the 1:1 C:P diet, at all diet concentrations above 1 g/L (Figure 3.2), which is not observed in *M. guizhouense.* Furthermore, at the most nutrient-poor diet concentration of 1 g/L, there is no significant difference in growth between the two higher protein diets (1:10 and 1:1 C:P) in *M. guizhouense.* This indicates protein was more of a limiting nutrient for *M. acridum,* where there was significantly more growth at the higher protein ratio (1:10 C:P).

The differential analysis comparing growth between the two species revealed that *M. acridum* consistently outperforms *M. guizhouense* in terms of overall growth at higher protein diets in high diet concentrations (Figure 3.3). This pattern persists until reaching a protein-limited 30:1 diet ratio, where the growth rates of both species converge. At this highly protein-limited diet, *M. guizhouense* demonstrates comparable efficiency to *M. acridum* in nutrient utilization. Notably, at the lower nutrient concentrations of 1 and 4 g/L, *M. guizhouense* exhibits higher growth compared to *M. acridum* on diets richer in carbohydrates (Figure 3.3 A, B). At a diet concentration of 1 g/L, a significant difference in overall growth was observed between *M. guizhouense* and *M. acridum*. The general linear mixed-effects model, with species, ratio, and their interaction as fixed effects and spore suspension/replicate as random effects, indicated that *M. guizhouense* exhibited less growth compared to *M. acridum* (estimate = -0.05828, standard error = 0.00361, $z = -16.14$, $p < 0.001$). At 4 g/L, *M. guizhouense* showed significantly greater overall growth compared to *M. acridum* (estimate = 0.04705, SE = 0.007477, $z = 6.293$, $p < 0.001$). This suggests that while protein is a key factor driving the growth advantage for *M. acridum*, *M. guizhouense's* broader dietary

flexibility allows it to better capitalize on carbohydrate availability, particularly under nutrient-scarce conditions. *M. guizhouense* exhibited significantly less overall growth than *M. acridum* at the higher concentrations of 8 g/L (estimate = -0.09108, SE = 0.004815, $z = -18.92$, $p < 0.001$) and 12 g/L (estimate = -0.08354, SE = 0.005483, $z = -15.24$, $p < 0.001$). These results indicate a consistent pattern where *M. acridum* outperforms *M. guizhouense* at higher nutrient concentrations, and the reverse is true of the nutrient-limited diets of 1 and 4 g/L concentration where the trend reverses.

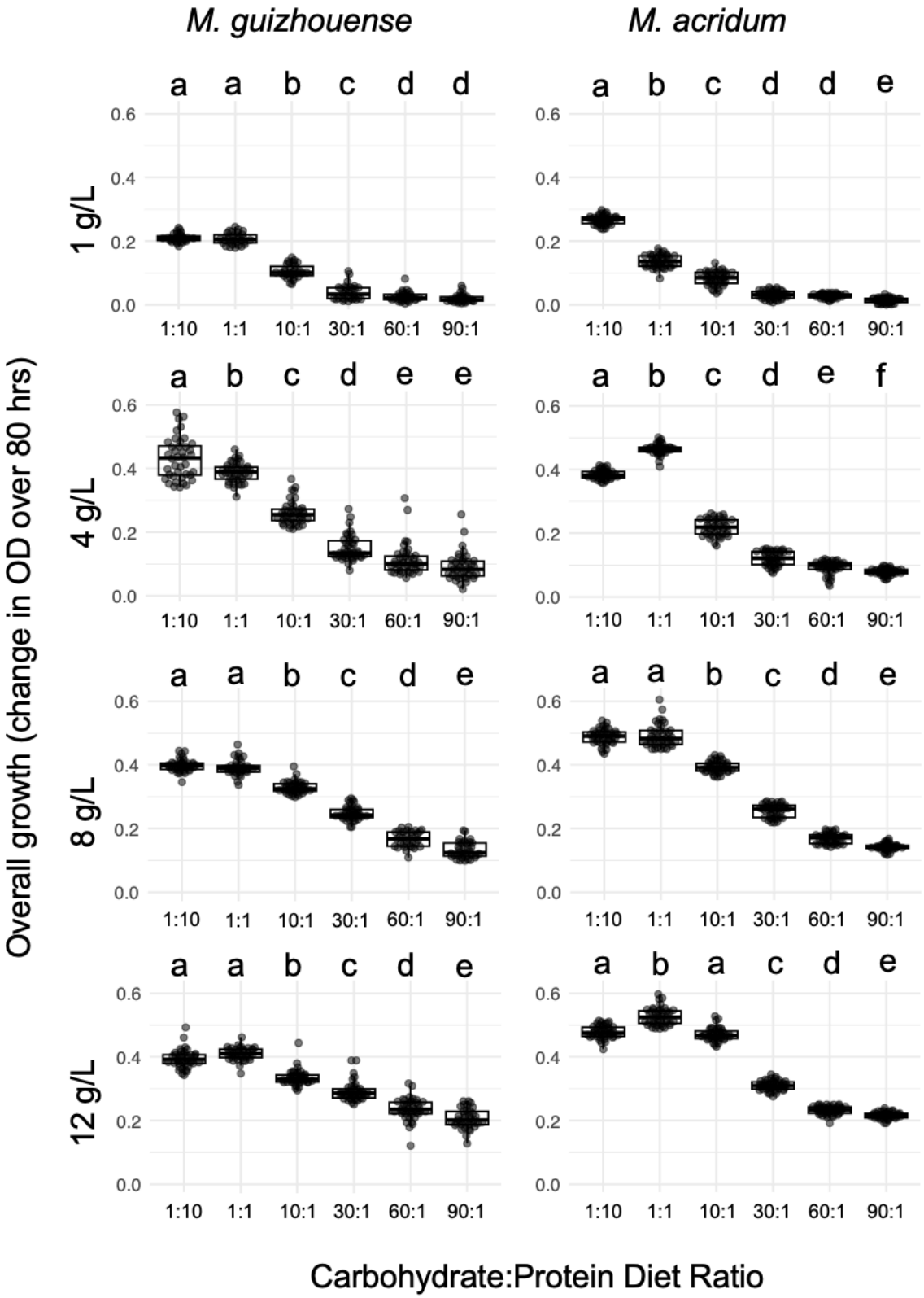

Figure 3.2 Comparative analysis of *M. guizhouense* and *M. acridum* growth response to varied carbohydrate to protein diet ratios and diet concentration. Overall growth is measured as the change in optical density (OD) over 80 hours. Each panel represents a different total nutrient concentration (1, 4, 8, and 12 g/L) and illustrates the growth pattern across ratios of 1:10 to 90:1 (C:P). The box

plots depict the distribution of growth responses within each nutrient ratio, with letters above the plots indicating statistically distinct groups at $p < 0.05$. The data points are individual growth measurements from replicated cultures.

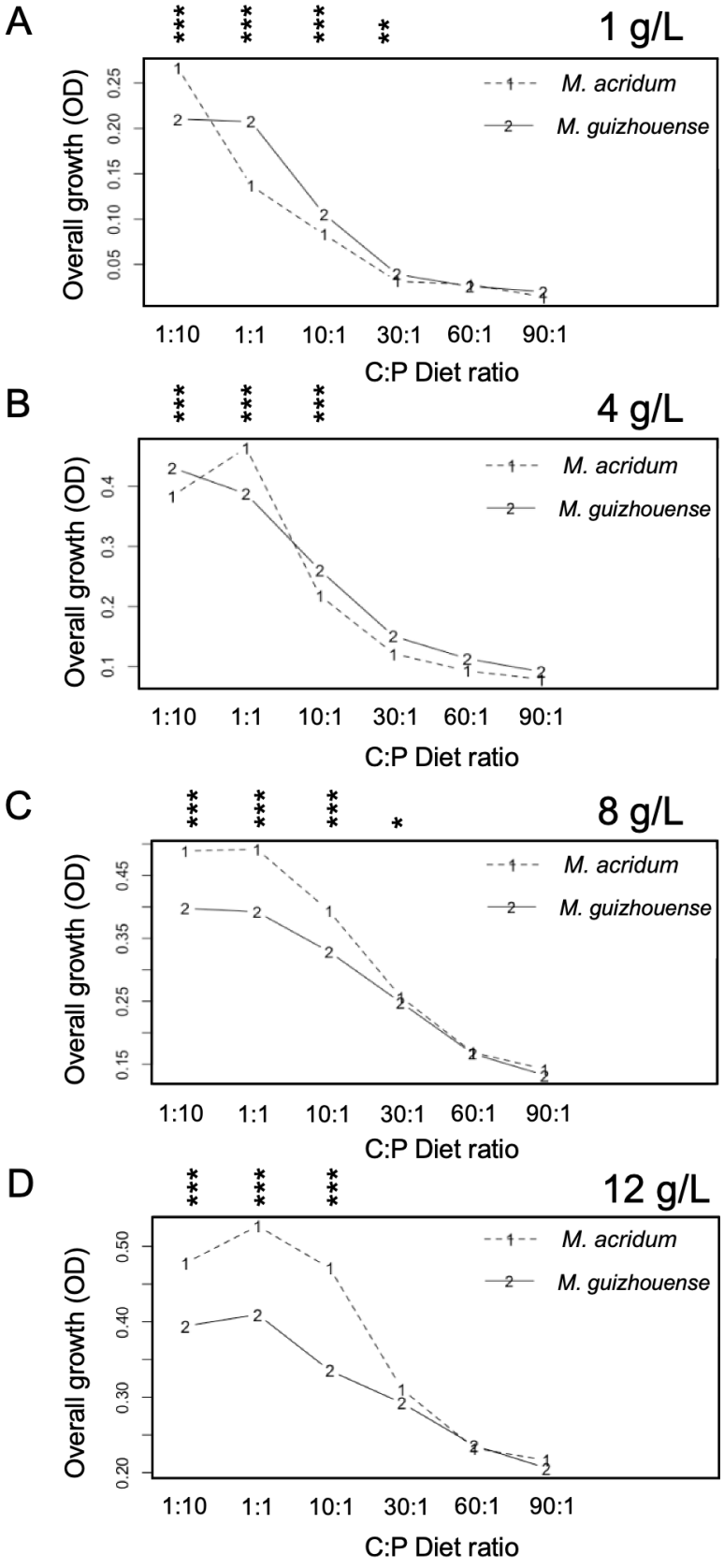
A
***
***
***
**
1 g/L
Overall growth (OD)
0.05
0.10
0.15
0.20
0.25
M. acridum
M. guizhouense
1:10
1:1
10:1
30:1
60:1
90:1
C:P Diet ratio
B
***
***
***
4 g/L
Overall growth (OD)
0.1
0.2
0.3
0.4
M. acridum
M. guizhouense
1:10
1:1
10:1
30:1
60:1
90:1
C:P Diet ratio
C
***
***
***
*
8 g/L
Overall growth (OD)
0.15
0.25
0.35
0.45
M. acridum
M. guizhouense
1:10
1:1
10:1
30:1
60:1
90:1
C:P Diet ratio
D
***
***
***
12 g/L
Overall growth (OD)
0.20
0.30
0.40
0.50
M. acridum
M. guizhouense
1:10
1:1
10:1
30:1
60:1
90:1
C:P Diet ratio

Figure 3.3 Differential growth dynamics of *M. guizhouense* and *M. acridum* across nutrient concentrations and C:P ratios. A statistical comparison of growth, measured in optical density (OD) over 80 hours, between *M. guizhouense* and *M. acridum*. Each graph corresponds to a different total nutrient concentration (1, 4, 8, and 12 g/L), plotted against a series of C:P diet ratios ranging from 1:10 to 90:1. Statistically significant differences in growth between the two species at each diet concentration and ratio are denoted by asterisks above the data points, with the level of significance indicated by the number of asterisks (*** = $p < 0.001$, ** = $p < 0.01$, * = $p < 0.05$).

3.5 Discussion

In this study, we explored the phenotypic variation in nutritional niches among two *Metarhizium* species, emphasizing the distinct differences between generalist and specialist fungi. Through the implementation of an experimentally constructed nutritional landscape and statistical comparisons of growth, we have quantified the breadth of their fundamental nutritional niches and the efficiency of their nutrient utilization strategies.

Our findings corroborate the prevailing hypothesis in the ecological literature that the breadth of an organism's ecological niche is intrinsically linked to its nutritional requirements and adaptability (Raubenheimer *et al.,* 2009; Simpson & Raubenheimer, 2012; Futuyma & Moreno, 1988; Verboom *et al.,* 2017). *Metarhizium guizhouense's* capability to grow well across a diverse range of nutrient ratios, especially under protein limitation, aligns with its generalist ecology and versatility (Figure 3.1B). This flexibility in nutrient utilization may confer an advantage in the variable and competitive soil environment where symbiotic interactions with plant roots provide access to carbohydrate-rich resources. The wider nutritional niche breadth of *M. guizhouense* could be reflective of potential resilience to fluctuating environmental conditions, a characteristic feature of generalist species (St. Leger & Wang, 2020). Conversely, the specialist *M. acridum*, exhibited a narrower, more specialized nutritional niche, reflecting its optimization for specific environmental and

nutritional conditions, which likely involves exploiting the protein-rich environments within its orthopteran hosts (Figure 3.1 A). Our growth analyses, modeled across a spectrum of diet ratios and concentrations, further support the notion of *M. acridum's* efficiency in nutrient use, particularly in protein-rich conditions (Figure 3.2). Interestingly, the growth rates of *M. acridum* and *M. guizhouense* converge at lower protein concentrations, suggesting a protein threshold beyond which *M. guizhouense* is as- or more-effective in utilizing the carbohydrate-heavy diet (Figure 3.3). This is evident from the differential growth dynamics, where *M. guizhouense* exhibits higher growth than *M. acridum* in carbohydrate-rich diets, especially at lower concentrations (Figure 3.3).

In the broader context of niche width correlations and the degree of specialization across varied life traits, our observations indicate a correlation between two axes of niche breadth, nutrition and host range, for these entomopathogenic fungi. Specialist organisms often exhibit heightened sensitivity and adaptability to specific environmental parameters, optimizing their survival and reproductive success within limited ecological spaces (Futumaya & Moreno, 1988). Generalists, conversely, tend to exhibit broader tolerances, enabling them to exploit a wider array of ecological opportunities but often at the expense of optimization for any single niche (Futumaya & Moreno, 1988). We can further understand the nutritional interactions between insects and EPF by contextualizing our findings within the established nutrient profiles of typical insect hosts and the nutrient-rich rhizosphere. For instance, *Tenebrio molitor*, a common insect host, comprises approximately 20% protein and 11.5% crude carbohydrate, with a soluble sugar fraction of 30% (Mariod, 2021; Son *et al*., 2021). This composition does not align perfectly with the 2:1 carbohydrate to protein ratios identified as optimal for *M. acridum*, however we did demonstrate that *M. acridum* is more effective at utilizing protein-rich diets than *M. guizhouense*. *Metarhizium* generalists, such as *M. guizhouense*, have been shown to associate with a variety of plant species, colonizing different plant tissues like roots, stems, and leaves, and are important rhizosphere colonizers (Flonc *et al.,* 2021; Stone & Bidochka, 2020; Sheng *et al.,* 2022). These interactions are often mediated by the carbohydrates available from root

exudates in the rhizosphere, which may explain the broader nutritional niche and the resilience of these generalists to variations in nutrient availability (Wang *et al.,* 2005; Nehls *et al.,* 2010).

In conclusion, this study advances the fundamental understanding of the nutritional ecology of EPF and underscores the connection between ecological lifestyles and nutritional ecology in the *Metarhizium* genus. The distinct variation in nutritional niches between the generalist and specialist species studied here illuminates the adaptive strategies that underlie their ecological distributions and interactions. While the correlations between different niche dimensions in fungal symbionts are not completely understood, this study demonstrates a correlation between the niche axes of host-specificity and nutritional requirements. These insights deepen our understanding of host-pathogen interactions, the fundamental ecological niche concept, and the ecology of entomopathogenic fungi.

3.6 References

Bates, D., Mächler, M., Bolker, B., & Walker, S. (2015). Fitting Linear Mixed-Effects Models Using lme4. *Journal of Statistical Software*, *67*(1), 1–48.

Bebber, D. P., & Chaloner, T. M. (2022). Specialists, generalists and the shape of the ecological niche in fungi. *The New Phytologist*, *234*(2), 345.

Blonder B., Lamanna, C., Violle, C., & Enquist, B. J. (2014). The n-dimensional hypervolume. *Global Ecology and Biogeography, 23*, 595–609.

Carscadden, K. A., Emery, N. C., Arnillas, C. A., Cadotte, M. W., Afkhami, M. E., Gravel, D., Livingstone, S. W., & Wiens, J. J. (2020). Niche breadth: causes and consequences for ecology, evolution, and conservation. *The Quarterly Review of Biology*, *95*(3), 179-214.

Cotter, S. C., & Al Shareefi, E. (2022). Nutritional ecology, infection and immune defence—exploring the mechanisms. *Current Opinion in Insect Science*, *50*, 100862.

Flonc, B., Barbercheck, M., & Ahmad, I. (2021). Observations on the relationships between endophytic *Metarhizium robertsii, Spodoptera frugiperda* (Lepidoptera: Noctuidae), and maize. *Pathogens*, *10*(6), 713.

Futuyma, D. J., & Moreno, G. (1988). The evolution of ecological specialization. *Annual Review of Ecology and Systematics 19*, 207–233.

Hothorn, T., Bretz., F., & Westfall, P. (2008). Simultaneous Interference in General Parametric Models. *Biometrical Journal, 50*(3), 346-363.

Hu, X., Xiao, G., Zheng, P., Shang, Y., Su, Y., Zhang, X., & Wang, C. (2014). Trajectory and genomic determinants of fungal-pathogen speciation and host adaptation. *Proceedings of the National Academy of Sciences*, *111*(47), 16796-16801.

Kamp, A. & Bidochka, M. (2002). Conidium production by insect pathogenic fungi on commercially available agars. *Letters in Applied Microbiology, 35*(1), 74-77.

Li, D., & Holdom, D. (1995). Effects of nutrients on colony formation, growth, and sporulation of *Metarhizium anisopliae* (Deuteromycotina: Hyphomycetes). *Journal of Invertebrate Pathology, 65*(3), 253-260.

Lovett, B., & St. Leger, R. J. (2015). Stress is the rule rather than the exception for Metarhizium. *Current genetics*, *61*, 253-261.

Mariod, A. A. (2020). Nutrient composition of mealworm (*Tenebrio molitor*). *African Edible Insects as Alternative Source of Food, Oil, Protein and Bioactive Components*, 275-280.

Nehls, U., Göhringer, F., Wittulsky, S., & Dietz, S. (2010). Fungal carbohydrate support in the ectomycorrhizal symbiosis: a review. *Plant Biology*, *12*(2), 292-301.

Nychka, D., Furrer, R., Paige, J., & Sain, S. (2021). fields: Tools for spatial data. R package version 15.2, <https://github.com/dnychka/fieldsRPackage>.

R Core Team. (2023). R: A Language and Environment for Statistical Computing. R Foundation for Statistical Computing, Vienna, Austria.

Raubenheimer, D., Simpson, S. J., & Mayntz, D. (2009). Nutrition, Ecology and Nutritional Ecology: Toward an Integrated Framework. *Functional Ecology*, *23*(1), 4–16.

Safavi, S. (2007). Effect of nutrition on growth and virulence of the entomopathogenic fungus *Beauveria bassiana*. *FEMS Microbiology Letters, 27*(1), 116-123.

Schluter, D., T. Price, A. Ø. Mooers, & D. Ludwig. (1997). Likelihood of ancestor states in adaptive radiation. *Evolution, 51,* 1699–1711.

Sheng, H., McNamara, P. J., & St. Leger, R. J. (2022). *Metarhizium*: an opportunistic middleman for multitrophic lifestyles. *Current Opinion in Microbiology*, *69*, 102176.

Simpson, S. J., & Raubenheimer, D. (2012). *The nature of nutrition: a unifying framework from animal adaptation to human obesity*. Princeton university press.

Slowik, A. R., Hesketh, H., Sait, S. M., & De Fine Licht, H. H. (2023). A Rapid Method for Measuring In Vitro Growth in Entomopathogenic Fungi. *Insects*, *14*(8), 703.

Son, Y. J., Hwang, I. K., Nho, C. W., Kim, S. M., & Kim, S. H. (2021). Determination of carbohydrate composition in mealworm (*Tenebrio*

molitor L.) larvae and characterization of mealworm chitin and chitosan. *Foods*, *10*(3), 640.

Stone, L. B., & Bidochka, M. J. (2020). The multifunctional lifestyles of *Metarhizium*: Evolution and applications. *Applied microbiology and biotechnology*, *104*(23), 9935-9945.

St. Leger, R. J. (2024). The evolution of complex *Metarhizium*-insect-plant interactions. *Fungal Biology*.

St. Leger, R. J., & Wang, J. B. (2020). *Metarhizium:* jack of all trades, master of many. *Open Biology*, *10*(12), 200307.

Sun, M. and Liu, X. (2006). Carbon requirements of some nematophagous, entomopathogenic and mycoparasitic hyphomycetes as fungal biocontrol agents. *Mycopathologia, 161*(5), 295-305.

Vega, F. E., & Kaya, H. K. (2012). *Insect pathology* (Vol. 2). Academic press.

Vega, F. E., Jackson, M. A., Mercadier, G., & Poprawski, T. J. (2003). The impact of nutrition on spore yields for various fungal entomopathogens in liquid culture. *World journal of Microbiology and Biotechnology*, *19*, 363-368.

Verboom, G. A., Stock, W. D., & Cramer, M. D. (2017). Specialization to extremely low-nutrient soils limits the nutritional adaptability of plant lineages. *The American Naturalist*, *189*(6), 684-699.

Wang, C., Hu, G., & St. Leger, R. J. (2005). Differential gene expression by *Metarhizium anisopliae* growing in root exudate and host (*Manduca sexta*) cuticle or hemolymph reveals mechanisms of physiological adaptation. *Fungal genetics and biology*, *42*(8), 704-718.

Williams, C. K. (1998). Prediction with Gaussian processes: From linear regression to linear prediction and beyond. In *Learning in graphical models* (pp. 599-621). Dordrecht: Springer Netherlands.

Zembrzuski, D., Woller, D. A., Jaronski, S., Black, L. R., Reuter, K. C., Grief, D., & Cease, A. J. (2023). Understanding how diet and temperature affect survival and subsequent sporulation in a major rangeland grasshopper pest, *Melanoplus sanguinipes*, infected with the entomopathogenic fungus, *Metarhizium robertsii*. *Biological Control*, *183*, 105268.

3.7 Supplemental materials

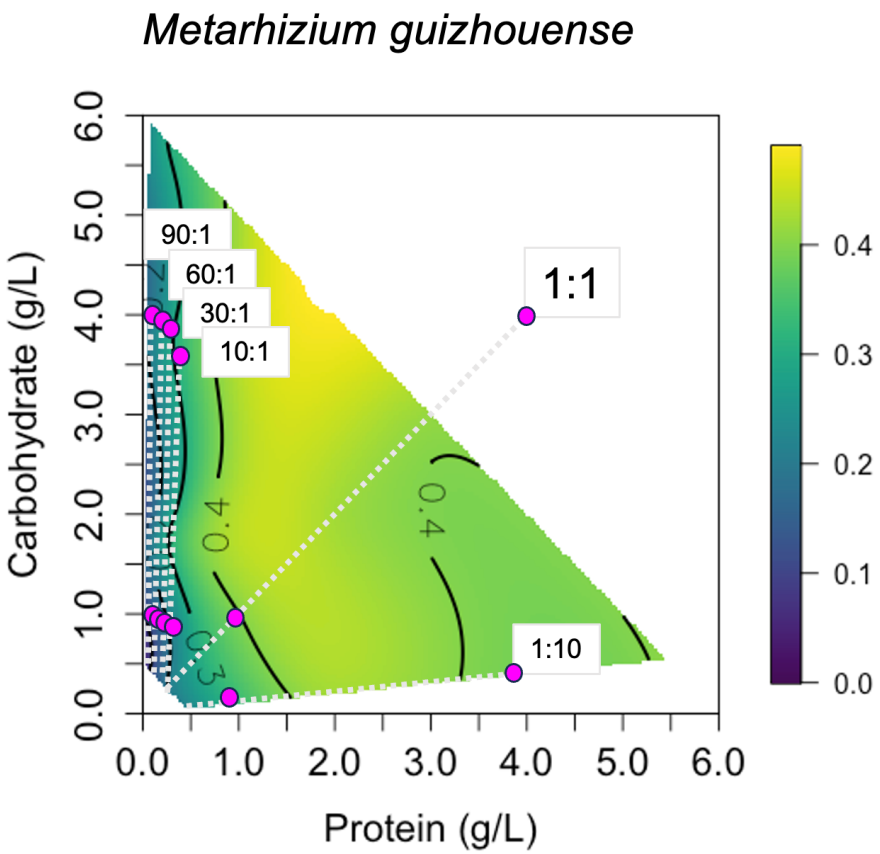

Supplementary Figure S3.4 Explanation of how nutritional landscape plots were generated using the *M. guizhouense* plot. Fungal isolate performance was mapped across a landscape of 12 experimentally defined artificial media varying in total amounts and relative (C:P ratio) amounts of carbohydrates and protein. Growth is measured as the increase in OD from the initial (blanked) to the final measurement. Dark blue indicates lowest value for growth area and yellow highest. The pink dots show roughly the actual ratios and concentrations measured. Six nutrient ratios are demarcated by grey dashed lines and labeled boxes, intersecting four concentrations along these ratios, as exemplified by the pink dots. Plots were capped at 6 g/L. This enabled the dimensionality of the heat maps to illustrate the areas of greatest growth.

Supplemental Table S3.1

Bonferroni contrasts for diet ratios: *M. guizhouense* at 1 g/L

Diet ratio contrast	Estimate	Std. Error	z value	Pr(>|z|)	
1to1 - 10to1 == 0	-0.002889	0.004466	-0.647	1.000000	
1to10 - 10to1 == 0	-0.104944	0.004466	-23.498	< 2e-16	***
1to30 - 10to1 == 0	-0.171190	0.004466	-38.330	< 2e-16	***
1to60 - 10to1 == 0	-0.184662	0.004466	-41.347	< 2e-16	***
1to90 - 10to1 == 0	-0.190328	0.004466	-42.616	< 2e-16	***
1to10 - 1to1 == 0	-0.102056	0.004466	-22.851	< 2e-16	***
1to30 - 1to1 == 0	-0.168301	0.004466	-37.684	< 2e-16	***
1to60 - 1to1 == 0	-0.181773	0.004466	-40.700	< 2e-16	***
1to90 - 1to1 == 0	-0.187439	0.004466	-41.969	< 2e-16	***
1to30 - 1to10 == 0	-0.066245	0.004466	-14.833	< 2e-16	***
1to60 - 1to10 == 0	-0.079717	0.004466	-17.849	< 2e-16	***
1to90 - 1to10 == 0	-0.085383	0.004466	-19.118	< 2e-16	***
1to60 - 1to30 == 0	-0.013472	0.004466	-3.016	0.038359	*
1to90 - 1to30 == 0	-0.019138	0.004466	-4.285	0.000274	***
1to90 - 1to60 == 0	-0.005666	0.004466	-1.269	1.000000	

Signif. codes: 0 '***' 0.001 '**' 0.01 '*' 0.05 '.' 0.1 ' ' 1

(Adjusted p values reported -- bonferroni method)

Supplemental Table S3.2

Bonferroni contrasts for diet ratios: *M. acridum* at 1 g/L

Diet ratio contrast	Estimate	Std. Error	z value	Pr(>|z|)	
1to1 - 10to1 == 0	-0.129662	0.002757	-47.032	< 2e-16	***
1to10 - 10to1 == 0	-0.183493	0.002757	-66.558	< 2e-16	***
1to30 - 10to1 == 0	-0.235224	0.002757	-85.322	< 2e-16	***
1to60 - 10to1 == 0	-0.238683	0.002757	-86.577	< 2e-16	***
1to90 - 10to1 == 0	-0.252412	0.002757	-91.557	< 2e-16	***
1to10 - 1to1 == 0	-0.053831	0.002757	-19.526	< 2e-16	***
1to30 - 1to1 == 0	-0.105562	0.002757	-38.290	< 2e-16	***
1to60 - 1to1 == 0	-0.109021	0.002757	-39.545	< 2e-16	***
1to90 - 1to1 == 0	-0.122750	0.002757	-44.525	< 2e-16	***
1to30 - 1to10 == 0	-0.051731	0.002757	-18.764	< 2e-16	***
1to60 - 1to10 == 0	-0.055191	0.002757	-20.019	< 2e-16	***
1to90 - 1to10 == 0	-0.068919	0.002757	-24.999	< 2e-16	***
1to60 - 1to30 == 0	-0.003460	0.002757	-1.255	1	
1to90 - 1to30 == 0	-0.017188	0.002757	-6.235	6.80e-09	***
1to90 - 1to60 == 0	-0.013728	0.002757	-4.980	9.56e-06	***

Signif. codes: 0 '***' 0.001 '**' 0.01 '*' 0.05 '.' 0.1 ' ' 1

(Adjusted p values reported -- bonferroni method)

Supplemental Table S3.3

Bonferroni contrasts for diet ratios: for *M. guizhouense* at 4 g/L

Diet ratio contrast	Estimate	Std. Error	z value	Pr(>|z|)	
1to1 - 10to1 == 0	-0.04350	0.01002	-4.341	0.000213	***
1to10 - 10to1 == 0	-0.17076	0.01002	-17.038	< 2e-16	***
1to30 - 10to1 == 0	-0.28070	0.01002	-28.008	< 2e-16	***
1to60 - 10to1 == 0	-0.31819	0.01002	-31.749	< 2e-16	***
1to90 - 10to1 == 0	-0.34002	0.01002	-33.927	< 2e-16	***
1to10 - 1to1 == 0	-0.12726	0.01002	-12.698	< 2e-16	***
1to30 - 1to1 == 0	-0.23720	0.01002	-23.668	< 2e-16	***
1to60 - 1to1 == 0	-0.27469	0.01002	-27.408	< 2e-16	***
1to90 - 1to1 == 0	-0.29652	0.01002	-29.587	< 2e-16	***
1to30 - 1to10 == 0	-0.10994	0.01002	-10.970	< 2e-16	***
1to60 - 1to10 == 0	-0.14743	0.01002	-14.711	< 2e-16	***
1to90 - 1to10 == 0	-0.16926	0.01002	-16.889	< 2e-16	***
1to60 - 1to30 == 0	-0.03749	0.01002	-3.741	0.002750	**
1to90 - 1to30 == 0	-0.05932	0.01002	-5.919	4.86e-08	***
1to90 - 1to60 == 0	-0.02183	0.01002	-2.178	0.440925	

Signif. codes: 0 '***' 0.001 '**' 0.01 '*' 0.05 '.' 0.1 ' ' 1

(Adjusted p values reported -- bonferroni method)

Supplemental Table S3.4

Bonferroni contrasts for diet ratios: *M. acridum* at 4 g/L

Diet ratio contrast	Estimate	Std. Error	z value	Pr(>|z|)	
1to1 - 10to1 == 0	0.07993	0.00331	24.148	< 2e-16	***
1to10 - 10to1 == 0	-0.16591	0.00331	-50.125	< 2e-16	***
1to30 - 10to1 == 0	-0.26290	0.00331	-79.430	< 2e-16	***
1to60 - 10to1 == 0	-0.29141	0.00331	-88.042	< 2e-16	***
1to90 - 10to1 == 0	-0.30541	0.00331	-92.273	< 2e-16	***
1to10 - 1to1 == 0	-0.24583	0.00331	-74.273	< 2e-16	***
1to30 - 1to1 == 0	-0.34283	0.00331	-103.578	< 2e-16	***
1to60 - 1to1 == 0	-0.37133	0.00331	-112.190	< 2e-16	***
1to90 - 1to1 == 0	-0.38534	0.00331	-116.421	< 2e-16	***
1to30 - 1to10 == 0	-0.09699	0.00331	-29.305	< 2e-16	***
1to60 - 1to10 == 0	-0.12550	0.00331	-37.917	< 2e-16	***
1to90 - 1to10 == 0	-0.13950	0.00331	-42.148	< 2e-16	***
1to60 - 1to30 == 0	-0.02850	0.00331	-8.612	< 2e-16	***
1to90 - 1to30 == 0	-0.04251	0.00331	-12.843	< 2e-16	***
1to90 - 1to60 == 0	-0.01401	0.00331	-4.231	0.000349	***

Signif. codes: 0 '***' 0.001 '**' 0.01 '*' 0.05 '.' 0.1 ' ' 1

(Adjusted p values reported -- bonferroni method)

Supplemental Table S3.5

Bonferroni contrasts for diet ratios: *M. guizhouense* at 8 g/L

Diet ratio contrast	Estimate	Std. Error	z value	Pr(>|z|)	
1to1 - 10to1 == 0	-0.006318	0.005128	-1.232	1	
1to10 - 10to1 == 0	-0.068957	0.004913	-14.036	< 2e-16	***
1to30 - 10to1 == 0	-0.150068	0.004978	-30.149	< 2e-16	***
1to60 - 10to1 == 0	-0.231462	0.005170	-44.768	< 2e-16	***
1to90 - 10to1 == 0	-0.264997	0.005128	-51.677	< 2e-16	***
1to10 - 1to1 == 0	-0.062639	0.005128	-12.215	< 2e-16	***
1to30 - 1to1 == 0	-0.143751	0.005188	-27.709	< 2e-16	***
1to60 - 1to1 == 0	-0.225145	0.005376	-41.878	< 2e-16	***
1to90 - 1to1 == 0	-0.258680	0.005339	-48.447	< 2e-16	***
1to30 - 1to10 == 0	-0.081111	0.004978	-16.295	< 2e-16	***
1to60 - 1to10 == 0	-0.162505	0.005170	-31.431	< 2e-16	***
1to90 - 1to10 == 0	-0.196040	0.005128	-38.229	< 2e-16	***
1to60 - 1to30 == 0	-0.081394	0.005231	-15.559	< 2e-16	***
1to90 - 1to30 == 0	-0.114929	0.005192	-22.135	< 2e-16	***
1to90 - 1to60 == 0	-0.033535	0.005377	-6.237	6.69e-09	***

Signif. codes: 0 ‘***’ 0.001 ‘**’ 0.01 ‘*’ 0.05 ‘.’ 0.1 ‘ ’ 1

(Adjusted p values reported -- bonferroni method)

Supplemental Table S3.6

Bonferroni contrasts for diet ratios: *M. acridum* at 8 g/L

Diet ratio contrast	Estimate	Std. Error	z value	Pr(>|z|)	
1to1 - 10to1 == 0	0.002523	0.004475	0.564	1	
1to10 - 10to1 == 0	-0.095530	0.004475	-21.346	< 2e-16	***
1to30 - 10to1 == 0	-0.232408	0.004475	-51.930	< 2e-16	***
1to60 - 10to1 == 0	-0.320371	0.004475	-71.585	< 2e-16	***
1to90 - 10to1 == 0	-0.346758	0.004504	-76.983	< 2e-16	***
1to10 - 1to1 == 0	-0.098054	0.004475	-21.909	< 2e-16	***
1to30 - 1to1 == 0	-0.234931	0.004475	-52.494	< 2e-16	***
1to60 - 1to1 == 0	-0.322894	0.004475	-72.149	< 2e-16	***
1to90 - 1to1 == 0	-0.349282	0.004504	-77.543	< 2e-16	***
1to30 - 1to10 == 0	-0.136877	0.004475	-30.584	< 2e-16	***
1to60 - 1to10 == 0	-0.224841	0.004475	-50.239	< 2e-16	***
1to90 - 1to10 == 0	-0.251228	0.004504	-55.775	< 2e-16	***
1to60 - 1to30 == 0	-0.087964	0.004475	-19.655	< 2e-16	***
1to90 - 1to30 == 0	-0.114351	0.004504	-25.387	< 2e-16	***
1to90 - 1to60 == 0	-0.026387	0.004504	-5.858	7.02e-08	***

Signif. codes: 0 ‘***’ 0.001 ‘**’ 0.01 ‘*’ 0.05 ‘.’ 0.1 ‘ ’ 1

(Adjusted p values reported -- bonferroni method)

Supplemental Table S3.7

Bonferroni contrasts for diet ratios: *M. guizhouense* at 12 g/L

Diet ratio contrast	Estimate	Std. Error	z value	Pr(>|z|)	
1to1 - 10to1 == 0	0.014718	0.006364	2.313	0.311	
1to10 - 10to1 == 0	-0.059205	0.006189	-9.566	< 2e-16	***
1to30 - 10to1 == 0	-0.102022	0.006150	-16.588	< 2e-16	***
1to60 - 10to1 == 0	-0.158110	0.006150	-25.708	< 2e-16	***
1to90 - 10to1 == 0	-0.187954	0.006273	-29.964	< 2e-16	***
1to10 - 1to1 == 0	-0.073923	0.006364	-11.616	< 2e-16	***
1to30 - 1to1 == 0	-0.116739	0.006327	-18.450	< 2e-16	***
1to60 - 1to1 == 0	-0.172828	0.006327	-27.315	< 2e-16	***
1to90 - 1to1 == 0	-0.202672	0.006447	-31.436	< 2e-16	***
1to30 - 1to10 == 0	-0.042816	0.006150	-6.962	5.04e-11	***
1to60 - 1to10 == 0	-0.098905	0.006150	-16.082	< 2e-16	***
1to90 - 1to10 == 0	-0.128749	0.006273	-20.526	< 2e-16	***
1to60 - 1to30 == 0	-0.056088	0.006111	-9.178	< 2e-16	***
1to90 - 1to30 == 0	-0.085933	0.006234	-13.785	< 2e-16	***
1to90 - 1to60 == 0	-0.029844	0.006234	-4.787	2.53e-05	***

Signif. codes: 0 ‘***’ 0.001 ‘**’ 0.01 ‘*’ 0.05 ‘.’ 0.1 ‘ ’ 1

(Adjusted p values reported -- bonferroni method)

Supplemental Table S3.8

Bonferroni contrasts for diet ratios: *M. acridum* at 12 g/L

Diet ratio contrast	Estimate	Std. Error	z value	Pr(>|z|)	
1to1 - 10to1 == 0	0.049042	0.003849	12.742	< 2e-16	***
1to10 - 10to1 == 0	-0.007132	0.003849	-1.853	0.958209	
1to30 - 10to1 == 0	-0.167610	0.003849	-43.549	< 2e-16	***
1to60 - 10to1 == 0	-0.245613	0.003849	-63.817	< 2e-16	***
1to90 - 10to1 == 0	-0.261614	0.003849	-67.974	< 2e-16	***
1to10 - 1to1 == 0	-0.056173	0.003849	-14.595	< 2e-16	***
1to30 - 1to1 == 0	-0.216652	0.003849	-56.292	< 2e-16	***
1to60 - 1to1 == 0	-0.294654	0.003849	-76.559	< 2e-16	***
1to90 - 1to1 == 0	-0.310656	0.003849	-80.716	< 2e-16	***
1to30 - 1to10 == 0	-0.160478	0.003849	-41.696	< 2e-16	***
1to60 - 1to10 == 0	-0.238481	0.003849	-61.964	< 2e-16	***
1to90 - 1to10 == 0	-0.254482	0.003849	-66.121	< 2e-16	***
1to60 - 1to30 == 0	-0.078003	0.003849	-20.267	< 2e-16	***
1to90 - 1to30 == 0	-0.094004	0.003849	-24.425	< 2e-16	***
1to90 - 1to60 == 0	-0.016001	0.003849	-4.158	0.000483	***

Signif. codes: 0 ‘***’ 0.001 ‘**’ 0.01 ‘*’ 0.05 ‘.’ 0.1 ‘ ’ 1

(Adjusted p values reported -- bonferroni method)

Supplementary Table S3.10. Bonferroni contrasts between species at 1 g/L

contrast	estimate	SE	t.ratio	p.value
acridum 10to1 - guizhouense 10to1	0.05828	0.00363	16.065	<.0001
acridum 1to1 - guizhouense 1to1	-0.06849	0.00723	18.878	<.0001
acridum 1to10 - guizhouense 1to10	-0.02026	0.00383	-5.586	<.0001
acridum 1to30 - guizhouense 1to30	-0.00575	0.00538	-1.585	0.9138
acridum 1to60 - guizhouense 1to60	0.00426	0.00231	1.175	0.9906
acridum 1to90 - guizhouense 1to90	-0.00380	0.00331	-1.047	0.9965

Supplementary Table S3.11. Bonferroni contrasts between species at 4 g/L

contrast	estimate	SE	t.ratio	p.value
acridum 10to1 - guizhouense 10to1	-0.04705	0.00513	-6.293	<.0001
acridum 1to1 - guizhouense 1to1	0.07638	0.00509	10.215	<.0001
acridum 1to10 - guizhouense 1to10	-0.0422	0.00507	-5.644	<.0001
acridum 1to30 - guizhouense 1to30	-0.02926	0.00502	-3.913	0.0058
acridum 1to60 - guizhouense 1to60	-0.02027	0.00485	-2.711	0.224
acridum 1to90 - guizhouense 1to90	-0.01245	0.00748	-1.665	0.8832

Supplementary Table S3.12. Bonferroni contrasts between species at 8 g/L

contrast	estimate	SE	t.ratio	p.value
acridum 10to1 - guizhouense 10to1	0.09108	0.00482	18.916	<.0001
acridum 1to1 - guizhouense 1to1	0.10019	0.00502	19.937	<.0001
acridum 1to10 - guizhouense 1to10	0.06451	0.00201	13.397	<.0001
acridum 1to30 - guizhouense 1to30	0.00886	0.00488	1.817	0.8083
acridum 1to60 - guizhouense 1to60	0.00216	0.00507	0.426	1
acridum 1to90 - guizhouense 1to90	0.0093	0.00505	1.84	0.795

Supplementary Table S3.13. Bonferroni contrasts between species at 12 g/L

contrast	estimate	SE	t.ratio	p.value
acridum 10to1 - guizhouense 10to1	0.08354	0.00548	15.236	<.0001
acridum 1to1 - guizhouense 1to1	0.11731	0.00564	20.783	<.0001
acridum 1to10 - guizhouense 1to10	0.13562	0.00383	24.732	<.0001
acridum 1to30 - guizhouense 1to30	0.0182	0.00502	3.34	0.0423
acridum 1to60 - guizhouense 1to60	-0.00372	0.00545	-0.683	0.9999
acridum 1to90 - guizhouense 1to90	0.01038	0.00556	1.867	0.7793

Chapter 4

Thermal ecology shapes disease outcomes of entomopathogenic fungi infecting warm-adapted insects

Anna R. Slowik[1, 2, 3], Helen H. Hesketh[2], Steven M. Sait[3], and Henrik H. De Fine Licht[1]

[1]University of Copenhagen, Department of Plant and Environmental Sciences, Thorvaldsensvej 40, 1871 Frederiksberg C., Denmark.
[2]UK Centre for Ecology & Hydrology, Maclean Building, Benson Lane, Crowmarsh Gifford, Wallingford, OX10 8BB, United Kingdom.
[3]School of Biology, Faculty of Biological Sciences, University of Leeds, Leeds, LS2 9JT, United Kingdom.

Submitted to the Journal of Invertebrate Pathology.

In this chapter, I investigated thermal ecology in host-pathogen interactions. I explored how temperature impacts the growth and disease-causing ability (virulence) of two fungi with distinct ecological lifestyles, *M. brunneum* and *M. flavoviride*, using the yellow mealworm, *Tenebrio molitor*, as a model. *M. brunneum* can infect a variety of host insects, while *M. flavoviride* typically parasitizes a smaller range. I measured individual growth in the fungi and the insect, as well as the interaction (virulence) of these organisms. This was performed at temperatures they've been acclimatized to and temperatures that were suboptimally hot and cold. The main findings showed that all three species grew best at 28°C. However, their virulence was different across temperatures. Specifically, *M. brunneum* was effective over a broader temperature span than *M. flavoviride*, which had more specific temperatures for maximum virulence. These outcomes highlight that evolutionary backgrounds and ecological adaptations play a pivotal role in how fungi interact with their hosts and challenge our understanding of how thermal ecology affects disease outcomes in host-pathogen interactions.

Thermal ecology shapes disease outcomes of entomopathogenic fungi infecting warm-adapted insects

4.1 Abstract

The thermal environment is a critical determinant of outcomes in host-pathogen interactions, yet the complexities of this relationship remain underexplored in many ecological systems. We examined the Thermal Mismatch Hypothesis (TMH) by measuring phenotypic variation in individual thermal performance profiles using a model system of two species of entomopathogenic fungi (EPF) that differ in their ecological niche, *Metarhizium brunneum* and *M. flavoviride*, and a warm-adapted model host, the mealworm *Tenebrio molitor*. We conducted experiments across ecologically relevant temperatures to determine the thermal performance curves for growth and virulence, measured as % survival, identify critical thresholds for these measures, and elucidate interactive host-pathogen effects. Both EPF species and the host exhibited a shared growth optima at 28°C, while the host's growth response was moderated in sublethal pathogen infections that depended on fungus identity and temperature. However, variances in virulence patterns were different between pathogens. The fungus *M. brunneum* exhibited a broader optimal temperature range (23–28°C) for virulence than *M. flavoviride*, which displayed a multiphasic virulence-temperature relationship with distinct peaks at 18 and 28°C. Contrary to predictions of the TMH, both EPF displayed peak virulence at the host's optimal temperature (28°C). The thermal profile for *M. brunneum* aligned more closely with that of *T. molitor* than that for *M. flavoviride*. Moreover, the individual thermal profile of *M. flavoviride* closely paralleled its virulence thermal profile, whereas the virulence thermal profile of *M. brunneum* did not track with its individual thermal performance. This suggests an indirect, midrange (23°C) effect, where *M. brunneum* virulence exceeded growth. These findings suggest that the evolutionary histories and ecological adaptations of these EPF species have produced distinct thermal niches during the host interaction. This study contributes to our understanding of thermal ecology in host-pathogen interactions, underpinning the ecological and evolutionary factors

that shape infection outcomes in entomopathogenic fungi, and has ecological implications for insect population dynamics in the face of a changing climate, as well as practically for the use of these organisms in biological control.

4.2 Introduction

Temperature plays a crucial role in host-pathogen interactions and disease dynamics in natural systems, particularly for ectothermic species (Rohr & Cohen, 2020). Body temperature significantly influences the performance and fitness of the interacting species, and taking temperature into account is therefore vital for understanding the ecology and evolution of host-pathogen interactions (Martin & Huey, 2008). For example, infection with a pathogen can affect the host's capacity to respond to thermal stress (Hector *et al.*, 2021), which may have important implications for pathogen transmission as the climate warms, including a greater likelihood of disease outbreaks (Elderd & Reilly, 2014).

Even when the thermal sensitivities of both host and pathogen align, the smaller size of pathogens compared to the host has led to the assumption that pathogens often have a broader range of optimal temperatures than hosts (Rohr & Cohen, 2020). However, individual performance across thermal gradients for hosts and pathogens is not always aligned and even small changes in environmental temperature can significantly affect host traits and the outcome of host pathogen interactions. The thermal mismatch hypothesis (TMH) accounts for such cases where host and pathogen fitness peak at different temperatures. The TMH asserts an increased susceptibility of hosts to pathogens under environmental conditions that diverge from their ideal thermal range (Cohen *et al.,* 2020, Rohr & Cohen, 2020). That is, warm-adapted hosts are more susceptible to pathogen infection at colder temperatures, and cold-adapted hosts are more susceptible at warmer temperatures.

There is broad support for the TMH across wildlife populations, with the most extensive evidence coming from amphibian systems (Cohen *et al.,* 2020). A significant effect of thermal mismatch has been observed for fungal pathogens infecting warm-adapted hosts at cold temperatures, where fungal pathogenicity

increases as temperature drops (Cohen *et al*., 2020). This pattern of thermal mismatch is, for example, evident between amphibian hosts from colder or warmer climatic conditions and the fungal pathogen *Batrachochytrium dendrobatidis*, which leads to temperature-dependent host susceptibility to fungal disease (Cohen, *et al*., 2020). However, this outcome is not universal for fungal pathogens (see for example, Sun *et al*., 2023), and it is challenging to predict the effect of warmer or colder temperatures on a particular host-fungal interaction.

Many of the host and pathogenic fungal traits that play crucial roles in determining infection outcomes are highly influenced by temperature, and insect-pathogenic fungi specifically are sensitive to microclimatic variations because they infect insects directly through the host cuticle (Cory & Ericsson, 2009). Temperature also influences key aspects of the interaction itself, such as host resistance, immune response and recovery, in addition to pathogen virulence, activation and replication (Herren *et al*., 2023, Hector *et al*., 2023). These effects are not always linear, as they arise from complex "genotype-by-genotype-by-environment" interactions. This implies that distinct thermal responses for various traits are the result of the interplay of genetic characteristics of both host and parasite, leading to a diverse range of responses that can variably impact both host survival and parasite virulence (Thomas & Blandford, 2003; Hector *et al*., 2023; Sinclair *et al.,* 2022; Gehman *et al*., 2017). Furthermore, temperature may have indirect effects on the host and pathogen that are not fully understood. For example, infection indirectly affects host responses to temperature (Hector *et al*., 2021), while the growth response of the host to changes in temperature may be critical for pathogen transmission because host growth affects the production of pathogen propagules, such as fungal spores (Boomsma *et al*., 2014). In experimental studies, the relationships between temperature and virulence are usually represented as a thermal virulence performance curve, which captures the dynamic interaction between the host and pathogen across different temperatures (Thomas & Blandford, 2003). Most pathogenic fungi do not perform well at warm temperatures, which, despite notable exceptions, helps to reduce risk of fungal infection for warm-blooded mammals (Robert & Casadevall, 2009). This has been proposed as a selective pressure in the evolution of endothermy,

aiding in the prevention of fungal infection for warm-blooded mammals (Casadevall, 2012). However, ectothermic organisms such as insects, amphibians, reptiles, and plants may be more susceptible to fungal infection, which is also reflected in recent fungal epidemics discovered in amphibians and plants (Casadevall, 2005; Fisher & Denning, 2023; Fisher *et al*., 2022; Fisher *et al*., 2020; Fisher *et al*., 2012; Fones, *et al.,* 2017; Harvell *et al*., 2002).

The ability to infect insects has evolved multiple times within the kingdom fungi, and today entomopathogenic fungi are globally widespread and present wherever insects are found (Humber, 2008). Entomopathogenic fungi exhibit diverse ecologies ranging from obligate and host-specific to facultative or opportunistic pathogens with a broad host-range, and includes some with extensive parts of their lifecycles occurring in the soil or as plant symbionts (Boomsma *et al*., 2014; Cory & Ericsson, 2009). In the latter group, the entomopathogenic fungal genus *Metarhizium* has evolved from root symbiotic fungi colonizing plant roots, and is primarily found in the soil environment (Sheng *et al*., 2022; Stone & Bidochka, 2020; Kaya & Vega, 2012). The genus *Metarhizium* is globally distributed, inhabiting a range of habitats across tropical and temperate soils where these fungi play an important role in regulating natural insect populations (St Leger & Wang, 2020; Roy *et al*., 2009). There is wide variation in fungal performance at different temperatures among *Metarhizium* species, in part correlating with geographical origin, resulting in significant isolate-specific temperature performance curves (Chandra Teja & Rahman, 2016; Ouedraogo *et al*., 1997; Driver *et al*., 2000). However, the effect of fluctuating or constant temperatures on *Metarhizum* growth does not always correlate with virulence in their insect host (Meissle *et al*., 2023). Acclimation and thermal history of both insect host and *Metarhizium* fungus can contribute to the outcome of infection at different thermal conditions (Ferguson & Sinclair, 2020). In general, many fungi perform best at cool to intermediate temperatures (Carlile *et al*., 2001), which suggests that entomopathogenic fungi may have a particular advantage when infecting warm-adapted hosts at cold temperatures.

A thermal performance curve describes how an organism performs for a given trait (growth, virulence, etc.) across a range of temperatures, whereas the

thermal niche is the range of temperatures within which an organism can survive, grow, and reproduce (Gvoždík, 2018). For pathogenic fungi, the thermal niche also delineates the temperatures at which they can effectively infect hosts. The thermal niche is a component of the infective niche (Rogers *et al.*, 2013), which is defined as the suite of conditions, including temperature, that permits a pathogen to infect and cause disease in a host. In the present study, we aimed to quantify the phenotypic variation in thermal performance curves of two entomopathogenic fungal species differing in their ecological niche and evolutionary histories and assess the thermal performance curve of the outcome of the interaction between entomopathogenic fungi and a warm-adapted insect host. In particular, we asked: (1) Do individual pathogens and hosts exhibit overlapping or distinct thermal performance curves and optima, and (2) How does host growth and the pathogen virulence outcomes reflect the interaction between the host and pathogen's individual thermal performance curve.

To answer these questions, we compared the ecological differences between species in the entomopathogenic genus *Metarhizium* that differ in their evolutionary history. We used *M. brunneum* and *M. flavoviride* as pathogens in virulence tests with a model insect host, larvae of the mealworm *Tenebrio molitor*, which were warm acclimated to 28°C and where temperature is known to influence the immune response (Catalán *et al.*, 2012). Both species of fungi are common soil fungi in Northern Europe, but vary in their global abundances and virulence (Keyser *et al.*, 2015; St Leger & Wang, 2020; Sheng *et al.*, 2022). *Metarhizium flavoviride* is locally abundant in Denmark, but is often reported as infrequently isolated in other parts of the world (Keyser *et al.*, 2015; Fisher *et al.*, 2011; Sun *et al.*, 2008; Wyrebek *et al.*, 2011). The *Metarhizium* genus contains species with broad host ranges and high global abundance. For example *M. brunneum*, part of the so-called PARB clade and *Metarhizium anisopliae* complex (Mongkolsamrit *et al.*, 2020), has a wide host range, in part due to an ancestral horizontal gene transfer of genes responsible for cuticle-degrading enzymes predating the PARB clade (Zhang *et al.*, 2019), and is among some of the most isolated *Metarhizium* species from soil globally (St. Leger & Wang, 2020). *Metarhizium brunneum's* wide host range and frequent isolation from soil is in

concordance with a broad ecological and infective niche (Meyling & Eilenberg, 2007). Conversely, *M. flavoviride*, outside the PARB clade, exhibits a narrower infective niche, targeting fewer insect host species (Mongkolsamrit *et al*., 2020; Moonjely & Bidochka, 2019; Keyser *et al*., 2016). Many isolates of *M. flavoviride*, previously designated *M. flavoviride var. flavoviride*, are known to be cold-active, germinating and growing at low temperatures (<10°C) (Driver, 2000). These distinct evolutionary histories and ecological adaptations may therefore have led to differences in their thermal and infective niches, and we expect *M. flavoviride* to be more cold-adapted than *M. brunneum.* Current predictions of the TMH thus suggest that *M. flavoviride* will have higher virulence towards warm-adapted *T. molitor* at colder temperatures, but differences in ecological niches and adaptive traits of the two pathogens will also affect their virulence and growth at various temperatures.

4.3 Materials and Methods

4.3.1 Insect strain and fungal isolates

A laboratory culture of *T. molitor* maintained at 28°C for at least 10 generations was used in experiments. Insects were kept in plastic boxes (750 mL volume with dimensions of 15 cm × width 9.5 cm × depth 4 cm) at 28°C in the dark, and provided a diet comprised of wheat bran, supplemented with 5% *w/w* egg white powder (Millipore® Merk). Insects were fed small plugs of 1% *w/v* water agar (Bacteriological (European Type) No. 1, Neogen Corp.) twice a week to provide a source of water.

Two species of *Metarhizium* spp. isolated in Denmark were used in this study, namely *M. brunneum* KVL 12_30 and *M. flavoviride* KVL 14_112 (Steinwender *et al*., 2014; Keyser *et al*., 2016), both of which were isolated from the soil using *T. molitor* larvae as a bait insect (Steinwender *et al*., 2014). The acronym KVL refers to the entomopathogenic fungus culture collection maintained at the Section for Organismal Biology, Department of Plant and Environmental Sciences, University of Copenhagen.

4.3.2 Preparation of fungal inoculum

The inoculum for experiments was prepared from in vitro cultures of each of the fungal isolates. Fungal cultures (3 replicate plates) of each isolate were grown on quarter- strength Sabouraud dextrose agar + yeast media (SDAY/4: 2.5 g/L 1:1 animal: bacterial peptone (Bacteriological Peptone & Acuferm Neoeptone, Neogen Corp.), 10 g/L dextrose (Bacteriological, Oxoid Ltd.), 2.5 g/L yeast extract (Neogen Corp.), 15 g/L agar (Bacteriological (European Type) No. 1, Neogen Corp.) in Petri dishes (90 mm × 15 mm triple-vented, Sterilin Ltd.,) at 23°C. Conidia were harvested from the surface of the agar after 14 days incubation by agitation with a Drigalski spatula on the sporulating colonies to remove the conidia, which were collected in 10 mL sterile 0.05% (*v/v*) Triton X-100 (Thermo Scientific). The resulting suspension was centrifuged for five minutes at 3000 g/rf, the supernatant removed, and the pellet rinsed twice with sterile 0.05% (*v/v*) Triton X-100 to remove all fragments of mycelia. The concentration of stock suspension was determined by counting conidia from 1000× serially diluted stock suspension in a Fuchs Rosenthal haemecytometer (×400 magnification) and diluted to required concentrations for experiments.

To assess the viability of conidial suspensions, a diluted suspension was prepared from each stock suspension, to give a concentration of 2×10^6 conidia per ml, using 0.05% (*v/v*) Triton X-100. To verify conidial germination, 100 µL of 100x diluted stock suspension was spread with a Drigalski spatula on an agar plate of SDAY/4 and incubated for 24 hours at 23°C. Four microscope coverslips (22 mm × 22 mm) were then placed on the culture surface and 100 conidia were counted under each coverslip. Conidia were considered to have germinated when the germ tube was at least as long as the width of the conidium. Conidial germination after 24 hours was verified as >98% for all prepared inoculate solutions before being used in assays.

4.3.3 Optimal and suboptimal temperatures for the host and pathogens

A range of four temperatures (18°C, 23°C, 28°C, and 33°C) were selected to construct growth curves for both the insects and fungi. These temperatures were

chosen to examine both optimal and suboptimal temperature conditions that are predicted to lead to increased and decreased host and pathogen growth. The fungi have been routinely cultivated and maintained at 23°C in the laboratory, a temperature to which we consider they are acclimatized. It has also been demonstrated that the optimal temperature for growth of *M. brunneum* is 24–25°C, and it does not grow above 35°C (Keyser *et al.,* 2014; Kryukov *et al.,* 2017). Conversely, the insects have been maintained at 28°C, a temperature known to maximize growth in *T. molitor* (Eberle *et al*., 2022). Therefore, the temperature of 33°C is predicted to be suboptimally high for both the host and pathogen, while 18°C represents conditions that are suboptimally low for both host and pathogen.

4.3.4 Insect & fungal growth curves

To determine whether pathogens and host exhibit overlapping or distinct thermal performance curves and optima, we produced thermal profiles using growth rates across the four thermal treatments in the three organisms individually. To determine growth rates of *T. molitor* at these temperatures, 20 insects weighing between 250–850 mg were placed individually in vented square 25-compartment Sterilin® Petri dishes (100 mm × 100 mm, Thermo Scientific, Basingstoke, UK) and provided wheat bran alone ad libitum and 0.2 g of 1% (*w/v*) water agar twice weekly. Insects were incubated at 18±1°C, 23±1°C, 28±1°C, and 33±1°C, which were all maintained at a consistent relative humidity of 70±5%. Temperature and relative humidity were recorded every 15 minutes using EasyLog™ EL-SIE-2 dataloggers (Lascar Electronics Ltd., Salisbury, UK). Every five days over a 15-day period, the insects were weighed on an OHAUS Pioneer PA114CM Precision Balance (110g / 1mg, Ohaus Corp.). The experiment was replicated three times resulting in a sample size of 60 for each temperature treatment. To reveal how fungal infection moderated the host's response to the different temperature treatments, the growth rates of sublethally-infected *T. molitor* (see section 4.3.5) were measured following the same protocol.

Growth rates for each insect were derived from the slopes of linear models constructed for each insect as larval mass ~ time using base R version 4.2.3 (R

Core Team, 2023). Pairwise comparisons of growth rates among temperature treatments were calculated based on the mixed-effects model slope ~ temp + (1|replicate) for each species, using the “lme4” package for constructing the models and the “multcomp” package for pairwise comparisons to apply Tukey's method for comparing a family of 4 estimates in R (Hothorn *et al.*, 2008; R Core Team, 2023). For sublethally-infected insects, pairwise comparisons of growth rates were calculated in the same manner at each temperature using the model slope ~ species * dose + (1|replicate). Insects were included in the sublethal analysis if they survived to pupation.

To determine growth rates of fungal isolates at different temperatures independent of the host, fungal growth was measured using microspectrophotometry in 96 well plates using the technique described in Slowik *et al*. (2023). Microcultures were prepared in 42 wells of a clear flat-bottom vented microplate (Starlab International GmbH, Neuer Höltigbaum 38, Hamburg, Germany) by inoculating 100 µL of 2×10^6 conidial suspension into 100 µL quarter- strength Sabouraud dextrose + yeast liquid media (SDY/4: 2.5 g/L 1:1 animal:bacterial peptone, 10 g/L dextrose, 2.5 g/L yeast extract). Microplates were incubated at 18±1°C, 23±1°C, 28±1°C, and 33±1°C all at 70±5 % relative humidity (RH). Temperature and RH were recorded every 15 minutes using EasyLog™ EL-SIE-2 dataloggers. The OD (optical density) of each well was measured at 405nm in a SpectraMax 340PC microplate reader (Molecular Devices UK Ltd., Wokingham, UK) with SoftMax® Pro Version 3.0 software every 12 hours from 24 – 84 hours after inoculation during the linear growth phase of the fungus (Slowik *et al.*, 2023). For each temperature, three replicates of 42 wells per treatment were prepared and measured, yielding a sample size of 126 per fungus isolate and temperature. To mitigate potential edge effects arising from temperature and evaporation, the 36 wells around the edge of the plate were excluded from analysis and loaded with 200 µL of blank media (Mansoury *et al.*, 2021). The OD values of all microplates were also measured after conidia settled (15 minutes post-inoculation) to establish the baseline reading OD of each culture. This baseline reading was subtracted from subsequent measurements to determine change in OD for the construction of growth curves.

To construct growth curves for the two fungal isolates at each temperature, linear models were fitted for each fungal culture as OD ~ time. Pairwise comparisons of growth rates among temperature treatments were calculated based on the mixed-effects model slope ~ temp + (1Ireplicate) for each species, using the "lme4" package for constructing the models and the "multcomp" package for pairwise comparisons to apply Tukey's method for comparing a family of 4 estimates in R (Hothorn *et al*., 2008; R Core Team, 2023).

4.3.5 Virulence thermal performance curves of the insect-fungus interaction

To investigate the effect of individual host-pathogen thermal performance curves on virulence and disease outcomes, we performed virulence assays across the four thermal treatments in *T. molitor* using two doses each for *M. brunneum* and *M. flavoviride.* To determine the effective doses for the host survival assay, initial virulence assays were carried out with the two fungal isolates to determine their lethal concentration LC50 and LC25 at 28°C, which represent conidial concentrations expected to induce 50% and 25% mortality respectively after 20 days (Supplementary materials and methods). For *M. flavoviride*, the effective lethal concentrations LC50 and LC25 were at 8.7×10^5 and 2.4×10^5 spores/mL when 2 µL of inoculum was applied to the metathorax, resulting in the delivery of approximately 1,740 and 480 spores, respectively. For *M. brunneum*, the values were 4.55×10^5 spores/mL (LC50) (910 spores) and 1.2×10^5 spores/mL (LC25) (240 spores). The lethal concentrations for the *M. flavoviride* isolate KVL 14_112 were almost twice that of *M. brunneum* (KVL 12_30), indicating the infective capacity of *M. brunneum* is greater than *M. flavoviride* by a factor of 1.9, which follows the findings of Keyser *et al.* (2016).

Conidial suspensions for both isolates were then prepared using previously outlined methods for preparing inoculum. The experiments were carried out in vented 25-compartment Sterilin® Petri dishes (100 mm × 100 mm, Thermo Scientific, Basingstoke, UK), each housing 20 separated insects weighing between 250 – 850 mg. A 2 µL droplet of the conidial suspension was applied to the metathorax of individual insects. Control insects received a 2 µL droplet of 0.05% *v/v* Triton X-100. Post-inoculation, dishes were lined with uniformly

moistened round 10mm filter papers (1 mL DI water) and sealed with Parafilm™. These setups were incubated at 28°C and 70±5% relative humidity for 24 hours. Following this, filter papers and Parafilm™ were removed, and the insects were provided wheat bran ad libitum and 0.2g of 1% (*w/v*) water agar twice weekly and incubated at the four constant treatment temperatures, 18±1°C, 23±1°C, 28±1°C, and 33±1°C, all under 70±5% relative humidity in complete darkness. Temperature and relative humidity were recorded every 15 minutes using EasyLogTM EL-SIE-2 dataloggers. Larval mortality was recorded every two days for 20 days post-inoculation, and to obtain growth of sublethal infections insects were weighed every five days on an OHAUS Pioneer PA114CM Precision Balance (110g / 1mg, Ohaus Corp.). Mortality due to fungal infection was confirmed through morphological observation of *Metarhizium* sporulation on cadavers. For this, cadavers were surface sterilized through a 20-second immersion in 5% *v/v* bleach solution and two subsequent DI (deionized) water rinses. Cadavers were then enclosed in tubes with moistened cotton wool and incubated at 23°C. No fungal infection was observed in any of the control treatments and plates for insect cadaver incubation were sealed to prevent cross-contamination. Only the weight of larvae that survived until the end of the experiment were included in the sublethal larval growth analysis. This experimental regime was replicated three times, yielding n = 60 per temperature and dose treatment.

To compare host survival outcomes for different temperatures, fungi and doses, survival models were constructed for each isolate at both doses using Cox proportional hazards regression in the R packages “coxme” and “survival” (Cox, 1972; Therneau, 2022; Therneau, 2023; R Core Team, 2023). Models were defined as (day, status) ~ treatment + temperature + (1 | replicate) for all four models. Pairwise comparisons for differences in survival probabilities among temperature treatments were calculated using Tukey’s HSD test on ANOVAs of each model with the package “multcomp” in R (Hothorn *et al.*, 2008; R Core Team, 2023).

4.4 Results

4.4.1 Thermal profiles of insect host and fungal pathogens

To assess the thermal sensitivity of *T. molitor* in terms of performance as growth, we measured growth rate and mortality at four different temperatures: 18°C, 23°C, 28°C, and 33°C (Figure 4.1). The overall linear model indicated significant differences in growth rates across temperatures ($p < 0.0001$) (Supp. Table S4.3). Pairwise comparisons using Tukey's post-hoc tests revealed that growth rates at 18°C and 23°C were different from all others, although there was no significant difference in insect growth rate between the two highest temperatures, 28°C and 33°C (Figure 4.1, Supp. Table S4.2). The significant differences in growth rates at varying temperatures suggest that *T. molitor* has a defined thermal preference for optimal growth. Growth rates at 28°C that are significantly higher than at 18°C and 23°C likely reflect the physiological constraints of *T. molitor's* homeostatic processes, which are more efficient within a moderate thermal range. The absence of significant differences in growth rates between 28°C and 33°C may indicate that *T. molitor* approaches an upper thermal threshold for growth at these temperatures. Beyond this threshold, the biological processes supporting growth may become heat-stressed or reach a plateau where further increases in temperature do not translate to enhanced metabolic efficiency or growth.

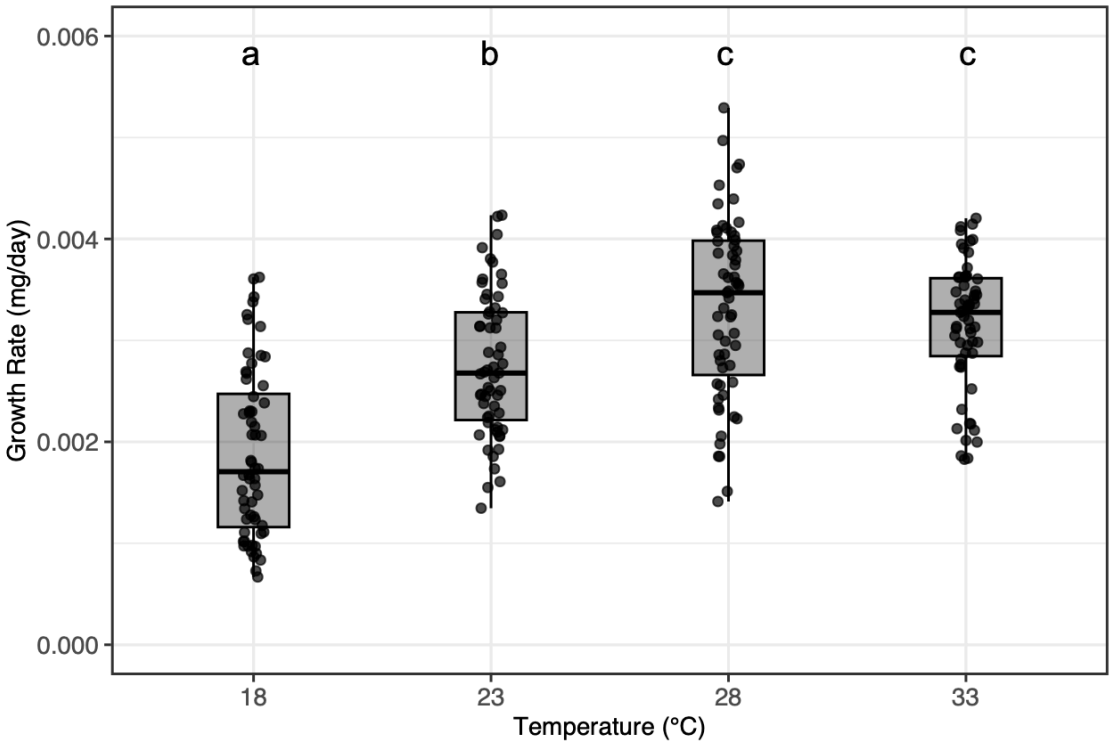

Figure 4.1 Temperature-dependent growth of *T. molitor.* Growth rates of *T. molitor* at different temperatures, where each box plot illustrates the distribution of average growth rates for insects within a specific temperature group. Points indicate growth rates of individual insects. Letters represent significant differences in growth rates from pairwise comparisons between temperatures at the $p < 0.05$ level.

We assessed the thermal sensitivity of two *Metarhizium* species, *M. brunneum* and *M. flavoviride*, by measuring their growth rates across a range of temperatures that align with those of their insect host, *T. molitor*. Both species displayed significantly different growth rates across the temperature range, with the highest growth rates observed at 28°C for both species ($p < 0.001$; Figure 4.2A, B; Supp. Tables S4.4 & S4.5). However, the response to temperature differed between the two species. In *M. brunneum*, there was a threshold effect, with growth rates increasing from 18°C to 28°C, and then significantly decreasing at 33°C (Figure 4.2B). On the other hand, *M. flavoviride* showed a different pattern, with the second-highest growth rate at 18°C (Figure 4.2A). While both

pathogens exhibited optimal growth at 28°C, their responses to suboptimal temperatures varied. *Metarhizium brunneum* showed a decrease in growth rate as the temperature deviated from the optimum, whereas *M. flavoviride* exhibited a narrower optimal niche, with consistent growth at lower temperatures and a sudden increase to optimal growth at 28°C.

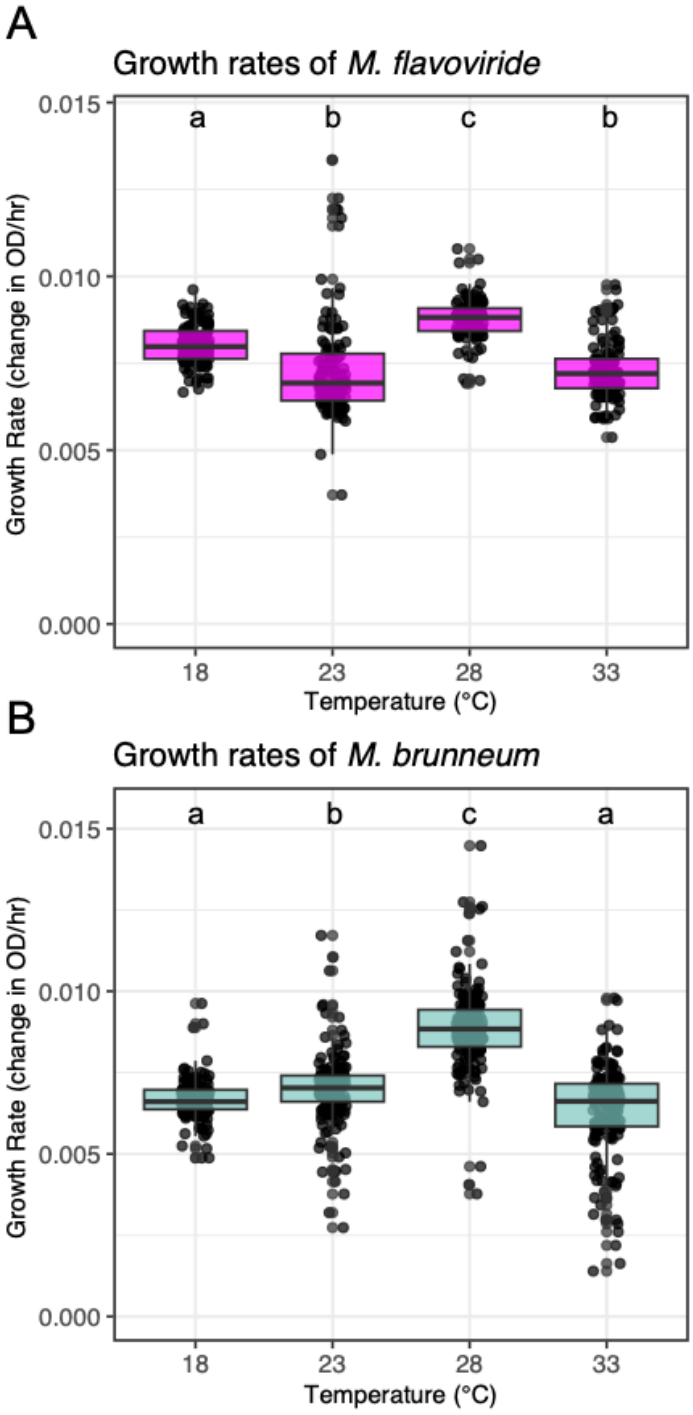

Figure 4.2 Temperature-dependent growth rates of *Metarhizium* spp. Growth rates of *Metarhizium flavoviride* **(A)** and *Metarhizium brunneum* **(B)** across a range of four temperatures. Each box plot depicts the distribution of average growth rates for cultures within a specific temperature group. Points indicate growth rates of individual cultures in microplate wells. Letters represent significant differences in growth rates from pairwise comparisons between temperatures at the $p < 0.05$ level.

4.4.2 Virulence thermal profiles

In this section, we examine the virulence thermal profiles of both *Metarhizium* species, evaluating the effects of different temperatures on their ability to induce mortality in *T. molitor*. To construct these profiles, we first performed a survival analysis to determine survival probabilities for both pathogens at each temperature using two doses, LC25 and LC50. We found a significant effect from pathogen treatment for *M. brunneum* at LC25 ($\chi^2 = 57.6$, df = 3, $p < 0.0002$) and LC50 ($\chi^2 = 105.7$, df = 3, $p < 0.0001$) as well as *M. flavoviride* LD25 ($\chi^2 = 23.8$, df = 3, $p < 0.001$) and LD50 ($\chi^2 = 62.2$, df = 3, $p < 0.0001$) (Supplementary tables S4.8 – S4.11). This implies that both fungi are able to infect and kill the host at both LC25 and LC50 doses. The overall model results did not indicate significant effect of temperature on survival when looking at all temperature levels simultaneously, however the a priori pairwise comparisons revealed significant effects between specific temperatures (Figure 4.3, Supp. Tables S4.8 – S4.11). The pairwise comparisons for survival among temperatures revealed no significant difference at lower doses (LC25) for *M. flavoviride* (Figure 4.3A). Planned pairwise comparisons revealed significant effects between temperatures in the various treatments (Fig. 4.3). For *M. brunneum* at LC25, the survival rate at 33°C was significantly lower than at 23°C ($p = 0.04$), and lower at 28°C, but short of significance ($p = 0.057$) (Figure 4.3C, Supp. Table S4.8). At higher doses (LC50), likewise the only significant difference in survival for *M. brunneum* was between 33°C and 23°C ($p = 0.03$) (Figure 4.3D). For *M. flavoviride* at LC50, we observed a greater differentiation in survival between temperatures; 28°C caused

significantly higher mortality than both 33°C and 23°C, although it did not significantly differ from 18°C (Figure 4.3B). The virulence rates at 23°C and 33°C were equally suboptimal for *M. flavoviride* at LC50 (Figure 4.3B). Taken together, the significant effects observed from pathogen treatment on survival rates, as indicated by the GLM, reflect the biological impact of the pathogens' virulence at different doses and temperatures on *T. molitor*. For *M. brunneum*, the stronger statistical significance at both LC25 and LC50 suggests a high virulence potential across the temperature range tested, which may correlate with its broader host range and environmental versatility. In contrast, the lack of significant temperature effect for *M. flavoviride* at LC25 may suggest a more stable virulence across the tested temperatures. However, the increased mortality at 28°C, could imply that *M. flavoviride's* virulence is optimized at this temperature, which may align with its individual thermal niche, allowing for more effective infection and proliferation.

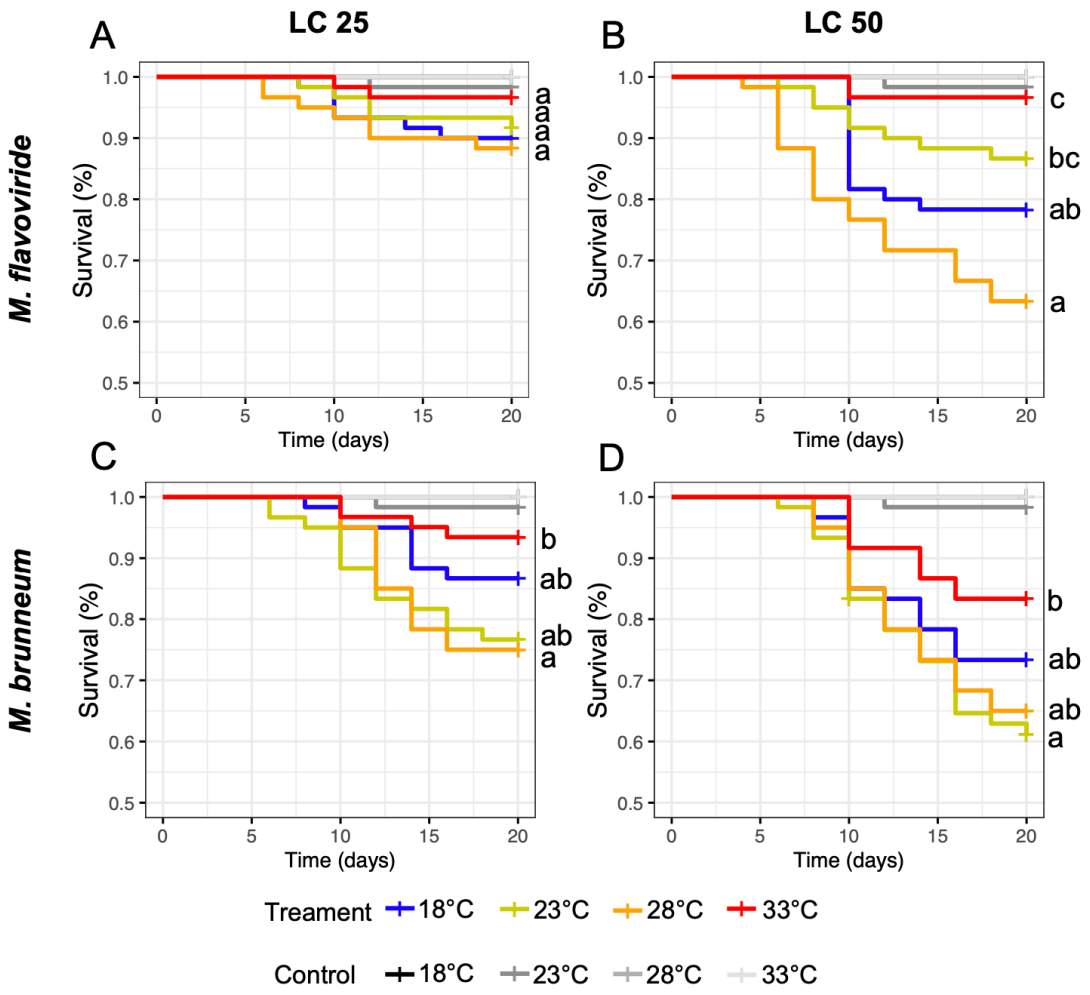

Figure 4.3 Temperature-dependent survival of *T. molitor* infected with *Metarhizium* spp. Survival probabilities of *Tenebrio molitor* infected with two species of *Metarhizium* fungi at two doses, LC25 and LC50, across a range of four temperatures from 18°C to 33°C. Letters represent significant differences in survival from pairwise comparisons between temperatures at the $p < 0.05$ level.

Adding to the thermal profiles of *T. molitor* and the two *Metarhizium* species, we investigated the growth rates of *T. molitor* larvae that survived fungal exposure with sublethal infections by either *M. brunneum* or *M. flavoviride* and subsequently reached pupation (Fig. 4.4). The growth rates of these sublethally infected insects provide insights into the effects of overcoming infection and its interaction with environmental temperature. We observed no significant differences in growth rates among the pathogen treatments at 18°C (Fig. 4.4A)

in the pairwise comparisons, indicating negligible effects of the suboptimal temperature or pathogen treatment on larval growth at this lower temperature. Conversely, at the acclimated temperature of 23°C, the control group presented significantly higher growth rates compared to the LC50 treatment groups of both fungi (F50 – Control $p = 0.025 \pm 0.0002$, df = 210; B50 – Control $p = 0.032 \pm 0.0002$, df = 210). Growth rates in the LC 25 groups were reduced compared to the control, but were not statistically different from either the control or the LC50 treatments (Fig. 4.4B). This pattern indicates that growth rate was influenced by the dosage of pathogen treatment rather than the pathogen species, although exposure to *M. flavoviride* consistently resulted in lower mean growth rates than exposure to *M. brunneum* at 23°C, 28°C, and 33°C (Fig. 4.4). At higher temperatures of 28°C (acclimated) and 33°C (suboptimal) (Fig. 4.4C, D), the control group's growth rates did not significantly differ from the LC25 groups. However, the *M. flavoviride* LC50 group presented a distinct response, showing significantly lower growth rates from the control group, but not differing from other treatment groups (at 28°C, F50 – Control $p = 0.04 \pm 0.0002$, df = 203; at 33°C F50 – Control $p = 0.01 \pm 0.0002$, df = 240).

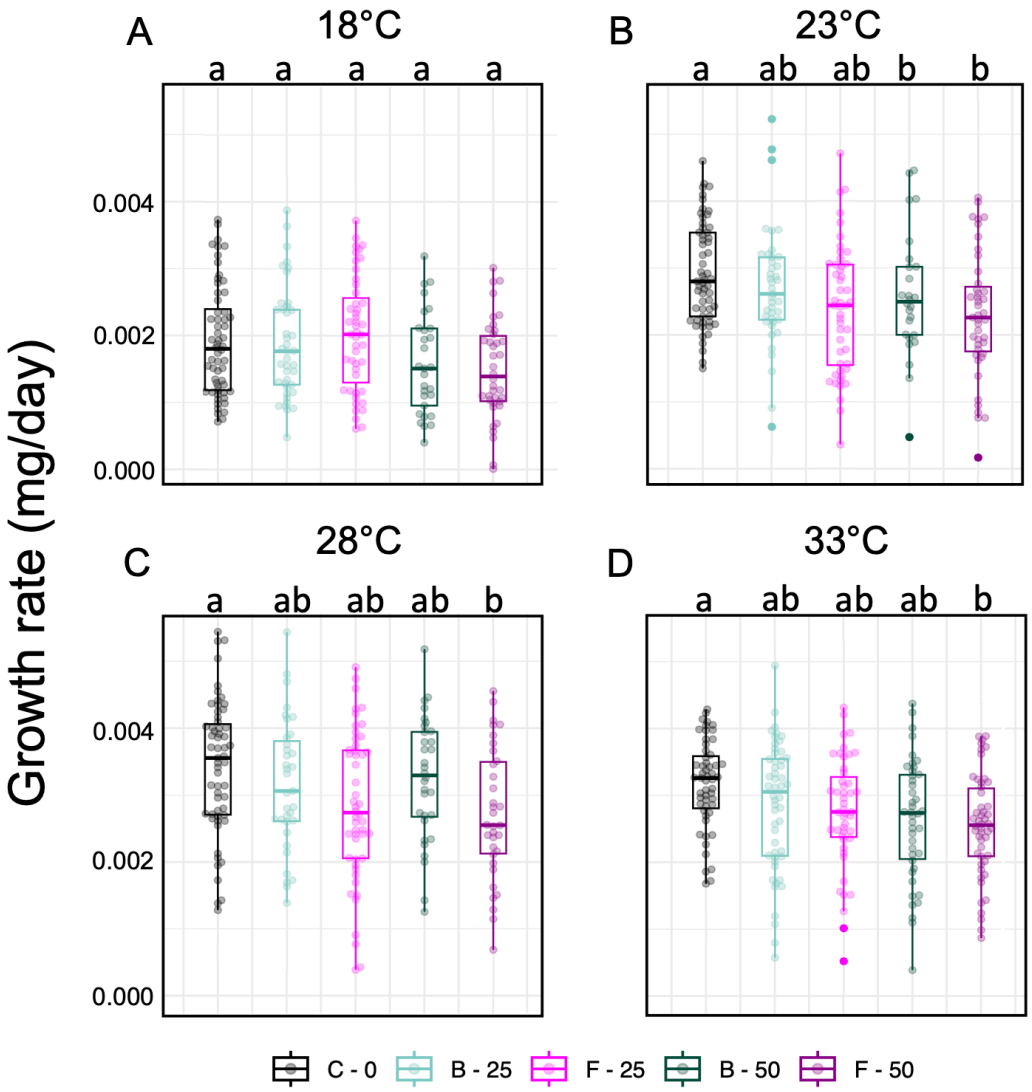

Figure 4.4 Growth rates over 15 days of *Tenebrio molitor* larvae at varying temperatures post sublethal infection with *Metarhizium* spp. The figure comprises four panels **(A–D)**, each corresponding to a different temperature setting: 18°C **(A)**, 23°C **(B)**, 28°C **(C)**, and 33°C **(D)**. Within each panel, box plots illustrate the growth rates (mg/day) of larvae across different treatments: control (C-0), *M. brunneum* at LC25 (B-25), *M. flavoviride* at LC25 (F-25), *M. brunneum* at LC50 (B-50), *and M. flavoviride* at LC50 (F-50). The central line of each box plot represents the median growth rate, the box boundaries indicate the interquartile range (IQR), and the whiskers extend to the furthest points within 1.5 times the IQR from the box. Points represent individual larval growth rates. Different letters above the box plots indicate statistically significant differences in growth rates

between treatment groups within the same temperature, based on pairwise comparisons.

After determining growth rates for each individual organism and assessing survival rates of *T. molitor* infected with each pathogen across temperatures, we integrated these findings to construct thermal profiles for the three species individually and the interaction, virulence. Comparing the growth of *T. molitor* (Fig. 4.5A) and the growth of the two fungi, *M. brunneum* and *M. flavoviride* (Fig. 4.5B) with the virulence thermal profiles of the infection of insects with fungi (Fig. 4.5C) show temperature dependent virulence. Thermal growth performance is similar for the pathogens *M. brunneum* and *M. flavoviride* and the host *T. molitor* (Figure 4.5A, B), as they share a thermal optimum at 28°C albeit with a steeper growth peak for *M. brunneum* around this temperature. The fungus *M. flavoviride* in addition show increased growth at the lowest temperature 18°C, which is expected based on the known biology of this species (Driver *et al*., 2000). Considering both the thermal and virulence performance profiles, there seems to be a common thermal optimum at 28°C for virulence for both pathogens and growth in all three species (Figure 4.5A, B, C). In *M. flavoviride*, the thermal profile closely aligns with the virulence profile, indicating that temperature has a similar effect on both growth and virulence (Figure 4.5B, C). Conversely, the reaction norm for *M. brunneum* diverges from the pattern of the thermal profile for growth at 23°C, where virulence is optimized and showing that the interaction of the host and the pathogen at this sub-optimal temperature for both, leads to increased virulence (Figure 4.5A, B, and C). These results collectively suggest that temperature has an important effect on the outcomes of interactions between these organisms, although the effects are not uniform across the different species.

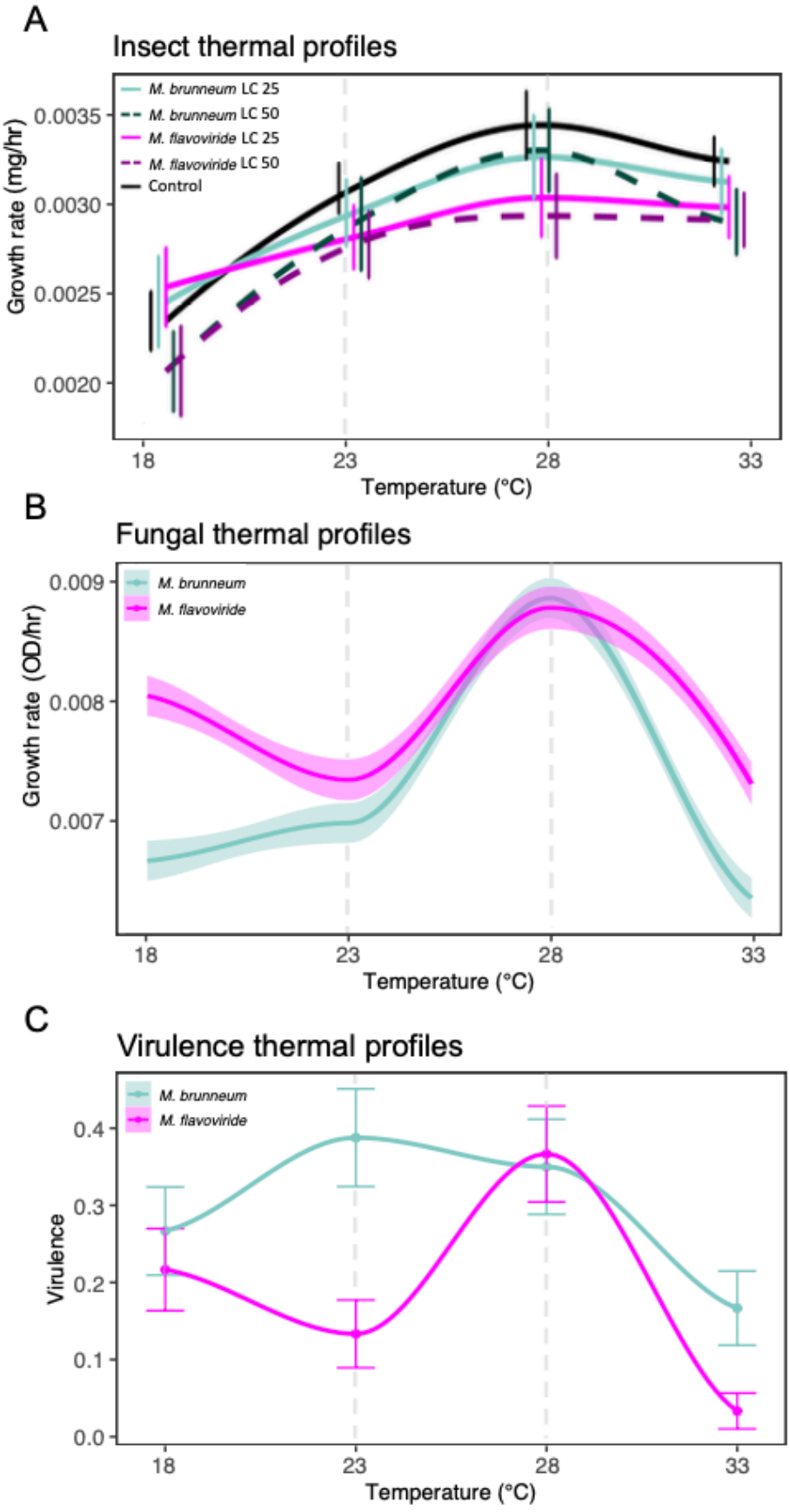
A
Insect thermal profiles
M. brunneum LC 25
M. brunneum LC 50
M. flavoviride LC 25
M. flavoviride LC 50
Control
Growth rate (mg/hr)
0.0035
0.0030
0.0025
0.0020
18
23
28
33
Temperature (°C)
B
Fungal thermal profiles
M. brunneum
M. flavoviride
Growth rate (OD/hr)
0.009
0.008
0.007
18
23
28
33
Temperature (°C)
C
Virulence thermal profiles
M. brunneum
M. flavoviride
Virulence
0.4
0.3
0.2
0.1
0.0
18
23
28
33
Temperature (°C)

Figure 4.5 Thermal responses in host and pathogen growth and virulence dynamics. **(A)** Thermal performance curves of *Tenebrio molitor,* differentiated by species and dose treatments. Error bars indicate 95% CI modeled from data in Figures 4.1 and 4.4. **(B)** Thermal performance curves of *M. brunneum* and *M. flavoviride* based on growth rates in Figure 4.2. Shaded bands indicate 95% CI. **(C)** Temperature-dependent virulence performance for *M. brunneum* and *M. flavoviride.* Virulence is defined as the likelihood of *Tenebrio* mortality after 20 days of infection at LC50 for each pathogen. Points indicate predicted probability of mortality for *Tenebrio* at day 20, bars are SE for these estimates.

4.5 Discussion

This study explored the thermal performance curves of the entomopathogenic fungi *M. brunneum* and *M. flavoviride*, and a model insect host *Tenebrio molitor*, at their acclimated temperatures (23°C and 28°C, respectively), and during both hot (33°C) and cold (18°C) sub-optimal temperatures. We found that both the uninfected and sublethally infeced insect hosts and fungal pathogens grew optimally at 28°C and that virulence of *M. flavoviride* was correlated with its temperature profile, whereas virulence for *M. brunneum* was also increased at 23°C, but its growth was not. These findings provide insights into the alignment of thermal performance optima, revealing that the effect of temperature on entomopathogenic fungal interactions is not uniform across pathogen species with different ecological niches and host ranges (Mongkolsamrit *et.al.,* 2020), and highlights that past evolutionary history of host-pathogen interactions may influence the outcome of infections under a thermal mismatch of host and pathogen.

The shared thermal optima at 28°C for individual growth across all three species suggests temperature alignment and minimal thermal mismatch. However, the complexity in virulence patterns, e.g. *M. brunneum*'s broader virulence thermal niche compared to its thermal profile for growth, reveals interactions influenced by factors beyond thermal optima for the single trait of growth individually in host and pathogens. While there is an obvious impact of

temperature on disease outcomes, the different responses observed in the two pathogens suggest that the TMH might have variable applicability based on the specific evolutionary and ecological contexts of the interacting organisms. Larval growth when sub-lethally infected highlighted the dynamic interactions between the dosage of pathogen and the influence of temperature on the host. Except at the coldest temperature of 18°C where there was no effect on growth, sublethal infections resulted in reduced growth of the host. This effect was highest for LC50 treatments and therefore dosage dependent, but there was also a consistent but non-significant trend of more reduced growth of sublethal infection with *M. flavoviride* than *M. brunneum.* This imply that sublethal fungal infections reduce growth at warmer temperatures but this effect likely is masked by the severity of the temperature treatment at 18°C. Also considering the survival outcomes, the data show that temperature affects both the overall outcomes of host-pathogen interactions (mortality) and the host's subsequent recovery and growth. These findings reveal that sublethal infections impose fitness costs on the host, evident through diminished growth rates, which could negatively affect the insects' reproductive success or other physiological processes and possibly pathogen transmission should the host eventually succumb to the infection.

Previous studies have examined the effect of temperature in EPF in the context of biocontrol, on traits such as germination and virulence (Couceiro *et al*., 2021; Brunner-Mendoza *et al*., 2019; Brunner-Mendoza *et al*., 2022; Seib *et al*., 2023). Here we capture the thermal sensitivity of both the host and pathogen individually as well as during the interaction of the host and pathogen at suboptimal temperatures. According to the thermal mismatch hypothesis (TMH), we anticipated peak virulence at colder temperatures where the warm-adapted host, *T. molitor*, performs suboptimally but where the pathogenic fungi would maintain high virulence (Cohen *et al.,* 2020; Rohr & Cohen, 2020). In the thermal virulence profile of *M. brunneum*, this was indeed what we observed with a broader thermal niche for virulence, which includes the thermal optima of the host (Figure 4.5A, C). In the more cold-adapted *M. flavoviride*, on the other hand, there is a narrower thermal niche for virulence, which aligns with that of the host's individual growth optima at (Figure 4.5C). Both host and pathogens have been

acclimated to specific temperatures through continued maintenance in laboratory conditions over many generations. The adaptation of the different pathogens according to their ecological evolutionary trajectories could have led to asynchronous development in thermal niches, where both organisms might have developed unique mechanisms to cope with thermal stress, leading to an unconventional pattern of virulence. For instance, while *M. brunneum's* virulence aligns with the TMH, the thermal performance patterns of *M. flavoviride* diverge from TMH predictions. Such divergence is reflective of a broader ecological phenomenon where species respond asymmetrically to climatic factors, a concept supported by findings in both herbivory and host-pathogen systems (Paudel *et al.,* 2020; Porras *et al.,* 2023). Paudel *et al.* (2020) described how temperature differentially affected insect herbivore and host plant responses, leading to an asymmetry in responses that was further complexed by the interaction between herbivore-associated elicitors and plant defense inducibility. Similarly, Porras *et al.* (2023) demonstrated that extreme heat events impacted the performance of both insect hosts and their pathogens, reducing the heat tolerance of hosts and the growth rate of pathogens. These studies underscore the complex and often species-specific impacts of temperature on biological interactions and suggest that the responses of *M. flavoviride* and *M. brunneum* to temperature stress may be part of a wider spectrum of thermal ecological strategies. Such asymmetrical responses to thermal stress noted in our study fungal species might reflect evolutionary pressures that have shaped unique virulence strategies, which could have significant implications for the dynamics of host-pathogen interactions in the context of a changing climate.

The shared thermal optima for the host and *M. flavoviride* in terms of growth and virulence could be a result of shared adaptive traits or environmental constraints. EPF and their insect hosts might have similar environmental pressures affecting them, given that they share the same soil environment (St Leger & Wang, 2020). Thus, soil insects and fungi may adapt to these pressures in ways that align their thermal optima. Specifically, soil-dwelling *Metarhizium* species appear adapted to their environmental habitat in the soil and plant root associations rather than insect hosts (Hu & Bidochka, 2021; Keyser *et al.*, 2014;

St. Leger & Wang, 2020), with an ecological strategy of exploiting of short lived, transitory insect hosts, and forming a beneficial mutualistic relationship with plants, which provide a stable environment (St. Leger & Wang, 2020). The interplay of the evolutionary forces in the shared soil and plant-root environmental niche could yield shared adaptive thermal traits, leading to a convergence in how both host and pathogen respond to thermal stress, forcing them into a shared optimum.

It is important to consider that the concept of thermal adaptation is intrinsically tied to the specific traits being evaluated, in our study these being growth and virulence. For example, there could be indirect effects and interactions that were not captured in this study that would expand our understanding of the system. The interplay of various adaptive traits, each responding to temperature differently, complicates our understanding of thermal adaptation. Considering this, there are indications that *T. molitor* may not be strictly warm-adapted. While growth is maximized at elevated temperatures, it does not encapsulate the entirety of the organism's adaptive traits. In natural environments, *T. molitor* can overwinter and endure extended periods at low temperatures (Graham *et al*., 2000). Furthermore, choice experiments with *T. molitor* show a preference for temperatures well below 28°C, indicating potential trade-offs and underlying physiological or ecological advantages linked to cooler environments (Catalán *et. al.,* 2012). The observed patterns of *Metarhizium* spp. virulence and thermal responses are likely idiosyncratic to the specific isolates under study, given that these fungi are known for extensive intraspecific variation among isolates for performance in virulence and temperature (Driver *et al*., 2000; Reingold *et al*., 2021; Couceiro *et al*., 2021; Tong & Feng, 2020). A broader exploration of traits important to virulence like conidia production and host immune responses (For an example from *Beauveria* see e.g. Maistrou *et al.,* 2020; Lu & St. Leger, 2016), and inclusive of a diverse array of isolates and an expanded temperature range, would be instrumental in drawing more generalized conclusions, but this study provides a framework for detecting different virulence and growth patterns outside of the thermal range investigated.

It is also important to note that during the initial 24 hours of the infection process, we maintained the experimental conditions at the insect's optimal temperature of 28°C with high humidity to ensure infection, as this is crucial for the initial pathogen establishment. During this early phase, the pathogens and host were not subjected to the varied experimental temperatures. This methodological nuance, while necessary to ensure successful infection, may have influenced the early interaction dynamics between the pathogens and the host, and as such is a critical consideration in interpreting the thermal performance curves we observed.

The differences in how each pathogen's individual thermal profile correlated with their respective thermal virulence profile was noteworthy for *M. brunneum*. This species is recognized for its ecological and pathogenic versatility that allows it to infect multiple insect orders and grow symbiotically with many plant hosts (St. Leger & Wang, 2020; Moonjely & Bidochka, 2019; Hu & Bidochka, 2021). Conversely, *M. flavoviride*, considered to be a less versatile pathogen primarily isolated from Coleoptera hosts and from soil (Keyser *et al*., 2016; Meyling *et al*., 2011), had a narrower optimum, which corresponded with its individual thermal profile. The alignment of growth and virulence thermal optima suggests that the thermal constraints and adaptations intrinsic to *M. flavoviride* may directly impact its virulence. The distinct responses exhibited by *M. brunneum* and *M. flavoviride* to temperature variations highlight the role of species-specific adaptations in determining infection outcomes.

In this study we found *M. flavoviride* exhibits two peaks in virulence, one critically at a lower temperature, and grows relatively well at lower temperatures (Driver *et al*., 2000). This is in concordance with *M. flavoviride* having a distinct ecology, which may be more locally adapted to performing well at lower temperatures as a weakly infective root symbiont, opportunistically infecting specific insects in the rhizosphere. We found *M. brunneum* to be twice as virulent in terms of number of spores needed to induce mortality, with a broader virulence thermal performance curve. This indicates *M. brunneum* is capable of infecting and killing insects over a broader range of temperatures beyond its own individual thermal niche for growth. The fungus *M. brunneum* is considered to be a

pathogen with a broad host range of insects, which could be due to its evolutionary history of together with fungi in the PARB-clade having acquired virulence genes through horizontal gene transfer (Zhang *et al*., 2019).

Our findings highlight the complex nature of thermal adaptation and its implications on the interactions between entomopathogenic fungi and their insect hosts. The variance in virulence, despite shared thermal growth optima, underscores the need to consider the specific ecological and evolutionary contexts of each species when incorporating broad theories, such as the Thermal Mismatch Hypothesis.

4.6 References

Boomsma, J. J., Jensen, A. B., Meyling, N. V., & Eilenberg, J. (2014). Evolutionary interaction networks of insect pathogenic fungi. *Annual Review of Entomology*, *59*, 467-485.

Brunner-Mendoza, C., Reyes-Montes, M. D. R., Moonjely, S., Bidochka, M. J., & Toriello, C. (2019). A review on the genus *Metarhizium* as an entomopathogenic microbial biocontrol agent with emphasis on its use and utility in Mexico. *Biocontrol Science and Technology, 29*(1), 83-102.

Carlile, M. J., Watkinson, S. C., & Gooday, G. W. (2001). *The fungi*. Gulf Professional Publishing.

Casadevall, A. (2005). Fungal virulence, vertebrate endothermy, and dinosaur extinction: is there a connection? *Fungal Genetics and Biology*, *42*(2), 98-106.

Casadevall, A. (2012). Fungi and the Rise of Mammals. *PLoS Pathog 8*(8): e1002808.

Catalán, T. P., Niemeyer, H. M., Kalergis, A. M., & Bozinovic, F. (2012). Interplay between behavioural thermoregulation and immune response in mealworms. *Journal of Insect Physiology, 58*, 1450–1455.

Chandra Teja, K. N. P., & Rahman, S. J. (2016). Characterisation and evaluation of *Metarhizium anisopliae* (Metsch.) Sorokin strains for their temperature tolerance. *Mycology*, *7*(4), 171-179.

Cohen, J. M., Venesky, M. D., Sauer, E. L., Civitello, D. J., McMahon, T. A., Roznik, E. A., & Rohr, J. R. (2017). The thermal mismatch hypothesis explains host susceptibility to an emerging infectious disease. *Ecology letters*, *20*(2), 184–193.

Cohen, J. M., Sauer, E. L., Santiago, O., Spencer, S. & Rohr, J. R. (2020). Divergent impacts of warming weather on wildlife disease risk across climates. *Science*, *370*, eabb1702

Cory, J. S., & Ericsson, J. D. (2010). Fungal entomopathogens in a tritrophic context. *The ecology of fungal entomopathogens*, 75-88. In: Roy, H.E., Vega, F.E., Chandler, D., Goettel, M.S., Pell, J., Wajnberg, E. (eds) The Ecology of Fungal Entomopathogens. Springer, Dordrecht.

Couceiro, J. D. C., Fatoretto, M. B., Demétrio, C. G. B., Meyling, N. V., & Delalibera Jr, Í. (2021). UV-B radiation tolerance and temperature-dependent activity within the entomopathogenic fungal genus *Metarhizium* in Brazil. *Frontiers in Fungal Biology, 2*, 645737.

Cox, D.R. (1972). Regression models and life-tables. *Journal of the Royal Statistical Society*. *Series B (Methodological), 34*(2), 187-220

Driver, F., Milner, R. J., & Trueman, J. W. (2000). A taxonomic revision of *Metarhizium* based on a phylogenetic analysis of rDNA sequence data. *Mycological research*, *104*(2), 134-150.

Eberle, S., Schaden, L. M., Tintner, J., Stauffer, C., & Schebeck, M. (2022). Effect of temperature and photoperiod on development, survival, and growth rate of mealworms, *Tenebrio molitor*. *Insects*, *13*(4), 321.

Elderd, B. D., & Reilly, J. R. (2014). Warmer temperatures increase disease transmission and outbreak intensity in a host–pathogen system. *Journal of Animal Ecology*, *83*(4), 838-849.

Ferguson, L. V., & Sinclair, B. J. (2020). Thermal variability and plasticity drive the outcome of a host-pathogen interaction. *The American Naturalist*, *195*(4), 603-615.

Fisher J.J., Rehner, S.A., & Bruck, D.J. (2011). Diversity of rhizosphere associated entomopathogenic fungi of perennial herbs, shrubs and coniferous trees. *Journal of Invertebrate Pathology, 106,* 289–95.

Fisher, M. C., & Denning, D. W. (2023). The WHO fungal priority pathogens list as a game-changer. *Nature Reviews Microbiology*, *21*(4), 211-212.

Fisher, M. C., Alastruey-Izquierdo, A., Berman, J., Bicanic, T., Bignell, E. M., Bowyer, P., Bromley, M., Brüggemann, R., Garber, G., Cornely, O. A. & Gurr, S. J. (2022). Tackling the emerging threat of antifungal resistance to human health. *Nature reviews microbiology*, *20*(9), 557-571.

Fisher, M. C., Gurr, S. J., Cuomo, C. A., Blehert, D. S., Jin, H., Stukenbrock, E. H., Stajich, J. E., Kahmann, R., Boone, C., Denning, D. W. & Gow, N. A. (2020). Threats posed by the fungal kingdom to humans, wildlife, and agriculture. *MBio*, *11*(3), 10-1128.

Fisher, M. C., Henk, D. A., Briggs, C. J., Brownstein, J. S., Madoff, L. C., McCraw, S. L., & Gurr, S. J. (2012). Emerging fungal threats to animal, plant and ecosystem health. *Nature*, *484*(7393), 186-194.

Fones, H. N., Fisher, M. C., & Gurr, S. J. (2017). Emerging fungal threats to plants and animals challenge agriculture and ecosystem resilience. *The fungal kingdom*, 787-809.

Gehman, A. L. M., Grabowski, J. H., Hughes, A. R., Kimbro, D. L., Piehler, M. F., & Byers, J. E. (2017). Predators, environment and host characteristics influence the probability of infection by an invasive castrating parasite. *Oecologia, 183*, 139-149.

Graham, L. A., Walker, V. K., & Davies, P. L. (2000). Developmental and environmental regulation of antifreeze proteins in the mealworm beetle *Tenebrio molitor. European Journal of Biochemistry, 267*(21), 6452-6458.

Gvoždík, L. (2018). "Just what is the thermal niche*?." Oikos 127*(12), 1701-1710.

Harvell, C. D., Mitchell, C. E., Ward, J. R., Altizer, S., Dobson, A. P., Ostfeld, R. S., & Samuel, M. D. (2002). Climate warming and disease risks for terrestrial and marine biota. *Science*, *296*(5576), 2158-2162.

Hector, T. E., Sgrò, C. M., & Hall, M. D. (2021). Thermal limits in the face of infectious disease: how important are pathogens? *Global Change Biology*, *27*(19), 4469-4480.

Hector, T. E., Gehman, A. L., & King, K. C. (2023). Infection burdens and virulence under heat stress: ecological and evolutionary considerations. *Philosophical Transactions of the Royal Society B*, *378*(1873), 20220018.

Hothorn, T., Bretz, F., & Westfall, P. (2008). Simultaneous Inference in General Parametric Models. *Biometrical Journal*, *50*(3), 346-363.

Hu, S., & Bidochka, M. J. (2021). Root colonization by endophytic insect-pathogenic fungi. *Journal of applied microbiology, 130*(2), 570-581.

Humber, R. A., 2008. Evolution of entomopathogenicity in fungi. *Journal of invertebrate pathology*, *98*(3), pp.262-266.

Keyser, C. A., Thorup-Kristensen, K., & Meyling, N. V. (2014). *Metarhizium* seed treatment mediates fungal dispersal via roots and induces infections in insects. *Fungal Ecology, 11*, 122-131.

Keyser, C. A., De Fine Licht, H. H., Steinwender, B. M., & Meyling, N. V. (2015). Diversity within the entomopathogenic fungal species *Metarhizium flavoviride* associated with agricultural crops in Denmark. *BMC microbiology*, *15*, 1-11.

Keyser, C. A., Jensen, B., & Meyling, N. V. (2016). Dual effects of *Metarhizium* spp. and *Clonostachys rosea* against an insect and a seed-borne pathogen in wheat. *Pest management science*, *72*(3), 517-526.

Keyser, C. A., Fernandes, É. K., Rangel, D. E., & Roberts, D. W. (2014). Heat-induced post-stress growth delay: a biological trait of many *Metarhizium* isolates reducing biocontrol efficacy?. *Journal of invertebrate pathology*, *120*, 67-73.

Kryukov, V., Yaroslavtseva, O., Tyurin, M., Akhanaev, Y., Elisaphenko, E., Wen, T.C., Tomilova, O., Tokarev, Y. and Glupov, V. (2017). Ecological preferences of *Metarhizium* spp. from Russia and neighboring territories and their activity against Colorado potato beetle larvae. *Journal of Invertebrate Pathology*, *149*, 1-7.

Lu, H.-L., & St. Leger, R. J. (2016). Insect Immunity to Entomopathogenic Fungi. *Advances in Genetics, 94*, 251-285.

Maistrou, S., Natsopoulou, M. E., Jensen, A. B., & Meyling, N. V. (2020). Virulence traits within a community of the fungal entomopathogen *Beauveria*: Associations with abundance and distribution. *Fungal Ecology*, *48*, 100992.

Mansoury, M., Hamed, M., Karmustaji, R., Al Hannan, F., & Safrany, S. T. (2021). The edge effect: A global problem. The trouble with culturing cells in 96-well plates. *Biochemistry and Biophysics Reports, 26,* 100987.

Martin, T. L., & Huey, R. B. (2008). Why “Suboptimal” Is Optimal: Jensen’s Inequality and Ectotherm Thermal Preferences. *The American Naturalist, 171*, E102–E118.

Meissle, M., Grabenweger, G., & Romeis, J. (2023). No interaction of fluctuating or constant temperature and virulence of entomopathogenic fungi in two noctuid species. *Journal of Pest Scien*ce, 1-15.

Meyling, N. V., & Eilenberg, J. (2007). Ecology of the entomopathogenic fungi *Beauveria bassiana* and *Metarhizium anisopliae* in temperate agroecosystems: Potential for conservation biological control. *Biological Control, 43*, 145–155.

Meyling, N. V., Thorup-Kristensen, K., & Eilenberg, J. (2011). Below-and aboveground abundance and distribution of fungal entomopathogens in experimental conventional and organic cropping systems. *Biological Control*, *59*(2), 180-186.

Mongkolsamrit, S., Khonsanit, A., Thanakitpipattana, D., Tasanathai, K., Noisripoom, W., Lamlertthon, S., Himaman, W., Houbraken, J., Samson, R. A. and Luangsa-Ard, J., 2020. Revisiting *Metarhizium* and the description of new species from Thailand. *Studies in Mycology, 95*(1), 171-251.

Moonjely, S., & Bidochka, M. J. (2019). Generalist and specialist *Metarhizium* insect pathogens retain ancestral ability to colonize plant roots. *Fungal Ecology*, *41*, 209-217.

Ouedraogo, A., Fargues, J., Goettel, M. S., & Lomer, C. J. (1997). Effect of temperature on vegetative growth among isolates of *Metarhizium anisopliae* and *M. flavoviride*. *Mycopathologia*, *137*, 37-43.

Paudel, S., Lin, P. A., Hoover, K., Felton, G. W. & Rajotte, E. G. (2020). Asymmetric responses to climate change: temperature differentially alters herbivore salivary elicitor and host plant responses to herbivory. *Journal of chemical ecology*, *46*, 891-905.

Porras, M. F., Navas, C. A., Agudelo-Cantero, G. A., Santiago-Martínez, M. G., Loeschcke, V., Sørensen, J. G., Crandall, S. G., Biddinger, D. & Rajotte, E. G. (2023). Extreme heat alters the performance of hosts and pathogen. *Frontiers in Ecology and Evolution, 11*, 1186452.

Reingold, V., Kottakota, C., Birnbaum, N., Goldenberg, M., Lebedev, G., Ghanim, M., & Ment, D. (2021). Intraspecies variation of *Metarhizium*

brunneum against the green peach aphid, *Myzus persicae,* provides insight into the complexity of disease progression. *Pest Management Science, 77*(5), 2557-2567.

Robert, V. A., & Casadevall, A. (2009). Vertebrate endothermy restricts most fungi as potential pathogens. *The Journal of infectious diseases*, *200*(10), 1623-1626.

Rogers, G. B., Hoffman, L. R., Carroll, M. P., & Bruce, K. D. (2013). "Interpreting infective microbiota: the importance of an ecological perspective." *Trends in microbiology, 21*(6), 271-276.

Roy, H. E., Hails, R. S., Hesketh, H., Roy, D. B., & Pell, J. K. (2009). Beyond biological control: non-pest insects and their pathogens in a changing world. *Insect Conservation and Diversity*, *2*(2), 65-72.

Rohr, J. R., & Cohen, J. M. (2020). Understanding how temperature shifts could impact infectious disease. *PLoS Biology*, *18*(11): e3000938.

Seib, T., Fischer, K., Sturm, A. M., & Stephan, D. (2023). Investigation on the Influence of Production and Incubation Temperature on the Growth, Virulence, Germination, and Conidial Size of *Metarhizium brunneum* for Granule Development. *Journal of Fungi, 9*(6), 668.

Sheng, H., McNamara, P. J., & St. Leger, R. J. (2022). *Metarhizium*: an opportunistic middleman for multitrophic lifestyles. C*urrent Opinion in Microbiology, 69*, 102176.

Sinclair, B. J., Sørensen, J. G., & Terblanche, J. S. (2022). Harnessing thermal plasticity to enhance the performance of mass-reared insects: Opportunities and challenges. *Bulletin of Entomological Research*, *112*(4), 441-450.

Slowik, A. R., Hesketh, H., Sait, S. M., & de Fine Licht, H. H. (2023). A Rapid Method for Measuring In Vitro Growth in Entomopathogenic Fungi. *Insects*, *14*(8), 703.

St. Leger, R. J., & Wang, J. B. (2020). *Metarhizium*: Jack of all trades, master of many. *Open Biology*, *10*(12), 200307.

Steinwender, B. M., Enkerli, J., Widmer, F., Eilenberg, J., Thorup-Kristensen, K., & Meyling, N. V. (2014). Molecular diversity of the entomopathogenic

fungal *Metarhizium* community within an agroecosystem. *Journal of invertebrate pathology, 123*, 6-12.

Stone, L. B., & Bidochka, M. J. (2020). The multifunctional lifestyles of *Metarhizium*: Evolution and applications. *Applied microbiology and biotechnology*, *104*, 9935-9945.

Sun, B. D., Yu, H. Y., Chen, A. J., Liu, X. Z. (2008). Insect-associated fungi in soils of field crops and orchards. *Crop Protection*, *27*, 1421–1426.

Sun, S. J., Dziuba, M. K., Jaye, R. N., & Duffy, M. A. (2023). Temperature modifies trait-mediated infection outcomes in a *Daphnia*–fungal parasite system. *Philosophical Transactions of the Royal Society B*, *378*(1873), 20220009.

Therneau, T.M. (2022). coxme: Mixed Effects Cox Models. R package version 2.2-18.1.

Therneau, T. (2023). A Package for Survival Analysis in R. R package version 3.5-7.

Thomas, M. B., & Blanford, S. (2003). Thermal biology in insect-parasite interactions. *Trends in Ecology & Evolution*, *18*(7), 344-350.

Tong, S. M., & Feng, M. G. (2020). Phenotypic and molecular insights into heat tolerance of formulated cells as active ingredients of fungal insecticides. *Applied Microbiology and Biotechnology, 104*, 5711-5724.

Tóthné Bogdányi, F., Petrikovszki, R., Balog, A., Putnoky-Csicsó, B., Gódor, A., Bálint, J., & Tóth, F. (2019). Current knowledge of the entomopathogenic fungal species *Metarhizium flavoviride* Sensu Lato and its potential in sustainable pest control. *Insects*, *10*(11), 385.

Vega, F. E., & Kaya, H. K. (2012). *Insect pathology* (Vol. 2). Academic press.

Velavan, V., Dhanapal, R., Ramkumar, G., Karthi, S., Senthil-Nathan, S., Ndomba, O. A., & Kweka, E. J. (2022). Characterization and Evaluation of *Metarhizium* spp.(Metsch.) Sorokin Isolates for Their Temperature Tolerance. *Journal of Fungi, 8*(1), 68.

Wyrebek, M., Huber, C., Sasan, R. K., & Bidochka, M. J. (2011). Three sympatrically occurring species of *Metarhizium* show plant rhizosphere specificity. *Microbiology, 157*, 2904–11.

Zhang, Q., Chen, X., Xu, C., Zhao, H., Zhang, X., Zeng, G., Qian, Y., Liu, R., Guo, N., Mi, W., Meng, G., St. Leger, R. J., & Fang, W. (2019). Horizontal gene transfer allowed the emergence of broad host range entomopathogens. *Proc Natl Acad Sci USA, 116,* 7982–7989.

4.7 Supplemental materials

Supplemental text – Materials and Methods for effective dose bioassays

To determine effective doses for the survival assay, initial virulence assays were performed for both fungal isolates. The experiments were carried out in 5x5 compartment lidded petri dishes with 25 separated insects per dish. Five concentrations of conidial suspension ($3.5x10^3$, $3.5x10^4$, $3.5x10^5$, $3.5x10^6$, and $3.5x10^7$ spores per mL) of each isolate were applied to 25 insects weighing 0.025 – 0.085 g, and replicated once in time. A droplet of 2µl of conidial suspension was applied to the metathorax of each insect. A droplet of 0.05 % v/v Triton X was used as a control. After inoculation, round filter papers evenly moistened with 1 mL DI water were placed between the chambers and the lid and the dishes were sealed with parafilm incubated for 24 hours at 28 °C and 70±5 % relative humidity. Filter papers and parafilm was removed after 24 hours and insects were each provided wheat bran and 0.2 g water agar twice every week. Mortality was checked every 2 days for 14 total days after inoculation. Infection was confirmed by sporulation of fungi from cadavers. To confirm sporulation, cadavers were surface sterilized by rinsing with 5 % v/v bleach water for 20 seconds followed by twice rinsing in DI water, then placed in small sealed tubes with 2 drops of DI water in cotton wool and incubated at 23 C. Effective doses were calculated using R package “drc” (Ritz et al. 2015).

References

Ritz, C., Baty, F., Streibig, J. C., & Gerhard, D. (2015). Dose-response analysis using R. *PloS one*, *10*(12), e0146021.

Supplemental Figure S4.1

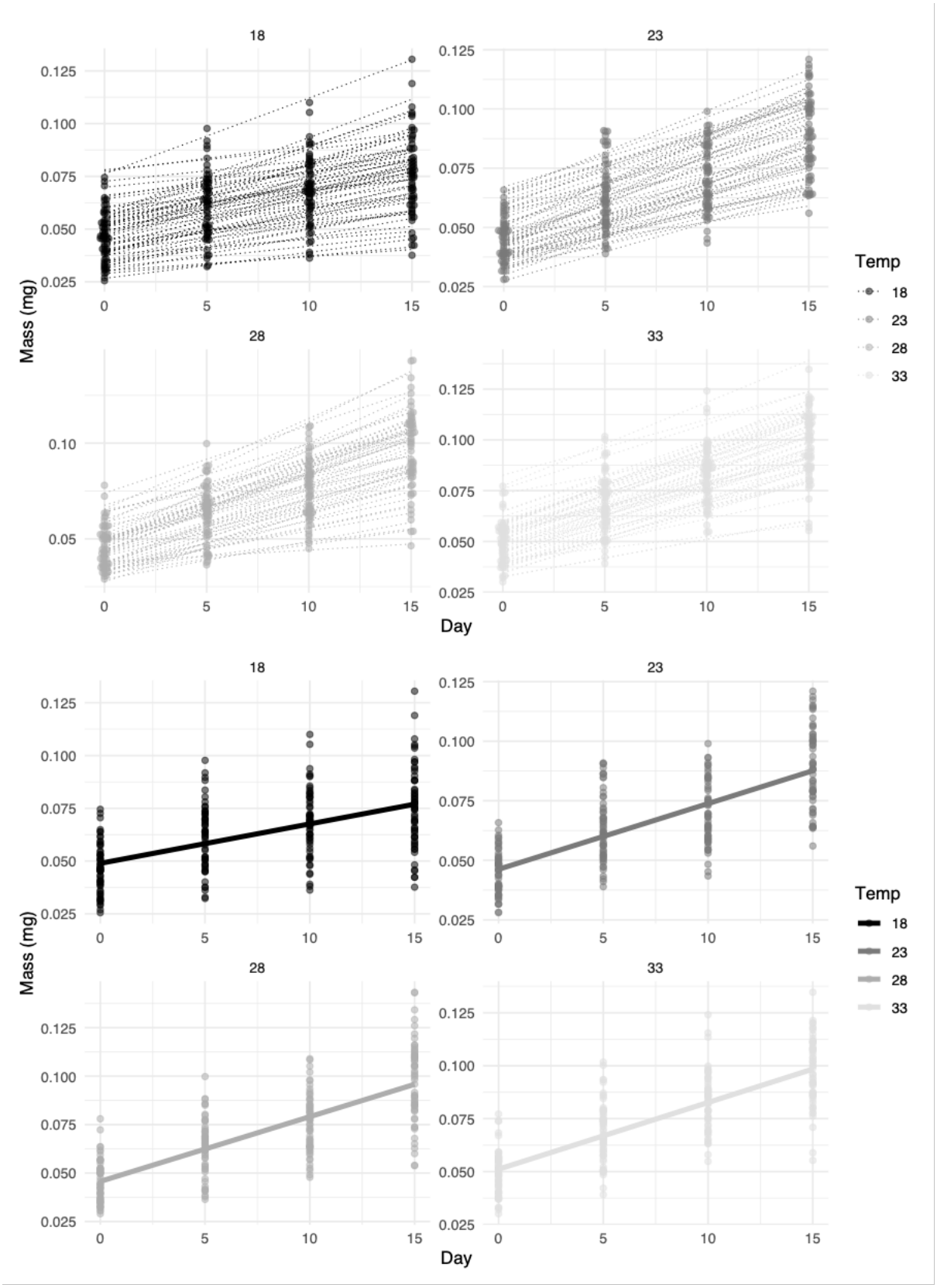

Supplemental Figure S4.1 Growth rates at four different temperatures for *Tenebrio molitor*. Top plots indicate regression lines for individual insects

Supplemental Table S4.1

Table S4.1 *Metarhizium* spp. biomass growth rates across temperatures in microculture

	M. flavoviride		*M. brunneum*	
Temperature(°C)	Average slope (change in OD/hr)	SE	Average slope (change in OD/hr)	SE
18	8.04E-03	5.27E-05	6.66E-03	4.40E-05
23	7.34E-03	1.35E-04	6.98E-03	8.46E-05
28	8.78E-03	5.68E-05	8.86E-03	9.50E-05
33	7.30E-03	7.98E-05	6.35E-03	1.04E-04

Supplemental Table S4.2

Bonferonni contrasts for comparison of *Tenebrio molitor* growth rates at different temperatures

```
         Simultaneous Tests for General Linear Hypotheses

Multiple Comparisons of Means: Tukey Contrasts


Fit: lmer(formula = growth_rate ~ temp + (1 | replicate), data = growth_rates)

Linear Hypotheses:
               Estimate Std. Error z value Pr(>|z|)
23 - 18 == 0  0.0008308  0.0001468   5.660   <0.001 ***
28 - 18 == 0  0.0013974  0.0001468   9.520   <0.001 ***
33 - 18 == 0  0.0012370  0.0001468   8.428   <0.001 ***
28 - 23 == 0  0.0005666  0.0001468   3.860   <0.001 ***
33 - 23 == 0  0.0004063  0.0001468   2.768   0.0287 *
33 - 28 == 0 -0.0001604  0.0001468  -1.093   0.6941
---
Signif. codes:  0 ‘***’ 0.001 ‘**’ 0.01 ‘*’ 0.05 ‘.’ 0.1 ‘ ’ 1
(Adjusted p values reported -- single-step method)
```

Supplemental Table S4.3
Model output for *Tenebrio molitor* growth model

```
Linear mixed model fit by REML ['lmerMod']
Formula: growth_rate ~ temp + (1 | replicate)
   Data: growth_rates

REML criterion at convergence: -2674.5

Scaled residuals:
    Min      1Q  Median      3Q     Max
-3.5986 -0.6271  0.0190  0.6778  2.3538

Random effects:
 Groups    Name        Variance  Std.Dev.
 replicate (Intercept) 2.498e-08 0.0001581
 Residual              6.463e-07 0.0008040
Number of obs: 240, groups:  replicate, 3

Fixed effects:
             Estimate Std. Error t value
(Intercept) 0.0018811  0.0001382  13.611
temp23      0.0008308  0.0001468   5.660
temp28      0.0013974  0.0001468   9.520
temp33      0.0012370  0.0001468   8.428

Correlation of Fixed Effects:
       (Intr) temp23 temp28
temp23 -0.531
temp28 -0.531  0.500
temp33 -0.531  0.500  0.500
```

Supplemental Table S4.4
Fungal growth rate contrasts – *M. brunneum*

```
         Simultaneous Tests for General Linear Hypotheses

Multiple Comparisons of Means: Tukey Contrasts


Fit: lmer(formula = slope ~ temp + (1 | replicate), data = filtered_slopes_brunneum)

Linear Hypotheses:
               Estimate Std. Error z value Pr(>|z|)
23 - 18 == 0  6.962e-05  2.488e-05   2.798   0.0262 *
28 - 18 == 0  4.611e-04  2.488e-05  18.531   <0.001 ***
33 - 18 == 0 -5.910e-05  2.488e-05  -2.375   0.0821 .
28 - 23 == 0  3.914e-04  2.488e-05  15.733   <0.001 ***
33 - 23 == 0 -1.287e-04  2.488e-05  -5.174   <0.001 ***
33 - 28 == 0 -5.202e-04  2.488e-05 -20.906   <0.001 ***
---
Signif. codes:  0 ‘***’ 0.001 ‘**’ 0.01 ‘*’ 0.05 ‘.’ 0.1 ‘ ’ 1
(Adjusted p values reported -- single-step method)
```

Supplemental Table S4.5
Fungal growth rate contrasts – *M. flavoviride*

```
         Simultaneous Tests for General Linear Hypotheses

Multiple Comparisons of Means: Tukey Contrasts


Fit: lmer(formula = slope ~ temp + (1 | replicate), data = filtered_slopes_flavoviride)

Linear Hypotheses:
               Estimate Std. Error z value Pr(>|z|)
23 - 18 == 0 -1.434e-04  2.442e-05  -5.871   <1e-06 ***
28 - 18 == 0  1.316e-04  2.501e-05   5.260   <1e-06 ***
33 - 18 == 0 -1.522e-04  2.484e-05  -6.129   <1e-06 ***
28 - 23 == 0  2.750e-04  2.518e-05  10.920   <1e-06 ***
33 - 23 == 0 -8.837e-06  2.500e-05  -0.353    0.985
33 - 28 == 0 -2.838e-04  2.555e-05 -11.108   <1e-06 ***
---
Signif. codes:  0 ‘***’ 0.001 ‘**’ 0.01 ‘*’ 0.05 ‘.’ 0.1 ‘ ’ 1
(Adjusted p values reported -- single-step method)
```

Supplemental Table S4.6
Model output for *M. brunneum* growth model

```
Linear mixed model fit by REML ['lmerMod']
Formula: slope ~ temp + (1 | replicate)
   Data: filtered_slopes_brunneum

REML criterion at convergence: -9746.8

Scaled residuals:
    Min      1Q  Median      3Q     Max
-4.5463 -0.3188  0.0494  0.4113  6.4317

Random effects:
 Groups    Name        Variance  Std.Dev.
 replicate (Intercept) 3.370e-09 5.805e-05
 Residual              5.478e-08 2.341e-04
Number of obs: 708, groups:  replicate, 3

Fixed effects:
             Estimate Std. Error t value
(Intercept)  1.812e-03  3.785e-05  47.884
temp23       6.962e-05  2.488e-05   2.798
temp28       4.611e-04  2.488e-05  18.531
temp33      -5.910e-05  2.488e-05  -2.375

Correlation of Fixed Effects:
       (Intr) temp23 temp28
temp23 -0.329
temp28 -0.329  0.500
temp33 -0.329  0.500  0.500
```

Supplemental Table S4.7
Model output for *M. flavoviride* growth model

```
Linear mixed model fit by REML ['lmerMod']
Formula: slope ~ temp + (1 | replicate)
   Data: filtered_slopes_flavoviride

REML criterion at convergence: -6540.3

Scaled residuals:
    Min      1Q  Median      3Q     Max
-3.6085 -0.5259 -0.0554  0.4646  6.2532

Random effects:
 Groups    Name        Variance  Std.Dev.
 replicate (Intercept) 2.407e-09 4.906e-05
 Residual              3.605e-08 1.899e-04
Number of obs: 463, groups:  replicate, 3

Fixed effects:
             Estimate Std. Error t value
(Intercept)  2.089e-03  3.317e-05  62.976
temp23      -1.434e-04  2.442e-05  -5.871
temp28       1.316e-04  2.501e-05   5.260
temp33      -1.522e-04  2.484e-05  -6.129

Correlation of Fixed Effects:
       (Intr) temp23 temp28
temp23 -0.360
temp28 -0.350  0.481
temp33 -0.352  0.485  0.475
```

Supplemental Table S4.8

Cox regression for *M. brunneum* LD50

```
Cox mixed-effects model fit by maximum likelihood
  Data: B50
  events, n = 71, 480
  Iterations= 20 163
                    NULL Integrated    Fitted
Log-likelihood -432.799  -379.9343 -377.5857

                    Chisq   df p    AIC   BIC
Integrated loglik 105.73 3.00 0  99.73 92.94
 Penalized loglik 110.43 3.58 0 103.26 95.16

Model:  Surv(day, status) ~ pathogen + temp + (1 | replicate)
Fixed coefficients
                 coef  exp(coef)   se(coef)     z       p
pathogenB  4.43810189 84.6141824 1.00722874  4.41 1.1e-05
temp      -0.02836842  0.9720302 0.02098424 -1.35 1.8e-01

Random effects
 Group     Variable  Std Dev   Variance
 replicate Intercept 0.4089532 0.1672427
```

Supplemental Table S4.9

Cox regression for *M. brunneum* LD25

```
Cox mixed-effects model fit by maximum likelihood
  Data: B25
  events, n = 42, 481
  Iterations= 7 53
                    NULL Integrated    Fitted
Log-likelihood -257.5426  -228.7415 -226.4875

                   Chisq   df          p   AIC   BIC
Integrated loglik 57.60 3.00 1.9114e-12 51.60 46.39
 Penalized loglik 62.11 3.55 5.1792e-13 55.01 48.84

Model:  Surv(day, status) ~ pathogen + temp + (1 | replicate)
Fixed coefficients
                 coef  exp(coef)   se(coef)     z       p
pathogenB  3.80723237 45.0256519 1.01217534  3.76 0.00017
temp      -0.02586058  0.9744709 0.02723788 -0.95 0.34000

Random effects
 Group     Variable  Std Dev   Variance
 replicate Intercept 0.5241104 0.2746918
```

Supplemental Table S4.10
Cox regression for *M. flavoviride* LD50

```
Call:
coxph(formula = Surv(day, status) ~ pathogen + temp, data = F50)

  n= 480, number of events= 46

              coef exp(coef) se(coef)      z Pr(>|z|)
pathogenF  3.90870  49.83389  1.01109  3.866 0.000111 ***
temp      -0.03631   0.96434  0.02637 -1.377 0.168571
---
Signif. codes:  0 ‘***’ 0.001 ‘**’ 0.01 ‘*’ 0.05 ‘.’ 0.1 ‘ ’ 1

          exp(coef) exp(-coef) lower .95 upper .95
pathogenF   49.8339    0.02007    6.8688   361.550
temp         0.9643    1.03698    0.9158     1.015

Concordance= 0.781  (se = 0.022 )
Likelihood ratio test= 60.53  on 2 df,   p=7e-14
Wald test            = 16.83  on 2 df,   p=2e-04
Score (logrank) test = 48.6  on 2 df,   p=3e-11
```

Supplemental Table S4.11
Cox regression for *M. flavoviride* LD25

```
Call:
coxph(formula = Surv(day, status) ~ pathogen + temp, data = F25)

  n= 480, number of events= 21

              coef exp(coef) se(coef)      z Pr(>|z|)
pathogenF  3.03776  20.85856  1.02471  2.965  0.00303 **
temp      -0.04347   0.95747  0.03967 -1.096  0.27321
---
Signif. codes:  0 ‘***’ 0.001 ‘**’ 0.01 ‘*’ 0.05 ‘.’ 0.1 ‘ ’ 1

          exp(coef) exp(-coef) lower .95 upper .95
pathogenF   20.8586    0.04794    2.7993   155.424
temp         0.9575    1.04442    0.8858     1.035

Concordance= 0.766  (se = 0.035 )
Likelihood ratio test= 23.07  on 2 df,   p=1e-05
Wald test            = 9.98  on 2 df,   p=0.007
Score (logrank) test = 19.19  on 2 df,   p=7e-05
```

Supplemental Table S4.12
Bonferroni contrasts for *M. brunneum* LD50

Multiple Comparisons of Means: Tukey Contrasts

Fit: coxme(formula = Surv(day, status) ~ pathogen + temp + (1 | replicate), data = B50)

Linear Hypotheses:

	Estimate	Std. Error	z value	Pr(>|z|)	
23 - 18 == 0	0.4788	0.3228	1.483	0.4443	
28 - 18 == 0	0.3013	0.3319	0.908	0.7986	
33 - 18 == 0	-0.5468	0.4031	-1.356	0.5236	
28 - 23 == 0	-0.1775	0.2989	-0.594	0.9332	
33 - 23 == 0	-1.0257	0.3765	-2.724	0.0319	*
33 - 28 == 0	-0.8482	0.3843	-2.207	0.1195	

Supplemental Table S4.13
Bonferroni contrasts for *M. brunneum* LD25

Fit: coxme(formula = Surv(day, status) ~ pathogen + temp + (1 | replicate), data = B25)

Linear Hypotheses:

	Estimate	Std. Error	z value	Pr(>|z|)	
23 - 18 == 0	0.73088	0.43795	1.669	0.3326	
28 - 18 == 0	0.67271	0.43793	1.536	0.4076	
33 - 18 == 0	-0.73783	0.61240	-1.205	0.6163	
28 - 23 == 0	-0.05817	0.36548	-0.159	0.9985	
33 - 23 == 0	-1.46872	0.56286	-2.609	0.0432	*
33 - 28 == 0	-1.41055	0.56288	-2.506	0.0567	.

Supplemental Table S4.14
Bonferroni contrasts for *M. flavoviride* LD50

Fit: coxph(formula = Surv(day, status) ~ pathogen + temp, data = F50)

Linear Hypotheses:

	Estimate	Std. Error	z value	Pr(>|z|)	
23 - 18 == 0	-0.4057	0.4337	-0.935	0.77427	
28 - 18 == 0	0.6483	0.3499	1.853	0.23395	
33 - 18 == 0	-1.9589	0.7597	-2.579	0.04449	*
28 - 23 == 0	1.0540	0.3958	2.663	0.03487	*
33 - 23 == 0	-1.5532	0.7817	-1.987	0.18009	
33 - 28 == 0	-2.6071	0.7387	-3.529	0.00201	**

Supplemental Table S4.15

Bonferroni contrasts for *M. flavoviride* LD25

Fit: coxph(formula = Surv(day, status) ~ pathogen + temp, data = F25)

Linear Hypotheses:

	Estimate	Std. Error	z value	Pr(>|z|)
23 - 18 == 0	-0.01336	0.57736	-0.023	1.000
28 - 18 == 0	0.17251	0.55635	0.310	0.989
33 - 18 == 0	-1.13072	0.81651	-1.385	0.502
28 - 23 == 0	0.18587	0.55636	0.334	0.987
33 - 23 == 0	-1.11736	0.81650	-1.368	0.512
33 - 28 == 0	-1.30323	0.80180	-1.625	0.357

Supplemental Table S4.16

Model output for 18°C sublethal insect growth model

```
Linear mixed model fit by REML. t-tests use Satterthwaite's method ['lmerModLmerTest']
Formula: overall_growth_rate ~ species * dose + (1 | replicate)
   Data: x18_dataset

REML criterion at convergence: -2377

Scaled residuals:
    Min      1Q  Median      3Q     Max
-1.8476 -0.7769 -0.1154  0.6593  2.5689

Random effects:
 Groups    Name        Variance  Std.Dev.
 replicate (Intercept) 7.077e-09 8.413e-05
 Residual              6.468e-07 8.042e-04
Number of obs: 215, groups:  replicate, 3

Fixed effects:
                 Estimate Std. Error         df t value Pr(>|t|)
(Intercept)      1.915e-03  1.146e-04  9.057e+00  16.707  4.1e-08 ***
speciesB        -3.479e-04  1.826e-04  2.100e+02  -1.906  0.05808 .
speciesF        -4.356e-04  1.672e-04  2.099e+02  -2.606  0.00982 **
dose25           5.463e-04  1.756e-04  2.088e+02   3.110  0.00213 **
speciesB:dose25 -2.457e-04  2.629e-04  2.094e+02  -0.935  0.35108
---
Signif. codes:  0 ‘***’ 0.001 ‘**’ 0.01 ‘*’ 0.05 ‘.’ 0.1 ‘ ’ 1

Correlation of Fixed Effects:
            (Intr) specsB specsF dose25
speciesB    -0.515
speciesF    -0.563  0.358
dose25       0.000 -0.002 -0.583
specsB:ds25  0.000 -0.464  0.390 -0.669
```

Supplemental Table S4.17

Model output for 23°C sublethal insect growth model

```
Linear mixed model fit by REML. t-tests use Satterthwaite's method ['lmerModLmerTest']
Formula: overall_growth_rate ~ species * dose + (1 | replicate)
   Data: x23_dataset

REML criterion at convergence: -2364.7

Scaled residuals:
    Min      1Q  Median      3Q     Max
-3.0065 -0.5545 -0.0344  0.6396  3.1942

Random effects:
 Groups    Name        Variance  Std.Dev.
 replicate (Intercept) 1.288e-07 0.0003588
 Residual              7.046e-07 0.0008394
Number of obs: 217, groups:  replicate, 3

Fixed effects:
                Estimate Std. Error         df t value Pr(>|t|)
(Intercept)    2.926e-03  2.342e-04  2.809e+00  12.490  0.00152 **
speciesB      -1.228e-04  3.293e-04  2.102e+02  -0.373  0.70953
speciesF      -5.044e-04  2.959e-04  2.102e+02  -1.704  0.08981 .
dose          -1.279e-06  7.088e-06  2.103e+02  -0.181  0.85693
speciesB:dose -1.526e-06  1.105e-05  2.104e+02  -0.138  0.89023
---
Signif. codes:  0 ‘***’ 0.001 ‘**’ 0.01 ‘*’ 0.05 ‘.’ 0.1 ‘ ’ 1

Correlation of Fixed Effects:
            (Intr) specsB specsF dose
speciesB    -0.155
speciesF    -0.173  0.118
dose         0.001  0.006 -0.880
speciesB:ds  0.000 -0.684  0.568 -0.644
```

Supplemental Table S4.18

Model output for 28°C sublethal insect growth model

```
Linear mixed model fit by REML. t-tests use Satterthwaite's method ['lmerModLmerTest']
Formula: overall_growth_rate ~ species * dose + (1 | replicate)
   Data: x28_dataset

REML criterion at convergence: -2212.3

Scaled residuals:
     Min       1Q   Median       3Q      Max
-2.75184 -0.58467  0.05086  0.75754  2.05659

Random effects:
 Groups    Name        Variance  Std.Dev.
 replicate (Intercept) 5.553e-08 0.0002357
 Residual              1.017e-06 0.0010086
Number of obs: 210, groups:  replicate, 3

Fixed effects:
               Estimate Std. Error         df t value Pr(>|t|)
(Intercept)    3.386e-03  1.891e-04  4.561e+00  17.906 2.11e-05 ***
speciesB      -2.959e-04  4.069e-04  2.031e+02  -0.727    0.468
speciesF      -4.271e-04  3.588e-04  2.031e+02  -1.191    0.235
dose          -5.141e-06  8.979e-06  2.032e+02  -0.573    0.568
speciesB:dose  8.430e-06  1.334e-05  2.031e+02   0.632    0.528
---
Signif. codes:  0 ‘***’ 0.001 ‘**’ 0.01 ‘*’ 0.05 ‘.’ 0.1 ‘ ’ 1

Correlation of Fixed Effects:
            (Intr) specsB specsF dose
speciesB    -0.224
speciesF    -0.254  0.120
dose         0.000 -0.002 -0.879
speciesB:ds  0.000 -0.663  0.590 -0.671
```

Supplemental Table S4.19

Model output for 33°C sublethal insect growth model

```
Linear mixed model fit by REML. t-tests use Satterthwaite's method ['lmerModLmerTest']
Formula: overall_growth_rate ~ species * dose + (1 | replicate)
   Data: subset_data33

REML criterion at convergence: -2714

Scaled residuals:
     Min       1Q   Median       3Q      Max
-2.76918 -0.58046  0.04371  0.73384  2.64487

Random effects:
 Groups    Name        Variance  Std.Dev.
 replicate (Intercept) 1.353e-08 0.0001163
 Residual              6.890e-07 0.0008301
Number of obs: 246, groups:  replicate, 3

Fixed effects:
                  Estimate Std. Error         df t value Pr(>|t|)
(Intercept)      3.130e-03  1.306e-04  1.090e+01  23.960 8.93e-11 ***
speciesB        -5.087e-04  1.704e-04  2.399e+02  -2.986 0.003121 **
speciesF        -5.895e-04  1.625e-04  2.400e+02  -3.628 0.000349 ***
dose25           2.141e-04  1.687e-04  2.393e+02   1.269 0.205679
speciesB:dose25  1.010e-05  2.412e-04  2.394e+02   0.042 0.966640
---
Signif. codes:  0 ‘***’ 0.001 ‘**’ 0.01 ‘*’ 0.05 ‘.’ 0.1 ‘ ’ 1

Correlation of Fixed Effects:
            (Intr) specsB specsF dose25
speciesB    -0.564
speciesF    -0.592  0.456
dose25      -0.001  0.001 -0.501
specsB:ds25  0.000 -0.401  0.350 -0.700
```

Supplemental Table S4.20

Bonferroni contrasts for sublethally-infected insects: 18°C

Fit: formula = growth rate ~ pathogen * dose + (1 | replicate), data = 18C)

contrast	estimate	SE	df	t.ratio	p.value
C dose0 - B dose25	4.73e-05	0.000165	210	0.286	1.0000
C dose0 - F dose25	-1.11e-04	0.000157	209	-0.705	0.9987
C dose0 - B dose50	3.48e-04	0.000184	210	1.887	0.6234
C dose0 - F dose50	4.36e-04	0.000168	210	2.588	0.1979
B dose25 - F dose25	-1.58e-04	0.000173	210	-0.913	0.9921
B dose25 - B dose50	3.01e-04	0.000196	209	1.533	0.8389
B dose25 - F dose50	3.88e-04	0.000181	208	2.143	0.4470
F dose25 - B dose50	4.59e-04	0.000191	209	2.400	0.2894
F dose25 - F dose50	5.46e-04	0.000176	209	3.102	0.0549
B dose50 - F dose50	8.77e-05	0.000199	209	0.440	1.0000

Degrees-of-freedom method: kenward-roger
P value adjustment: tukey method for comparing a family of 9 estimates

Supplemental Table S4.21

Bonferroni contrasts for sublethally-infected insects: 23°C

Fit: formula = growth rate ~ pathogen * dose + (1 | replicate), data = 23C)

contrast	estimate	SE	df	t.ratio	p.value
C dose0 - B dose25	1.93e-04	0.000171	210	1.128	0.9694
C dose0 - F dose25	1.93e-04	0.000171	210	1.128	0.9694
C dose0 - B dose50	5.36e-04	0.000163	210	3.285	0.0321
C dose0 - F dose50	5.68e-04	0.000169	210	3.364	0.0252
B dose25 - F dose25	3.43e-04	0.000179	210	1.914	0.6046
B dose25 - B dose50	7.01e-05	0.000211	210	0.332	1.0000
B dose25 - F dose50	3.75e-04	0.000183	210	2.047	0.5123
F dose25 - B dose50	-2.73e-04	0.000205	210	-1.334	0.9201
F dose25 - F dose50	3.20e-05	0.000177	210	0.180	1.0000
B dose50 - F dose50	3.05e-04	0.000209	210	1.460	0.8727

Degrees-of-freedom method: kenward-roger
P value adjustment: tukey method for comparing a family of 9 estimates

Supplemental Table S4.22

Bonferroni contrasts for sublethally-infected insects: 28°C

Fit: formula = growth rate ~ pathogen * dose + (1 | replicate), data = 28C)

contrast	estimate	SE	df	t.ratio	p.value
C dose0 - B dose25	2.14e-04	0.000215	203	0.992	0.9863
C dose0 - F dose25	5.56e-04	0.000194	203	2.866	0.1035
C dose0 - B dose50	1.31e-04	0.000223	204	0.590	0.9996
C dose0 - F dose50	6.84e-04	0.000218	203	3.146	0.0486
B dose25 - F dose25	3.42e-04	0.000222	203	1.538	0.8362
B dose25 - B dose50	-8.22e-05	0.000248	203	-0.332	1.0000
B dose25 - F dose50	4.71e-04	0.000244	203	1.932	0.5922
F dose25 - B dose50	-4.24e-04	0.000229	204	-1.849	0.6491
F dose25 - F dose50	1.29e-04	0.000225	203	0.572	0.9997
B dose50 - F dose50	5.53e-04	0.000249	203	2.220	0.3970

Degrees-of-freedom method: kenward-roger
P value adjustment: tukey method for comparing a family of 9 estimates

Supplemental Table S4.23

Bonferroni contrasts for sublethally-infected insects: 33°C

Fit: formula = growth rate ~ pathogen * dose + (1 | replicate), data = 33C)

contrast	estimate	SE	df	t.ratio	p.value
C dose0 - B dose25	2.84e-04	0.000161	240	1.767	0.7038
C dose0 - F dose25	3.75e-04	0.000166	241	2.258	0.3719
C dose0 - B dose50	5.09e-04	0.000171	240	2.980	0.0760
C dose0 - F dose50	5.89e-04	0.000163	240	3.619	0.0107
B dose25 - F dose25	9.09e-05	0.000167	240	0.543	0.9998
B dose25 - B dose50	2.24e-04	0.000172	239	1.300	0.9305
B dose25 - F dose50	3.05e-04	0.000164	239	1.854	0.6459
F dose25 - B dose50	1.33e-04	0.000176	239	0.755	0.9979
F dose25 - F dose50	2.14e-04	0.000169	239	1.268	0.9394
B dose50 - F dose50	8.08e-05	0.000174	239	0.465	0.9999

Degrees-of-freedom method: kenward-roger
P value adjustment: tukey method for comparing a family of 9 estimates

Chapter 5

General discussion

The *Metarhizium* genus is distinguished by its evolutionary and ecological spectrum that spans from species with recent divergences, to those tracing back over 150 million years. The genus includes varied species like the foliage pest specialist *M. acridum,* to broad host range, soil-dwelling plant root endophytes like *M. brunneum* and *M. guizhouense* (Gao *et al.,* 2011; Islam *et al.,* 2021; Matar *et al.,* 2022; Jaber & Enkerli, 2016). Such diversity positions *Metarhizium* species as essential models that have independently evolved, offering experimentally tangible insights into adaptation, be it generalization or specialization, across varied environments and insect hosts (St. Leger & Wang, 2020). In *Metarhizium* species, comparative analyses reveal that examining the significant differences in metabolism, host range, and root colonization capabilities in the context of their diverse lifestyles provides a more accurate comparative understanding of these fungi (Hu *et al*., 2014; St. Leger, 2024). Moreover, our perception of entomopathogenic fungi (EPF) and host interactions has largely been built within the confines of their individual niches and environmental variables (Thomas & Blandford, 2003). Within this thesis, the research presented has highlighted the complex interplay between pathogen and host, focusing on the thermal and nutritional environments as key determinants in their mutual interactions.

In order to achieve a multidimensional analysis of the niches mediating these interactions, I began by developing a high throughput method for rapidly measuring fungal growth, an important measure of performance (Metcalfe & Monaghan, 2003). I then utilized this method to investigate the nutritional niche of EPF and investigate the correlation of fungal growth with host range. In the final experimental chapter, I explored how the combined thermal niches of both the host and the pathogen converge to define the thermal niche of the host-pathogen interaction, in terms of virulence. The collective findings derived from

the successive chapters reinforce the overarching hypothesis that the thermal and nutritional ecology of EPF and their level of specialization, or rather their different lifestyles, are intrinsically linked and play an important role in the dynamics of infection and virulence.

In the first data chapter I utilized microspectrophotometry to achieve a precise quantification of in situ fungal growth, offering insights beyond the capabilities of traditional radial expansion measurement methods typically using agar media. This technique enabled a detailed examination of the niche width of *Metarhizium* species, providing a granular view of their adaptive responses to environmental parameters of diet and temperature. While traditional radial expansion methods provide a general overview, microspectrophotometry offers an improved resolution, capturing early growth rates and deviations in growth patterns. This demonstrated the complexity and variability inherent in the growth dynamics of different *Metarhizium* species. Although the focus here remained on assessing environmental factors individually, the accuracy and efficiency of microspectrophotometry presents opportunities for future studies to explore their interactive effects, offering a more comprehensive perspective on the ecological adaptability of these fungi.

In Chapter 3, I explored the nutritional niche width of both a specialist and a broad host-range EPF, using an experimentally constructed nutritional landscape. The findings confirmed that the broad host-range species, *M. guizhouense*, exhibited a broader nutritional niche compared to the specialist, *M. acridum*. This demonstrated that the method developed in Chapter 2 serves as a useful technique for providing data for such studies, as well as that host-specialist EPF tend to have a more narrow and specialized nutritional niche. Notably, the observations pointed to a correlation between two axes of niche breadth - diet and host range.

In Chapter 4, the focus shifted to examining the thermal performance curves of the entomopathogenic fungi, specifically *M. brunneum* and *M. flavoviride*, in relation to the model host, *Tenebrio molitor.* I found that both the insect host and the fungi optimally grew at 28°C. However, virulence patterns

varied between the fungi. *Metarhizium brunneum* displayed a broader thermal niche for virulence that exceeded its growth thermal niche, whereas *M. flavoviride's* virulence aligned closely with its individual thermal growth profile. These observations partially corroborated my hypothesis. I had initially speculated that *M. brunneum*, as a generalist species, would be more versatile and possess a more expansive thermal performance curve than *M. flavoviride*. However, both species exhibited similar niche widths in terms of thermal optima. Intriguingly, *M. brunneum* displayed a wider thermal virulence niche, despite sharing comparable niche widths for individual thermal optima with *M. flavoviride.* This suggests there are secondary effects that are at play in this relationship that we are yet to understand. Additionally, the study showed the nuanced interaction effects of temperature on EPF-insect relationships, reaffirming the importance of species-specific adaptations in infection outcomes.

Niche breadth, as a measure of the adaptability of an organism to various environmental conditions, often signifies its evolutionary history, phenotypic plasticity, and survival strategy (Carscadden *et al.,* 2020). Previous to this study, it had not been specifically investigated whether specialization in host range in EPF correlates with specialization on other axes. In this work, it was found that generalist species (e.g. *M. brunneum* and *M. guizhouense*) exhibited expanded niche breadths in diet and virulence compared to more specialized species like *M. acridum* and *M. flavoviride*. This broad adaptability aligns with the ability of generalist species to parasitize a diverse array of insects and foster symbiotic relationships with plants in the rhizosphere (Hu & Bidochka, 2021; Barelli *et al.,* 2016). In the nitrogen-limited study environment in this study, there was a clear correlation between nutritional niche width and host specificity.

It has been proposed that correlation between niche breadths on multiple axes, such as thermal niche width and host specificity, is influenced by two primary factors, namely environmental drivers and functional constraints (Carscadden *et al.,* 2020). Environmental drivers, such as nutrient availability or temperature variations, can directly shape the adaptability of an organism (Wolinska & King, 2009). On the other hand, functional constraints, such as genetic limitations or metabolic restrictions, also limit the niche breadth

(Carscadden *et al.,* 2020). I propose these findings point towards a significant influence of environmental drivers in the context of the adaptation of *Metarhizium* species, aligning with the hypothesis that environmental drivers play the determining role in whether niche breadth correlates across different axes (Bebber & Chaloner, 2022; Carscadden *et al.,* 2020). Furthermore, this supports one of the main theories of the evolutionary ecology of the genus *Metarhzium*: that its adaptation is driven by ecological habitat as opposed to the availability of insect hosts (St. Leger & Wang, 2020).

The findings that are presented in this thesis, integrated with theory in niche breadth axes correlations, underscore the "opportunistic, versatile middleman" narrative for evolutionary strategies employed by generalist *Metarhizium* species (Sheng & Leger, 2022; Stone & Bidochka, 2020). In specialist species, the observed narrow nutritional niche, aligned with a constricted host range, reflects their adaptation to more specific ecological niches. In contrast, the generalist species exhibit a broader nutritional niche and infective capability, indicative of their opportunistic versatility. This versatility reflects their ecological adaptability, where they are not limited to a particular host but have developed multitrophic lifestyles (Shen & Leger, 2020). This could be attributed to their inherent traits, allowing them to maximize infection opportunities in diverse habitats. Generalist *Metarhizium* spp. are known to possess factors contributing to rhizosphere fitness, notably ecological and nutritional versatility, in abundance (Odelade & Babalola, 2019; St. Leger & Wang, 2020). Genomic studies have shown that generalists, compared to specialists, possess expanded gene families linked with pathogenesis (Wang *et al.,* 2016). The broader infective capability observed in generalist *Metarhizium* spp., paired with their pronounced nutritional versatility, corroborates the idea that these species are prime examples of opportunistic adaptors.

The findings presented in Chapter 4 on the thermal mismatch between host and pathogens proved intriguing and contrary to our expectations. It was initially predicted that at cooler temperatures the pathogens would have a competitive edge over the warm-adapted insect host, *T. molitor,* in accordance with the Thermal Mismatch Hypothesis and given the acclimatization of the

pathogens to the warmer temperatures of 28°C, as well as previous establishment of this growth optima in the literature (Rohr *et al.,* 2017; Graham *et al.,* 2000; Sinclair *et al.,* 2022). Contrary to this prediction, it seems that the pathogens are thermally synchronized with this host, with both performing optimally at 28°C. This alignment led to a scenario where the pathogens displayed peak virulence at the host's optimal growth temperature. I propose that this ability of the pathogen to outcompete the host, even when individually constrained, e.g. performing relatively worse than the host at a given temperature, may be a defining characteristic of a "true generalist" for EPF.

On the other hand, this unexpected result might arise from extraneous underlying factors. It could be that the artificial experimental set up in our model does not capture the complexity of the niche interactions in natural settings. Laboratory conditions differ from the natural environment in a multitude of ways. One particularly relevant aspect is the dose of spores applied to the host to induce mortality. The LC 50 value for *M. flavoviride* was quite high and almost twice that, of *M. brunneum*, which brings into question how ecologically relevant this dose is. Given the intense exposure of the insect to spores in optimal germination conditions in our experiment, it raises questions about real-world dynamics going on in the soil environment. We need to know more about the dynamics of natural infections in order to truly elucidate what the relationship is in natural systems between these particular hosts and pathogens. Further specific considerations could include: the frequency and quantity of spores that a host such as *T. molitor* encounters in the natural soil environment, the most vulnerable points in the lifecycle (e.g. after molting) and how frequently this happens, along with how often the humidity conditions are optimal for germination, in order to better understand disease progression in nature, and moreover, how these pathogens are operating as entomopathogens in soil environments. This would provide a clearer picture of disease ecology and the pathogenic strategies employed by these fungi in soil ecosystems.

It has been proposed that generalist *Metarhizium* fungi are only opportunistically parasitizing insects, and rely mostly on their stable associations with plants. This raises the question of how integral insect parasitism truly is to

EPF lifecycle and survival, and furthermore, if their predominant associations are with plants, what evolutionary dynamics maintain their entomopathogenic traits? The nitrogen transfer from insects to plants in these associations offers another intriguing dimension to explore (Behie & Bidochka, 2014). It is possible insect parasitism might serve more as a periodic nutritional enrichment rather than a primary survival mechanism, creating specific ecological scenarios where insect pathogenesis becomes crucial for EPF proliferation and survival. It is essential to consider the significance of these fungi infecting an insect host periodically to evolutionarily sustain insect pathogenesis as a lifestyle. While this research has provided new insight into the dynamics between entomopathogens and their insect hosts, a holistic understanding demands exploration of multitrophic interactions in this system.

Lastly, while *T. molitor* might appear to be acclimatized to warm temperatures in some respects, especially after being reared in laboratory conditions for numerous generations, its ability to withstand colder temperatures shouldn't be overlooked (Catalán *et al.*, 2020). It's plausible that this insect retains defensive mechanisms or immune responses which are active at temperatures cooler than those tested in this work, allowing it to overcome pathogen infections (Graham *et al.,* 2000). This dynamic might drive up the observed optimal temperature for virulence. Investigating the immune responses of cold-resistant insects in tandem with fungal virulence bioassays to deduce thermal profiles for immune response as well as virulence could yield crucial insights into the dynamic interplay between these factors and the disease outcomes observed at different temperatures.

Conclusions & Perspectives

In this body of work, I investigated the dynamics of host-pathogen interactions within the genus *Metarhizium*, a fungal group known for its evolutionary and ecological diversity. From soil-dwelling plant symbionts to specialists in foliar insect pathogens, *Metarhizium* species offer a valuable window into the

evolutionary paths of generalization versus specialization across varied environments and hosts.

The research presented in this thesis developed a novel high-throughput microspectrophotometry method for rapid fungal growth assessment, enabling us to explore the nutritional and thermal ecologies of these EPF and supporting our hypothesis for Chapter 1. This method, validated against traditional measures, facilitated a detailed analysis of nutritional niche widths, highlighting a correlation between the breadth of nutritional and host range niches in EPF.

In the pursuit of quantifying niche breadth, we discovered that generalist species, such as *M. brunneum* and *M. guizhouense*, exhibited greater versatility in diet and virulence compared to the more specialized *M. acridum and M. flavoviride,* which aligns with the hypotheses proposed in Chapter 3. This versatility is likely tied to their wider ability to exploit varied nutrititive sources and establish symbiotic relationships within the rhizosphere, potentially driven by an expanded repertoire of pathogenesis-related genes.

The exploration of thermal ecology within host-pathogen dynamics, as delineated in Chapter 4, advances our understanding of how temperature influences entomopathogenic fungal interactions with their insect hosts. The investigation into the Thermal Mismatch Hypothesis through the thermal performance profiles of *M. brunneum* and *M. flavoviride* against *T. molitor* resulted in both consistencies and deviations from our original hypotheses. While we anticipated finding distinct thermal performance curves that could pinpoint effective infection hotspots, both pathogens and the host exhibited shared growth optima at 28°C, challenging the expectation of a strict thermal mismatch. Furthermore, the discovery that both EPF species reached peak virulence at the host's optimal temperature nuances our understanding of thermal ecology's role in pathogenicity, diverging from the TMH's predictions and with the specific TMH predictions for Chapter 4. On the other hand, *M. brunneum's* broader thermal range for virulence and *M. flavoviride's* multiphasic virulence-temperature relationship underscore the complexity of thermal influences on host-pathogen interactions. These findings substantiate the hypothesis for Chapter 4 that

generalists will have broader thermal virulence niches and suggest that the thermal ecology of EPF and their insect hosts reflect their evolutionary histories and ecological strategies, offering critical insights into the ecological and evolutionary dynamics that govern infection outcomes.

Looking forward, the techniques and insights from this study could be applied to optimize the use of EPF in biological control systems and ensure the health of industrially farmed insect populations. Broadly, this research informs basic theory in host-pathogen interactions and disease dynamics, which forms the basis for any applied study. Specifically, the contribution of this work to the applied fields of biocontrol and insect farming hinges on its potential to refine and enhance current practices through evidence-based insights. In the realm of biocontrol, the detailed understanding of host-pathogen interactions, especially involving *Metarhizium* species, offers a nuanced perspective on how fungal pathogens can be more effectively used to target and manage pest populations in agriculture. This could lead to the development of more precise biopesticides that are not only highly effective against specific pests but also minimize collateral impact on non-target species and the environment. Such advancements could improve the efficacy, sustainability, and public acceptance of biocontrol methods. For the insect farming industry, this research provides critical information on protecting farmed insects from diseases, particularly those caused by EPF. By identifying the conditions under which EPF become pathogenic to beneficial insects, operators can develop better biosecurity measures and management practices to prevent outbreaks and ensure the health and productivity of farmed insects. This is particularly relevant for industries reliant on insects for pollination, food production, or as feedstock, where disease management is crucial for operational success. Moreover, this work's contributions to basic science—understanding the ecological and evolutionary dynamics of EPF-host interactions—equip practitioners with the knowledge to anticipate and mitigate potential challenges. This includes the development of resistance in pest populations and the adaptation of biocontrol agents to changing environmental conditions, ensuring long-term viability and effectiveness of biocontrol strategies.

In terms of research trajectories, the door is now open to explore the interactive effects of nutritional and thermal factors in defining the ecological adaptability of EPF. Such multidimensional studies will be crucial for a holistic understanding of EPF ecology and their role in agroecosystems. Furthermore, while this thesis has advanced our knowledge on the niche breadth correlations in EPF, continued exploration is warranted, especially in the context of multitrophic interactions and their influence on EPF life histories. As we contemplate the role of insect parasitism in the lifecycle of EPF, future studies may also delve into the evolutionary pressures that preserve entomopathogenic traits, even as some species exhibit closer associations with plant hosts.

In conclusion, the findings from this research underscore the complex dynamics that define the ecologies of different *Metarhizium* species and shed light on the environmental parameters and interactions that distinguish a generalist pathogen from a specialist. Exploring these dynamics offers insights into their adaptability, evolutionary narratives, and the critical role of thermal factors in their pathogenic success. Furthermore, this work has also contributed to the discourse on niche breadth correlation. The exploration of niche breadth correlation further enriches our understanding, demonstrating that variance in one dimension (e.g., nutrition) can reflect breadth in another (e.g., host range) for EPF. Additionally, the introduction of a rapid microspectrophotometry method for measuring fungal performance represents a significant advancement, offering a valuable tool for assessing multifactorial niche dimensions, which could facilitate more comprehensive investigations into the ecological strategies of EPF. The findings here not only advance the theoretical framework of host-pathogen interactions but also have practical implications for biocontrol strategies and insect production, guiding the development of more effective and sustainable agricultural practices. This thesis stands as a contribution to the evolving tapestry of knowledge surrounding EPF, their insect hosts, and their shared ecological interactions.

5.2 References

Barelli, L., Moonjely, S., Behie, S. W., & Bidochka, M. J. (2016). Fungi with multifunctional lifestyles: endophytic insect pathogenic fungi. *Plant molecular biology*, *90*, 657-664.

Behie, S. W., & Bidochka, M. J. (2014). Ubiquity of insect-derived nitrogen transfer to plants by endophytic insect-pathogenic fungi: an additional branch of the soil nitrogen cycle. *Applied and environmental microbiology*, *80*(5), 1553-1560.

Carscadden, K. A., Emery, N. C., Arnillas, C. A., Cadotte, M. W., Afkhami, M. E., Gravel, D., & Wiens, J. J. (2020). Niche breadth: causes and consequences for ecology, evolution, and conservation. *The Quarterly Review of Biology*, *95*(3), 179-214.

Catalán, T. P., Niemeyer, H. M., Kalergis, A. M., & Bozinovic, F. (2012). Interplay between behavioural thermoregulation and immune response in mealworms. *Journal of Insect Physiology, 58*, 1450–1455.

Cohen, J. M., Venesky, M. D., Sauer, E. L., Civitello, D. J., McMahon, T. A., Roznik, E. A., & Rohr, J. R. (2017). The thermal mismatch hypothesis explains host susceptibility to an emerging infectious disease. *Ecology letters*, *20*(2), 184-193.

Gao, Q., Jin, K., Ying, S. H., Zhang, Y., Xiao, G., Shang, Y., & Wang, C. (2011). Genome sequencing and comparative transcriptomics of the model entomopathogenic fungi *Metarhizium anisopliae* and *M. acridum. PLoS genetics*, *7*(1), e1001264.

Hu, S., & Bidochka, M. J. (2021). Root colonization by endophytic insect-pathogenic fungi. *Journal of applied microbiology, 130*(2), 570-581.

Hu, X., Xiao, G., Zheng, P., Shang, Y., Su, Y., Zhang, X., & Wang, C. (2014). Trajectory and genomic determinants of fungal-pathogen speciation and host adaptation. *Proceedings of the National Academy of Sciences*, *111*(47), 16796-16801.

Islam, W., Adnan, M., Shabbir, A., Naveed, H., Abubakar, Y. S., Qasim, M., & Ali, H. (2021). Insect-fungal-interactions: A detailed review on

entomopathogenic fungi pathogenicity to combat insect pests. *Microbial Pathogenesis*, *159*, 105122.

Jaber, L. R., & Enkerli, J. (2016). Effect of seed treatment duration on growth and colonization of *Vicia faba* by endophytic *Beauveria bassiana* and *Metarhizium brunneum. Biological Control*, *103*, 187-195.

Odelade, K. A., & Babalola, O. O. (2019). Bacteria, fungi and archaea domains in rhizospheric soil and their effects in enhancing agricultural productivity. *International Journal of Environmental Research and Public Health*, *16*(20), 3873.

Liao, X., O'Brien, T. R., Fang, W., & St. Leger, R. J. (2014). The plant beneficial effects of *Metarhizium* species correlate with their association with roots. *Applied microbiology and biotechnology*, *98*, 7089-7096.

Matar, N., Macadre, C., Ammar, G. A., Peres, A., Collet, B., Boustany, N. E., & Ratet, P. (2022). Identification of beneficial Lebanese *Trichoderma* spp. wheat endophytes. *Frontiers in Plant Science*, *13*, 1017890.

Metcalfe, N. B., & Monaghan, P. (2003). Growth versus lifespan: perspectives from evolutionary ecology. *Experimental gerontology*, *38*(9), 935-940.

Meyling, N. V., Thorup-Kristensen, K., & Eilenberg, J. (2011). Below-and aboveground abundance and distribution of fungal entomopathogens in experimental conventional and organic cropping systems. *Biological Control*, *59*(2), 180-186.

Sheng, H., McNamara, P. J., & Leger, R. J. S. (2022). *Metarhizium*: an opportunistic middleman for multitrophic lifestyles. *Current Opinion in Microbiology*, *69*, 102176.

Sinclair, B. J., Sørensen, J. G., & Terblanche, J. S. (2022). Harnessing thermal plasticity to enhance the performance of mass-reared insects: Opportunities and challenges. *Bulletin of Entomological Research*, *112*(4), 441-450.

St. Leger, R. J. (2024). The evolution of complex *metarhizium*-insect-plant interactions. *Fungal Biology*.

Stone, L. B., & Bidochka, M. J. (2020). The multifunctional lifestyles of *Metarhizium*: Evolution and applications. *Applied microbiology and biotechnology*, *104*, 9935-9945.

Wang, J. B., Leger, R. S., & Wang, C. (2016). Advances in genomics of entomopathogenic fungi. *Advances in genetics*, *94*, 67-105.

Wolinska, J., & King, K. C. (2009). Environment can alter selection in host–parasite interactions. *Trends in parasitology*, *25*(5), 236-244.

Appendix

insects

MDPI

Article

A Rapid Method for Measuring In Vitro Growth in Entomopathogenic Fungi

Anna R. Slowik [1,2,3,*], Helen Hesketh [2], Steven M. Sait [3] and Henrik H. de Fine Licht [1,*]

[1] Department of Plant and Environmental Sciences, University of Copenhagen, Thorvaldsensvej 40, 1871 Frederiksberg, Denmark
[2] UK Centre for Ecology & Hydrology, Maclean Building, Benson Lane, Crowmarsh Gifford, Wallingford OX10 8BB, UK; hhesketh@ceh.ac.uk
[3] School of Biology, Faculty of Biological Sciences, University of Leeds, Leeds LS2 9JT, UK; s.m.sait@leeds.ac.uk
* Correspondence: slowik@plen.ku.dk (A.R.S.); hhdefinelicht@plen.ku.dk (H.H.d.F.L.)

Simple Summary: This study aimed to develop a rapid and efficient method for measuring the growth of entomopathogenic fungi, which are used as environmentally friendly alternatives to chemical insecticides. The traditional methods used to measure fungal growth are time-consuming and limited in their ability to capture important aspects of growth. In this research, we implemented an indirect measure using a microplate reader, which uses the optical density of small-volume cultures to estimate fungal growth. We directly related changes in optical density to the amount of fungal biomass, and compared the results of this method with traditional measurements on solid agar plates. We found that the microspectrophotometric approach provided accurate and reliable measurements. Our findings revealed differences in growth rates and biomass production among different species and isolates of the fungi. This technique offers a valuable tool for studying the growth dynamics of entomopathogenic fungi, and has practical applications in assessing their virulence and pathogenic potential. It can contribute to our understanding of how these fungi grow during infection, and aid in the development of effective biological control strategies against insect pests.

Abstract: Quantifying the growth of entomopathogenic fungi is crucial for understanding their virulence and pathogenic potential. Traditional methods for determining growth, such as biomass determination or colony growth area, are time-consuming and quantitatively and spatially limited in scope. In this study, we introduce a high-throughput method for rapidly measuring fungal growth using spectrophotometry in small-volume, liquid media cultures in 96-well microplates. Optical density (OD) changes were directly correlated with dry weight of samples for six isolates from three species of the genus *Metarhizium* to validate spectrophotometric growth measurements, and investigate species- and isolate-specific effects. We quantified fungal biomass from the microcultures by extracting, drying, and weighing mycelial mats. From the relationship established between OD and biomass, we generated standard curves for predicting biomass based on the OD values. The OD measurements clearly distinguished growth patterns among six isolates from three *Metarhizium* species. The logistic growth phase, as captured by the OD measurements, could be accurately assessed within a span of 80 h. Using isolates of *M. acridum*, *M. brunneum*, and *M. guizhouense*, this technique was demonstrated to be an effective, reproducible, and simple method for rapidly measuring filamentous fungal growth with high precision. This technique offers a valuable tool for studying the growth dynamics of entomopathogenic fungi and investigating the factors that influence their growth.

Keywords: *Metarhizium*; fungal growth; filamentous fungi; bioassay technique; spectrophotometry; microspectrophotometry; microplate reader; biomass quantification

Citation: Slowik, A.R.; Hesketh, H.; Sait, S.M.; de Fine Licht, H.H. A Rapid Method for Measuring In Vitro Growth in Entomopathogenic Fungi. *Insects* **2023**, *14*, 703. https://doi.org/10.3390/insects14080703

Academic Editors: Monique M. van Oers, Annete Bruun Jensen and Christina Nielsen-LeRoux

Received: 11 July 2023
Revised: 10 August 2023
Accepted: 11 August 2023
Published: 13 August 2023

1. Introduction

Entomopathogenic fungi are important natural regulators of insect populations, and are widely used as environmentally friendly biological control alternatives to synthetic chemical insecticides [1–4]. In biological studies, measurements of fungal growth over time on different defined media serve as a standard measure to assess performance and evaluate efficacy during isolation and testing [5,6]. Being heterotrophic organisms with indeterminate growth, fungal growth often responds directly to the quality and availability of nutrients in the immediate environment [7,8]. Fungal growth over time can be evaluated using various methods, generally classified as direct or indirect measures [9]. The most widely applied direct methods include measurement of hyphal extension [10], dry weight from liquid cultures, and radial expansion on solid agar [11,12]. Accepted indirect methods make use of spectrophotometry in liquid macro- or micro-cultures [10,13,14], fluorescence of labeled fungi and light sheet fluorescence [15,16], multispectral imaging [17], quantification of chitin production [18,19], and advances in the spectrophotometric analysis of microcultures on agar media [20].

Measurement of the radial expansion of fungal colonies on solid media is a widely-used direct method to quantify growth. The method is straightforward, and allows for measurement of other phenotypic traits such as spore production and colony morphology (e.g., color, branching pattern) [6,8,21]. However, this approach fails to account for some important aspects of growth, such as the density of the mycelium [20]. An expanding colony can exhibit varying degrees of mycelial density while covering the same area, which is not captured when using radial expansion measurements. Using a dry weight method to measure growth in liquid macrocultures accounts for this discrepancy in mycelial density, but requires interference with cultures through direct sampling for quantification, making real-time monitoring of in situ growth impractical [13,22].

In addition to this, the solid media environment may not be biologically appropriate for some fungi based on their specific ecologies. In entomopathogenic fungi, in vivo growth progresses primarily through the insect hemocoel, which is a submerged liquid environment [23]. The physiological and developmental biology of fungi can vary considerably, depending on whether they grow on a solid or liquid medium. For instance, solid media may support a higher production of secondary metabolites or enzymes compared to liquid media in some fungal isolates [24,25]. In terms of practicality, fungal growth on agar plates is also time-consuming to conduct. The timescale for growth of many entomopathogenic fungi when analyzing radial expansion spans multiple days, and in the case of measuring dry weight, the processing of samples involves a lengthy process of collection, drying, and weighing [3,9,21].

In situ spectrophotometry provides a viable alternative to these methods by directly correlating optical density (OD) values with an increase in fungal biomass. It is generally understood that growing fungus changes the OD of liquid cultures, because turbidity directly correlates with unit population size, which serves as the basis for the traditional spectrophotometric analysis of fungal growth [26]. In this study, we apply spectrophotometric analysis to measure the growth of entomopathogenic fungi, which are typically performed on solid agar media, as previously described. Previous studies have demonstrated the use of spectrophotometric measurements for assessing filamentous fungal growth in microcultures. However, in these studies, the relationship between dry mycelial mass and OD is extrapolated using correlation coefficients [13], or hyphal extension is employed as a growth metric [10]. The aim of this study was to establish a direct correlation between the dry weight of mycelial cultures and their corresponding OD values for six isolates of *Metarhizium* spp. This correlation allows for the construction of isolate-specific standard curves, enabling the quantification of biomass based on OD measurements.

2. Materials and Methods

2.1. Fungal Isolates and Preparation of Inoculum

The growth of two isolates within each of three different species of *Metarhizium* were compared to investigate variations among species and isolates. This was assessed in addition to the effect on the relationship between dry weight and OD. Six fungal isolates of the genus *Metarhizium* were used to produce standard curves of OD by dry weight: *M. brunneum* KVL 16_36 (Isolated from the commercial product Met52, Novozymes A/S, Krogshøjvej 36, Bagsværd, Denmark), *M. brunneum* KVL 12_30 [27], *M. acridum* KVL 18_06 (ARSEF 6421), *M. acridum* KVL 04_55 (ARSEF 7486), *M. guizhouense* KVL 19_24 (ARSEF 977), and *M guizhouense* KVL 19_28 (ARSEF 3611). The acronym ARSEF refers to the United States Department of Agriculture (USDA) Agricultural Research Service (ARS) collection of Entomopathogenic Fungal cultures (https://data.nal.usda.gov/dataset/ars-collection-entomopathogenic-fungal-cultures-arsef. URL accessed on 11 March 2022). The acronym KVL refers to the entomopathogenic fungus culture collection maintained at the Section for Organismal Biology, Department of Plant and Environmental Sciences, University of Copenhagen. *Metarhizium* (Metschnikoff) Sorokin (Order Hypocreales: Family Clavicipitaceae) was selected as the focus of our study, due to its multifaceted importance in both evolutionary ecology and practical applications in pest management [2–4].

The fungal cultures were grown on quarter-strength Sabouraud dextrose agar + yeast media (SDAY/4: 2.5 g/L 1:1 animal:bacterial peptone (bacteriological peptone and Acuferm Neoeptone, Neogen Corp., 620 Lesher Place, Lansing, MI, USA), 10 g/L dextrose (Bacteriological, Oxoid Ltd., Wade Road, Hampshire, UK), 2.5 g/L yeast extract (Neogen Corp.), 15 g/L agar (Bacteriological (European Type) No. 1, Neogen Corp.))) in Petri dishes (90 mm × 15 mm triple-vented, Sterilin Ltd., 1 Ashley Road, Altrincham, Cheshire, UK) at 23 °C, and conidia were harvested after 14 days. The conidia were collected in 0.1% (*v*/*v*) Tween® 80 (Merk KgaA, Frankfurter Straße 250, Darmstadt, Germany) via agitation with a Drigalski spatula from sporulating colonies, and the resulting suspension was centrifuged; the supernatant was removed, and the colonies were rinsed twice with 0.1% (*v*/*v*) Tween® 80 to remove all fragments of mycelia. Conidial suspensions were prepared at a concentration of 2×10^6 conidia per mL by dilution using 0.1% (*v*/*v*) Tween® 80. The concentration of the stock suspension was determined by counting conidia from 1000× serially diluted stock suspension in a Fuchs Rosenthall hemocytometer (×400 magnification). To verify germination, 100 µL of 100× diluted stock suspension was spread with a Drigalski spatula on an agar plate of SDAY/4 and incubated for 24 h at 23 °C. Four microscope coverslips (22 mm × 22 mm) were then placed over the culture surface, and 100 conidia were counted under each coverslip. Conidia were considered to have germinated with the germ tube that was at least as long as the width of the conidium, and conidial germination after 24 h was verified as >98% in all cases before being used in further assays.

2.2. Continuous Growth Curve

To determine whether measurement by spectrophotometry in liquid microcultures can accurately capture the growth curve of an entomopathogenic fungus, a growth curve of *M. brunneum* KVL 12_30 was produced. The microcultures were prepared in 96 wells of a clear flat-bottom vented microplate (Starlab International GmbH, Neuer Höltigbaum 38, Hamburg, Germany) by inoculating 100 µL of 2×10^6 conidial suspension into 100 µL Sabouraud dextrose + yeast media (SDY/4: 2.5 g/L 1:1 animal:bacterial peptone, 10 g/L dextrose, 2.5 g/L yeast extract). The OD of each well was measured at 405 nm in a Synergy™ HT MultiDetection Microplate Reader (BioTek Instruments Ltd., Cheadle, UK) with Gen5 software Version 2.00.18 every 10 min for 96 h at 24 °C, without removal of the microplate from the plate reader. The wavelength of 405 nm was previously described as being fit for this purpose [10]. Pilot assays were performed comparing a range of wavelengths for measuring growth in microcultures that confirmed this. The microcultures were checked visually for bacteria using a compound microscope upon completion to ensure they were uncontaminated.

2.3. Standard Curve for Fungal Dry Weight and OD

To establish a correlation between OD and fungal biomass, OD values were measured, and the mycelial mats were subsequently extracted and weighed for the six isolates at four time points (20, 40, 60, and 80 h post-inoculation) during the linear growth phase. The period of logistic growth was determined from the continuous growth curve generated, as detailed in Section 2.2, utilizing the described parameters for media and conidial suspension. The fungal microcultures were prepared as described in Section 2.2. For each measurement at the four time points, a single microplate containing 60 wells was utilized to assess the determination of dry weight, resulting in a total of 240 wells analyzed across the four measurements. To mitigate edge effects arising from temperature and evaporation, the 36 wells around the edge of the plate were excluded from analysis and loaded with 200 µL of blank media [28]. The microplates were incubated at 23 ± 0.5 °C, and the OD measured at 405 nm at 20, 40, 60, and 80 h post-inoculation using a Synergy^{TM} HT MultiDetection microplate reader with Gen5 software. At each time point, one microplate per isolate was collected after OD measurement and stored at −20 °C. The OD values of all of the microplates were also measured after conidia settled (15 min post-inoculation) to establish the baseline reading OD of each culture. This baseline reading was subtracted from subsequent measurements to determine changes in OD for the construction of standard curves.

To quantify the changes in biomass of the microcultures, mycelial mats were extracted for the determination of dry weight. Thawed microplates were centrifuged in an Eppendorf Centrifuge 5810R (1968× *g*) at 4000 rpm for three minutes to force fungal material to the bottom of the wells, and the remaining media supernatant was removed using a pipette. The wells were then filled with 200 µL of 99% ethanol, and mycelia were scraped from the bottom of the well with a pipette tip to re-suspend the fungal material. The entire content of the well was then transferred to a pre-weighed aluminum weigh boat using a cut pipette tip. The process was repeated three times, refilling each well with 200 µL of ethanol and scraping to ensure complete removal of residual mycelial matter and rinsing of the pipette tip. Thus, a total of 600 µL of ethanol was utilized to thoroughly wash each well. Complete extraction of mycelial material from the wells was confirmed through microscopic examination of the microplates. If any residual mycelial material was observed, the extraction process was repeated until the wells were free of any remaining matter. For each isolate, ten replicate wells containing resultant mycelial suspensions were pooled into pre-weighed aluminum boats, resulting in a total of six pooled dry weight measurements per microplate with an approximate volume of 6 mL. The pooled samples were subsequently dried in an oven for 72 h at 60 °C within a heat-resistant, lidded box. Finally, the dried samples were weighed on a precision scale (Sartorius ME36S Ultra Micro Balance, 31 g × 0.001 mg (Sartorius UK Ltd., Epsom, UK).

Standard curves were produced to establish the correlation between OD and change in biomass using the OD measurements and their corresponding pooled biomass samples. At each measurement time point, the base OD values were subtracted from the measured OD values, and the resulting OD values for the 10 pooled wells in the sample were averaged. Regression analysis was performed to construct standard curves of OD by dry weight using the R package stats [29]. To test for differences in relationships between the OD and dry weight between isolates, a pairwise comparison of slope estimates was conducted using lsmeans [30]. This analysis applies a p value multiplicity adjustment to the least squares means of each isolate using Tukey's HSD. Linear regression was also performed to determine slope estimates for biomass added over time for each isolate. All statistical calculations were conducted in R Version 1.4.1717 [29].

2.4. Comparison of OD Growth Measure to Radial Growth Measure on Agar Plates

To evaluate how the microspectrophotometric method compared to traditional growth assays performed on solid media, the growth of two isolates (*M. guizhouense* KVL 19_28 and *M. acridum* KVL 04_55) was measured using both microspectrophotometry and radial

expansion methods. These experiments were conducted under the same conditions at 23 °C in SDY/4 and SDAY/4 media, respectively. For the microspectrophotmetric analysis, media and conidial suspensions were prepared as described in Section 2.2 in a microplate (n = 96). OD measurements were taken during the linear phase of the logistic growth curve (24 h post-inoculation) at 405 nm in 8-hour intervals. This provided a total of five measurements. To estimate the biomass, the linear equations deduced from the standard curves were applied to the spectrophotometric measurements. This allowed for the determination of the biomass estimation based on the spectrophotometric data.

To conduct the radial expansion analysis, for each isolate, four Petri dishes (90 mm × 15 mm, vented) of SDAY/4 were each inoculated with five cultures (n = 20). The inoculation was performed using 5 µL of a conidial suspension with a concentration of 2.4×10^4 spores per mL, prepared according to the methods described in Section 2.1. Germination of the conidial suspension was confirmed as >99% after 24 h on a plate of SDAY/4, following the methods detailed in Section 2.1. The growth was recorded every 4 days, starting from the first day of detectable mycelium formation (day 4) until day 11. To calculate the radial expansion, the plates were digitally photographed at each measurement time point, and the colony area was calculated in ImageJ Version 1.53s [31].

3. Results

3.1. Growth Curves and Correlation of Biomass with OD

First, it was determined that the entire growth curve of a *Metarhizium* fungus (isolate KVL 12_37, *M. brunneum*) could be captured within a short time period (96 h) using microspectrophotometry (Figure 1A). The distinct phases of fungal growth, namely the lag, log (exponential), and stationary phases, were clearly discernible in the preliminary growth curves obtained during the pilot study (Figure A1). Second, standard curves were produced to quantify the change in culture OD with a corresponding increase in dry weight of fungal biomass over the linear growth phase of the logistic growth curve for two isolates each of *M. guizhouense* (Figure 1B), *M. acridum* (Figure 1C) and *M. brunneum* (Figure 1D). The linear growth phase was determined between 20 and 80 h after inoculation, based on the specified parameters for media and concentration of conidial suspension (Figure 1A). The resulting standard curves for dry weight and OD showed high correlation coefficients across all isolates (R^2 = 0.93–0.95) (Figure 1), but with varying biomass incorporation (i.e., slopes) between isolates (Figure 2). In the pairwise comparison of the slope estimates for different isolates, some slope estimates for the relationship between OD and dry weight significantly differed from others (Figure 2 and Table 1). Notably, the *M. guizhouense* isolates (KVL 19_28 and KVL 19_24) exhibited distinct slope estimates compared to most other isolates, as well as each other (Table 1). The slope for isolate KVL 19_28 differed from all other isolates, with significantly larger dry weight estimation compared to all other isolates, with the exception of KVL 16_36 (*M. brunneum*; Table 1). Isolate KVL 19_24 was significantly different from KVL 18_06 (*M. acridum*) and KVL 16_36 ($p < 0.05$), with a smaller dry weight estimation compared to these two isolates (Figure A2).

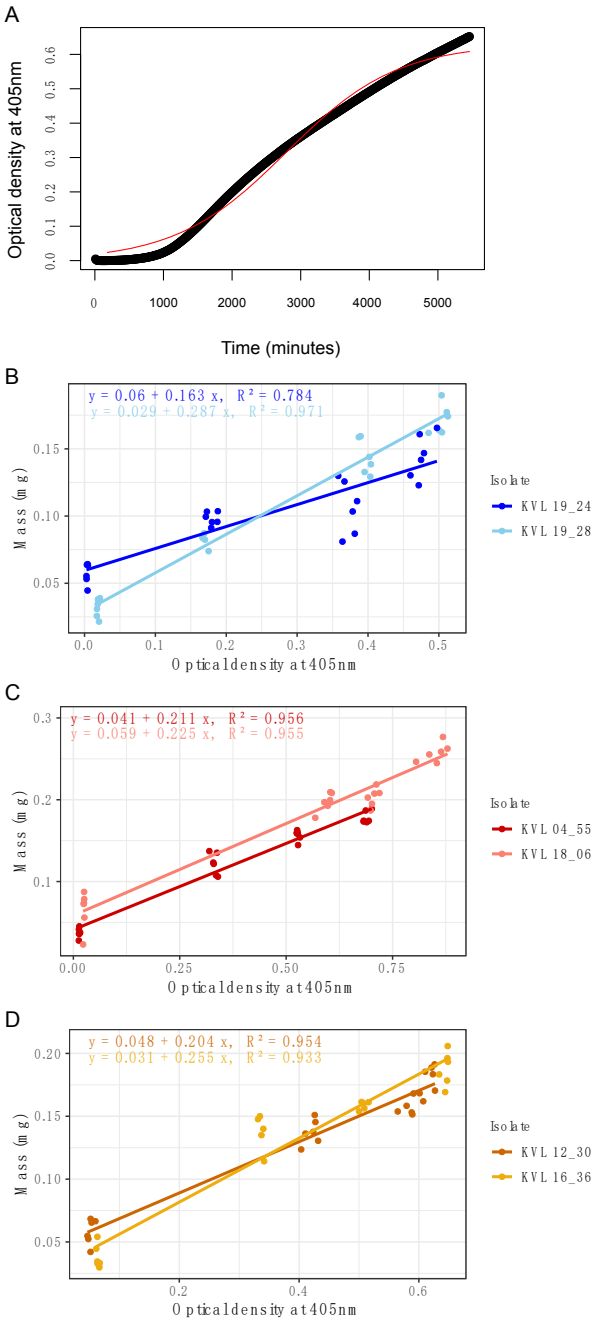

Figure 1. Standard curves and growth curve for *Metarhizium* spp. (**A**) Fitted growth curve over 96 h using continuous measurement (every 10 minutes) for *M. brunneum* KVL 12_30 for 96 averaged microcultures. The red line indicates fitted logistic growth model, and the black line is average absorbance readings for 96 wells at each time point. Standard curves for change in dry weight as a function of optical density (OD) for three species of *Metarhizium*: (**B**) *M. guizhouense* KVL 19_24 and KVL 19_28 (blue and light blue), (**C**) *M. acridum* KVL 04_55 and KVL 18_06 (red and light red) and (**D**) *M. brunnuem* KVL 12_30 and KVL 16_36 (dark yellow and yellow) cultured in a 96-well microplate. Shaded bands around regression lines indicate 95% confidence intervals.

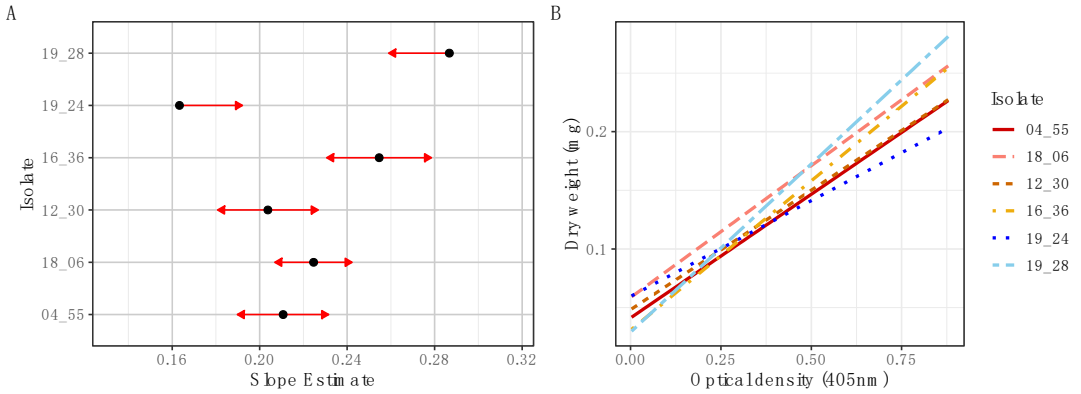

Figure 2. Comparison of slope estimates for dry weight as a function of change in optical density (OD) among six *Metarhizium* isolates. (**A**) Graphical comparisons of least squares means for each isolate's slope estimate. Black dots indicate slope estimates for biomass as a function of change in OD. The shaded bands are corresponding confidence intervals at an alpha level of 0.1. Arrow lengths indicate the amount by which confidence intervals for differences cover the value 0. (**B**) Corresponding regression lines for dry weight as a function of change in OD for six *Metarhizium* isolates.

Table 1. Pairwise comparison of slope estimates for dry weight as a function of change in OD for six *Metarhizium* isolates.

Contrast	Estimate	SE	*p* Value [1]
04_55–12_30	0.0069	0.0167	0.998
04_55–16_36	−0.0439	0.0171	0.113
04_55–18_06	−0.0139	0.0142	0.924
04_55–19_24	0.0474	0.019	0.133
04_55–19_28	−0.076	0.0185	0.001
12_30–16_36	−0.0509	0.018	0.059
12_30–18_06	−0.0209	0.0153	0.746
12_30–19_24	0.0404	0.0198	0.324
12_30–19_28	−0.0829	0.0194	0.0005
16_36–18_06	0.03	0.0158	0.406
16_36–19_24	0.0913	0.0202	0.0002
16_36–19_28	−0.0321	0.0197	0.583
18_06–19_24	0.0613	0.0178	0.009
18_06–19_28	−0.062	0.0173	0.006
19_24–19_28	−0.123	0.0214	<0.0001

[1] *p* values were adjusted for multiplicity using Tukey's HSD.

The biomass accumulated over time was determined for each isolate using slope coefficients extracted from the linear models (Figure 3A), and differences in the growth rates among isolates were clearly distinguishable between some isolates (Figure 3B). Isolates KVL 19_24 (*M. guizhouense*) grew more slowly, and had a lower overall biomass than all other isolates (Figures 2B and A2). In contrast, isolate KVL 18_06 of *M. acridum* displayed more rapid growth, and achieved a higher overall biomass compared to the other isolates (Figures 2B and A2).

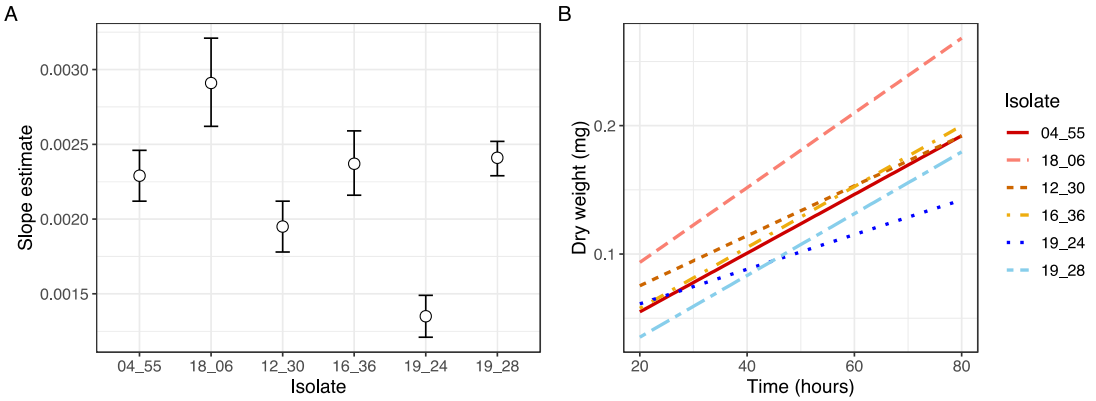

Figure 3. Biomass added over time for six *Metarhizium* isolates. (**A**) Slope estimates for linear phase growth rate of six isolates and three species of *Metarhizium* calculated using dry weight measured at 20-hour intervals from 20 to 80 h (milligrams of dry weight ~ time*isolate). Estimates are for ten pooled microcultures collected from 60 wells in a 96-well microplate, n = 6. White dots indicate the slope estimates, with SE bars calculated at an alpha level of 0.1. (**B**) Corresponding regression lines for dry weight (mg) as a function of time in hours in six *Metarhizium* isolates.

3.2. Comparison to Traditional Method and Proof of Concept

We applied this method to measure the growth rates of two species of *Metarhizium* (*M. guizhouense* KVL 19_28 and *M. acridum* KVL 04_55) over 56 h, from 20 to 80 h after inoculation (Figure 4A), in conjunction with performing the same growth analysis using a radial expansion assay over 11 days (Figure 4B). In the microspectrophotometric analysis, the respective linear equations for the two isolates derived from the standard curves were applied to the measured OD values to predict the dry weight per well. End point values between both methods showed similar results: the KVL 04_55 (*M. acridum*) isolate had a faster growth rate, growing more overall compared to KVL 19_28 (*M. guizhouense*), whether that was on the solid agar medium (Figure 4A) or using the new technique in the liquid medium (Figure 4B).

It is important to note that Figure 4A represents a shorter time period of 9 days, whereas Figure 4B covers the first 56 h only (approximately 2.33 days). This distinction underscores the significance of our method, as it reveals detailed differences in growth rates that would not be apparent otherwise. While the end points in both figures show similar results, the microspectrophotometric method provides a more detailed analysis, exposing variations in the initial growth rate. For instance, the KVL 04_55 isolate exhibits slower initial growth, only overtaking the KVL 19_28 isolate after the 40-hour sampling time point (Figure 4B). This level of detail allows us to discern growth rate differences that would not be evident from the 1–3 day growth analysis on solid media. Furthermore, an important aspect of the new assay (Figure 4A) is the low measurement error observed over this short time period. This reduced error enhances the reliability and accuracy of the growth rate measurements obtained. Finally, we developed linear models to assess the relationship between time and growth for the two measurement methods. Despite the inability to directly compare the regression lines due to the utilization of different measurement methods, the relationship between time and growth appears similar for the different isolates. The remarkable similarity observed in the regression lines (Figure 4C,D) indicates that the slopes of the growth rates for the two species of *Metarhizium* are quite similar between assays, although they are at different time scales. This similarity suggests that, regardless of potential variations in initial growth rates or growth patterns observed between the two assays (Figure 4A,B), the overall growth rates for both species exhibit a comparable trajectory over time in the context of both measurement methods.

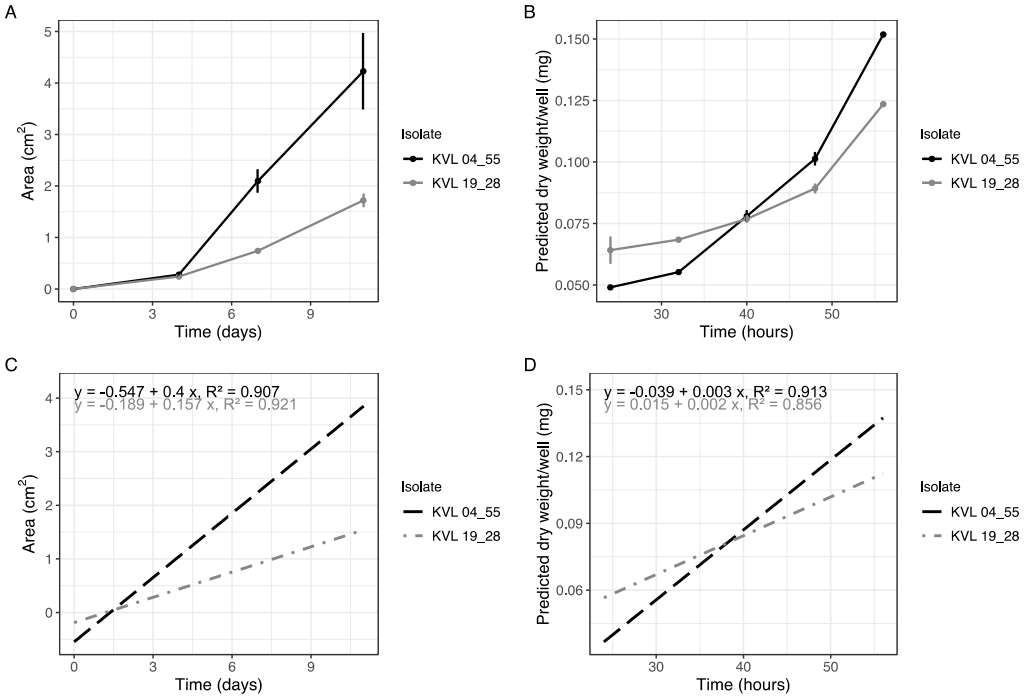

Figure 4. Growth curves for *Metarhizium acridum* KVL 04_55 and *M. guizhouense* KVL 19_28 produced on solid agar SDAY/4 media (n = 20) (**A**), using the new technique in SDY/4 liquid media (n = 96) (**B**), and regression lines for each (**C**,**D**). The equations derived from the standard curves for the relationship between absorbance and dry weight were applied to OD values measured from plates of *Metarhizium* grown over 56 h to deduce the biomass added over time for each isolate (**A**). Dots represent the mean increase in area/colony or predicted biomass/well at each time point, and bars indicate standard deviation. Regression lines (**C**,**D**) were obtained using the lm function with the method of least squares.

Continuous measurement of OD over time allowed in situ fungal growth to be monitored at a fine scale and with low measurement error, which demonstrated this as a feasible technique for the two isolates of *M. brunneum* (Figures 1D and A1). This method can also be used to measure ODs at greater intervals, or for end point determination of growth (Figure 4). The growth curve generated for *M. brunneum* KVL 12_37 and KVL 12_30 clearly differentiates the lag, exponential, and stationary phases of the growth curve from continuous readings (Figures 1A and A1).

4. Discussion

In this study, we demonstrate that microspectrophotometry can be used to capture the growth curve of entomopathogenic fungi in situ, and that the change in absorbance can be directly correlated with an increase in fungal biomass. Optical density (OD) values correlated strongly with biomass, and it was demonstrated that it is possible to produce a standard curve for the quantification of dry weight from OD by extracting, drying, and weighing the microcultures of mycelia on a precision scale (Figure 1).

In addition, we showed that change in the OD accurately represents biomass accumulation. This is not always the case in measurements of radial expansion, as the expansion of fungal colonies on solid media can often be equal in area, while having significantly different densities of mycelial growth [20]. Fungal cultures grow in multiple planar dimensions on agar (i.e., upwards and downwards, as well as across the substrate surface), and the hyphal mass can thus be more or less dense depending on nutrient availability [32].

The microspectrophotometric technique provides a quantitative measurement of hyphal density that is more uniformly distributed throughout the microculture, which produces a better representation of three-dimensional hyphal density than measuring two dimensions. This technique also makes it possible to capture specific effects from environmental changes on different fungal growth phase features that are only detectable at small time scales (Figure 4B), which produce atypical growth curves, e.g., rapid depletion of a primary nutrient source followed by a secondary phase of logarithmic growth [33]. Furthermore, the solid medium does not accurately represent the environment which entomopathogenic fungi encounter during infection (i.e., insect hemolymph). Given that most entomopathogenic fungi are filamentous with similar ecologies (i.e., penetration of host cuticle and subsequently spreading as individual cells through the insect hemocoel), this technique could be applied to investigate growth in other entomopathogenic species [34]. However, differences in biomass accumulation during growth as represented in the relationship between fungal dry weight and OD necessitates the production of standard curves specific to the isolate under investigation, although this would only need to be undertaken once per isolate to be applied to subsequent high throughput measurements.

In this study, we compared the use of microspectrophotometry with radial expansion analysis to assess the growth dynamics of two species of *Metarhizium, M. acridum* and *M. guizhouense*. Our findings demonstrated that the microspectrophotometric analysis yielded similar end point results and linear growth rates compared to the radial growth assay (Figure 4A–C). However, the microspectrophotometric technique provided the additional advantage of capturing differences in early growth rates that were not evident in the radial growth assay (Figure 4). The finer scale of measurement provided by the microspectrophotometric technique illustrates its value in accurately capturing different aspects of fungal growth curves that might be otherwise undetectable when measuring macroculture growth over many days. Compared to methods with fewer measurement points, this technique is better suited for detecting subtle differences in growth (Figure 4).

Importantly, our study revealed a different relationship between *M. acridum* and *M. guizhouense* through finer measurement intervals during critical growth phases, particularly the early linear phase, which could not be discerned through radial expansion measurements performed over several days (Figure 4). This development is significant for understanding the growth dynamics of fungi, as it has been previously shown that the classical growth curve does not always adequately describe the growth patterns of filamentous fungi [33]. Different aspects of the growth curve can change due to variables such as nutrition and the host insect environment. Capturing the growth pattern can offer important insights into various aspects of how fungi grow during infection. Notably, atypically shaped growth curves have been suggested to be the rule rather than the exception [33]. This arises from the depletion of distinct nutrients occurring at different rates, resulting in atypical-shaped growth curves, like bimodal growth peaks [33]. These curves reveal nutritive preferences that might be otherwise overlooked without the necessary sensitivity in measurements. Our study revealed that the *M. acridum* KVL 04_55 isolate generally exhibited more growth over time compared to other isolates (Figure 4). However, a notable finding was that in the early stages, this isolate displayed a significantly slower growth rate compared to the other isolate examined, *M. guizhouense* KVL 19_28. This observation provides important insights into the growth dynamics and pathogenic potential during early infection processes for this particular isolate [35].

Additionally, our findings have practical implications regarding the pathogenic potential of the different isolates and species measured. By comparing the growth rates and total biomass produced between isolates, our findings shed light on the potential speed of host invasion across different species of *Metarhizium*. Significantly differing slope estimates and total biomass production were observed not only between species, but also among isolates, indicating variations in pathogenicity potential within this in vitro setting (Figures 3 and A2). This highlights the practical application of the method in assessing the virulence and pathogenic potential of the examined isolates and species.

Previous studies demonstrated the use of microspectrophotometry in monitoring the growth of filamentous fungi, but were unable to determine the dry weight of individual microcultures, and therefore relied on comparisons of indirect metrics to extrapolate the relationship between OD and fungal dry weight [10,13], or used microscopic measurements of hyphal extension to infer growth [10]. In this research, we inferred growth in microculture using mycelial dry weight, and generated standard curves for direct correlation. While the microspectrophotometric technique may provide limited phenotypic information compared to solid media bioassays, such as the measurement of spore production and colony color, it offers complementary advantages in capturing biomass build-up during the early phases of the growth curve, and obtains data rapidly. The speed at which growth data can be obtained using microspectrophotometry is a clear advantage, as linear growth of the tested *Metarhizium* isolates could be measured within a few days, whereas radial growth on agar plates typically takes 10–14 days.

The need to produce entomopathogenic fungi for biocontrol at massive scales makes it important to be able to investigate the effects of different media and nutrients on entomopathogenic fungal growth, and identify optimal growth parameters [36]. In addition, for experimental biologists, this method allows for large-scale experiments using growth as a primary measure of performance in areas of research such as fitness costs, adaptation [37], and niche quantification [38]. A more detailed picture of the different growth phases could provide an understanding of nutritional adaptation, for example, in revealing nutritive preferences [33].

In conclusion, this technique allows for the rapid generation of growth curves of entomopathogenic fungi at a fine timescale with many replicates, and in a medium that is more ecologically relevant to entomopathogenic fungi than what typical solid media bioassays provide. Furthermore, this approach has the potential for application to other species of filamentous entomopathogenic fungi under investigation, such as *Beauveria* spp., *Hirsutella* spp., *Cordyceps* spp., and *Lecanicillium* spp. [3]. The methodological developments described advance the applications of spectrophotometry to the monitoring of filamentous fungal growth in entomopathogenic fungi, and resolve the infeasibility of producing standard curves directly correlating change in OD with mycelial mass. This automated and high-throughput method for monitoring in situ fungal growth presented here will aid further studies on aspects affecting growth of these ecologically and commercially important organisms.

Author Contributions: Conceptualization, A.R.S., H.H., S.M.S. and H.H.d.F.L.; methodology, A.R.S. and H.H.d.F.L.; formal analysis, A.R.S.; investigation, A.R.S.; writing—original draft preparation, A.R.S.; writing—review and editing, A.R.S., H.H., S.M.S. and H.H.d.F.L.; supervision, H.H., S.M.S. and H.H.d.F.L. All authors have read and agreed to the published version of the manuscript.

Funding: This research has received funding from the European Union's Horizon 2020 research and innovation program INSECT DOCTORS under the Marie Skłodowska-Curie grant agreement No 859850. H.H.d.F.L. was also supported by a Sapere Aude Starting Grant from the Independent Research Fund Denmark (No. 8049-00086B).

Data Availability Statement: The data supporting the findings of this study are available upon reasonable request. Requests for access to the data can be directed to the corresponding authors and will be subject to approval by the data owners. Availability of the data is contingent upon compliance with relevant data use and privacy regulations.

Acknowledgments: We would like to express our gratitude to Daisy Fairchild and Fie Rübner-Petersen for their assistance in data collection.

Conflicts of Interest: The authors declare no conflict of interest.

Appendix A

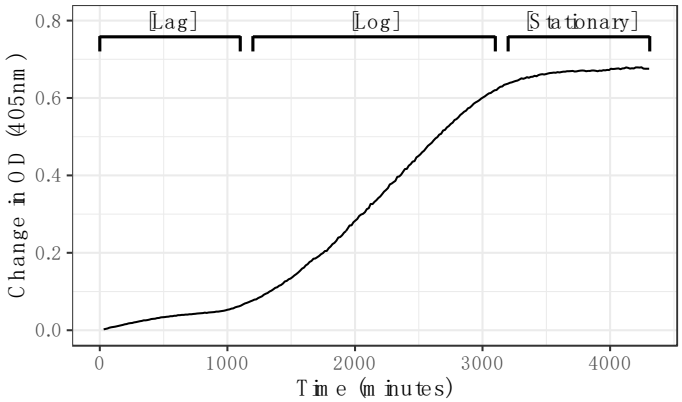

Figure A1. Growth curve of *M. brunneum* KVL 12_37. Line indicates average change in OD of 12 cultures grown at 24° C in 100 µL of SDY/4 liquid media in a 96-well plate over 96 h. Absorbance readings were taken every 10 min at 405 nanometers. Demonstrates full growth curve can be captured rapidly using high concentration conidial suspensions. For our purposes we used a lower concentration and a longer period of measurement.

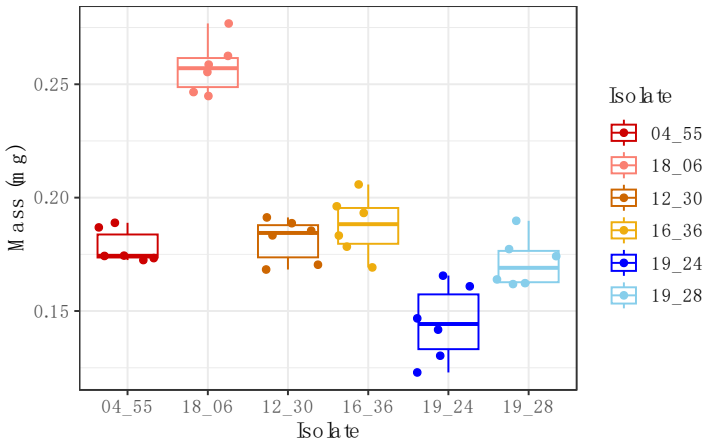

Figure A2. Change in dry weight over 80 h in six *Metarhizium* isolates. Dry weight was calculated for mycelial material extracted from ten pooled microcultures grown for 80 h in 60 wells of a microplate (n = 6).

References

1. Augustyniuk-Kram, A.; Kram, K.J. Entomopathogenic fungi as an important natural regulator of insect outbreaks in forests. In *Forest Ecosystems-More Than Just Trees*; InTech: Rijeka, Croatia, 2012; pp. 265–294.
2. Goettel, M.S.; Glare, T. 11 Entomopathogenic Fungi and their Role in Regulation of Insect Populations. In *Insect Control: Biological and Synthetic Agents*; Elsevier: Amsterdam, The Netherlands, 2010.
3. Shah, P.A.; Pell, J.K. Entomopathogenic fungi as biological control agents. *Appl. Microbiol. Biotechnol.* **2003**, *61*, 413–423. [CrossRef] [PubMed]
4. Roberts, D.W.; Hajek, A.E. Entomopathogenic fungi as bioinsecticides. In *Frontiers in Industrial Mycology*; Springer: Boston, MA, USA, 1992; pp. 144–159.
5. Jaronski, S.T. Mass production of entomopathogenic fungi—State of the art. In *Chapter 11—Mass Production of Entomopathogenic Fungi—State of the Art*; Academic Press: Cambridge, MA, USA, 2023; pp. 317–357.
6. Yeo, H.; Pell, J.K.; Alderson, P.G.; Clark, S.J.; Pye, B.J. Laboratory evaluation of temperature effects on the germination and growth of entomopathogenic fungi and on their pathogenicity to two aphid species. *Pest Manag. Sci. Former. Pestic. Sci.* **2003**, *59*, 156–165. [CrossRef]

7. Gow, N.A.; Gadd, G.M. *Growing Fungus*; Springer Science Business Media: Berlin/Heidelberg, Germany, 1995.
8. Shah, F.A.; Wang, C.S.; Butt, T.M. Nutrition influences growth and virulence of the insect-pathogenic fungus *Metarhizium anisopliae*. *FEMS Microbiol. Lett.* **2005**, *251*, 259–266. [CrossRef] [PubMed]
9. Lee, S.K.; Lee, J.H.; Kim, H.R.; Chun, Y.; Lee, J.H.; Park, C.; Yoo, H.Y.; Kim, S.W. Rapid and concise quantification of mycelial growth by microscopic image intensity model and application to mass cultivation of fungi. *Sci. Rep.* **2021**, *11*, 24157. [CrossRef] [PubMed]
10. Meletiadis, J.; Meis, J.F.; Mouton, J.W.; Verweij, P.E. Analysis of growth characteristics of filamentous fungi in different nutrient media. *J. Clin. Microbiol.* **2001**, *39*, 478–484. [CrossRef] [PubMed]
11. Trinci, A.P.J. Influence of the width of the peripheral growth zone on the radial growth rate of fungal colonies on solid media. *Microbiology* **1971**, *67*, 325–344. [CrossRef]
12. Taniwaki, M.H.; Pitt, J.I.; Hocking, A.D.; Fleet, G.H. *Comparison of Hyphal Length, Ergosterol, Mycelium Dry Weight, and Colony Diameter for Quantifying Growth of Fungi from Foods*; Springer: Boston, MA, USA, 2006.
13. Granade, T.C.; Hehmann, M.F.; Artis, W.M. Monitoring of filamentous fungal growth by in situ microspectrophotometry, fragmented mycelium absorbance density, and 14C incorporation: Alternatives to mycelial dry weight. *Appl. Environ. Microbiol.* **1985**, *49*, 101–108.
14. Langvad, F. A rapid and efficient method for growth measurement of filamentous fungi. *J. Microbiol. Methods* **1999**, *37*, 97–100. [CrossRef]
15. Hickey, P.C.; Swift, S.R.; Roca, M.G.; Read, N.D. Live-cell imaging of filamentous fungi using vital fluorescent dyes and confocal microscopy. *Methods Microbiol.* **2004**, *34*, 63–87.
16. Gutiérrez–Medina, B.; Vázquez-Villa, A. Visualizing three-dimensional fungal growth using light sheet fluorescence microscopy. *Fungal Genet. Biol.* **2021**, *150*, 103549. [CrossRef]
17. Ebrahimi, P.; van den Berg, F.; Aunsbjerg, S.D.; Honoré, A.; Benfeldt, C.; Jensen, H.M.; Engelsen, S.B. Quantitative determination of mold growth and inhibition by multispectral imaging. *Food Control* **2015**, *55*, 82–89. [CrossRef]
18. Plassard, C.S.; Mousain, D.G.; Salsac, L.E. Estimation of mycelial growth of basidiomycetes by means of chitin determination. *Phytochemistry* **1982**, *21*, 345–348. [CrossRef]
19. Aidoo, K.E.; Hendry, R.; Wood, B.J.B. Estimation of fungal growth in a solid state fermentation system. *Eur. J. Appl. Microbiol. Biotechnol.* **1981**, *12*, 6–9. [CrossRef]
20. Cánovas, D.; Studt, L.; Marcos, A.T.; Strauss, J. High-throughput format for the phenotyping of fungi on solid substrates. *Sci. Rep.* **2017**, *7*, 1–9. [CrossRef] [PubMed]
21. Poprawski, T.J.; Majchrowicz, I. Effects of herbicides on in vitro vegetative growth and sporulation of entomopathogenic fungi. *Crop Prot.* **1995**, *14*, 81–87. [CrossRef]
22. Banerjee, U.C.; Chisti, Y.; Moo-Young, M. Spectrophotometric determination of mycelial biomass. *Biotechnol. Tech.* **1993**, *7*, 313–316. [CrossRef]
23. Lovett, B.; St. Leger, R.J. The insect pathogens. *Microbiol. Spectr.* **2017**, *5*. [CrossRef] [PubMed]
24. VanderMolen, K.M.; Raja, H.A.; El-Elimat, T.; Oberlies, N.H. Evaluation of culture media for the production of secondary metabolites in a natural products screening program. *AMB Express* **2013**, *3*, 1–7. [CrossRef]
25. Viniegra-González, G.; Favela-Torres, E.; Aguilar, C.N.; de Jesus Rómero-Gomez, S.; Dıaz-Godınez, G.; Augur, C. Advantages of fungal enzyme production in solid state over liquid fermentation systems. *Biochem. Eng. J.* **2003**, *13*, 157–167. [CrossRef]
26. Stanier, R.Y.; Doudoroff, M.; Adelberg, E.A. *The Microbial World*; Prentice-Hall, Inc.: Englewood Clifs, NJ, USA, 1963; pp. 321–341.
27. Steinwender, B.M.; Enkerli, J.; Widmer, F.; Eilenberg, J.; Thorup-Kristensen, K.; Meyling, N.V. Molecular diversity of the entomopathogenic fungal Metarhizium community within an agroecosystem. *J. Invertebr. Pathol.* **2014**, *123*, 6–12. [CrossRef]
28. Mansoury, M.; Hamed, M.; Karmustaji, R.; Al Hannan, F.; Safrany, S.T. The edge effect: A global problem. The trouble with culturing cells in 96-well plates. *Biochem. Biophys. Rep.* **2021**, *26*, 100987. [CrossRef] [PubMed]
29. R Core Team. *R: A Language and Environment for Statistical Computing*; R Foundation for Statistical Computing: Vienna, Austria, 2023.
30. Lenth, R.V. Least-Squares Means: The R Package lsmeans. *J. Stat. Softw.* **2016**, *69*, 1–33. [CrossRef]
31. Schneider, C.A.; Rasband, W.S.; Eliceiri, K.W. NIH Image to ImageJ: 25 years of image analysis. *Nat. Methods* **2012**, *9*, 671–675. [CrossRef] [PubMed]
32. Olsson, S. Colonial growth of fungi. In *Biology of the Fungal Cell*; Springer: Berlin/Heidelberg, Germany, 2001; pp. 125–141.
33. Vrabl, P.; Schinagl, C.W.; Artmann, D.J.; Heiss, B.; Burgstaller, W. Fungal growth in batch culture–what we could benefit if we start looking closer. *Front. Microbiol.* **2019**, *10*, 2391. [CrossRef] [PubMed]
34. Mantzoukas, S.; Kitsiou, F.; Natsiopoulos, D.; Eliopoulos, P.A. Entomopathogenic fungi: Interactions and applications. *Encyclopedia* **2022**, *2*, 646–656. [CrossRef]
35. Frank, S.A. Models of parasite virulence. *Q. Rev. Biol.* **1996**, *71*, 37–78. [CrossRef] [PubMed]
36. Barra-Bucarei, L.; Vergara, P.; Cortes, A. Conditions to optimize mass production of Metarhizium anisopliae (Metschn.) Sorokin 1883 in different substrates. *Chil. J. Agric. Res.* **2016**, *76*, 448–454. [CrossRef]

37. Schoustra, S.E.; Bataillon, T.; Gifford, D.R.; Kassen, R. The properties of adaptive walks in evolving populations of fungus. *PLoS Biol.* **2009**, *7*, e1000250. [CrossRef]
38. Shik, J.Z.; Kooij, P.W.; Donoso, D.A.; Santos, J.C.; Gomez, E.B.; Franco, M.; Boomsma, J.J.; Crumière, A.J.J.; Arnan, X.; Howe, J.; et al. Nutritional niches reveal fundamental domestication trade-offs in fungus-farming ants. *Nat. Ecol. Evol.* **2021**, *5*, 122–134. [CrossRef]

Journal of Insects as Food and Feed, 2023 online **ARTICLE IN PRESS** Wageningen Academic Publishers

Harmful and beneficial symbionts of *Tenebrio molitor* and their implications for disease management

A.R. Slowik[1,2,3], P. Herren[1,2,3], E. Bessette[2,4*], F.S. Lim[5,6], L. Hernández-Pelegrín[6,7] and C. Savio[8,9*]

[1]University of Leeds, Faculty of Biological Sciences, Leeds LS2 9JT, United Kingdom; [2]University of Copenhagen, Department of Plant and Environmental Sciences, Thorvaldsensvej 40, 1871 Frederiksberg C., Denmark; [3]UK Centre for Ecology & Hydrology, Maclean Building, Benson Lane, Crowmarsh Gifford, Wallingford OX10 8BB, United Kingdom; [4]Living Systems Institute, Biosciences, College of Life and Environmental Sciences, University of Exeter, Exeter EX4 4QD, United Kingdom; [5]Julius Kühn-Institut (JKI), Institute of Biological Control, Schwabenheimerstrasse 101, 69221 Dossenheim, Germany; [6]Department of Genetics and University Institute of Biotechnology and Biomedicine (BIOTECMED), Universitat de València, 46100 Valencia, Spain; [7]Laboratory of Virology, Wageningen University and Research, Droevendaalsesteeg 1, 6708 PB Wageningen, the Netherlands; [8]University of Paris Saclay, INRAE, Micalis, 78350 Jouy en Josas, France; [9]Laboratory of Entomology, Wageningen University, Department of Plant Sciences, 6708 PB Wageningen, the Netherlands; e.bessette@exeter.ac.uk; carlotta.savio@inrae.fr; all authors contributed equally to this work

Received: 21 November 2022 / Accepted: 14 March 2023

REVIEW ARTICLE

Abstract

The yellow mealworm, *Tenebrio molitor*, is currently one of the most important insect species produced for livestock feed and human consumption. High-density rearing conditions make the risk of disease and infections by parasitic symbionts a challenge in the mass production of these insects. However, certain symbionts are beneficial and should be favoured in order to promote healthy insect populations. Knowledge of parasitic symbionts and their management is essential for the insect rearing industry and its associated research. Here we review the documented microbial infectious agents, invertebrate parasites, and beneficial symbionts occurring in *T. molitor*. Furthermore, we discuss detection, prevention, and treatment methods for disease management in *T. molitor* production systems to inform future management and decision making in *T. molitor* rearing.

Keywords: mass-rearing, insect diseases, beneficial microorganisms, entomopathogens, probiotics, yellow mealworm

1. Introduction

The insect rearing industry has grown rapidly in recent years to meet the global demand for alternative and sustainable sources of feed and food (Francuski and Beukeboom, 2020). In 2017, 6,000 tons of insects were produced for animal feed in Europe alone (Derrien and Boccuni, 2018) and the global production of insects for food and feed is estimated to reach up to 500,000 tons by 2030 (De Jong, 2021). The yellow mealworm, *Tenebrio molitor* L. (Coleoptera: Tenebrionidae), is one of the major insect species produced on a large scale due to its high protein and fat content, its efficient feed conversion rate and its comparatively simple rearing process (Costa *et al.*, 2020; Grau *et al.*, 2017b). Such characteristics make *T. molitor* an ideal candidate for addressing societal issues like sustainable food production and hunger. Consequently, the European Food Safety Authority (EFSA) (Reg EU 2021/882, Reg EU 2015/2083) permitted in 2021 the processing and commercialisation of dried *T. molitor* larvae for human consumption in Europe (European Commission, 2021).

One important challenge in the mass-production of insects is the risk of diseases and infections in these systems (Eilenberg *et al.*, 2015, 2018; Van Huis, 2017). Mass-produced insects are generally kept at high densities. This favours the spread of microbial infectious agents and invertebrate parasites (either endo- or ectoparasites) between individuals if environmental conditions are conducive and no preventive measures are taken (Eilenberg *et al.*, 2018). Pathogens can be a major barrier in scaling up insect production, as well as an economic obstacle causing

ISSN 2352-4588 online, DOI 10.3920/JIFF2022.0171

significant losses for insect production companies (Bhat *et al.*, 2009; Liu *et al.*, 2011). Furthermore, the ecological risk of pathogen spillover from mass-rearing facilities into natural insect populations further emphasises the importance of disease management (Bang and Courchamp, 2021).

Like in other animals, infectious diseases in insects are diverse and can be enigmatic, manifesting as lethal or sublethal, and as single or co-infections. Moreover, mutualistic and commensal symbionts can appear as etiological agents if their ecology is unknown, but in actuality are beneficial to the insect host, and in certain cases can protect the insects from disease (Lecocq *et al.*, 2021). Beneficial symbionts are therefore candidates for introduction as probiotics in mass-reared insects (Savio *et al.*, 2022).

To date, harmful and beneficial symbionts of *T. molitor* and their management have not been comprehensively reviewed. Understanding the variety of symbiotic interactions and their implications for disease outcomes is critical to the success of insect farming. Here we review the symbionts known to occur in *T. molitor*, and document the symptoms they cause, present detection methods, and discuss potential innovative treatment and prevention strategies.

2. Harmful symbionts

In this section, parasitic symbionts harmful to *T. molitor* are addressed, although it is worth mentioning diseased states can be induced by a range of non-infectious factors, *e.g.* malnutrition (Kaya and Vega, 2012). Here, we distinguish between 'microbial infectious agents' (bacteria, fungi, protists, viruses) and 'invertebrate parasites' (mites, cestodes, nematodes, and parasitoids). Microbial infectious agents that infect insects are often also referred to as 'entomopathogens' or 'insect pathogens' in the literature (Eilenberg *et al.*, 2015; Hajek and Shapiro-Ilan, 2018).

Infections in insects manifest as acute or chronic and covert or overt. The most obvious and easily observable are acute infections, which are of short duration and may result in sudden death of the host. Chronic infections, on the other hand, are less apparent and can often be overlooked due to sublethal effects and the long incubation period before death. Covert or latent infections, primarily observed in viral infections, are a dormant form of disease, presenting no visible symptoms in the host. These have the potential to become overt or acute infections when triggered by appropriate abiotic or biotic factors, e.g. environmental effects (Hajek and Shapiro-Ilan, 2018) or transfer from one host to another (Martin and Brettell, 2019).

Parasites can occur in different life stages of *T. molitor* given the vast difference in body composition, behaviour, and environmental requirements throughout the insect lifecycle. For this reason, we specify the life stage in which each pathogen or parasite has been identified in *T. molitor* (Supplementary Table S1). This classification should not be considered exhaustive, as bioassays may not have been performed on every life stage, rather it is the sum of current knowledge on *T. molitor* diseases.

Infections in insects can both be naturally occurring or experimentally induced. Given that the artificial environments in which *T. molitor* is mass-produced are ecologically novel relative to the evolutionary time scale on which symbiotic relationships have been formed, it is possible some parasites might be able to extend their ecological host ranges under these new conditions. We

Definitions of terms used in this review

Symbiosis	Refers to any ecological relationship between two species, whether beneficial or detrimental to either partner, and is further subdivided into different forms.
Mutualism	A symbiotic relationship in which both partners benefit from each other.
Commensalism	A symbiotic relationship in which one partner benefits and the other partner is neither harmed nor benefits.
Parasitism	A symbiotic relationship in which one partner causes harm to the other partner (Martin and Schwab, 2012).
Symbiont	An organism living in some form of symbiosis with another species.
Parasite	An organism living on or in a host organism, deriving nutrition at the expense of the host's health (Hajek and Shapiro-Ilan, 2018).
Pathogen	Microorganisms, including viruses, that have the potential to cause disease (Pirofski and Casadevall, 2012).
Facultative pathogen or parasite	Pathogenic or parasitic symbionts capable of surviving and reproducing outside of a host organism.
Obligate pathogen or parasite	Pathogenic or parasitic symbionts reliant on a host organism for survival and reproduction.
Ecological host range	The sum of all host species a parasite is capable of encountering and infecting in the natural environment; also refers to natural infection.
Physiological host range	The sum of all host species a parasite has been found to infect under laboratory conditions; also refers to experimental infection.

therefore include parasites that have *T. molitor* in their ecological as well as physiological host range to give a complete overview (Supplementary Table S1).

Microbial infectious agents

Bacteria

The microbial communities of *T. molitor* are characterised by the presence of a resident microbiota, mainly composed of the bacterial phyla of Proteobacteria and Firmicutes, which can be shaped by feed and environmental conditions (Urbanek *et al.*, 2020). Bacteria can exploit different relationships with insects from mutualistic to pathogenic interactions (Vallet-Gely *et al.*, 2008). Assurance of safety for food and feed necessarily raises several questions regarding bacterial pathogens, including susceptibility, persistence, and transmission of pathogens in the host organism. This is especially relevant in mass-rearing systems characterised by high-density conditions and the practice of using organic side streams as insect feed (Jensen *et al.*, 2020; Maciel-Vergara *et al.*, 2021; Urbanek *et al.*, 2020; Wynants *et al.*, 2019). *T. molitor* is not naturally associated with food-borne and environmental bacterial pathogens considered infectious to humans, reducing their risk of acting as a biological vector between different trophic levels (Urbanek *et al.*, 2020).

Infection mainly occurs via oral ingestion of bacteria, although insect haemocoel can be directly infected when exposed through injuries or damage from fungi or nematodes (Maciel-Vergara *et al.*, 2018; Vallet-Gely *et al.*, 2008). A pathogenic bacterial species of *T. molitor, Bacillus thuringiensis* var. *tenebrionis,* was first isolated from *T. molitor* in 1982 (Krieg *et al.*, 1983) and is commercially used in biocontrol of certain pest species from Coleoptera. This Gram-positive spore-forming bacterium belonging to the phylum Bacillota is well known for causing death of the larval stages of many insects. Mortality occurs via sepsis-related organ failure (Nielsen-Leroux *et al.*, 2012), when the insect gut is perforated through the action of bacterial pore forming toxins, followed by infection of the whole body. Bacterial spores then germinate and proliferate throughout the haemocoel. In the case of *T. molitor* larvae, the extensive gut leakage has not been correlated to the killing mechanism of *B. thuringiensis,* but reduced feeding behaviour has been observed in infected individuals (Zanchi *et al.*, 2020). Other bacteria, such as *Serratia marcescens* (phylum Pseudomonadota), act mainly as opportunistic pathogens, when the insects are already physiologically weakened (Dupriez *et al.*, 2022).

A first indication of the presence of pathogenic bacteria is the observation of reduced feeding behaviour and decreased movement. In the case of bacterial proliferation and sepsis-related organ failure, the insect cadavers change colour, presenting a flaccid consistency and a foul odour (Maciel-Vergara *et al.*, 2021). Specific insect colorations can sometimes be related to the presence of bacterial infection such as pink or red for *S. marcescens,* and dark colours for other bacterial species (Dupriez *et al.*, 2022; Eilenberg *et al.*, 2015). The application of molecular techniques such as Next Generation Sequencing (NGS) are recommended for identifying bacterial pathogens to the species level (Verma *et al.*, 2017).

Fungi

Several fungal species of the orders Hypocreales, Eurotiales, Capnodiales and Saccharomycetales have been shown to affect *T. molitor*. Most of the studies are based on experimental infections and focus on the application of entomopathogenic fungi as biocontrol agents for tenebrionid pest species. Fungal infections either lead to mortality of the insects or induce sublethal effects, such as a modification of the lipid composition (Gołębiowski *et al.*, 2020) or a negative effect on the number of offspring (Pedrini *et al.*, 2010) as shown in other species of Tenebrionidae. It is important to note that different fungal isolates from the same species can have highly variable virulence (Praprotnik *et al.*, 2021).

In insects, infections by fungi are typically transmitted when a spore from their surrounding environment encounters an appropriate insect host cuticle, and there is sufficient humidity and temperature for the spore to adhere and germinate (Vega *et al.*, 2012). The germinating spores penetrate the host cuticle by producing chitinase and induce mortality as fungal structures are produced throughout the host body (Vega *et al.*, 2012).

Within the order Hypocreales, members of the genera *Metarhizium* (Barnes and Siva-Jothy, 2000; Bharadwaj and Stafford, 2011; Keyser *et al.*, 2014, 2016; Korosi *et al.*, 2019; Mathulwe *et al.*, 2021; Moret and Siva-Jothy, 2003; Praprotnik *et al.*, 2021) and *Beauveria* (Korosi *et al.*, 2019; Lee *et al.*, 2014; Maistrou *et al.*, 2018) have been described to infect *T. molitor*. Many members of these two genera are generalist pathogens having many different host species (Maciel-Vergara *et al.*, 2021). They are highly relevant in production systems of *T. molitor* because they can be found in stored grains (Wakil *et al.*, 2014). Stored grains are not only a natural habitat of *T. molitor*, but they are also frequently used to feed *T. molitor* larvae in production facilities (Cortes Ortiz *et al.*, 2016). A typical symptom of *T. molitor* infected with fungi from the order Hypocreales is white fungal outgrowth when cadavers are kept at high humidity. After mycosis, the fungi start to produce conidia (green conidia: *Metarhizium* spp.; white conidia: *Beauveria bassiana*). The genera can often be determined based on characteristics of the conidia using light microscopy (Maciel-Vergara *et al.*, 2021), whereas

molecular methods are needed to identify the species (Castrillo and Humber, 2009).

Several fungal species not classified as entomopathogens have been shown to affect *T. molitor* when they were ingested together with the feed. Guo *et al.* (2014) found that *T. molitor* larvae fed with *Fusarium avenaceum*- and *Fusarium culmorum*-colonised wheat kernels had an increased mortality compared to the control. This was despite having found none of the tested *Fusarium* species multiplied inside the insect haemocoel, indicating that mycotoxins produced by the fungi are responsible for the mortality of the larvae (Guo *et al.*, 2014). Other fungal species growing on grains (*Aspergillus niger*, *Aspergillus flavus*, *Penicillium expansum*, *Cladosporium herbarum*, *Fusarium nivale*, *Fusarium equiseti*, *Fusarium roseum* and *Fusarium tricinctum*) have been shown to inhibit the growth of *T. molitor* larvae (Davis *et al.*, 1975; Reiss, 1973). The growth inhibition by mycotoxins might be a combination of the effect of the toxins inside the insect and deterrence in feeding behaviour of the contaminated feed (Davis *et al.*, 1975).

Studies investigating the effect of the mycotoxin deoxynivalenol (DON) on *T. molitor* larvae report contradicting results. Jankovic-Tomanic *et al.* (2019) found growth-inhibiting effects of larvae reared on wheat containing 4.9 to 25 mg/kg DON (Janković-Tomanić *et al.*, 2019). Other studies, however, describe no effect on weight gain when the larvae of *T. molitor* were fed with wheat flour containing up to 8 mg/kg (Van Broekhoven *et al.*, 2017) or even up to 12 mg/kg DON (Ochoa Sanabria *et al.*, 2019). This indicates that mycotoxins from different fungal species or strains might have different effects on the larvae of *T. molitor*. Additionally, the human pathogenic yeast species *Candida albicans* and *Candida neoformans* have been found to cause mortality in *T. molitor* when directly injected into the haemocoel of the larvae (De Souza *et al.*, 2015).

Microsporidia

Microsporidia are obligate, intracellular, spore-forming parasites, considered to be most closely related to fungi based on recent phylogenetic studies (Capella-Gutiérrez *et al.*, 2012; Strassert and Monaghan, 2022) and are common parasites of insects: 93 of the 200 described genera of microsporidia have an insect as a host (Becnel and Andreadis, 2014). The most common pathway of microsporidia transmission to a new insect host is through direct oral ingestion of infectious spores, which are found in food, faeces, or liquids within the host's immediate environment (e.g. soil, water, plant, insect cadaver). Vertical transmission, where infection is transferred directly from parent to progeny, can also occur in the case of transovarial transmission (Becnel and Andreadis, 2014).

Microsporidian infection in *T. molitor* thus far appears to be rare, with the only account of natural infection reported by Armitage and Siva-Jothy (2005), who identified unnamed microsporidians in a *T. molitor* lineage. In total, 87% of the beetles in the infected culture carried microsporidia, although they determined the infections were not harmful for the insect (Armitage and Siva-Jothy, 2005). Fisher and Sanborn (1962) experimentally induced infection in *T. molitor* using the microsporidium *Paranosema whitei* (natural host: *Tribolium* spp.) with infected feed, but susceptibility to infection was limited to second and third-instar larvae immediately post-moult (Fisher and Sanborn, 1962). Moreover, Milner also found that first instar *T. molitor* larvae were not susceptible to *P. whitei* infection (Milner, 1973). Based on the limited evidence of the ability of microsporidians to induce diseased states in *T. molitor,* further research is required to evaluate the disease-risk of microsporidians in mass-rearing systems.

Protists

Protists, historically called protozoans, are an informal group describing free-living or parasitic single-celled eukaryotes other than fungi, animals, and plants. They are found in a myriad of cellular forms with diverse biochemistries, which allow them to colonise every biome and many different types of hosts. Multiple protistan groups have the capacity to infect animals and may cause serious disease (Kolářová *et al.*, 2022). However, compared to prokaryotic microbes, fungi, and viruses, protists are often overlooked as potential pathogens of mass-reared insects (Bessette and Williams, 2022; Garofalo *et al.*, 2019; Maciel-Vergara *et al.*, 2021).

In insects, protist parasites typically start their life cycle when their environmental cysts or spores are ingested by a susceptible host (Lange and Lord, 2012). All protists identified as symbionts of *T. molitor* are typically transmitted via this route, causing infection after oral ingestion of the infectious stages of the protist. Infection by protistans is not typically obvious, as it is generally chronic with no external indications of disease. An infection of high intensity with neogregarines or coccidians can cause insects to become lethargic with a swollen, whitish appearance (Lange and Lord, 2012). The detection and identification of protist parasites has historically relied on microscopy and morphological identification in combination with knowledge of biological parameters, such as host specificity, tissues tropism, and route of infection (Solter *et al.*, 2012). Presently, the use of polymerase chain reaction (PCR) and, more recently, NGS, are being widely applied for discovering novel protist lineages and to understand their contribution to microbiomes (Bass and del Campo, 2020). The 18S (small subunit) ribosomal RNA gene (18S) is the most extensively used genetic barcode for protist surveys (Vaulot *et al.*, 2022).

Amoebozoa

The Amoebozoa group includes unicellular eukaryotes that possess pseudopodia for their motility and ingestion (Anderson, 2017). Six amoebae species are reported to be parasitic to insects. Moreover, it is possible for insects to act as mechanical vectors for amoebae pathogenic to humans and other animal hosts (Lange and Lord, 2012). Entomopathogenic amoebae are known to form resilient uninucleate cysts in the environment that will excyst within a suitable host and release trophozoites (i.e. active feeding stages) found either in the midgut or Malpighian tubules (Lange and Lord, 2012). Newly formed cysts are then released in the environment through the insect frass. Specific parasitic amoebae of the mealworm have yet not been described, but *T. molitor* has been found to carry *Entamoeba* spp., with the amoebae species *Entamoeba histolytica* known to cause dysentery to humans (Gałęcki and Sokół, 2019) (Supplementary Table S1).

Coccidia

Coccidians, also called haemogregarines, are similar to neogregarines. These endoparasites primarily infect vertebrates but are also found in invertebrates, with less than 1% of the described species infecting insect hosts (Lange and Lord, 2012). Few studies have examined coccidians within *T. molitor*, but some species are known to infect other Tenebrionidae, such as *Adelina castana* and *Adelina picei,* parasites of *Tribolium castaneum* and *Alphitobius piceus*, respectively (Ghosh *et al.*, 2000). *Adelina* spp. are not well studied in *T. molitor*, and only one reference from 1930 has reported a natural infection from reared *T. molitor* with *Adelina tenebriosis* (Sautet, 1930). The potential effects of coccidian infections on *T. molitor* are not studied, but lag in development time has been reported in another Tenebrionidae, which could impact insect production (Park and Frank, 1950).

Cryptosporidia

Recently, *Cryptosporidium* has been proposed as a gregarine (Adl *et al.*, 2019) but later this was abandoned to place *Cryptosporidium* as a basal group of apicomplexans (Salomaki *et al.*, 2021). Interestingly, *Cryptosporidium* spp., a vertebrate parasite, can be found on the surface or in the intestines of different insects, which could serve as mechanical vectors. A parasitological evaluation undertaken in European farms (with insect stock from all over the world) has reported that *T. molitor* could be a vector of this pathogen, presenting a risk for human health (Gałęcki and Sokół, 2019). The same study also found *Isospora* spp. in *T. molitor*, a coccidian pathogen that can induce gastrointestinal symptoms in humans, livestock, and exotic animals (Gałęcki and Sokół, 2019).

Gregarines

The most well studied protist group infecting *T. molitor* is Gregarinasina, known commonly as gregarines. Gregarines are the most abundant group of Apicomplexa that infect invertebrates (Desportes and Schrével, 2013; Votýpka *et al.*, 2017). Gregarines are mainly extracellular parasites and attach to the host via anchoring structures which allow them to feed on host cell cytoplasm (Lange and Lord, 2012). Two main orders compose the subclass Gregarinasina, the Eugregarinorida and the Neogregarinorida. In contrast to the eugregarines, the neogregarines (syn. schizogregarines) can develop intracellularly in the host tissues. This development induces more serious disease than eugregarines, as the intensity of infection of the eugregarines is limited to the number of oocysts that are ingested by the host (Lange and Lord, 2012).

Five species are known to infect *T. molitor*: *Gregarina polymorpha*, *Gregarina niphandrodes*, *Gregarina cuneata*, *Gregarina steini* and *Mattesia* spp. (Berndt, 1902; Clopton *et al.*, 1991; Hammerschmidt, 1838; Harry, 1967; Kleespies *et al.*, 2008; Koura and Kamel, 1993; Lipa, 1967; Rodriguez *et al.*, 2007; Schawang and Janovy, 2001; Stein, 1848; Valigurova, 2012). Gregarines are naturally present in *T. molitor* populations with controversial effects on their host. Rueckert *et al.*, 2019 did an extensive review on the effects of gregarines and how they transgress the symbiosis spectrum (Rueckert *et al.*, 2019). Two references showed positive effects on *T. molitor* infected by *Gregarina* spp. with enlarged host growth and positive impact on host development, fitness and longevity (Sumner, 1936; Valigurova, 2012). Other studies showed negative or no effect on the development and fitness of *Tenebrio* hosts. They can include a destruction of the gut cells (Lipa, 1967) and a decrease of the longevity of highly infected hosts (Rodriguez *et al.*, 2007) (Supplementary Table S1).

Viruses

The first report of a virus naturally infecting *T. molitor* dates back to 1969 (Huger, 1969). Viral particles similar to densovirus were identified in diseased larvae using an electron microscope, however, no further molecular analysis was carried out (Huger, 1969). These larvae presented a grey discoloration and cytopathic modifications on diverse tissues such as the epidermis, or the fat body. Moreover, *T. molitor* may act as a mechanical vector for *Acheta domesticus* densovirus (AdDV). AdDV-positive *T. molitor* individuals were detected in a colony reared together with infected house crickets (*A. domesticus*) within the same facility (Szelei *et al.*, 2011). These results indicate the possibility of horizontal transmission of densovirus between insect species. Apart from densovirus, viruses of the family Iridoviridae were found and demonstrated to be capable of infecting *T. molitor*. Particles of small iridescent

virus (type 29) were identified in *T. molitor* larvae using electron microscopy (Black *et al.*, 1981; Kelly *et al.*, 1979). Wild type and recombinant invertebrate iridescent virus 6 (IIV6) have also been shown to cause disease in *T. molitor* via injection. Symptoms of infection include paralysis of larvae and darkening of cadaver three days after infection (Gencer *et al.*, 2020).

Regarding detection, molecular techniques are the most suitable method to correlate viral infection with the disease symptoms. Moreover, the advent of high-throughput sequencing has spurred the discovery of covert viruses in insects (Käfer *et al.*, 2019; Shi *et al.*, 2016; Wu *et al.*, 2020), including mass-reared edible species (Bertola and Mutinelli, 2021). Most of these viruses infect the host in a covert state with no visible biological costs. Therefore, it is likely that the number of viruses described for *T. molitor* and related species increases in the near future. In this scenario, analysing the risk of a potential viral outbreak and the sublethal effects caused by covert infections will be of high value to assess the level of risk for the mass-rearing industry.

Invertebrate parasites

Acari

Acari are ectoparasites capable of colonising many orders of insects. A parasitological evaluation of farmed insects found that *T. molitor* can carry mites belonging to the Acaridae (Gałęcki and Sokół, 2019). However, further research is needed to determine whether mites are parasites of *T. molitor*. Furthermore, mite debris should be considered as a potential hazard in insects produced for human consumption due to dust mite allergies. Other Tenebrionidae, such as *Alphitobius diaperinus,* are known to be parasitised by *Acarophenax mahunkai*, which feed on the eggs of this species (Steinkraus and Cross, 1993).

Cestodes

Cestodes are a group of intestinal endoparasites. In their adult stage, cestodes mainly affect vertebrates. However, the larval stages (cysticercoids) can infect invertebrates via oral ingestion as intermediate hosts while they develop their infective capacity on the definitive host (Saari *et al.*, 2019). Most literature concerning cestodes focuses on the family Hymenolepididae. Natural infections of this cestode have been reported in *T. molitor* and other species of Tenebrionidae such as *T. castaneum* and *Tribolium confusum* (Heyneman and Voge, 1971; Hurd *et al.*, 1990; Makki *et al.*, 2017) but most of the studies report experimental infections.

Although cestodes are not considered direct insect parasites, some studies have shown sublethal effects of cestode infection in the insect host. For instance, infection with *Hymenolepis diminuta* reduced the locomotion of *T. molitor* larvae in comparison to healthy individuals (Hurd *et al.*, 1990; Hurd and Parry, 1991; Sheiman *et al.*, 2006). Moreover, infection with *H. diminuta* was related to a decrease in the reproductive vigour of infected males and the fertility of females (Cole *et al.*, 2003; Hurd and Parry, 1991; Maema, 1986). In addition, we should avoid the presence of cestodes in mass-reared insects for assuring the food safety of the final product (Boelaert *et al.*, 2021).

To detect the infective stage of cestodes in insects, the use of a light microscope is recommended, while the application of molecular techniques may be required for characterisation at the species level.

Nematodes

No natural nematode infections have been described in *T. molitor* to date. However, diverse studies have assessed the physiological host range and pathogenicity of nematodes through experimental infection. These studies, which aim to unravel the potential of nematodes as biocontrol agents, concluded that several nematode species can infect *T. molitor* when added to the diet (de Carvalho Barbosa Negrisoli *et al.*, 2013; Ramos-Rodríguez *et al.*, 2006; Shapiro-Ilan *et al.*, 2008) (Supplementary Table S1). Species belonging to the genera *Steinernema* and *Heterorhabditis* are the main entomopathogenic nematodes described in *T. molitor*. These nematodes require high moisture conditions for infection (Eilenberg *et al.*, 2015) and desiccation tolerance is strain dependent (Shapiro-Ilan *et al.*, 2014). Similarly, the heat tolerance and the virulence of nematodes are influenced by the behavioural and physiological characteristics of the specific isolates and the environmental conditions (Lulamba and Serepa-Dlamini, 2020; Ramakuwela *et al.*, 2018). Members of the *Oscheius* spp. are also capable of infecting *T. molitor* both through experimental infection and using *T. molitor* as a bait (Foelkel *et al.*, 2017; Torrini *et al.*, 2015).

Nematode infections can be directly detected using a magnifying lens, while the species characterisation requires the application of molecular techniques.

Parasitoids

Like nematodes, no natural parasitoid infection of *T. molitor* has been described to date. However, due to its high accessibility and low production costs, *T. molitor* has been used as an alternate factitious host to rear multiple parasitoid species for biocontrol. Several studies were conducted to investigate the use of *T. molitor* as a host for rearing parasitoids at various life stages, including different pupal ages and eggs (Supplementary Table S1). *T. molitor* was demonstrated to be a highly suitable host

for rearing parasitoids of lepidopteran species, with the level of parasitism in *T. molitor* reaching 100% of efficacy and an emergence rate above 90% (Andrade *et al.*, 2012; Favero *et al.*, 2014; Zanuncio *et al.*, 2008).

3. Beneficial symbionts

Mutualistic associations between hosts and their microbiota are well-known in the animal kingdom. Several microorganisms, especially prokaryotes, have been shown to have beneficial effects on *T. molitor,* all of which increased the growth of the larvae (Table 1). Increased larval survival and adult emergence was conferred by *Pediococcus pentosaceus* when provided in both vital and inactivated form (Lecocq *et al.*, 2021). *Bacillus subtilis*, *Bacillus toyonensis*, and *Enterococcus faecalis* had effects on the nutritional contents of the larvae (Rizou *et al.*, 2022), all of which increased crude protein content. Additionally, it has been shown that the gut biome of *T. molitor* larvae affects the parasite establishment of the tapeworm *Hymenolepis diminuta* (Fredensborg *et al.*, 2020). Controversial effects have been recorded on Gregarines impact on host development, fitness and longevity. Sumner (1933, 1936) and Valigurova (2012) observed an increased larval growth and longevity in *T. molitor* larvae infected with *Gregarina* spp. In addition, the exposure of *T. molitor* larvae to the fungal species *Neurospora sitophila* (Reiss, 1973) and *Pithomyces chartarum* (Davis *et al.*, 1975) resulted in beneficial effects on larval weight gain of individuals fed with contaminated products (Table 1).

Bacteria also present the possibility for use as probiotics to prevent diseases in reared insects, as is practiced in other livestock populations (Grau *et al.*, 2017b; Savio *et al.*, 2022). Probiotics are usually bacteria that either inhibit parasites (*e.g.* via inhibition of the expression of virulence genes or the increased production of antimicrobial substances) or increase the resistance of the insects by the stimulation of the host immune response (Grau *et al.*, 2017b). The *in vivo* application of probiotics to make *T. molitor* more resistant to parasites has not been demonstrated thus far. However, in the red flour beetle *T. castaneum*, the feeding of a probiotic (*Enterococcus mundtii*) increased the survival of larvae after exposure to *B. thuringiensis* (Grau *et al.*, 2017a), and *in vitro* studies of *P. pentosaceus* demonstrated growth-inhibiting effects on different entomopathogenic bacteria (*B. thuringiensis*, *S. marcescens*, *Serratia plymuthica* and *Pseudomonas aeruginosa*) (Lecocq *et al.*, 2021).

4. Implications for mass-rearing systems

Methods for detection and isolation

Diagnostic techniques used in detection, identification, and characterisation of parasites in diseased insects have evolved considerably over the past decades. Conventional methods to examine these parasites include microscopic analysis, observation of the respective signs and symptoms, and isolation using specific selective media (Bing *et al.*, 2021; Vandeweyer *et al.*, 2021). Gałęcki and Sokół (2019) demonstrated the use of microscopic analysis and Ziehl-Neelsen application of staining methods (Carter and Cole Jr, 2012) in identifying various parasites in *T. molitor* production facilities (Gałęcki and Sokół, 2019).

However, many of these parasites are unculturable (Masson and Lemaitre, 2020) on artificial media (e.g. *Ichthyosporea* spp.). In addition to that, parasites like protists and viruses may be present in covert states, presenting no observable signs or symptoms. The advent of new technologies in

Table 1. Overview of beneficial symbiont species and their effects on *Tenebrio molitor*.

Classification	Species	Effect on *T. molitor*	References
Bacteria	*Enterococcus faecalis*	Increased larval growth, reduced larval development time, increased crude protein content of larvae	Rizou *et al.*, 2022
	Bacillus subtilis	Increased larval growth, increased crude protein content of larvae, decreased crude fat content of larvae, decreased microbial counts of *Enterobacteriaceae*	Rizou *et al.*, 2022
	Bacillus toyonensis	Increased larval growth, increased crude protein content of larvae, decreased microbial counts of *Enterobacteriaceae*	Rizou *et al.*, 2022
	Pediococcus pentosaceus	Increased larval survival and growth, increased adult emergence	Lecocq *et al.*, 2021
	Mixed culture of *Bifidobacterium bifidum*, *Clostridium butyricum*, *Bacillus subtilis* and *Bacillus licheniformis*	Increased larval survival and growth, increased crude protein content of larvae, decreased calcium and phosphorus contents of larvae	Zhong *et al.*, 2017
Fungi	*Neurospora sitophila*	Increased larval growth	Reiss, 1973
	Pithomyces chartarum	Increased larval growth	Davis *et al.*, 1975
Gregarinasina	*Gregarina* spp.	Increased larval growth and longevity	Sumner, 1933; 1936; Valigurova, 2012

the field of molecular biology allows for the identification of these parasites via PCR by targeting parasite-specific genome regions. For example, by amplifying the non-structural protein 1 (NS1) coding region in densovirus, it was possible to identify AdDV positive *T. molitor* colonies reared together with *A. domesticus* within the same facility (Szelei *et al.*, 2011). In another case, confirmation of the presence of IIV6 in *T. molitor* larvae was determined using PCR in larvae showing symptoms of paralysis (Gencer *et al.*, 2020).

The rapid development of NGS technology in recent years allows for the detection of unsuspected and novel parasites via a metagenomics approach, as well as providing the possibility to simultaneously assess the microbiome and macrobiome of species of interest (Gibson *et al.*, 2014). A general estimate of the relative abundance of particular organisms within a sample is also possible using metagenomic approaches, which can help determine the clinical significance of a parasite of interest. The initial culturing procedure or preliminary knowledge of signs and symptoms of parasites are not necessary in this technique (Frey and Bishop-Lilly, 2015). The use of metagenomics has already revealed novel pathogens in several commonly reared insect species, such as the presence of a new iflavirus in *A. domesticus* colonies (de Miranda *et al.*, 2021). Reference databases of parasite genomic sequences are crucial for untargeted metagenomic screening approaches (de Miranda *et al.*, 2021). Regardless of the detection method, storage conditions such as temperature (-80 °C) prior to analysis are essential to maintain the stability of the genetic material for long periods (Bing *et al.*, 2021; Yang *et al.*, 2021).

In many cases, conventional detection methods are sufficient to identify common parasites with well-described signs and symptoms. Routine surveillance can be performed for the detection of previously recorded parasites in insect farming with standard PCR assays. In scenarios where unknown or suspected chronic diseases covertly reduce the fitness of the insects, the metagenomics approach is helpful in discovering the potential causative agent. In the future, it is possible that NGS techniques could be used to detect diseases even before infection, for example in the feed or in the circulating air (Sikorowski and Lawrence, 1994; Szelei *et al.*, 2011).

Management of harmful symbionts

Previous reviews and protocols of measures and good practice used in insect mass-rearing systems provide a useful framework for prevention and management of diseases in insects (Eilenberg *et al.*, 2015; IPIFF, 2022; Maciel-Vergara and Ros, 2017; Maciel-Vergara *et al.*, 2021). These general guidelines include hygiene and facility design, and are largely applicable to the production of *T. molitor.* While diligent hygienic practices are the most important aspect of disease prevention in insect production, research into new prevention methods is continuously ongoing. Here we focus on research with future potential for innovative methods in the context of *T. molitor* disease management.

Insights in insect ecology offer promising potential for managing disease in the future. For example, it has recently been discovered that insects have a form of innate immune memory called 'immune priming', which protects them from pathogens when previously exposed to a pathogen or a pathogen-derived compound (Little and Kraaijeveld, 2004; Vigneron *et al.*, 2019). Several authors have suggested making use of immune priming in the commercial production of insects (Grau *et al.*, 2017b; Maciel-Vergara and Ros, 2017). The application of immune priming has been shown to be successful in another invertebrate system, the production of giant tiger prawns (*Penaeus monodon*), providing protection from infections caused by white spot syndrome virus (Witteveldt *et al.*, 2004). In *T. molitor,* immune priming has been shown to have both intra- and transgenerational effects (Dhinaut *et al.*, 2018). Immune priming of *T. molitor* using Gram-positive bacteria conferred protection from infections with pathogenic Gram-positive and -negative bacteria within generation and the next generation (Dhinaut *et al.*, 2018). To reduce the risk of insects becoming infected during the immune priming treatment, heat inactivated microorganisms could be used, as it has been successfully demonstrated in *T. molitor* larvae (González-Acosta *et al.*, 2022). This could be useful in the future as a preventative treatment for parasites known to be problematic in insect facilities.

Modification of diet components might be another useful tool to prevent or treat parasites. For example, beneficial compounds found in diets, like flavonoids, could confer protection from parasites. In a study on amoeba in locusts, hosts collected in the field had lower infection rates by the amoeba *Malamoeba locustae* (Abdel Rahman *et al.*, 2015), compared to reared hosts (King and Taylor, 1936; Kleespies *et al.*, 2010). Abdel Rahman *et al.,* (2015) hypothesised that orthopterans living in natural conditions acquired immunity associated with feeding on the plant *Portulaca oleracea*, which contains flavonoids with potential anti-protist properties. Moreover, prevention of harmful symbionts could also be achieved by providing probiotics, as discussed in section 3.

Temperature treatments could prevent and treat disease outbreaks in *T. molitor* populations, in particular heat shock. Curative heat treatments can, for example, reduce the effects of viral pathogens in insects (Cevallos and Sarnow, 2010; Inoue and Tanada, 1977). Another interesting finding in this regard is that temperature stress can pre-emptively increase the immune responses of insect hosts and thereby decrease the susceptibility to pathogen infection (Browne *et*

al., 2014; Wojda and Taszłow, 2013). These findings have, however, not been tested in *T. molitor* thus far.

Previous work in selective breeding has shown it is possible to fix particular traits and produce lines of *T. molitor* with altered phenotypes (Song *et al.*, 2022). In the future, selective breeding of *Tenebrio* for the purposes of withstanding certain conditions or diseases might be of interest to insect producers. The knowledge necessary for producing resistant lines of insects will be developed from our understanding of different aspects that contribute to disease resistance, like insect behaviour, ecology, and evolution. For example, it might be possible to promote grooming behaviours, which is important in high-density conditions, based on our understanding of insect grooming.

5. Concluding remarks

The mass-production of *T. molitor* is a relatively young industry, and information on symbionts of this insect species is therefore still limited. However, *T. molitor* has been used as a model organism to study host-parasite interactions for several decades, providing valuable insights into its life history and ecology (Barnes and Siva-Jothy, 2000; Dhinaut *et al.*, 2018). In the future, it will be important to consider how diseases are classified in terms of host range, as insect rearing facilities are neither natural conditions nor optimised laboratory conditions. Under unnatural, high-density breeding conditions, it is possible that new and emerging parasites may adapt to infect insects that were formerly only capable of colonisation under experimental circumstances. It is largely unknown what effects altered environments like mass rearing facilities will have on host-parasite interactions and disease outcomes, which could be positive or negative for insect production. For this reason, it is important to understand a parasite's physiological as well as ecological host range, and the environmental and evolutionary forces driving adaptation and host-shifts. Interactive effects arising from co-infection must also be considered. Different parasite species or strains might infect simultaneously, resulting in unpredictable outcomes that are impossible to determine when studying parasites individually (Cory and Deschodt, 2018).

As the mass production of *T. molitor* grows alongside global demand for insect protein, it will be important to maintain awareness of the type and severity of organisms affecting insect stocks. This is especially true for disease-causing agents, given that mass-rearing is practised at high insect densities that are conducive to outbreaks. Likewise, continued research into the possible benefits of mutualistic organisms will also help to ensure the health and well-being of farmed insects. These areas of research could largely benefit from partnerships between academic institutions, government programs, and industry in order to identify and address emerging parasites of particular concern and ensure the best practices for maintaining insect health are known and implemented.

Supplementary material

Supplementary material can be found online at https://doi.org/10.3920/JIFF2022.0171.

Table S1. Overview of *Tenebrio molitor* parasites, symptoms, detection methods, and prevention or treatment.

Authors contributions

A.R.S., P.H., E.B., F.S.L., L.H.-P., C.S. conceptualisation, investigation, writing – original draft preparation. A.R.S. and P.H. writing – reviewing and editing.

Acknowledgements

We wish to thank Florent Dupriez, Jørgen Eilenberg, Thomas Lefebvre, Joop van Loon, Christina Nielsen-Leroux and Niek Steeghs for their valuable remarks and feedback, which contributed to the refinement of this review.

Funding

The writing of this review has received funding from the European Union's Horizon 2020 research and innovation programme INSECT DOCTORS under the Marie Skłodowska-Curie grant agreement No 859850.

Conflict of interest

The authors declare no conflict of interest.

References

Abdel Rahman, K., El-Shazly, M. and Ghazawy, N., 2015. The incidence of the protozoa *Malamoeba locustae* and *Gregarina granhami* in three acridian aommunities during summer month. Donnish Journal of Entomology and Nematology 1: 1-8.

Adl, S.M., Bass, D., Lane, C.E., Lukes, J., Schoch, C.L., Smirnov, A., Agatha, S., Berney, C., Brown, M.W., Burki, F., Cardenas, P., Cepicka, I., Chistyakova, L., del Campo, J., Dunthorn, M., Edvardsen, B., Eglit, Y., Guillou, L., Hampl, V., Heiss, A.A., Hoppenrath, M., James, T.Y., Karnkowska, A., Karpov, S., Kim, E., Kolisko, M., Kudryavtsev, A., Lahr, D.J.G., Lara, E., Le Gall, L., Lynn, D.H., Mann, D.G., Massana, R., Mitchell, E.A.D., Morrow, C., Park, J.S., Pawlowski, J.W., Powell, M.J., Richter, D.J., Rueckert, S., Shadwick, L., Shimano, S., Spiegel, F.W., Torruella, G., Youssef, N., Zlatogursky, V. and Zhang, Q.Q., 2019. Revisions to the classification, nomenclature, and diversity of eukaryotes. Journal of Eukaryotic Microbiology 66: 4-119. https://doi.org/10.1111/jeu.12691

Anderson, O.R., 2017. Amoebozoan Lobose Amoebae (Tubulinea, Flabellinea, and others). In: Archibald, J.M., Simpson, A.G.B. and Slamovits, C.H. (eds) Handbook of the protists. Springer International Publishing, Cham, Switzerland, pp. 1279-1309. https://doi.org/10.1007/978-3-319-28149-0_2

Andrade, G.S., Sousa, A.H., Santos, J.C., Gama, F.C., Serrao, J.E. and Zanuncio, J.C., 2012. Oogenesis pattern and type of ovariole of the parasitoid *Palmistichus elaeisis* (Hymenoptera: Eulophidae). Anais Da Academia Brasileira De Ciencias 84: 767-774. https://doi.org/10.1590/s0001-37652012000300019

Armitage, S.A.O. and Siva-Jothy, M.T., 2005. Immune function responds to selection for cuticular colour in *Tenebrio molitor*. Heredity 94: 650-656. https://doi.org/10.1038/sj.hdy.6800675

Bang, A. and Courchamp, F., 2021. Industrial rearing of edible insects could be a major source of new biological invasions. Ecology Letters 24: 393-397. https://doi.org/10.1111/ele.13646

Barnes, A.I. and Siva-Jothy, M.T., 2000. Density-dependent prophylaxis in the mealworm beetle *Tenebrio molitor* L. (Coleoptera: Tenebrionidae): cuticular melanization is an indicator of investment in immunity. Proceedings of the Royal Society B-Biological Sciences 267: 177-182. https://doi.org/10.1098/rspb.2000.0984

Bass, D. and del Campo, J., 2020. Microeukaryotes in animal and plant microbiomes: Ecologies of disease? European Journal of Protistology 76: 1-10. https://doi.org/10.1016/j.ejop.2020.125719

Becnel, J.J. and Andreadis, T.G., 2014. Microsporidia in insects. In: Weiss, L.M. and Becnel, J.J. (eds) Microsporidia: pathogens of opportunity. John Wiley & Sons, Inc. Ames, IA, USA, pp. 521-570. https://doi.org/10.1002/9781118395264.ch21

Berndt, A., 1902. Beitrag zur Kenntnis der im Darme der Larve von *Tenebrio molitor* lebenden Gregarinen. Archiv für Protistenkunde 1: 375.

Bertola, M. and Mutinelli, F., 2021. A systematic review on viruses in mass-reared edible insect species. Viruses 13: 1-31. https://doi.org/10.3390/v13112280

Bessette, E. and Williams, B., 2022. Protists in the insect rearing industry: benign passengers or potential risk? Insects 13: 1-32. https://doi.org/10.3390/insects13050482

Bharadwaj, A. and Stafford, K.C., 2011. Potential of *Tenebrio molitor* (Coleoptera: Tenebrionidae) as a bioassay probe for *Metarhizium brunneum* (Hypocreales: Clavicipitaceae) activity against *Ixodes scapularis* (Acari: Ixodidae). Journal of Economic Entomology 104: 2095-2098. https://doi.org/10.1603/ec11170

Bhat, S.A., Bashir, I. and Kamili, A.S., 2009. Microsporidiosis of silkworm, *Bombyx mori* L. (Lepidoptera-bombycidae): A review. African Journal of Agricultural Research 4: 1519-1523. https://doi.org/10.5897/AJAR.9000490

Bing, X.L., Winkler, J., Gerlach, J., Loeb, G. and Buchon, N., 2021. Identification of natural pathogens from wild *Drosophila suzukii*. Pest Management Science 77: 1594-1606. https://doi.org/10.1002/ps.6235

Black, P.N., Blair, C.D., Butcher, A., Capinera, J.L. and Happ, G.M., 1981. Biochemistry and ultrastructure of iridescent virus type 29. Journal of Invertebrate Pathology 38: 12-21. https://doi.org/10.1016/0022-2011(81)90028-8

Boelaert, F., Stoicescu, A., Amore, G., Messens, W., Hempen, M., Rizzi, V., Antoniou, S.E., Baldinelli, F., Dorbek-Kolin, E., Van der Stede, Y., Niskanen, T., Haussig, J., Kaczmarek, M., Dias, J.G., Barco, L., Mancin, M., Mantovani, C., Sardella, A., Antonelli, P., Leati, M., Lettini, A.A., Losasso, C., Morabito, S., Scavia, G., Knijn, A., Tozzoli, R., Iacoponi, F., Moro, O., D'Errico, M.L., Gattuso, A., Suffredini, E., Di Bartolo, I., Delibato, E., Anniballi, F., Ianiro, G., Altieri, I., Morales, M.A.G., Casulli, A., Caccio, S., Danan, C. and Felix, B., 2021. The European Union one health 2019 zoonoses report. EFSA Journal 19(2): e06406. https://doi.org/10.2903/j.efsa.2021.6406

Browne, N., Surlis, C. and Kavanagh, K., 2014. Thermal and physical stresses induce a short-term immune priming effect in *Galleria mellonella* larvae. Journal of Insect Physiology 63: 21-26. https://doi.org/10.1016/j.jinsphys.2014.02.006

Capella-Gutiérrez, S., Marcet-Houben, M. and Gabaldón, T., 2012. Phylogenomics supports microsporidia as the earliest diverging clade of sequenced fungi. BMC Biology 10: 1-13. https://doi.org/10.1186/1741-7007-10-47

Carter, G.R. and Cole Jr, J.R., 2012. Diagnostic procedure in veterinary bacteriology and mycology. Academic Press, San Diego, CA, USA.

Castrillo, L. and Humber, R., 2009. Molecular methods for identification and diagnosis of fungi. In: Stock, S.P. Vandenberg, J., Glazer, I. and Boemare, N. (eds) Insect pathogens molecular approaches and techniques. CABI International, Wallingford, UK.

Cevallos, R.C. and Sarnow, P., 2010. Temperature protects insect cells from infection by cricket paralysis virus. Journal of Virology 84: 1652-1655. https://doi.org/10.1128/JVI.01730-09

Clopton, R.E., Percival, T.J. and Janovy, J., 1991. *Gregarina niphandrodes* N. Sp. (Apicomplexa: Eugregarinorida) from adult *Tenebrio molitor* (L.) with oocyst descriptions of other gregarine parasites of the yellow mealworm. Journal of Protozoology 38: 472-479. https://doi.org/10.1111/j.1550-7408.1991.tb04819.x

Cole, T.J., Eggleston, P. and Hurd, H., 2003. Juvenile hormone titre and egg production in *Tenebrio molitor* infected by *Hymenolepis diminuta*: effect of male and/or female infection, male age and mating. Journal of Insect Physiology 49: 583-590. https://doi.org/10.1016/S0022-1910(03)00030-1

Cortes Ortiz, J.A., Ruiz, A.T., Morales-Ramos, J.A., Thomas, M., Rojas, M.G., Tomberlin, J.K., Yi, L., Han, R., Giroud, L. and Jullien, R.L., 2016. Insect mass production technologies. Chapter 6. In: Dossey, A.T., Morales-Ramos, J.A. and Guadalupe Rojas, M. (eds) Insects as sustainable food ingredients. Academic Press, San Diego, CA, USA, pp. 153-201. https://doi.org/10.1016/b978-0-12-802856-8.00006-5

Cory, J.S. and Deschodt, P.S., 2018. The biotic environment. In: Hajek, A.E. and Shapiro-Ilan, D.I. (eds) Ecology of invertebrate diseases (1st ed.). John Wiley & Sons, Hoboken, NJ, USA, pp. 187-212.

Costa, S., Pedro, S., Lourenço, H., Batista, I., Teixeira, B., Bandarra, N.M., Murta, D., Nunes, R. and Pires, C., 2020. Evaluation of *Tenebrio molitor* larvae as an alternative food source. NFS Journal 21: 57-64. https://doi.org/10.1016/j.nfs.2020.10.001

Davis, G.R.F., Smith, J.D., Schiefer, B. and Loew, F.M., 1975. Screening for mycotoxins with larvae of *Tenebrio molitor*. Journal of Invertebrate Pathology 26: 299-303. https://doi.org/10.1016/0022-2011(75)90225-6

de Carvalho Barbosa Negrisoli, C.R., Negrisoli Júnior, A.S., Bernardi, D. and Garcia, M.S., 2013. Activity of eight strains of entomopathogenic nematodes (Rhabditida: Steinernematidae, Heterorhabditidae) against five stored product pests. Experimental Parasitology 134: 384-388. https://doi.org/10.1016/j.exppara.2013.03.008

De Jong, B., 2021. No longer crawling: insect protein to come of age in the 2020s. Available at: https://research.rabobank.com/far/en/sectors/animal-protein/insect-protein-to-come-of-age-in-the-2020s.html.

de Miranda, J.R., Granberg, F., Low, M., Onorati, P., Semberg, E., Jansson, A. and Berggren, Å., 2021. Virus diversity and loads in crickets reared for feed: Implications for husbandry. Frontiers in Veterinary Science 8: 1-10. https://doi.org/10.3389/fvets.2021.642085

De Souza, P.C., Morey, A.T., Castanheira, G.M., Bocate, K.P., Panagio, L.A., Ito, F.A., Furlaneto, M.C., Yamada-Ogatta, S.F., Costa, I.N., Mora-Montes, H.M. and Almeida, R.S., 2015. *Tenebrio molitor* (Coleoptera: Tenebrionidae) as an alternative host to study fungal infections. Journal of Microbiological Methods 118: 182-186. https://doi.org/10.1016/j.mimet.2015.10.004

Derrien, C. and Boccuni, A., 2018. Current status of the insect producing industry in europe. In: A. Halloran, R. Flore, P. Vantomme and N. Roos (eds) Edible insects in sustainable food systems. Springer, Cham, Switzerland, pp. 471-479. https://doi.org/10.1007/978-3-319-74011-9_30

Desportes, I. and Schrével, J., 2013. Treatise on zoology – anatomy, taxonomy, biology. The gregarines: The early branching Apicomplexa. Brill, Leiden, the Netherlands. https://doi.org/10.1163/9789004256057

Dhinaut, J., Chogne, M. and Moret, Y., 2018. Immune priming specificity within and across generations reveals the range of pathogens affecting evolution of immunity in an insect. Journal of Animal Ecology 87: 448-463. https://doi.org/10.1111/1365-2656.12661

Dupriez, F., Rejasse, A., Rios, A., Lefebvre, T. and Nielsen-Leroux, C., 2022. Impact and persistence of *Serratia marcescens* in *Tenebrio molitor* larvae and feed under optimal and stressed mass rearing conditions. Insects 13: 1-14. https://doi.org/10.3390/insects13050458

Eilenberg, J., Van Oers, M.M., Jensen, A.B., Lecocq, A., Maciel-Vergara, G., Santacoloma, L.P.A., van Loon, J.J.A. and Hesketh, H., 2018. Towards a coordination of European activities to diagnose and manage insect diseases in production facilities. Journal of Insects as Food and Feed 4: 157-166. https://doi.org/10.3920/jiff2018.0002

Eilenberg, J., Vlak, J.M., Nielsen-LeRoux, C., Cappellozza, S. and Jensen, A.B., 2015. Diseases in insects produced for food and feed. Journal of Insects as Food and Feed 1: 87-102. https://doi.org/10.3920/jiff2014.0022

European Commission, 2021. Commission Implementing Regulation (EU) 2021/882 of 1 June 2021 authorising the placing on the market of dried *Tenebrio molitor* larva as a novel food under Regulation (EU) 2015/2283 of the European Parliament and of the Council, and amending Commission Implementing Regulation (EU) 2017/2470. Official Journal of the European Union L 194: 16-20. Available at: .http://data.europa.eu/eli/reg_impl/2021/882/oj

Favero, K., Pereira, F.F., Kassab, S.O., Costa, D.P. and Zanuncio, J.C., 2014. Life and fertility tables of *Trichospilus diatraeae* (Hymenoptera: Eulophidae) with *Tenebrio molitor* (Coleoptera: Tenebrionidae) pupae. Annals of the Entomological Society of America 107: 621-626. https://doi.org/10.1603/an13082

Fisher, F.M. and Sanborn, R.C., 1962. Observations on the susceptibility of some insects to *Nosema* (Microsporidia: Sporozoa). The Journal of Parasitology 48: 926-932. https://doi.org/10.2307/3275124

Foelkel, E., Voss, M., Monteiro, L.B. and Nishimura, G., 2017. Isolation of entomopathogenic nematodes in an apple orchard in Southern Brazil and its virulence to *Anastrepha fraterculus* (Diptera: Tephritidae) larvae, under laboratory conditions. Brazilian Journal of Biology 77: 22-28. https://doi.org/10.1590/1519-6984.08315

Francuski, L. and Beukeboom, L.W., 2020. Insects in production – an introduction. Entomologia Experimentalis et Applicata 168: 422-431. https://doi.org/10.1111/eea.12935

Fredensborg, B.L., Kalvalio, I.F.I., Johannesen, T.B., Stensvold, C.R., Nielsen, H.V. and Kapel, C.M.O., 2020. Parasites modulate the gut-microbiome in insects: a proof-of-concept study. Plos One 15: 1-18. https://doi.org/10.1371/journal.pone.0227561

Frey, K.G. and Bishop-Lilly, K.A., 2015. Next-Generation sequencing for pathogen detection and identification. In: Sails, A. and Tang, Y.-W. (eds) Methods in microbiology. Academic Press, San Diego, CA, USA, pp. 525-554. https://doi.org/10.1016/bs.mim.2015.06.004

Gałęcki, R. and Sokół, R., 2019. A parasitological evaluation of edible insects and their role in the transmission of parasitic diseases to humans and animals. Plos One 14: 1-19. https://doi.org/10.1371/journal.pone.0219303

Garofalo, C., Milanović, V., Cardinali, F., Aquilanti, L., Clementi, F. and Osimani, A., 2019. Current knowledge on the microbiota of edible insects intended for human consumption: a state-of-the-art review. Food Research International 125: 1-32. https://doi.org/10.1016/j.foodres.2019.108527

Gencer, D., Yesilyurt, A., Gullu, M., Demir, I. and Nalcacioglu, R., 2020. Insecticidal activities of wild type and recombinant invertebrate iridescent viruses on five common pests. Turkish Journal of Entomology 44: 365-373. https://doi.org/10.16970/entoted.700189

Ghosh, C., Choudhury, A. and Misra, K.K., 2000. Life histories of three new coccidian parasites from three coleopteran stored-grain pests of India. Acta Protozoologica 39: 233-240.

Gibson, J., Shokralla, S., Porter, T.M., King, I., Van Konynenburg, S., Janzen, D.H., Hallwachs, W. and Hajibabaei, M., 2014. Simultaneous assessment of the macrobiome and microbiome in a bulk sample of tropical arthropods through DNA metasystematics. Proceedings of the National Academy of Sciences 111: 8007-8012. https://doi.org/10.1073/pnas.1406468111

Gołębiowski, M., Urbanek, A., Pietrzak, A., Naczk, A.M., Bojke, A., Tkaczuk, C. and Stepnowski, P., 2020. Effects of the entomopathogenic fungus *Metarhizium flavoviride* on the fat body lipid composition of *Zophobas morio* larvae (Coleoptera: Tenebrionidae). The Science of Nature 107: 1-11. https://doi.org/10.1007/s00114-019-1662-5

González-Acosta, S., Baca-González, V., Asensio-Calavia, P., Otazo-Pérez, A., López, M.R., Morales-Delanuez, A. and Pérez De La Lastra, J.M., 2022. Efficient oral priming of *Tenebrio molitor* larvae using heat-inactivated microorganisms. Vaccines 10: 1-11. https://doi.org/10.3390/vaccines10081296

Grau, T., Vilcinskas, A. and Joop, G., 2017a. Probiotic *Enterococcus mundtii* isolate protects the model insect *Tribolium castaneum* against *Bacillus thuringiensis*. Frontiers in Microbiology 8: 1-10. https://doi.org/10.3389/fmicb.2017.01261

Grau, T., Vilcinskas, A. and Joop, G., 2017b. Sustainable farming of the mealworm *Tenebrio molitor* for the production of food and feed. Zeitschrift für Naturforschung C 72: 337-349. https://doi.org/10.1515/znc-2017-0033

Guo, Z.Q., Doll, K., Dastjerdi, R., Karlovsky, P., Dehne, H.W. and Altincicek, B., 2014. Effect of fungal colonization of wheat grains with *Fusarium* spp. on food choice, weight gain and mortality of meal beetle larvae (*Tenebrio molitor*). Plos One 9: 1-9. https://doi.org/10.1371/journal.pone.0100112

Hajek, A.E. and Shapiro-Ilan, D.I., 2018. General concepts in the ecology of invertebrate diseases. In: Hajek, A.E. and Shapiro-Ilan, D.I. (eds) Ecology of invertebrate diseases. John Wiley & Sons Ltd., Oxford, UK, pp. 3-18.

Hammerschmidt, K.E.I., 6: 3 5 8, 1838. Ueber die Spermatozoon der Insecten. Isis: 358.

Harry, O.G., 1967. The effect of a eugregarine *Gregarina polymorpha* (Hammerschmidt) on the mealworm larva of *Tenebrio molitor* (L.). The Journal of Protozoology 14: 539-547. https://doi.org/10.1111/j.1550-7408.1967.tb02039.x

Heyneman, D. and Voge, M., 1971. Host response of the flour beetle, *Tribolium confusum*, to infections with *Hymenolepis diminuta*, *H. microstoma*, and *H. citelli* (Cestoda: Hymenolepididae). Journal of Parasitology 57: 881-886. https://doi.org/10.2307/3277820

Huger, A.M., 1969. Virose bei Larven des Mehlkäfers. Naturwissenschaften 56: 466-467. https://doi.org/10.1007/BF00601081

Hurd, H. and Parry, G., 1991. Metacestode-induced depression of the production of, and response to, sex pheromone in the intermediate host *Tenebrio molitor*. Journal of Invertebrate Pathology 58: 82-87. https://doi.org/10.1016/0022-2011(91)90165-M

Hurd, H., Strambi, C. and Beckage, N.E., 1990. *Hymenolepis diminuta*: an investigation of juvenile hormone titre, degradation and supplementation in the intermediate host, *Tenebrio molitor*. Parasitology 100: 445-452. https://doi.org/10.1017/s0031182000078744

Inoue, H. and Tanada, Y., 1977. Thermal therapy of the flacherie virus disease in the silkworm, *Bombyx mori*. Journal of Invertebrate Pathology 29: 63-68. https://doi.org/10.1016/0022-2011(77)90173-2

International Platform of Insects for Food and Feed (IPIFF), 2022. Guide on good hygiene practices for European (EU) producers of insects as food and feed. Available at: https://ipiff.org/wp-content/uploads/2019/12/IPIFF-Guide-on-Good-Hygiene-Practices.pdf.

Janković-Tomanić, M., Petković, B., Todorović, D., Vranković, J. and Perić-Mataruga, V., 2019. Physiological and behavioral effects of the mycotoxin deoxynivalenol in *Tenebrio molitor* larvae. Journal of Stored Products Research 83: 236-242. https://doi.org/10.1016/j.jspr.2019.07.008

Jensen, A.N., Hansen, S.H. and Baggesen, D.L., 2020. *Salmonella typhimurium* level in mealworms (*Tenebrio molitor*) after exposure to contaminated substrate. Frontiers in Microbiology 11: 1-9. https://doi.org/10.3389/fmicb.2020.01613

Käfer, S., Paraskevopoulou, S., Zirkel, F., Wieseke, N., Donath, A., Petersen, M., Jones, T.C., Liu, S., Zhou, X., Middendorf, M., Junglen, S., Misof, B. and Drosten, C., 2019. Re-assessing the diversity of negative strand RNA viruses in insects. PLOS Pathogens 15: 1-32. https://doi.org/10.1371/journal.ppat.1008224

Kaya, H.K. and Vega, F.E., 2012. Scope and basic principles of insect pathology. In: Kaya, H.K. and Vega, F.E. (eds) Insect pathology (second edition). Academic Press, San Diego, CA, USA, pp. 1-12. https://doi.org/10.1016/B978-0-12-384984-7.00001-4

Kelly, D.C., Ayres, M.D., Lescott, T., Robertson, J.S. and Happ, G.M., 1979. Small Iridescent Virus (Type-29) isolated from *Tenebrio molitor* – comparison of its proteins and antigens with 6 other iridescent viruses. Journal of General Virology 42: 95-105. https://doi.org/10.1099/0022-1317-42-1-95

Keyser, C.A., Jensen, B. and Meyling, N.V., 2016. Dual effects of *Metarhizium* spp. and *Clonostachys rosea* against an insect and a seed-borne pathogen in wheat. Pest Management Science 72: 517-526. https://doi.org/10.1002/ps.4015

Keyser, C.A., Thorup-Kristensen, K. and Meyling, N.V., 2014. *Metarhizium* seed treatment mediates fungal dispersal via roots and induces infections in insects. Fungal Ecology 11: 122-131. https://doi.org/10.1016/j.funeco.2014.05.005

King, R.L. and Taylor, A.B., 1936. *Malpighamœba locustae*, n. sp. (Amoebidae), a protozoan parasitic in the malpighian tubes of grasshoppers. Transactions of the American Microscopical Society 55: 6-10. https://doi.org/10.2307/3223005

Kleespies, R.G., Huger, A.M. and Zimmermann, G., 2008. Diseases of insects and other arthropods: results of diagnostic research over 55 years. Biocontrol Science and Technology 18: 439-482. https://doi.org/10.1080/09583150802011618

Kleespies, R.G., Huger, A.M. and Zimmermann, G., 2010. Database on diagnosis of arthropod diseases in the Internet of the Julius Kuhn-Institute. Journal of Applied Entomology 134: 1-80. https://doi.org/10.1111/j.1439-0418.2009.01431.x

Kolářová, I., Florent, I. and Valigurová, A., 2022. Parasitic protists: diversity of adaptations to a parasitic lifestyle. Microorganisms 10: 1-3. https://doi.org/10.3390/microorganisms10081560

Korosi, G.A., Wilson, B.A.L., Powell, K.S., Ash, G.J., Reineke, A. and Savocchia, S., 2019. Occurrence and diversity of entomopathogenic fungi (*Beauveria* spp. and *Metarhizium* spp.) in Australian vineyard soils. Journal of Invertebrate Pathology 164: 69-77. https://doi.org/10.1016/j.jip.2019.05.002

Koura, E.A. and Kamel, E.G. 1993. A survey of gregarines associated with *Tenebrio molitor* and *Opatriodes vicinus* in the central region of Saudi Arabia. Journal of the Egyptian Society of Parasitology 23: 213-220.

Krieg, A., Huger, A.M., Langenbruch, G.A. and Schnetter, W., 1983. *Bacillus thuringiensis* var. *tenebrionis*: ein neuer, gegenüber Larven von Coleopteren wirksamer Pathotyp. Zeitschrift für Angewandte Entomologie 96: 500-508. https://doi.org/10.1111/j.1439-0418.1983.tb03704.x

Lange, C.E. and Lord, J.C., 2012. Protistan entomopathogens. In: Vega, F.E. and Kaya, H.K. (eds) Insect pathology (second edition). Academic Press, San Diego, CA, USA, pp. 367-394. https://doi.org/10.1016/B978-0-12-384984-7.00010-5

Lecocq, A., Natsopoulou, M.E., Berggreen, I.E., Eilenberg, J., Heckmann, L.H.L., Nielsen, H.V., Stensvold, C.R. and Jensen, A.B., 2021. Probiotic properties of an indigenous *Pediococcus pentosaceus* strain on *Tenebrio molitor* larval growth and survival. Journal of Insects as Food and Feed 7: 975-986. https://doi.org/10.3920/jiff2020.0156

Lee, S.J., Kim, S.H., Nai, Y.S., Je, Y.H., Parker, B.L. and Kim, J.S., 2014. Management of entomopathogenic fungi in cultures of *Tenebrio molitor* (Coleoptera: Tenebrionidae). Entomological Research 44: 236-243. https://doi.org/10.1111/1748-5967.12068

Lipa, J.J., 1967. Studies on gregarines (Gregarinomorpha) of arthropods in Poland. Acta Protozoologica 5: 97-179.

Little, T.J. and Kraaijeveld, A.R., 2004. Ecological and evolutionary implications of immunological priming in invertebrates. Trends in Ecology & Evolution 19: 58-60. https://doi.org/10.1016/j.tree.2003.11.011

Liu, S.J., Vijayendran, D. and Bonning, B.C., 2011. Next generation sequencing technologies for insect virus discovery. Viruses 3: 1849-1869. https://doi.org/10.3390/v3101849

Lulamba, T.E. and Serepa-Dlamini, M.H., 2020. Molecular identification of a *Heterorhabditis* entomopathogenic nematode isolated from the northernmost region of South Africa. Egyptian Journal of Biological Pest Control 30: 1-9. https://doi.org/10.1186/s41938-020-00279-0

Maciel-Vergara, G., Jensen, A. and Eilenberg, J., 2018. Cannibalism as a possible entry route for opportunistic pathogenic bacteria to insect hosts, exemplified by *Pseudomonas aeruginosa*, a pathogen of the giant mealworm *Zophobas morio*. Insects 9: 1-15. https://doi.org/10.3390/insects9030088

Maciel-Vergara, G., Jensen, A.B., Lecocq, A. and Eilenberg, J., 2021. Diseases in edible insect rearing systems. Journal of Insects as Food and Feed 7: 621-638. https://doi.org/10.3920/jiff2021.0024

Maciel-Vergara, G. and Ros, V.I.D., 2017. Viruses of insects reared for food and feed. Journal of Invertebrate Pathology 147: 60-75. https://doi.org/10.1016/j.jip.2017.01.013

Maema, M., 1986. Experimental infection of *Tribolium confusum* (Coleoptera) by *Hymenolepis diminuta* (Cestoda): host fecundity during infection. Parasitology 92: 405-412. https://doi.org/10.1017/S0031182000064167

Maistrou, S., Paris, V., Jensen, A.B., Rolff, J., Meyling, N.V. and Zanchi, C., 2018. A constitutively expressed antifungal peptide protects *Tenebrio molitor* during a natural infection by the entomopathogenic fungus *Beauveria bassiana*. Developmental and Comparative Immunology 86: 26-33. https://doi.org/10.1016/j.dci.2018.04.015

Makki, M.S., Mowlavi, G., Shahbazi, F., Abai, M.R., Najafi, F., Hosseini-Farash, B.R., Teimoori, S., Hasanpour, H. and Naddaf, S.R., 2017. Identification of *Hymenolepis diminuta* cysticercoid larvae in *Tribolium castaneum* (Coleoptera: Tenebrionidae) beetles from Iran. Journal of arthropod-borne diseases 11: 338-343.

Martin, B.D. and Schwab, E.R., 2012. Current usage of symbiosis and associated terminology. International Journal of Biology 5: 32-35. https://doi.org/10.5539/ijb.v5n1p32

Martin, S.J. and Brettell, L.E., 2019. Deformed wing virus in honeybees and other insects. In: Enquist, L., DiMaio, D. and Demody, T. (eds) Annual review of virology, Vol 6, 2019. Annual Review of Virology. Annual Reviews, Palo Alto, CA, USA, pp. 49-69. https://doi.org/10.1146/annurev-virology-092818-015700

Masson, F. and Lemaitre, B., 2020. Growing ungrowable bacteria: overview and perspectives on insect symbiont culturability. Microbiology and Molecular Biology Reviews 84: 1-22. https://doi.org/10.1128/mmbr.00089-20

Mathulwe, L.L., Jacobs, K., Malan, A.P., Birkhofer, K., Addison, M.F. and Addison, P., 2021. Characterisation of *Metarhizium majus* (Hypocreales: Clavicipitaceae) isolated from the Western Cape Province, South Africa. Plos One 16: 1-11. https://doi.org/10.1371/journal.pone.0240955

Milner, R.J., 1973. *Nosema whitei*, a microsporidan pathogen of some species of *Tribolium* V. Comparative pathogenicity and host range. Entomophaga 18: 383-390. https://doi.org/10.1007/BF02371014

Moret, Y. and Siva-Jothy, M.T., 2003. Adaptive innate immunity? Responsive-mode prophylaxis in the mealworm beetle, *Tenebrio molitor*. Proceedings of the Royal Society B-Biological Sciences 270: 2475-2480. https://doi.org/10.1098/rspb.2003.2511

Nielsen-Leroux, C., Gaudriault, S., Ramarao, N., Lereclus, D. and Givaudan, A., 2012. How the insect pathogen bacteria *Bacillus thuringiensis* and *Xenorhabdus*/*Photorhabdus* occupy their hosts. Current Opinion in Microbiology 15: 220-231. https://doi.org/10.1016/j.mib.2012.04.006

Ochoa Sanabria, C., Hogan, N., Madder, K., Gillott, C., Blakley, B., Reaney, M., Beattie, A. and Buchanan, F., 2019. Yellow mealworm larvae (*Tenebrio molitor*) fed mycotoxin-contaminated wheat – a possible safe, sustainable protein source for animal feed? Toxins 11: 1-13. https://doi.org/10.3390/toxins11050282

Park, T. and Frank, M.B., 1950. The population history of *Tribolium* free of sporozoan infection. Journal of Animal Ecology 19: 95-105. https://doi.org/10.2307/1520

Pedrini, N., Villaverde, M.L., Fuse, C.B., Dal Bello, G.M. and Juarez, M.P., 2010. *Beauveria bassiana* infection alters colony development and defensive secretions of the beetles *Tribolium castaneum* and *Ulomoides dermestoides* (Coleoptera: Tenebrionidae). Journal of Economic Entomology 103: 1094-1099. https://doi.org/10.1603/ec10072

Pirofski, L.-A. and Casadevall, A., 2012. Q&A: What is a pathogen? A question that begs the point. BMC Biology 10: 1-3. https://doi.org/10.1186/1741-7007-10-6

Praprotnik, E., Lončar, J. and Razinger, J., 2021. Testing virulence of different species of insect associated fungi against yellow mealworm (Coleoptera: Tenebrionidae) and their potential growth stimulation to maize. Plants 10: 1-17. https://doi.org/10.3390/plants10112498

Ramakuwela, T., Hatting, J., Laing, M.D., Thiebaut, N. and Hazir, S., 2018. Biological characterization of the entomopathogenic nematode, *Steinernema innovationi*: a South African isolate. Journal of Nematology 50: 507-516. https://doi.org/10.21307/jofnem-2018-049

Ramos-Rodríguez, O., Campbell, J.F. and Ramaswamy, S.B., 2006. Pathogenicity of three species of entomopathogenic nematodes to some major stored-product insect pests. Journal of Stored Products Research 42: 241-252. https://doi.org/10.1016/j.jspr.2004.08.004

Reiss, J., 1973. Toxicity of molds to the larvae of *Tenebrio molitor*. Journal of Invertebrate Pathology 21: 112-113. https://doi.org/10.1016/0022-2011(73)90120-1

Rizou, E., Kalogiouri, N., Bisba, M., Papadimitriou, A., Kyrila, G., Lazou, A., Andreadis, S., Hatzikamari, M., Mourtzinos, I. and Touraki, M., 2022. Amelioration of growth, nutritional value, and microbial load of *Tenebrio molitor* (Coleoptera: Tenebrionidae) through probiotic supplemented feed. European Food Research and Technology 248: 727-739. https://doi.org/10.1007/s00217-021-03925-5

Rodriguez, Y., Omoto, C.K. and Gomulkiewicz, R., 2007. Individual and population effects of eugregarine, *Gregarina niphandrodes* (Eugregarinida: Gregarinidae), on *Tenebrio molitor* (Coleoptera: Tenebrionidae). Environmental Entomology 36: 689-693. https://doi.org/10.1093/ee/36.4.689

Rueckert, S., Betts, E.L. and Tsaousis, A.D., 2019. The symbiotic spectrum: where do the gregarines fit? Trends in Parasitology 35: 687-694. https://doi.org/10.1016/j.pt.2019.06.013

Saari, S., Näreaho, A. and Nikander, S., 2019. Cestoda (tapeworms). In: S. Saari, A. Näreaho and S. Nikander (Eds.), Canine parasites and parasitic diseases. Academic Press, San Diego, CA, USA, pp. 55-81. https://doi.org/10.1016/B978-0-12-814112-0.00004-0

Salomaki, E.D., Terpis, K.X., Rueckert, S., Kotyk, M., Varadinova, Z.K., Cepicka, I., Lane, C.E. and Kolisko, M., 2021. Gregarine single-cell transcriptomics reveals differential mitochondrial remodeling and adaptation in apicomplexans. BMC Biology 19: 1-19. https://doi.org/10.1186/s12915-021-01007-2

Sautet, J., 1930. A propos d'*Adelina tenebrionis*, coccidie cœlomique de *Tenebrio molitor*. Annales de Parasitologie Humaine et Comparée 8: 582-589. https://doi.org/10.1051/parasite/1930086582

Savio, C., Mugo-Kamiri, L. and Upfold, J.K., 2022. Bugs in bugs: The role of probiotics and prebiotics in maintenance of health in mass-reared insects. Insects 13: 1-18. https://doi.org/10.3390/insects13040376

Schawang, J.E. and Janovy, J., 2001. The response of *Gregarina niphandrodes* (Apicomplexa: Eugregarinida: Septatina) to host starvation in *Tenebrio molitor* (Coleoptera: Tenebrionidae) adults. The Journal of Parasitology 87: 600-605. https://doi.org/10.2307/3285099

Shapiro-Ilan, D., Rojas, M.G., Morales-Ramos, J.A., Lewis, E.E. and Tedders, W.L., 2008. Effects of host nutrition on virulence and fitness of entomopathogenic nematodes: lipid- and protein-based supplements in *Tenebrio molitor* diets. Journal of Nematology 40: 13-19.

Shapiro-Ilan, D.I., Blackburn, D., Duncan, L., El-Borai, F.E., Koppenhöfer, H., Tailliez, P. and Adams, B.J., 2014. Characterization of biocontrol traits in *Heterorhabditis floridensis*: a species with broad temperature tolerance. Journal of Nematology 46: 336-345.

Sheiman, I.M., Shkutin, M.F., Terenina, N.B. and Gustafsson, M.K.S., 2006. A behavioral study of the beetle *Tenebrio molitor* infected with cysticercoids of the rat tapeworm *Hymenolepis diminuta*. Naturwissenschaften 93: 305-308. https://doi.org/10.1007/s00114-006-0103-4

Shi, M., Lin, X.-D., Vasilakis, N., Tian, J.-H., Li, C.-X., Chen, L.-J., Eastwood, G., Diao, X.-N., Chen, M.-H., Chen, X., Qin, X.-C., Widen, S.G., Wood, T.G., Tesh, R.B., Xu, J., Holmes, E.C., Zhang, Y.-Z. and Ou, J.-H.J., 2016. Divergent viruses discovered in arthropods and vertebrates revise the evolutionary history of the flaviviridae and related viruses. Journal of Virology 90: 659-669. https://doi.org/10.1128/JVI.02036-15

Sikorowski, P.P. and Lawrence, A.M., 1994. Microbial contamination and insect rearing. American Entomologist 40: 240-353. https://doi.org/10.1093/ae/40.4.240

Solter, L.F., Becnel, J.J. and Vávra, J., 2012. Research methods for entomopathogenic microsporidia and other protists. Chapter XI. In: Lacey, L.A. (ed.) Manual of techniques in invertebrate pathology (second edition). Academic Press, San Diego, CA, USA, pp. 329-371. https://doi.org/10.1016/B978-0-12-386899-2.00011-7

Song, J.-H., Chang, G.-D., Ji, S., Kim, S.-Y. and Kim, W., 2022. Selective breeding and characterization of a black mealworm strain of *Tenebrio molitor* Linnaeus (Coleoptera: Tenebrionidae). Journal of Asia-Pacific Entomology 25: 1-7. https://doi.org/10.1016/j.aspen.2022.101978

Stein, F., 1848. Ueber die Natur der Gregarinen. Archiv für Anatomie, Physiologie und Wissenschaftliche Medicin: 182-223.

Steinkraus, D.C. and Cross, E.A., 1993. Description and life history of *Acarophenax mahunkai*, n. sp. (Acari, Tarsonemina: Acarophenacidae), an egg parasite of the lesser mealworm (Coleoptera: Tenebrionidae). Annals of the Entomological Society of America 86: 239-249. https://doi.org/10.1093/aesa/86.3.239

Strassert, J.F.H. and Monaghan, M.T., 2022. Phylogenomic insights into the early diversification of fungi. Current Biology 32: 3628-3635. https://doi.org/10.1016/j.cub.2022.06.057

Sumner, R., 1933. Influence of gregarines on growth in the mealworm. Science 78: 125. https://doi.org/10.1126/science.78.2015.125.a

Sumner, R., 1936. Relation of gregarines to growth and longevity in the mealworm *Tenebrio molitor* L. Annals of the Entomological Society of America 29: 645-648. https://doi.org/10.1093/aesa/29.4.645

Szelei, J., Woodring, J., Goettel, M.S., Duke, G., Jousset, F.X., Liu, K.Y., Zadori, Z., Li, Y., Styer, E., Boucias, D.G., Kleespies, R.G., Bergoin, M. and Tijssen, P., 2011. Susceptibility of North-American and European crickets to *Acheta domesticus* densovirus (AdDNV) and associated epizootics. Journal of Invertebrate Pathology 106: 394-399. https://doi.org/10.1016/j.jip.2010.12.009

Torrini, G., Mazza, G., Carletti, B., Benvenuti, C., Roversi, P.F., Fanelli, E., de Luca, F., Troccoli, A. and Tarasco, E., 2015. *Oscheius onirici* sp n. (Nematoda: Rhabditidae): a new entomopathogenic nematode from an Italian cave. Zootaxa 3937: 533-548. https://doi.org/10.11646/zootaxa.3937.3.6

Urbanek, A.K., Rybak, J., Wrobel, M., Leluk, K. and Mironczuk, A.M., 2020. A comprehensive assessment of microbiome diversity in *Tenebrio molitor* fed with polystyrene waste. Environmental Pollution 262: 1-10. https://doi.org/10.1016/j.envpol.2020.114281

Valigurova, A., 2012. Sophisticated adaptations of *Gregarina cuneata* (Apicomplexa) feeding stages for epicellular parasitism. Plos One 7: 1-11. https://doi.org/10.1371/journal.pone.0042606

Vallet-Gely, I., Lemaitre, B. and Boccard, F., 2008. Bacterial strategies to overcome insect defences. Nature Reviews Microbiology 6: 302-313. https://doi.org/10.1038/nrmicro1870

Van Broekhoven, S., Gutierrez, J.M., De Rijk, T.C., De Nijs, W.C.M. and Van Loon, J.J.A., 2017. Degradation and excretion of the *Fusarium* toxin deoxynivalenol by an edible insect, the Yellow mealworm (*Tenebrio molitor* L.). World Mycotoxin Journal 10: 163-169. https://doi.org/10.3920/wmj2016.2102

van Huis, A., 2017. Edible insects and research needs. Journal of Insects as Food and Feed 3: 3-5. https://doi.org/10.3920/JIFF2017.x002

Vandeweyer, D., De Smet, J., Van Looveren, N. and Van Campenhout, L., 2021. Biological contaminants in insects as food and feed. Journal of Insects as Food and Feed 7: 807-822. https://doi.org/10.3920/jiff2020.0060

Vaulot, D., Geisen, S., Mahé, F. and Bass, D., 2022. pr2-primers: An 18S rRNA primer database for protists. Molecular Ecology Resources 22: 168-179. https://doi.org/10.1111/1755-0998.13465

Vega, F.E., Meyling, N.V., Luangsa-ard, J.J. and Blackwell, M., 2012. Fungal Entomopathogens. In: Vega, F.E. and Kaya, H.K. (eds) Insect pathology (second edition). Academic Press, San Diego, CA, USA, pp. 171-220. https://doi.org/10.1016/B978-0-12-384984-7.00006-3

Verma, M., Kulshrestha, S. and Puri, A., 2017. Genome sequencing. In: Keith, J. (ed.) Bioinformatics. Humana Press, New York, NY, USA, pp. 3-33. https://doi.org/10.1007/978-1-4939-6622-6_1

Vigneron, A., Jehan, C., Rigaud, T. and Moret, Y., 2019. Immune defenses of a beneficial pest: The mealworm beetle, *Tenebrio molitor*. Frontiers in Physiology 10: 1-17. https://doi.org/10.3389/fphys.2019.00138

Votýpka, J., Modrý, D., Oborník, M., Šlapeta, J. and Lukeš, J., 2017. Apicomplexa. In: Archibald, J.M., Simpson, A.G.B., Slamovits, C.H., Margulis, L., Melkonian, M., Chapman, D.J. and Corliss, J.O. (eds) Handbook of the protists. Springer International Publishing, Cham, Switzerland, pp. 1-58. https://doi.org/10.1007/978-3-319-32669-6_20-1

Wakil, W., Ghazanfar, M.U. and Yasin, M., 2014. Naturally occurring entomopathogenic fungi infecting stored grain insect species in Punjab, Pakistan. Journal of Insect Science 14: 1-7. https://doi.org/10.1093/jisesa/ieu044

Witteveldt, J., Cifuentes, C.C., Vlak, J.M. and van Hulten, M.C.W., 2004. Protection of *Penaeus monodon* against white spot syndrome virus by oral vaccination. Journal of Virology 78: 2057-2061. https://doi.org/10.1128/jvi.78.4.2057-2061.2004

Wojda, I. and Taszłow, P., 2013. Heat shock affects host-pathogen interaction in *Galleria mellonella* infected with *Bacillus thuringiensis*. Journal of Insect Physiology 59: 894-905. https://doi.org/10.1016/j.jinsphys.2013.06.011

Wu, H., Pang, R., Cheng, T., Xue, L., Zeng, H., Lei, T., Chen, M., Wu, S., Ding, Y., Zhang, J., Shi, M., Wu, Q. and Cristea, I.M., 2020. Abundant and diverse RNA viruses in insects revealed by RNA-Seq analysis: Ecological and evolutionary implications. mSystems 5: 1-14. https://doi.org/10.1128/mSystems.00039-20

Wynants, E., Frooninckx, L., Van Miert, S., Geeraerd, A., Claes, J. and Van Campenhout, L., 2019. Risks related to the presence of *Salmonella* sp. during rearing of mealworms (*Tenebrio molitor*) for food or feed: Survival in the substrate and transmission to the larvae. Food Control 100: 227-234. https://doi.org/10.1016/j.foodcont.2019.01.026

Yang, Z.W., Men, Y., Zhang, J., Liu, Z.H., Luo, J.Y., Wang, Y.H., Li, W.J. and Xie, Q., 2021. Evaluation of sample preservation approaches for better insect microbiome research according to next-generation and third-generation sequencing. Microbial Ecology 82: 971-980. https://doi.org/10.1007/s00248-021-01727-6

Zanchi, C., Lindeza, A.S. and Kurtz, J., 2020. Comparative mortality and adaptation of a smurf assay in two species of tenebrionid beetles exposed to *Bacillus thuringiensis*. Insects 11: 1-14. https://doi.org/10.3390/insects11040261

Zanuncio, J.C., Pereira, F.F., Jacques, G.C., Tavares, M.T. and Serrão, J.E., 2008. *Tenebrio molitor* Linnaeus (Coleoptera: Tenebrionidae), a new alternative host to rear the pupae parasitoid *Palmistichus elaeisis* Delvare & Lasalle (Hymenoptera: Eulophidae). The Coleopterists Bulletin 62: 64-66. https://doi.org/10.1649/1015.1

Zhong, J., Zhang, F., Peng, Y.J., Ji, Z.X., Li, H.Q., Li, S.C., Zhang, X.Z., Shi, Q.M. and Zhang, J., 2017. Mixed culture of probiotics on a solid-state medium: An efficient method to produce an affordable probiotic feed additive. Biotechnology and Bioprocess Engineering 22: 758-766. https://doi.org/10.1007/s12257-017-0038-y